

**M A S A R Y K O V A
U N I V E R Z I T A**

PŘÍRODOVĚDECKÁ FAKULTA

**Charakterizace
stafylokokových
bakteriofágů
využitelných ve
veterinární praxi**

Disertační práce

MGR. MICHAL ZEMAN

Vedoucí práce: doc. RNDr. Roman Pantůček, Ph.D.

Ústav experimentální biologie
program Molekulární a buněčná biologie a genetika

Brno 2021



Bibliografický záznam

Autor:	Mgr. Michal Zeman Přírodovědecká fakulta Masarykova univerzita Ústav experimentální biologie
Název práce:	Staphylococcal phages for application in veterinary medicine
Studijní program:	Molekulární a buněčná biologie a genetika
Vedoucí práce:	doc. RNDr. Roman Pantůček, Ph.D.
Rok:	2021
Počet stran:	116
Klíčová slova:	bakteriofág; Staphylococcus pseudintermedius; fágová terapie; genomika; proteomika

Bibliographic record

Author: Mgr. Michal Zeman
Faculty of Science
Masaryk University
Department of Experimental Biology

Title of Thesis: Staphylococcal phages for application in
veterinary medicine

Degree Programme: Molecular and Cell Biology and Genetics

Supervisor: doc. RNDr. Roman Pantůček, Ph.D.

Year: 2021

Number of Pages: 116

Keywords: bacteriophage; Staphylococcus
pseudintermedius; phage therapy; genomics;
proteomics

Abstrakt

Rezistence bakterií k antibiotikům není problémem pouze humánní ale i veterinární medicíny. *Staphylococcus pseudintermedius*, který je jednou z příčin onemocnění u domácích zvířat, může podobně jako *Staphylococcus aureus* nést různé faktory virulence a geny rezistence k antibiotikům. Možností léčby rezistentních kmenů *Staphylococcus* spp. je fágová terapie. Tato práce popisuje morfologickou, genomickou a proteomickou stavbu dvou fágů bakterie *S. pseudintermedius*. Fág QT1 je zástupcem nově popsaneho rodu, který má na konci bičíku dlouhé vlákno a jeho popis rozšiřuje znalosti temperovaných fágů tohoto druhu. Fág 40 je prvním popsáným fágem z čeledi *Herelleviridae* infikující *S. pseudintermedius* a mohl by sloužit jako modelový organismus pro fágovou terapii onemocnění způsobených tímto patogenem. V této práci jsou navíc popsány nové bakteriální druhy Pseudomonád a mobilní genetické elementy u zástupců *Staphylococcus intermedius* group.

Abstract

The problem of bacterial antibiotic resistance is not limited only to human medicine. *Staphylococcus pseudintermedius* can cause serious diseases in companion animals. This bacterium often harbours virulence and resistance genes similarly to *Staphylococcus aureus*. One possibility of how to treat resistant strains is to use phage therapy. Two phages that lyse *S. pseudintermedius* are described in this work at the physiological, genomic, and proteomic level. Phage QT1 widens the knowledge of temperate phages of *S. pseudintermedius* and is an example of a newly described genus of phages with long tail fibre. Phage 40 is the first *S. pseudintermedius*-infecting phage described belonging to the *Herelleviridae* family. This phage might serve as a model phage for phage therapy of *S. pseudintermedius* infection. Moreover, mobile genetic elements in *Staphylococcus intermedius* group members were characterised and new bacterial species were described.

Declaration

I declare that I have worked on this thesis independently using only the sources listed in the bibliography. All resources, sources, and literature, which I used in preparing or I drew on them, I quote in the thesis properly by stating the full reference to the source.

In Brno 19th March 2021

.....
Mgr. Michal Zeman

Acknowledgement and dedication

I would like to thank my supervisor doc. Pantůček for his valuable scientific insight and benevolent attitude during my whole studies. I appreciate it a lot. I am grateful to Brno metropolitan police animal shelter, Brno ZOO, Animal shelter Interpespenzion, MB PHARMA s.r.o. and the University of Veterinary and Pharmaceutical Sciences Brno, who kindly offered me samples for my thesis. I would like to acknowledge the National Reference Laboratory for Staphylococci and the National Institute of Public Health for their biochemical tests and additional sensitivity tests. I am grateful to prof. Sedláček for the possibility to undertake research at the J. G. Mendel Czech Antarctic Station. I thank the people who have read my work in advance and gave me advice on how to improve its structure or grammar. We kindly thank the Czech Science Foundation (13-05069P and 18-13064S), the Czech Health Research Council (16-29916A), and the Grant Agency of Masaryk University (MUNI/A/0877/2016, MUNI/A/0824/2017, MUNI/A/0958/2018, MUNI/A/1127/2019) for their funding.

Many thanks belong to all my colleagues/fellow students from the Laboratory of microbial molecular diagnostics – former and present, with which I have spent countless days and nights in the lab solving scientific and personal riddles alike. Namely, I must mention at least, Ben, Veronika, Dáda, Tibor, Lenka, Vojtěch, Hanka, Kristína, Jirka, Zuzana... they were always there for me as I was always there for them.

My heartiest thanks go to Ad'a and Pa'lo from which I think I took the most. From Ad'a I gained different perspectives on how to look at some problems and learnt that even when no one supports your decision, to stand true to yourself. With Pa'lo we tackled plenty of teaching and laboratory problems, his scientific spirit motivated me to be a better scientist, and he showed me that it's possible to live life to the full – both inside and outside of the lab.

This thank you goes to the numbers of students that “went through my hands” because it is not only them who takes something from the classes, but even the teacher is rewarded with a bit of knowledge or ideas he collects from their minds.

To the people outside of our lab including, but not limited to, Ondrej, Marek, Staša, Juro, Šeriff, Martinovia, Steve, and a great many others. Without them, it would have been a sad student life. I have the privilege

to call them my friends. They are those poor unfortunates that I always bored with my purely academic questions, and they thought I meant it for real.

I would like to thank all the people that made my journey through university a bit more bearable.

Ku koncu by som chcel poďakovať mojim rodičom za ich príkladnú starostlivosť o mňa. Za to, že som strávil roky študovaním niečoho čomu nerozumejú a aj tak boli zvedaví čo to vlastne tých 10 rokov robím a prečo ešte stále nemajú vnúčatá. Vždy ma doma čakalo niečo teplé v hrnci a miesto ktoré som mohol volať domov. Bez ich podpory by som to nebol dokázal.

Moje posledné vd'aka patrí Veronike. Ďakujem! Ďakujem, za to že si to so mnou vydržala aj keď som ti doslova utiekol na opačnú stranu zeme. Za to, že si mi bola oporou, aj keď už sa mi nechcelo ďalej. Verím, že toto už je posledná prekážka, ktorej sa zbavujem na ceste k spoločnej budúcnosti.

List of publications and author's share

Zeman, Michal, Pavol Bárdy, Veronika Vrbovská, Pavel Roudnický, Zbyněk Zdráhal, Vladislava Růžičková, Jiří Doškař, and Roman Pantůček. 'New genus *Fibralongavirus* in *Siphoviridae* phages of *Staphylococcus pseudintermedius*'. *Viruses* 11, no. 12 (2019): 1143.

<https://doi.org/10.3390/v11121143>.

MZ under the supervision of his supervisor designed the study. MZ isolated phages and experimentally investigated their characteristics. Revision, analysis, and integration of partial results from co-authors were done by MZ. MZ wrote an article draft and revised its text with co-authors' suggestions.

Zeman, Michal, Ivana Mašlaňová, Adéla Indráková, Marta Šiborová, Kamil Mikulášek, Kamila Bendíčková, Pavel Plevka, Veronika Vrbovská, Zbyněk Zdráhal, Jiří Doškař and Roman Pantůček. '*Staphylococcus sciuri* bacteriophages double-convert for staphylokinase and phospholipase, mediate interspecies plasmid transduction, and package *mecA* gene'. *Scientific Reports* 7, no. 1 (2017): 46319.

<https://doi.org/10.1038/srep46319>.

MZ with his supervisor designed the study. MZ described phages on a molecular level with a focus on the genome of phages. MZ integrated and interpreted obtained results. MZ wrote an article and revised it during rounds of revisions.

Vrbovská, Veronika, Ivo Sedláček, Michal Zeman, Pavel Švec, Vojtěch Kovařovic, Ondrej Šedo, Monika Laichmanová, Jiří Doškař, and Roman Pantůček. 'Characterization of *Staphylococcus intermedius* group isolates associated with animals from Antarctica and emended description of *Staphylococcus delphini*'. *Microorganisms* 8, no. 2 (2020): 204.

<https://doi.org/10.3390/microorganisms8020204>.

MZ assembled genomes used in this article for further analysis. Comparative genomics and visualisation of data were done by MZ. The presence of mobile genetic elements and their characterisation was done by MZ. MZ wrote part of the draft.

Nováková, Dana, Pavel Švec, Michal Zeman, Hans-Jürgen Busse, Ivana Mašlaňová, Roman Pantůček, Stanislava Králová, Lucie Křištofová, and Ivo Sedláček. '*Pseudomonas leptonychotis* sp. nov., isolated from Weddell seals in Antarctica'. *International Journal of Systematic and*

Evolutionary Microbiology, 70, no. 1 (2020): 302–8.

<https://doi.org/10.1099/ijsem.0.003753>.

MZ designed sequencing primers for the *gyrB* gene and sequenced that gene. MZ prepared whole-genome sequencing data and assembled the draft genome. Phylogenetic analyses based on core gene set and overall genome relatedness index was done by MZ, similarly to the annotation of genes of interest. MZ wrote part of the article dealing with genomics and made the genome publicly available.

Original research articles not connected to this thesis:

Švec, Pavel, Marcel Kosina, Michal Zeman, Pavla Holočová, Stanislava Králová, Eva Němcová, Lenka Micenková, Urvashi, Vipin Gupta, Utkarsh Sood, Rup Lal, Suresh Korpole and Ivo Sedláček. ‘*Pseudomonas karstica* sp. nov. and *Pseudomonas spelaei* sp. nov., isolated from calcite moon-milk deposits from caves’. *International Journal of Systematic and Evolutionary Microbiology*, 70, no. 9 (2020): 5131–40.

<https://doi.org/10.1099/ijsem.0.004393>.

MZ processed sequencing data and assembled draft genomes. Phylogenetic analyses based on core gene set and overall genome relatedness index was done by MZ. MZ advised on the remaining phylogenetic analyses. MZ wrote part of the article dealing with genomics and made the genome publicly available.

Sedláček, Ivo, Roman Pantůček, Michal Zeman, Pavla Holočová, Ondrej Šedo, Eva Staňková, Pavel Švec, Stanislava Králová, Petra Vídeňská, Lenka Micenková, Urvashi, Suresh Korpole, Rup Lal. ‘*Hymenobacter terrestris* sp. nov. and *Hymenobacter lapidiphilus* sp. nov., isolated from regoliths in Antarctica’. *International Journal of Systematic and Evolutionary Microbiology*, 70, no. 12 (2020): 6364–72.

<https://doi.org/10.1099/ijsem.0.004540>.

MZ pre-processed sequencing data and assembled draft genomes. Phylogenetic analyses based on core gene set and overall genome relatedness index was done by MZ. MZ wrote part of the article dealing with genomics and made the genome publicly available.

Original research article in preparation:

Zeman, Michal, Kristína Oremová, Pavol Bárdy, Veronika Vrbovská, Pavel Roudnický, Zbyněk Zdráhal, and Roman Pantůček. ‘Promising phage vB_SpsH_40 for veterinary phage therapy of *S. pseudintermedius*’.

Contents

List of abbreviations	17
1 Introduction	18
1.1 Phage therapy	19
1.1.1 Application of phages in veterinary medicine.....	20
1.2 <i>Staphylococcus intermedius</i> group (SIG).....	25
1.3 <i>Staphylococcus pseudintermedius</i>	26
1.4 Phages of <i>Staphylococcus pseudintermedius</i>	28
2 Research aims	30
3 Methodology	31
3.1 Phage isolation.....	31
3.2 Bacterial cultures and phage origin.....	32
3.3 Phage propagation and purification.....	33
3.4 Deposition of biological material.....	33
3.5 DNA extraction	33
3.6 DNA restriction analysis	34
3.7 Genome analysis	34
3.8 Phylogenetic analysis.....	36
3.9 Polymerase chain reactions.....	37
3.10 Phage transduction and relative quantification of bacterial genes in phage particles.....	37
3.11 Polyacrylamide gel electrophoresis	38
3.12 Filter-aided sample preparation for mass spectrometry and LC- MS/MS Analysis	38
3.13 Optical microscopy.....	39
3.14 Electron and cryo-electron microscopy.....	39
3.15 Image analysis.....	40
4 Results and discussion	41

CONTENTS

4.1	Isolation of phages from the environment	41
4.2	Phage vB_SpsS_QT1 and a new genus of phages	43
4.2.1	Growth characteristics of phage QT1	43
4.2.2	Virion morphology of phages QT1 and 2638A.....	44
4.2.3	Reclassification of the propagating strain <i>Staphylococcus aureus</i> 2854 for phage 2638A as <i>Staphylococcus pseudintermedius</i> and phage host range	45
4.2.4	Phage structural proteins.....	46
4.2.5	QT1 genome description	48
4.2.6	Taxonomical classification and proposal of new genus <i>Fibralongavirus</i>	53
4.2.7	Genome Description of Propagating Strain for Phage QT1	56
4.3	Phage vB_SpsH_40 as therapeutical phage for <i>S. pseudintermedius</i> infections.....	57
4.3.1	Growth characteristics and host range of phage 40	57
4.3.2	Morphology of phage 40	58
4.3.3	Structural proteins of phage 40	60
4.3.4	The genome of phage 40.....	61
4.3.5	Classification of phage 40 into a taxonomical group	66
4.3.6	Description of propagating strain 253 for phage 40	69
4.4	Prophages in <i>Staphylococcus delphini</i> from Antarctic penguins	73
4.5	Phages and transfer of mobile genetic elements in <i>Staphylococcus sciuri</i>	77
4.5.1	Horizontal transfer of pSTS7-like plasmid between <i>S. sciuri</i> and <i>S. aureus</i> strains	79
4.5.2	Packaging of <i>Staphylococcus sciuri</i> SCCmec element.....	79
4.6	Search for phage propagating strains in genus <i>Pseudomonas</i> .	80
5	Conclusion	81
6	Závěr	83

7	Reference list	85
8	Appendix	108
8.1	Appendix A.....	108
8.2	Appendix B.....	110
8.3	Appendix C.....	111
8.4	Appendix D.....	114
9	Author's publications	116

List of abbreviations

CCM –	Czech Collection of Microorganisms
CEITEC –	Central European Institute of Technology
CoPS –	Coagulase-positive staphylococci
CRISPR –	Clustered regularly interspaced short palindromic repeats
DSMZ –	German Collection of Microorganisms and Cell Cultures
HER –	the Félix d'Hérelle Reference Center for bacterial viruses
LC-MS/MS –	Liquid chromatography and tandem mass spectrometry
LMDM –	the Laboratory of microbial molecular diagnostics
LTR –	Long terminal repeats
MALDI-TOF MS –	Matrix-assisted laser desorption/ionization mass spectrometry
MRSP –	Methicillin-resistant strains of <i>S. pseudintermedius</i>
NCBI –	National Center for Biotechnology Information
PFGE –	Pulsed-field gel electrophoresis
PCR –	Polymerase chain reaction
PCR-RFLP –	Polymerase chain reaction-restriction fragment length polymorphism
SDS-PAGE –	Sodium dodecyl sulphate–polyacrylamide gel electrophoresis
SIG –	Staphylococcus intermedius group
TSA –	Tryptone soya agar
TSB –	Tryptone soya broth
WGS –	Whole-genome shotgun

1 Introduction

Staphylococcus pseudintermedius is a natural commensal bacterium that lives on the skin or other surfaces of human companion animals. When the immunity of these animals is compromised by e.g. environmental stress this opportunistic pathogen might lead to severe complications and further degrade their health. But as those animals are in contact with their owners, an infection might spread to owners as well (Gómez-Sanz et al., 2013). This underlines the importance of this bacterial species not just as a valid veterinary target but also as a target for human medicine.

Some strains of *S. pseudintermedius* are equipped with several virulence factors that promote inflammation and make an infection more serious (Bannoehr and Guardabassi, 2012). Besides, strains resistant to multiple drugs are becoming more prevalent. Multidrug-resistant *Staphylococcus aureus* is a serious threat in human medicine and outbreaks of multidrug-resistant *S. pseudintermedius* were also observed. *S. pseudintermedius* is with its prevalence between animals, virulence potential and growing insusceptibility to antibiotics the *S. aureus* of the animal world.

Treatment of resistant bacteria is becoming ever more difficult. The discovery of new and improvement of the existing antibiotics is a laborious and time-consuming process. We have more than 100 different classes of antibiotics at our hands. At the time of writing, there are more than 11.000 entries for bacteriophages that have their genome sequenced (NCBI Resource Coordinators, 2018). Bacteriophages (or phages in short) are the most abundant entities on our planet, and they are natural predators of bacteria. The application of phages to treat bacterial infections is called phage therapy. Phage therapy is one of the answers to our growing need for new antimicrobials. Phages can multiply at the site of the infection and their host spectrum is often narrow, represented by a small number of strains. This high specificity means that normal microflora would not be destroyed as it would be if we had used broad-spectrum antibiotics.

This is the reason why this work focuses on isolation and description of phages that might be used to treat *S. pseudintermedius* infections.

1.1 Phage therapy

Phage therapy is the use of bacteriophages (viruses that lyse bacteria) to treat bacterial infections. Bacteriophages were discovered a long time ago by Twort (Twort, 1915), and from the very beginning, people think about how to use them against bacterial infections (Chanishvili, 2012). Insufficient knowledge of phage biology led phage therapy into recession, however, phages became a model organism for molecular biology (Campbell, 2003). Only after DNA sequencing and electron microscopy become more accessible by scientists, phage therapy had seen a renaissance. Especially in the last 20 years, there is an increased interest in the molecular characterisation of phages. This interest is motivated partially by the rise in antibiotic resistance of bacteria, to which phages offer an alternative treatment (Lin et al., 2017).

At the time of writing, there are 7 active clinical studies based on the phage therapy listed at The National Institutes of Health clinical trials (ClinicalTrials.gov, 2021). Interest in this type of research is underlined with studies funded by U.S. Food & Drug Administration and US Army (Voelker, 2019; Duplessis and Biswas, 2020). But the use of phages does not limit to whole particles. Phages are a source of biotechnologically exploitable bactericidal enzymes sometimes called enzybiotics (Drulis-Kawa et al., 2015). One of the most recent technologies is the use of genetically modified phages to deliver antibacterial macromolecules into bacteria or vaccinate macroorganisms where they were delivered (Clark and March, 2006).

Phages also have a huge impact on the physiology and ecology of microorganisms as they contribute to horizontal gene transfer and are able of lysogenic conversion (Chibani-Chennoufi et al., 2004; Xia and Wolz, 2014). Phages that transfer genes are undesirable when they are considered for medical treatment. This is the reason why the scientific community predominantly focus on the characterisation of strictly virulent phages.

1.1.1 Application of phages in veterinary medicine

Bacterial infections are causing problems for humans and animals alike. Considering this, phage therapy is a suitable approach in veterinary medicine (Johnson et al., 2008). The use of phages or their proteins in agriculture has several benefits. The improved health of raised animals is an obvious one that enhances the quality of their life. The advantage of having healthy animals turns into better food safety of meat products made from these animals. European Union reports campylobacteriosis and salmonellosis as the most frequent bacterial diseases acquired from animals (Figure 1) (European Food Safety Authority and European Centre for Disease Prevention and Control (EFSA and ECDC), 2019). Healthy animals improve the efficiency of feed conversion and have reduced mortality. Therefore, the phage therapy could have a positive economic impact. Limiting animal pathogens help to reduce zoonotic transfer from animals to humans, especially in domestic and companion animals.

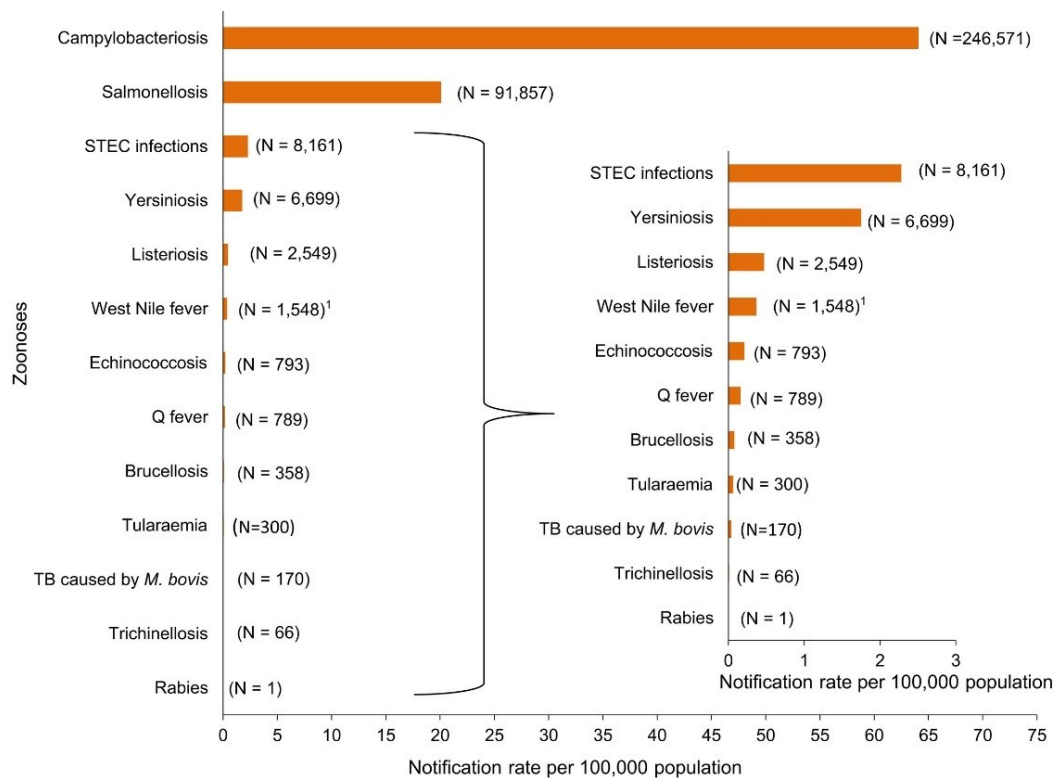


Figure 1 The reported number of cases for human zoonoses in the European Union in the year 2018. The image is used from The European Union One Health 2018 Zoonoses Report. ¹Exception: West Nile fever where the total number of cases was used.

Phages might be used even indirectly for preserving the pet food or disinfection of enclosures for livestock animals.

Phages had been isolated against many bacteria causing various diseases in livestock. Some pathogens are shared across several animal species and broad-host-range phages isolated against one bacterial species in one animal might work against the same bacterial species in a different animal. Such bacteria are *Escherichia coli*, *Salmonella* and *Staphylococcus* which are readily found in poultry, swine, and cattle.

E. coli is a very heterogeneous species with some strains causing serious diseases. A well-known representative is Shiga toxin-producing *E. coli*. Several studies readily isolated phages against these strains (Dini and De Urraza, 2010; Niu et al., 2012; Litt et al., 2018). Where previous studies have isolated phages of cattle origin (minced meat, faecal samples, water samples from the farm), recent article isolated phages from goat faeces that might be used to tackle asymptotically carriage in ruminants (Lennon et al., 2020). Skaradzińska et al. had shown that it is possible to isolate as much as 22 phages against extended-spectrum β -lactamase and AmpC β -lactamase producing *E. coli* from pig and turkey farms (Skaradzińska et al., 2017). Other authors conclude that the addition of phages into the feed promote growth and reduce enterotoxigenic *E. coli* concentrations in pigs (Cha et al., 2012; Yan et al., 2012). The improved survival, reduced manifestations of the disease, and lower numbers of enteropathogenic *E. coli*, were detected in piglets and lambs when phages were applied before the onset of diarrhoea (Smith and Huggins, 1983). Rabbits which are both companion animals and a source of meat often serve as an experimental model organism for infections common in different organisms. Rabbits that were orally infected with pathogenic *E. coli* were cured by oral administration of bacteriophage with minimal impact on the caecal microbiota (Zhao et al., 2017).

Salmonella spp. are causing salmonellosis in many different animals, as well as humans. *Salmonella* phages were able to control salmonellosis caused by serovars enterica and typhimurium in broiler chickens (Atterbury et al., 2007). Atterbury et al. in their study found out that phages are a suitable biocontrol agent against *Salmonella* on the broiler chicken skin (Atterbury et al., 2020). Phage therapy reduced bacterial load by one order of magnitude in market-weight swine (Wall et al., 2010). Challenged pigs have reduced caecal and ileal *Salmonella* counts after application of phage cocktail. After a challenge of weaned pigs by *Salmonella* and application of different phage cocktails, Seo et al. observed a reduced level of *Salmonella* shedding in faeces up to the 8th day post-infection when

there was no *Salmonella* in phage treated group (Seo et al., 2018). There was a drop in the Enterobacteriaceae family (include *Salmonella* spp. and *E. coli*) in the intestine microbiome of phage-cured pigs, and no significant negative impacts on the normal intestinal microflora were observed.

Staphylococcal phage SA was isolated on a bovine mastitis strain and was shown to be active in a wide range of pH and temperatures (Hamza et al., 2016). *S. aureus* from cow mastitis was eliminated by phages ϕ SA012 and ϕ SA039 in mice model (Iwano et al., 2018). Gill et al. have tested the effect of Staphylococcus phage K on mammary glands infection caused by *S. aureus* (Gill et al., 2006). Results of this field trial on subclinical mastitis were rather negative. A small number of phage-treated udder quarters improved but it was not statistically significant. They also report that the survival of phage inside the gland was limited. In a different case (Verstappen et al., 2016), the authors tested *in vitro*, *in vivo* and *ex vivo* efficacy of phages K and P68 on MRSA infection in pigs. *In vitro* they detected superb efficiency, but *in vivo* and *ex vivo* phages were unable to decrease MRSA counts when compared to antibiotic active against MRSA. Apart from the mastitis of cattle, phages were isolated against *S. aureus* causing goat mastitis (Mishra et al., 2014). Staphylococcal chronic osteomyelitis in rabbits was cured by a cocktail of seven virulent bacteriophages (Kishor et al., 2016). The use of these phages led to health improvement in the next two weeks.

Phages have been isolated for all major poultry pathogens (Żbikowska et al., 2020). It was shown that control of *Campylobacter jejuni* by phages did not have a significant effect on the gut microbiome in chickens and reduced *Campylobacter* counts (Richards et al., 2019). Most of the *Campylobacter* phages that are described come from chicken or poultry origin (Jäckel et al., 2019).

Clostridium perfringens infection in chicken was controlled by a mix of two phages and bacteriocin (Heo et al., 2018). Five phages were isolated from poultry farms and processing plants and were prepared into phage cocktail INT-401 that was able to control active *C. perfringens* infection more efficiently than toxoid vaccine (Miller et al., 2010). A virulent phage Susfortuna was also isolated from pig faeces against this pathogen (Pedersen et al., 2020).

There are no lytic phages identified so far that would infect *Actinobacillus pleuropneumonia*, a respiratory pathogen of pigs. This bacterium might be a valid target for the isolation of broad-host-range phages or phage enzymes that act against this pathogen.

Pasteurella multocida is a cause of haemorrhagic septicaemia in cattle, fowl cholera in poultry and rhinitis in pigs. Lytic phages and depolymerase isolated from the phage PHB02 had a protective effect on the survival of mice, although phages were more effective (Chen et al., 2018b, 2018c; Qureshi et al., 2018). Patented phage Pas-MUP-1 shows a dose-dependent reduction of *P. multocida* infection and downregulation of inflammatory responses in swine cells (Park et al., 2020).

Vibrio cholerae infected rabbits were successfully treated by single phage vB_VchoP_1 and the authors did not recover any phage-resistant mutants (Bhandare et al., 2019). Similar results were achieved when the cocktail of three phages was administered to infant mice and infant rabbits (Yen et al., 2017).

Major fish pathogens *Aeromonas salmonicida* (Kim et al., 2015; Silva et al., 2016) and *Aeromonas hydrophila* (Akmal et al., 2020), were treated with a single dose of a single phage. Mortality was reduced in groups treated with phages when compared to untreated controls.

Several studies show promising results in the treatment of *Paenibacillus larvae*, an important honeybee pathogen. When phages were used as a prophylactic measure or as a post-treatment, honeybees were protected from the infection of *P. larvae* (Ghorbani-Nezami et al., 2015; Yost et al., 2016). The application of phages did not affect standard bee death rates (Brady et al., 2017).

Companion animals are another target for phage therapy, which shows promising results when used to treat *Pseudomonas aeruginosa* ocular infection and otitis in dogs (Hawkins et al., 2010; Santos et al., 2011). Treatment of uropathogenic *E. coli* in cats and dogs shows that 94% out of 53 tested bacterial strains were sensitive to at least one of naturally occurring phages (Freitag et al., 2008).

Pet owners and veterinarians are in favour of phage therapy (Rhys-Davies and Ogden, 2020). It seems that it is possible to isolate phages against the majority of pathogens that cause problems in a wide range of animals. The animal rumen microbiome is a promising source of phages (Gilbert et al., 2020). For isolation of phages important in human phage therapy sewage water (Mattila et al., 2015), sewers leading from a hospital (Nikkhahi et al., 2017) or rivers (Bhetwal et al., 2017) are often a source of new phages. Apart from the basic research done on isolation and description of phages, there is a transfer of technologies to applied science and a large number of phage-based products are already

INTRODUCTION

available to the public (Table 1). Several companies offer phage solutions tailored to the requirements of a customer instead of a premade product.

Table 1 List of currently available phage products for the treatment of infections caused by veterinary pathogens. Listed are only products that use active phage particles. Products are grouped by producing company.

Name of the product	Bacterial targets	Company	Country
Stafal®	<i>Staphylococcus aureus</i>	Bohemia Pharmaceuticals, s.r.o.	Czech republic
Staphage Lysate (SPL)®	<i>Staphylococcus aureus</i>	DELMONT LABORATORIES	Pennsylvania, USA
Enko Bacteriophage	<i>Staphylococcus spp., Shigella spp., E. coli, Salmonella</i>	Eliava BioPreparations	Georgia
FERSISI BACTERIOPHAGE	<i>Staphylococcus and Streptococcus spp.</i>	Eliava BioPreparations	Georgia
Intesti bacteriophage	<i>Shigella spp., Salmonella, Escherichia coli, Proteus spp., Staphylococcus aureus, Pseudomonas aeruginosa, Enterococcus faecalis</i>	Eliava BioPreparations	Georgia
Pyo bacteriophage	<i>Staphylococcus aureus, Streptococcus spp., E.coli, Pseudomonas aeruginosa, Proteus spp.</i>	Eliava BioPreparations	Georgia
SES Bacteriophage	<i>Staphylococcus spp., Streptococcus spp., E. coli</i>	Eliava BioPreparations	Georgia
Staphylococcal bacteriophage	<i>Staphylococcus aureus</i>	Eliava BioPreparations	Georgia
Secure Shield E1	<i>Escherichia coli</i>	FINKTEC GmbH	Germany
Ecolicide PX™	<i>Escherichia coli</i> O157:H7	Intralytix Inc.	Maryland, USA
Ecolicide®	<i>Escherichia coli</i> O157:H7	Intralytix Inc.	Maryland, USA
EcoShield PX™	<i>Escherichia coli</i> and Shiga toxin producing <i>E. coli</i>	Intralytix Inc.	Maryland, USA
ListPhage™	<i>Listeria monocytogenes</i>	Intralytix Inc.	Maryland, USA
ListShield™	<i>Listeria monocytogenes</i>	Intralytix Inc.	Maryland, USA
SalmoFresh™	<i>Salmonella enterica</i>	Intralytix Inc.	Maryland, USA
SalmoLyse®	<i>Salmonella enterica</i>	Intralytix Inc.	Maryland, USA
ShigaShield™	<i>Shigella spp.</i>	Intralytix Inc.	Maryland, USA
PHAGESTAPH	<i>Staphylococcus aureus</i>	JSC Biochimpharm	Georgia
PHAGYO	<i>Streptococcus, Staphylococcus, E.Coli, Pseudomonas aeruginosa, Proteus</i>	JSC Biochimpharm	Georgia
Septaphage®	<i>Shigella, Salmonella, E.coli, Proteus, Staphylococcus, Pseudomonas, Enterococcus</i>	JSC Biochimpharm	Georgia
TRAVELPHAGE™	<i>Shigella, Salmonella, E. Coli, Proteus, Staphylococcus, Pseudomonas, Enterococcus</i>	JSC Biochimpharm	Georgia

Table 1 – (continued) List of currently available phage products for the treatment of infections caused by veterinary pathogens. Listed are only products that use active phage particles. Products are grouped by producing company.

Name of the product	Bacterial targets	Company	Country
Complex pyobacteriophage	<i>Staphylococcus</i> , <i>Enterococcus</i> , <i>Streptococcus</i> , <i>Pseudomonas aeruginosa</i> , <i>Klebsiella spp.</i> , enteropathogenic <i>Escherichia coli</i> , <i>Proteus spp.</i>	Microgen	Russia
Dysentery polyvalent bacteriophage	<i>Shigella flexneri</i> , <i>Shigella sonnei</i>	Microgen	Russia
E. coli bacteriophage	enterotoxigenic <i>Escherichia coli</i>	Microgen	Russia
E.coli-Proteus bacteriophage	<i>Proteus vulgaris</i> , <i>Proteus mirabilis</i> , <i>Escherichia coli</i>	Microgen	Russia
Intesti-bacteriophage	<i>Shigella spp.</i> , <i>Salmonella spp.</i> , enteropathogenic <i>Escherichia coli</i> , <i>Proteus spp.</i> , <i>Enterococcus</i> , <i>Staphylococcus</i> , <i>Pseudomonas aeruginosa</i>	Microgen	Russia
Sextaphag® polyvalent pyobacteriophage	<i>Staphylococcus</i> , <i>Streptococcus</i> , <i>Proteus spp.</i> , <i>Pseudomonas aeruginosa</i> , enteropathogenic <i>Escherichia coli</i> , <i>Klebsiella pneumoniae</i>	Microgen	Russia
Bronchophage Vet	21 respiratory disease associated bacterial species	Micromir	Russia
Phagovet	18 bacteria associated with diseases at farming broilers or egg-laying hens	Micromir	Russia
Vetagyn	<i>Escherichia coli</i> , <i>Enterococcus faecalis</i> , <i>Klebsiella pneumoniae</i> , <i>Pseudomonas aeruginosa</i> , <i>Proteus vulgaris</i> , <i>Staphylococcus aureus</i> , <i>Streptococcus pyogenes</i>	Micromir	Russia
Intestifag®	<i>Shigella flexneri</i> , <i>Shigella sonnei</i> , <i>Salmonella enterica</i> , <i>Escherichia coli</i> , <i>Pseudomonas aeruginosa</i> , <i>Proteus vulgaris</i> , <i>Proteus mirabilis</i> , <i>Enterococcus faecalis</i> , <i>Staphylococcus aureus</i>	NeoProbioCare Inc.	Ukraine
Pyofag®	<i>Streptococcus pyogenes</i> , <i>Staphylococcus aureus</i> , <i>Escherichia coli</i> , <i>Pseudomonas aeruginosa</i> , <i>Proteus vulgaris</i> , <i>Proteus mirabilis</i>	NeoProbioCare Inc.	Ukraine
SniPha 360 Bacteriophage	<i>Streptococcus pyogenes</i> , <i>Staphylococcus aureus</i> , <i>Escherichia coli</i> , <i>Pseudomonas aeruginosa</i> , <i>Proteus spp.</i>	Phage24	Germany
Bafador®	<i>Pseudomonas</i> , <i>Aeromonas</i>	Proteon Pharmaceuticals	Poland
Bafasal®	<i>Salmonella</i>	Proteon Pharmaceuticals	Poland

1.2 Staphylococcus intermedius group (SIG)

S. pseudintermedius (Devriese et al., 2005) belong to the group of staphylococci that was excluded from the *Staphylococcus intermedius* complex (Hájek, 1976). Other members of this group are *Staphylococcus delphini* (Sasaki et al., 2007), *Staphylococcus cornubiensis* (Murray et al., 2018), and *Staphylococcus ursii* (Perreten et al., 2020). This group is commonly isolated from animals and all members are considered opportunistic pathogens. Their pathogenicity is not limited only to animals and the rising number of human infections caused by SIG is detected (Yarbrough et al., 2018), underlining their zoonotic potential.

Staphylococci were and still are divided by the presence of coagulase or clumping factor. Coagulase-positive staphylococci (CoPS) used to

be often classified as *S. aureus*. While this assumption works well for *Staphylococcus saprophyticus*, *Staphylococcus epidermidis* and *Staphylococcus lugdunensis* that are associated with veterinary infections, SIG members represent an exception to this rule (Pottumarthy et al., 2004). Routine clinical diagnostics of staphylococci often ends with a result of coagulase-positive/negative *Staphylococcus*. Phenotypic methods are not sensitive enough to distinguish between different SIG. Only *S. intermedius* might be distinguished from other SIG by negative arginine dihydrolase reaction and utilization of β -gentiobiose (Sasaki et al., 2007). But this was proven before the discovery of *S. cornubiensis* and *S. ursii*, in whose production of acid from β -gentiobiose was not tested. Routine diagnostic laboratories currently rely on the fact that SIG species other than *S. pseudintermedius* are virtually absent in dogs. If the patient was in close contact with animals and shows signs of CoPS infection, diagnostics have to include molecular methods for correct diagnosis and surveillance.

1.3 *Staphylococcus pseudintermedius*

This bacterial species was first recognised in 2005 (Devriese et al., 2005) and is considered one of the major pathogens in dogs causing mostly dermatitis and otitis (van Duijkeren et al., 2011). It is part of skin microflora and lives on mucous membranes (Ma et al., 2020) but in some cases, it might turn into a pathogen. The most notable pathologies are pyoderma (Bajwa, 2016), otitis externa (Bugden, 2013) and urinary tract infections (McMeekin et al., 2017).

Methicillin-resistant strains of *S. pseudintermedius* (MRSP) are being identified in veterinary ambulances (Haenni et al., 2014; Melter et al., 2017) and officials are starting to acknowledge raising resistance to antibiotics in bacteria (Laxminarayan et al., 2016). These MRSP have a weaker response to all β -lactam antibiotics, and there is a concern that by wide use of human antibiotics, an increase in resistance of MRSP and MRSA might be expected. MRSP is not a direct concern for humans, although infections in form of endocarditis (Riegel et al., 2011), systemic infections (Blondeau et al., 2020; Kitagawa et al., 2021), and skin-related infections - mostly foot ulcers (Lozano et al., 2017; Gagetti et al., 2020) were reported in older or immunocompromised patients. The main risk of excessive use of systemic antibiotics on MRSP is that *S. aureus* living on such animals might become resistant to antibiotics, and then spreads

to their human owners. The horizontal transfer of resistance genes is also a major concern in this case.

S. pseudintermedius was isolated from several animals other than a dog, however, suborder Caniformia is its primal niche. Its first isolate that became type strain originates from the cat sample (Devriese et al., 2005). Authors also describe isolates from a dog, parrot, and horse, although infections in horses are not very common (Ruscher et al., 2009; Haenni et al., 2010). *S. pseudintermedius* was commonly isolated from wild foxes and might lead to fatal infections (Guardabassi et al., 2012; Iwata et al., 2018). Cats are carrying less *S. pseudintermedius* when compared to dogs with differences between domestic and feral cats (Abraham et al., 2007; Hanselman et al., 2009; Hariharan et al., 2011). Recently *S. pseudintermedius* was isolated from Weddell seals from Antarctica (Vrbovská et al., 2020).

In routine diagnostics, physiological tests are not specific enough to discriminate between SIG species. Molecular methods are capable of classification on the species level. Four widely used techniques are used: PCR-RFLP where *pta* gene is amplified by PCR and further restricted by MboI endonuclease (Bannoehr et al., 2009), rep-PCR fingerprinting relying on amplification with (GTG)₅ primer (Švec et al., 2010), MALDI-TOF MS where mass spectra of expressed proteins of whole cells are compared to known profiles (Decristophoris et al., 2011), and multiplex PCR (Sasaki et al., 2010). *S. intermedius* formerly isolated from dogs should be considered *S. pseudintermedius*. Older canine *S. aureus* isolates or isolates from wounds caused by dogs also require caution when evaluated (Kempker et al., 2009).

Shampooing and debridement are usual ways how to treat infections on the surface of animal skin. Pyoderma responds well to topical chlorhexidine or iodine-based treatment if the owner and pet are compliant with the washing routine. The treatment of MRSP is complicated by its resistance to β -lactams. Topical use of antimicrobials is always preferred to systemic use in these cases (Morris et al., 2017). Antiseptics that use chlorhexidine and fusidic acid as an active ingredient are commonly used to decontaminate the coat of MRSP infected animal. When systematic therapy is needed antibacterials have to be selected according to microbial susceptibility test results. Some authors suggest that amoxicillin/clavulanic acid and first-generation cephalosporins should be antibiotics of the first choice for MRSP infections (Wegener et al., 2020). The use of bacterin - a suspension of killed or attenuated bacteria used as a vaccine, was proven to be effective in recurrent pyoderma (Curtis et al.,

2006). However, no vaccines are commercially available for this bacterium.

European medicines agency published reflection paper where phage therapy and use of enzybiotics are considered as alternative therapeutic strategies on how to battle MRSP infections (European Medicines Agency, 2011). Researchers already reacted to this need and isolated phages against *S. pseudintermedius*.

1.4 Phages of *Staphylococcus pseudintermedius*

Phages of *S. pseudintermedius* were observed in the past but were not described in detail (Overturf et al., 1991; Wakita et al., 2002). They were mostly used for phage typing of different staphylococcal strains. Nowadays, phages are considered as a potential treatment and having a completely sequenced genome of phage is one of the requirements for utilisation of phages in phage therapy (Pirnay et al., 2015).

At the time of writing, there are twenty genomes of phages that were isolated against *S. pseudintermedius*. All of them belong to the family *Siphoviridae* and are presumably temperate. All but one phage genomes were published in the last 5 years underlining the current interest in this topic. There are no specific *Herelleviridae* phages active against *S. pseudintermedius*. However, phages ν B_SauM-fRuSau02 (Leskinen et al., 2017) and ϕ 812 (data not published) were observed to infect at least some *S. pseudintermedius* strains.

Phages SpT5, SpT152, SpT252, SpT99F3 are described in a thesis written by Breteau (Breteau et al., 2017). She aimed to isolate lytic phages from the environment and she was partially successful, isolating temperate phages. In the following research, she proposed mutational sites for the production of lytic Vir mutants of SpT5 based on the structure of the CI repressor.

Phages SN8, SN10, SN11 and SN13 were described by Moodley et al. (Moodley et al., 2019). These phages are active against methicillin-resistant *S. pseudintermedius*. Phages acted lytic on a small number of MRSP samples despite their temperate character. Interesting is that they were able to lyse even lysogenic strains. Their lysogenic modules recombined with modules from prophages during the infection of lysogens. The most similar phage to these phages is *S. aureus* virus 187 (Kwan et al., 2005).

Phages SP120, SP197 and SP276 were isolated from *S. pseudintermedius* by mitomycin C induction (Azam et al., 2019). Azam et al. have

analysed the mechanism of cell recognition by phage and found out that glycosylation of wall teichoic acid is essential for the protection of *S. aureus* against SP phages.

Wipf et al. described prophages ϕ SP15-1, ϕ SP119-1, ϕ SP119-2, ϕ SP119-3 from human and canine clinical isolate (Wipf et al., 2019).

Some *S. pseudintermedius* phages do not have any linked literature in the NCBI database and are probably in process of description. Those phages are namely: pSp_SNUABM-J (GenBank accession: MT423823), pSp_SNUABM-S (GenBank accession: MT423824), and vB_SpsM_WIS42 (GenBank accession: MN028536). Phage vB_SpsM_WIS42 that was isolated from river water. SpsM in its name stands for – '*S. pseudintermedius* Myoviriade phage' but according to its genome, it is a phage from the *Siphoviridae* family.

Phage 2638A was described as *S. aureus* phage (Kwan et al., 2005). In the study, they compared genome sequences of 27 *S. aureus* phages. Phage 2638A together with *S. aureus* virus 187 were deemed unique and did not cluster with other phages. The reason for this is, that the host strain for this phage is in fact *S. pseudintermedius*. Phage was even shown to be active against recent clinical strains of *S. pseudintermedius* (Zeman et al., 2019).

And finally, phage QT1 was described in 2019 (Zeman et al., 2019). The authors established a new genus *Fibralongavirus* around phages QT1 and 2638A. They share similar morphological features and are genetically related.

2 Research aims

This thesis is focused on tailed bacteriophages of the bacterium *S. pseudintermedius*. The research is multidisciplinary and crosses borders between microbiology, molecular biology, and bioinformatics to describe the biology of novel phages. The thesis has three main objectives and several minor goals.

1. Isolation of phages with a broad host spectrum against veterinary important pathogen *Staphylococcus pseudintermedius*
 - Find a suitable reservoir of phages
 - Acquire samples from various niches
 - Optimise isolation methods
 - Purify phage for further characterisation
2. Detailed physiological and molecular description of isolated phages
 - Propagation of phages to a high titre
 - Describe the growth characteristics
 - Susceptibility testing on host strains
 - Acquire morphological information
 - Analyse genome and proteome of phages
 - Describe the genome of propagating bacterial strain
3. Taxonomical classification of novel phages according to the current system
 - Find phages that are most similar to the ones described
 - Classify phages in relation to other known viruses at family, genus and species level

5 Conclusion

In this thesis, we describe two new phages vB_SpsS_QT1 and vB_SpsH_40 that are able to propagate on *S. pseudintermedius* strains.

The author of the thesis obtained samples from different habitats: dog bowls, living animals, animal enclosure, and wastewater plants. Several phage isolation protocols were used and one form of induction of prophages was developed and tested. The isolation of phages from the environment was successful but we isolated only temperate phages that are not suitable for phage therapy. Two *S. pseudintermedius* and two *S. sciuri* phages were described in detail. Genomes of their propagating strains were also extensively described. We established a new viral genus – *Fibralongavirus* in temperate *S. pseudintermedius* phages and described a new species for phage 40.

Phage QT1 is a temperate phage and is distinguishable by a single long tail fibre at the tip of the tail. Based on genome similarity most similar phage to phage QT1 is phage 2638A. We compared phages QT1 and 2638A at the genomic, proteomic, and morphological level. Host strain for phage 2638A was reclassified from *S. aureus* to *S. pseudintermedius*. Genus *Fibralongavirus* has been established by the author for phages of similar properties. The host strain for phage QT1 was described in detail and genomic analysis confirms its clinical character. Several haemolysins, enterotoxin, exfoliative toxin and plasmid-borne bacteriocin cytotoxic to mammalian cells were present in the genome of this host strain.

Phage 40 is a polyvalent phage that is able to lyse 72% of tested *S. pseudintermedius* strains. Different species than *S. pseudintermedius* that are of veterinary importance were also sensitive to phage 40. Phage 40 has a *Herelleviridae* morphology similar to other phages that belong to the subfamily *Twortvirinae* and is the most similar to phage Twort. Regarding nucleotide identity, phage 40 creates a new species in the genus *Twortvirus*. The description of phage Twort was amended as the true host for phage Twort is *Staphylococcus agnetis*, not *Staphylococcus hyicus*. Twenty-seven proteins were observed as structural in the mature virion of phage 40. The genome of phage 40 is 154 kbp long, has 14 kbp long long-terminal repeats and encode for 234 proteins. The genome is complex including the number of direct and indirect repeats and multiple introns and transposons. Several enzymes that are able to lyse bacterial cell wall were predicted. Propagating strain *S. pseudintermedius* 253

CONCLUSION

for phage 40 have been described but considering its genomic analysis, the strain originated from clinical material as seen on several virulence factors encoded in the genome. Mutants of strain 253 that are resistant to phage 40 were prepared and evident changes in phenotype were observed and described. Results suggest that phage 40 is able to persist inside the bacterial host in a pseudolysogenic state. Phage 40's broad spectrum and activity against additional animal staphylococci is interesting for veterinary research. This basic research and molecular description of phage 40 lay the foundation for its use in veterinary phage therapy.

Analysed *S. sciuri* phages are encoding bacterial virulence factors and are able to package and transduce mobile genetic elements to other staphylococcal species. The genome of phage ϕ 575 encoded genes for staphylokinase and phospholipase. The phage ϕ 879 was able to pack and transduce a plasmid that encodes tetracycline efflux protein and aminoglycoside adenylyltransferase. The phage ϕ 879 similarly packaged SCC-*mec* into its capsid. However, we did not observe any successful transduction of SCC*mec* element into recipient strains.

6 Závěr

Tato práce popisuje dva nové bakteriofágy vB_SpsS_QT1 a vB_SpsH_40, které jsou aktivní proti zvířecímu patogenu *S. pseudintermedius*.

Podářilo se nám získat vzorky z několika typů prostředí: žijící zvířata, misky na žrádlo, výběh zvířat a odpadová voda z čističek odpadních vod. Vyzkoušeli jsme několik protokolů na izolaci fágů a navrhli jsme jeden způsob indukce profágů. Po izolaci fágů z prostředí jsme získali pouze temperované fágy, které nejsou vhodné na použití ve fágové terapii. Podrobně byly popsány fágy bakterií *S. pseudintermedius* a *S. sciuri* a rovněž byly popsány genomy jejich pomnožovacích kmenů. V taxonomii mírných fágů *S. pseudintermedius* jsme založili nový rod *Fibralongavirus* a také jsme popsali nový druh patřící fágu 40.

Fág QT1 patří mezi temperované fágy a vyznačuje se přítomností jednoho dlouhého vlákna vycházejícího z konce bičíku. Při porovnání genomu fága QT1 s ostatními fágy se jako nejpodobnější jeví fág 2638A. Porovnali jsme tyto dva fágy na úrovni genomu, proteomu a morfologie a na základě porovnání byl hostitelský kmen fága 2638A přeřazen z druhu *S. aureus* na *S. pseudintermedius*. Popsali jsme nový druh *Fibralongavirus*, do kterého patří fágy s podobnými vlastnostmi. U pomnožovacího kmene fága QT1 jsme provedli detailní analýzu genomu, která potvrdila jeho klinický charakter. V genomu hostitelské bakterie jsme identifikovali geny kódující hemoliziny, endotoxiny, exfoliativní toxin a plazmidově kódovaný bakteriocin, který je cytotoxický pro savčí buňky.

Fág 40 je polyvalentní fág, který je schopný lyzovat 72 % testovaných kmenů *S. pseudintermedius*, a i jiné, veterinárně důležité druhy rodu *Staphylococcus*, se jeví být vůči němu citlivé. Fág 40 se nejvíce podobá fágu Twort a podobně jako ostatní fágy z podčeledi *Twortvirinae* patří morfologicky do čeledi *Herelleviridae*. Fág 40 bude zařazen jako nový druh rodu *Twortvirus*. Ověřili jsme, že hostitelem fága Twort není dříve označovaný druh *Staphylococcus hyicus*, ale *Staphylococcus agnetis*. Analýzou strukturních proteinů na hmotnostní spektrometrii jsme potvrdili přítomnost 27 proteinů ve zralém virionu fága 40. Genom tohoto fága je velký 154 kb a kóduje 234 genů. Na obou jeho koncích se nacházejí 14kb dlouhé koncové repetice. Genom je komplexní s množstvím přímých a obrácených repetit, introny a transpozony. Podářilo se nám detekovat několik enzymů, které mohou štěpit buněčnou stěnu. Pomnožovací kmen *S. pseudintermedius* 253 pro fága 40 se jeví být klinický s přihlédnutím

na přítomnost genů zvyšujících jeho virulenci. Podařilo se nám získat mutanty kmene 253 odolné k fágu 40 a popsat jejich odlišnosti ve fenotypu. Zdá se, že fág 40 může za určitých podmínek přežívat v genomu bakterií v pseudolyzogenním stavu. Pro veterinární výzkum a biotechnologické použití je široké spektrum hostitelů fága 40 a jeho schopnost cílit i na jiné zvířecí stafylokoky ideální. Tento základní výzkum a detailní molekulární popis fága 40 bude sloužit jako základ pro jeho další použití ve veterinární fágové terapii.

Analyzované fágy *S. sciuri* kódují bakteriální faktory virulence a jsou schopné transdukovat různé mobilní elementy na jiné stafylokokové druhy. Genom fága ϕ 575 kódoval geny pro stafylokinázu a fosfolipázu. Fág ϕ 879 byl schopen transdukovat plazmid, který kóduje aminoglykosid-adenyltransferázu a také protein tetracyklinové efluxní pumpy. Fág ϕ 879 je také schopen zabalit SCC*mec* kazetu do své kapsidy, avšak transdukce elementu SCC*mec* nebyla pozorována.

7 Reference list

- Abaev, I., Foster-Frey, J., Korobova, O., Shishkova, N., Kiseleva, N., Kopylov, P., et al. (2013). Staphylococcal Phage 2638A endolysin is lytic for *Staphylococcus aureus* and harbors an inter-lytic-domain secondary translational start site. *Appl. Microbiol. Biotechnol.* 97, 3449–3456. doi:10.1007/s00253-012-4252-4.
- Abedon, S. T. (2011). Lysis from without. *Bacteriophage* 1, 46–49. doi:10.4161/bact.1.1.13980.
- Abraham, J. L., Morris, D. O., Griffeth, G. C., Shofer, F. S., and Rankin, S. C. (2007). Surveillance of healthy cats and cats with inflammatory skin disease for colonization of the skin by methicillin-resistant coagulase-positive staphylococci and *Staphylococcus schleiferi* ssp. *schleiferi*. *Vet. Dermatol.* 18, 252–259. doi:10.1111/j.1365-3164.2007.00604.x.
- Ågren, J., Sundström, A., Håfström, T., and Segerman, B. (2012). Geenees: Fragmented Alignment of Multiple Genomes for Determining Phylogenomic Distances and Genetic Signatures Unique for Specified Target Groups. *PLoS ONE* 7, e39107. doi:10.1371/journal.pone.0039107.
- Akmal, M., Rahimi-Midani, A., Hafeez-ur-Rehman, M., Hussain, A., and Choi, T.-J. (2020). Isolation, Characterization, and Application of a Bacteriophage Infecting the Fish Pathogen *Aeromonas hydrophila*. *Pathogens* 9, 215. doi:10.3390/pathogens9030215.
- Andrews, S. (2019). Babraham Bioinformatics - FastQC A Quality Control tool for High Throughput Sequence Data. Available at: <https://www.bioinformatics.babraham.ac.uk/projects/fastqc/> [Accessed March 21, 2021].
- Armenteros, J. J. A., Tsirigos, K. D., Sønderby, C. K., Petersen, T. N., Winther, O., Brunak, S., et al. (2019). SignalP 5.0 improves signal peptide predictions using deep neural networks. *Nat. Biotechnol.* 37, 420–423. doi:10.1038/s41587-019-0036-z.
- Atterbury, R. J., Gigante, A. M., Rubio Lozano, M. de la S., Méndez Medina, R. D., Robinson, G., Alloush, H., et al. (2020). Reduction of *Salmonella* contamination on the surface of chicken skin using bacteriophage. *Virology* 17, 98. doi:10.1186/s12985-020-01368-0.

REFERENCE LIST

- Atterbury, R. J., Van Bergen, M. A. P., Ortiz, F., Lovell, M. A., Harris, J. A., De Boer, A., et al. (2007). Bacteriophage Therapy To Reduce Salmonella Colonization of Broiler Chickens. *Appl. Environ. Microbiol.* 73, 4543–4549. doi:10.1128/AEM.00049-07.
- Azam, A. H., Kadoi, K., Miyanaga, K., Usui, M., Tamura, Y., Cui, L., et al. (2019). Analysis host-recognition mechanism of staphylococcal kayvirus ϕ SA039 reveals a novel strategy that protects *Staphylococcus aureus* against infection by *Staphylococcus pseudintermedius* Siphoviridae phages. *Appl. Microbiol. Biotechnol.* 103, 6809–6823. doi:10.1007/s00253-019-09940-7.
- Bajwa, J. (2016). Canine superficial pyoderma and therapeutic considerations. *Can. Vet. J. Rev. Veterinaire Can.* 57, 204–206.
- Bannoehr, J., Franco, A., Iurescia, M., Battisti, A., and Fitzgerald, J. R. (2009). Molecular Diagnostic Identification of *Staphylococcus pseudintermedius*. *J. Clin. Microbiol.* 47, 469–471. doi:10.1128/JCM.01915-08.
- Bannoehr, J., and Guardabassi, L. (2012). *Staphylococcus pseudintermedius* in the dog: taxonomy, diagnostics, ecology, epidemiology and pathogenicity. *Vet. Dermatol.* 23, 253-e52. doi:https://doi.org/10.1111/j.1365-3164.2012.01046.x.
- Becker, S. C., Foster-Frey, J., Stodola, A. J., Anacker, D., and Donovan, D. M. (2009). Differentially conserved staphylococcal SH3b_5 cell wall binding domains confer increased staphylolytic and streptolytic activity to a streptococcal prophage endolysin domain. *Gene* 443, 32–41. doi:10.1016/j.gene.2009.04.023.
- Bellaousov, S., Reuter, J. S., Seetin, M. G., and Mathews, D. H. (2013). RNAstructure: web servers for RNA secondary structure prediction and analysis. *Nucleic Acids Res.* 41, W471–W474. doi:10.1093/nar/gkt290.
- Belley, A., Callejo, M., Arhin, F., Dehbi, M., Fadhil, I., Liu, J., et al. (2006). Competition of bacteriophage polypeptides with native replicase proteins for binding to the DNA sliding clamp reveals a novel mechanism for DNA replication arrest in *Staphylococcus aureus*. *Mol. Microbiol.* 62, 1132–1143. doi:10.1111/j.1365-2958.2006.05427.x.

- Ben Zakour, N. L., Beatson, S. A., van den Broek, A. H. M., Thoday, K. L., and Fitzgerald, J. R. (2012). Comparative Genomics of the *Staphylococcus intermedius* Group of Animal Pathogens. *Front. Cell. Infect. Microbiol.* 2. doi:10.3389/fcimb.2012.00044.
- Benešík, M., Nováček, J., Janda, L., Dopitová, R., Pernisová, M., Melková, K., et al. (2018). Role of SH3b binding domain in a natural deletion mutant of Kayvirus endolysin LysF1 with a broad range of lytic activity. *Virus Genes* 54, 130–139. doi:10.1007/s11262-017-1507-2.
- Besemer, J. (2001). GeneMarkS: a self-training method for prediction of gene starts in microbial genomes. Implications for finding sequence motifs in regulatory regions. *Nucleic Acids Res.* 29, 2607–2618. doi:10.1093/nar/29.12.2607.
- Bhandare, S., Colom, J., Baig, A., Ritchie, J. M., Bukhari, H., Shah, M. A., et al. (2019). Reviving Phage Therapy for the Treatment of Cholera. *J. Infect. Dis.* 219, 786–794. doi:10.1093/infdis/jiy563.
- Bhetwal, A., Maharjan, A., Shakya, S., Satyal, D., Ghimire, S., Khanal, P. R., et al. (2017). Isolation of Potential Phages against Multidrug-Resistant Bacterial Isolates: Promising Agents in the Rivers of Kathmandu, Nepal. *BioMed Res. Int.* 2017, 1–10. doi:10.1155/2017/3723254.
- Blondeau, L. D., Rubin, J. E., Deneer, H., Kanthan, R., Morrison, B., Sanche, S., et al. (2020). Persistent infection with *Staphylococcus pseudintermedius* in an adult oncology patient with transmission from a family dog. *J. Chemother.* 32, 151–155. doi:10.1080/1120009X.2020.1735142.
- Blouse, L., and Meekins, W. E. (1968). Isolation and use of experimental phages for typing *Staphylococcus aureus* isolates from sentry dogs. *Am. J. Vet. Res.* 29, 1817–1822.
- Brady, T. S., Merrill, B. D., Hilton, J. A., Payne, A. M., Stephenson, M. B., and Hope, S. (2017). Bacteriophages as an alternative to conventional antibiotic use for the prevention or treatment of *Paenibacillus* larvae in honeybee hives. *J. Invertebr. Pathol.* 150, 94–100. doi:10.1016/j.jip.2017.09.010.
- Breteau, M., Hodgson, D. A., Wellington, E. M. H., Moodley, A., and Vogensen, F. K. (2017). Study of *Staphylococcus pseudintermedius* phages: towards the development of phage therapy.

REFERENCE LIST

- Bugden, D. (2013). Identification and antibiotic susceptibility of bacterial isolates from dogs with otitis externa in Australia. *Aust. Vet. J.* 91, 43–46. doi:10.1111/avj.12007.
- Campbell, A. (2003). The future of bacteriophage biology. *Nat. Rev. Genet.* 4, 471–477. doi:10.1038/nrg1089.
- Candiano, G., Bruschi, M., Musante, L., Santucci, L., Ghiggeri, G. M., Carnemolla, B., et al. (2004). Blue silver: A very sensitive colloidal Coomassie G-250 staining for proteome analysis. *ELECTROPHORESIS* 25, 1327–1333. doi:10.1002/elps.200305844.
- Cernooka, E., Rumnieks, J., Tars, K., and Kazaks, A. (2017). Structural Basis for DNA Recognition of a Single-stranded DNA-binding Protein from Enterobacter Phage Enc34. *Sci. Rep.* 7, 15529. doi:10.1038/s41598-017-15774-y.
- Cha, S. B., Yoo, A. N., Lee, W. J., Shin, M. K., Jung, M. H., Shin, S. W., et al. (2012). Effect of Bacteriophage in Enterotoxigenic Escherichia coli (ETEC) Infected Pigs. *J. Vet. Med. Sci.* 74, 1037–1039. doi:10.1292/jvms.11-0556.
- Chanishvili, N. (2012). “Phage Therapy—History from Twort and d’Herelle Through Soviet Experience to Current Approaches,” in *Advances in Virus Research* (Elsevier), 3–40. doi:10.1016/B978-0-12-394438-2.00001-3.
- Chen, L., Zheng, D., Liu, B., Yang, J., and Jin, Q. (2016). VFDB 2016: hierarchical and refined dataset for big data analysis—10 years on. *Nucleic Acids Res.* 44, D694–D697. doi:10.1093/nar/gkv1239.
- Chen, S., Wang, Y., Chen, F., Yang, H., Gan, M., and Zheng, S. J. (2007). A Highly Pathogenic Strain of Staphylococcus sciuri Caused Fatal Exudative Epidermitis in Piglets. *PLoS ONE* 2, e147. doi:10.1371/journal.pone.0000147.
- Chen, S., Zhou, Y., Chen, Y., and Gu, J. (2018a). fastp: an ultra-fast all-in-one FASTQ preprocessor. *Bioinformatics* 34, i884–i890. doi:10.1093/bioinformatics/bty560.
- Chen, Y., Sun, E., Song, J., Yang, L., and Wu, B. (2018b). Complete Genome Sequence of a Novel T7-Like Bacteriophage from a Pasteurella

- multocida Capsular Type A Isolate. *Curr. Microbiol.* 75, 574–579. doi:10.1007/s00284-017-1419-3.
- Chen, Y., Sun, E., Yang, L., Song, J., and Wu, B. (2018c). Therapeutic Application of Bacteriophage PHB02 and Its Putative Depolymerase Against *Pasteurella multocida* Capsular Type A in Mice. *Front. Microbiol.* 9, 1678. doi:10.3389/fmicb.2018.01678.
- Chibani-Chennoufi, S., Bruttin, A., Dillmann, M.-L., and Brüssow, H. (2004). Phage-Host Interaction: an Ecological Perspective. *J. Bacteriol.* 186, 3677–3686. doi:10.1128/JB.186.12.3677-3686.2004.
- Christie, G. E., Matthews, A. M., King, D. G., Lane, K. D., Olivarez, N. P., Tallent, S. M., et al. (2010). The complete genomes of *Staphylococcus aureus* bacteriophages 80 and 80 α —Implications for the specificity of SaPI mobilization. *Virology* 407, 381–390. doi:10.1016/j.virol.2010.08.036.
- Chung, C.-H., Walter, M. H., Yang, L., Chen, S.-C., Winston, V., and Thomas, M. A. (2017). Predicting genome terminus sequences of *Bacillus cereus*-group bacteriophage using next generation sequencing data. *BMC Genomics* 18, 350. doi:10.1186/s12864-017-3744-0.
- Clark, J. R., and March, J. B. (2006). Bacteriophages and biotechnology: vaccines, gene therapy and antibacterials. *Trends Biotechnol.* 24, 212–218. doi:10.1016/j.tibtech.2006.03.003.
- ClinicalTrials.gov (2021). Available at: <https://clinicaltrials.gov/> [Accessed March 19, 2021].
- Curtis, C. F., Lamport, A. I., and Lloyd, D. H. (2006). Masked, controlled study to investigate the efficacy of a *Staphylococcus intermedius* auto-genous bacterin for the control of canine idiopathic recurrent superficial pyoderma. *Vet. Dermatol.* 17, 163–168. doi:10.1111/j.1365-3164.2006.00512.x.
- Daniel, A., Bonnen, P. E., and Fischetti, V. A. (2007). First Complete Genome Sequence of Two *Staphylococcus epidermidis* Bacteriophages. *J. Bacteriol.* 189, 2086–2100. doi:10.1128/JB.01637-06.
- Decristophoris, P., Fasola, A., Benagli, C., Tonolla, M., and Petrini, O. (2011). Identification of *Staphylococcus intermedius* Group by

REFERENCE LIST

- MALDI-TOF MS. *Syst. Appl. Microbiol.* 34, 45–51.
doi:10.1016/j.syapm.2010.11.004.
- Dehbi, M., Moeck, G., Arhin, F. F., Bauda, P., Bergeron, D., Kwan, T., et al. (2009). Inhibition of Transcription in *Staphylococcus aureus* by a Primary Sigma Factor-Binding Polypeptide from Phage G1. *J. Bacteriol.* 191, 3763–3771. doi:10.1128/JB.00241-09.
- Dempsey, R. M., Carroll, D., Kong, H., Higgins, L., Keane, C. T., and Coleman, D. C. (2005). Sau42I, a Bcgl-like restriction–modification system encoded by the *Staphylococcus aureus* quadruple-converting phage π 42. *Microbiology* 151, 1301–1311. doi:10.1099/mic.0.27646-0.
- Devriese, L. A., Vancanneyt, M., Baele, M., Vaneechoutte, M., De Graef, E., Snauwaert, C., et al. (2005). *Staphylococcus pseudintermedius* sp. nov., a coagulase-positive species from animals. *Int. J. Syst. Evol. Microbiol.* 55, 1569–1573. doi:10.1099/ijs.0.63413-0.
- Dini, C., and De Urraza, P. J. (2010). Isolation and selection of coliphages as potential biocontrol agents of enterohemorrhagic and Shiga toxin-producing *E. coli*(EHEC and STEC) in cattle: Selection of coliphages as biocontrol agents. *J. Appl. Microbiol.* 109, 873–887.
doi:10.1111/j.1365-2672.2010.04714.x.
- Doster, E., Lakin, S. M., Dean, C. J., Wolfe, C., Young, J. G., Boucher, C., et al. (2020). MEGARes 2.0: a database for classification of antimicrobial drug, biocide and metal resistance determinants in metagenomic sequence data. *Nucleic Acids Res.* 48, D561–D569.
doi:10.1093/nar/gkz1010.
- Drulis-Kawa, Z., Majkowska-Skrobek, G., and Maciejewska, B. (2015). Bacteriophages and Phage-Derived Proteins – Application Approaches. *Curr. Med. Chem.* 22, 1757–1773.
doi:10.2174/0929867322666150209152851.
- Duplessis, C. A., and Biswas, B. (2020). A Review of Topical Phage Therapy for Chronically Infected Wounds and Preparations for a Randomized Adaptive Clinical Trial Evaluating Topical Phage Therapy in Chronically Infected Diabetic Foot Ulcers. *Antibiotics* 9, 377.
doi:10.3390/antibiotics9070377.
- European Food Safety Authority and European Centre for Disease Prevention and Control (EFSA and ECDC) (2019). The European Union

- One Health 2018 Zoonoses Report. *EFSA J.* 17. doi:10.2903/j.efsa.2019.5926.
- European Medicines Agency (2011). Reflection paper on meticillin-resistant *Staphylococcus pseudintermedius*. *Eur. Med. Agency*. Available at: <https://www.ema.europa.eu/en/meticillin-resistant-staphylococcus-pseudintermedius> [Accessed March 20, 2021].
- Feldgarden, M., Brover, V., Haft, D. H., Prasad, A. B., Slotta, D. J., Tolstoy, I., et al. (2019). Validating the AMRFinder Tool and Resistance Gene Database by Using Antimicrobial Resistance Genotype-Phenotype Correlations in a Collection of Isolates. *Antimicrob. Agents Chemother.* 63, e00483-19, /aac/63/11/AAC.00483-19.atom. doi:10.1128/AAC.00483-19.
- Freitag, T., Squires, R. A., and Schmid, J. (2008). Naturally occurring bacteriophages lyse a large proportion of canine and feline uropathogenic *Escherichia coli* isolates in vitro. *Res. Vet. Sci.* 85, 1–7. doi:10.1016/j.rvsc.2007.09.004.
- Fu, L., Niu, B., Zhu, Z., Wu, S., and Li, W. (2012). CD-HIT: accelerated for clustering the next-generation sequencing data. *Bioinformatics* 28, 3150–3152. doi:10.1093/bioinformatics/bts565.
- Gagetti, P., Errecalde, L., Wattam, A. R., De Belder, D., Ojeda Saavedra, M., Corso, A., et al. (2020). Characterization of the First *mec A*-Positive Multidrug-Resistant *Staphylococcus pseudintermedius* Isolated from an Argentinian Patient. *Microb. Drug Resist.* 26, 717–721. doi:10.1089/mdr.2019.0308.
- Ghorbani-Nezami, S., LeBlanc, L., Yost, D. G., and Amy, P. S. (2015). Phage Therapy is Effective in Protecting Honeybee Larvae from American Foulbrood Disease. *J. Insect Sci.* 15, 84. doi:10.1093/jis-esa/iev051.
- Gilbert, R. A., Townsend, E. M., Crew, K. S., Hitch, T. C. A., Friedersdorff, J. C. A., Creevey, C. J., et al. (2020). Rumen Virus Populations: Technological Advances Enhancing Current Understanding. *Front. Microbiol.* 11. doi:10.3389/fmicb.2020.00450.
- Gill, J. J., Pacan, J. C., Carson, M. E., Leslie, K. E., Griffiths, M. W., and Sabor, P. M. (2006). Efficacy and Pharmacokinetics of Bacteriophage Therapy in Treatment of Subclinical *Staphylococcus aureus* Mastitis in

REFERENCE LIST

- Lactating Dairy Cattle. *Antimicrob. Agents Chemother.* 50, 2912–2918. doi:10.1128/AAC.01630-05.
- Gómez-Sanz, E., Torres, C., Lozano, C., and Zarazaga, M. (2013). High diversity of *Staphylococcus aureus* and *Staphylococcus pseudintermedius* lineages and toxigenic traits in healthy pet-owning household members. Underestimating normal household contact? *Comp. Immunol. Microbiol. Infect. Dis.* 36, 83–94. doi:10.1016/j.cimid.2012.10.001.
- Grazziotin, A. L., Koonin, E. V., and Kristensen, D. M. (2017). Prokaryotic Virus Orthologous Groups (pVOGs): a resource for comparative genomics and protein family annotation. *Nucleic Acids Res.* 45, D491–D498. doi:10.1093/nar/gkw975.
- Guardabassi, L., Schmidt, K. R., Petersen, T. S., Espinosa-Gongora, C., Moodley, A., Agersø, Y., et al. (2012). Mustelidae are natural hosts of *Staphylococcus delphini* group A. *Vet. Microbiol.* 159, 351–353. doi:10.1016/j.vetmic.2012.04.004.
- Gupta, S. K., Padmanabhan, B. R., Diene, S. M., Lopez-Rojas, R., Kempf, M., Landraud, L., et al. (2014). ARG-ANNOT, a New Bioinformatic Tool To Discover Antibiotic Resistance Genes in Bacterial Genomes. *Antimicrob. Agents Chemother.* 58, 212–220. doi:10.1128/AAC.01310-13.
- Gurevich, A., Saveliev, V., Vyahhi, N., and Tesler, G. (2013). QUASt: quality assessment tool for genome assemblies. *Bioinformatics* 29, 1072–1075. doi:10.1093/bioinformatics/btt086.
- Gutiérrez, D., Martínez, B., Rodríguez, A., and García, P. (2012). Genomic characterization of two *Staphylococcus epidermidis* bacteriophages with anti-biofilm potential. *BMC Genomics* 13, 228. doi:10.1186/1471-2164-13-228.
- Haenni, M., de Moraes, N. A., Châtre, P., Médaille, C., Moodley, A., and Madec, J.-Y. (2014). Characterisation of clinical canine meticillin-resistant and meticillin-susceptible *Staphylococcus pseudintermedius* in France. *J. Glob. Antimicrob. Resist.* 2, 119–123. doi:10.1016/j.jgar.2014.02.002.
- Haenni, M., Targant, H., Forest, K., Sévin, C., Tapprest, J., Laugier, C., et al. (2010). Retrospective Study of Necropsy-Associated Coagulase-Positive *Staphylococci* in Horses. *J. Vet. Diagn. Invest.* 22, 953–956. doi:10.1177/104063871002200617.

- Hájek, V. (1976). *Staphylococcus intermedius*, a New Species Isolated from Animals. *Int. J. Syst. Bacteriol.* 26, 401–408. doi:10.1099/00207713-26-4-401.
- Hamza, A., Perveen, S., Abbas, Z., and Ur Rehman, S. (2016). The Lytic SA Phage Demonstrate Bactericidal Activity against Mastitis Causing *Staphylococcus aureus*. *Open Life Sci.* 11, 39–45. doi:10.1515/biol-2016-0005.
- Hanselman, B. A., Kruth, S. A., Rousseau, J., and Weese, J. S. (2009). Coagulase positive staphylococcal colonization of humans and their household pets. *Can. Vet. J. Rev. Veterinaire Can.* 50, 954–958.
- Hariharan, H., Matthew, V., Fountain, J., Snell, A., Doherty, D., King, B., et al. (2011). Aerobic bacteria from mucous membranes, ear canals, and skin wounds of feral cats in Grenada, and the antimicrobial drug susceptibility of major isolates. *Comp. Immunol. Microbiol. Infect. Dis.* 34, 129–134. doi:10.1016/j.cimid.2010.05.001.
- Hawkins, C., Harper, D., Burch, D., Änggård, E., and Soothill, J. (2010). Topical treatment of *Pseudomonas aeruginosa* otitis of dogs with a bacteriophage mixture: A before/after clinical trial. *Vet. Microbiol.* 146, 309–313. doi:10.1016/j.vetmic.2010.05.014.
- Hedin, G., and Widerström, M. (1998). Endocarditis due to *Staphylococcus sciuri*. *Eur. J. Clin. Microbiol. Infect. Dis.* 17, 673–675. doi:10.1007/BF01708356.
- Heo, S., Kim, M. G., Kwon, M., Lee, H. S., and Kim, G.-B. (2018). Inhibition of *Clostridium perfringens* using Bacteriophages and Bacteriocin Producing Strains. *Food Sci. Anim. Resour.* 38, 88–98. doi:10.5851/kosfa.2018.38.1.88.
- Hiroshi, S., Hiroshi, H., Keiji, I., Taizo, H., Tohru, K., and G. Nigel, G. (1988). Role of the potential secondary structures in phage g4 origin of complementary dna strand synthesis. *Gene* 71, 323–330. doi:10.1016/0378-1119(88)90049-2.
- Iwano, H., Inoue, Y., Takasago, T., Kobayashi, H., Furusawa, T., Taniguchi, K., et al. (2018). Bacteriophage Φ SA012 Has a Broad Host Range against *Staphylococcus aureus* and Effective Lytic Capacity in a Mouse Mastitis Model. *Biology* 7, 8. doi:10.3390/biology7010008.

REFERENCE LIST

- Iwata, K., Kasuya, K., Takayama, K., Nakahara, Y., Kobayashi, Y., Kato, A., et al. (2018). Systemic *Staphylococcus pseudintermedius* infection in an arctic fox (*Vulpes lagopus*) with severe multifocal suppurative meningoencephalitis and nephritis. *J. Vet. Med. Sci.* 80, 1219–1222. doi:10.1292/jvms.18-0061.
- Jäckel, C., Hammerl, J., and Hertwig, S. (2019). Campylobacter Phage Isolation and Characterization: What We Have Learned So Far. *Methods Protoc.* 2, 18. doi:10.3390/mps2010018.
- Jia, B., Raphenya, A. R., Alcock, B., Waglechner, N., Guo, P., Tsang, K. K., et al. (2017). CARD 2017: expansion and model-centric curation of the comprehensive antibiotic resistance database. *Nucleic Acids Res.* 45, D566–D573. doi:10.1093/nar/gkw1004.
- Johnson, R. P., Gyles, C. L., Huff, W. E., Ojha, S., Huff, G. R., Rath, N. C., et al. (2008). Bacteriophages for prophylaxis and therapy in cattle, poultry and pigs. *Anim. Health Res. Rev.* 9, 201–215. doi:10.1017/S1466252308001576.
- Jones, P., Binns, D., Chang, H.-Y., Fraser, M., Li, W., McAnulla, C., et al. (2014). InterProScan 5: genome-scale protein function classification. *Bioinforma. Oxf. Engl.* 30, 1236–1240. doi:10.1093/bioinformatics/btu031.
- Kang, J.-H., and Hwang, C.-Y. (2020). First detection of multiresistance pRE25-like elements from Enterococcus spp. in *Staphylococcus pseudintermedius* isolated from canine pyoderma. *J. Glob. Antimicrob. Resist.* 20, 304–308. doi:10.1016/j.jgar.2019.08.022.
- Kempker, R., Eaton, M., Mangalat, D., and Kongphet-Tran, T. (2009). Beware of the Pet Dog: A Case of *Staphylococcus intermedius* Infection. *Am. J. Med. Sci.* 338, 425–427. doi:10.1097/MAJ.0b013e3181b0baa9.
- Kim, J. H., Choresca, C. H., Shin, S. P., Han, J. E., Jun, J. W., and Park, S. C. (2015). Biological Control of *Aeromonas salmonicida* subsp. *salmonicida* Infection in Rainbow Trout (*Oncorhynchus mykiss*) Using *Aeromonas* Phage PAS-1. *Transbound. Emerg. Dis.* 62, 81–86. doi:10.1111/tbed.12088.
- Kishor, C., Mishra, R. R., Saraf, S. K., Kumar, M., Srivastav, A. K., and Nath, G. (2016). Phage therapy of staphylococcal chronic osteomyelitis in

- experimental animal model. *Indian J. Med. Res.* 143, 87.
doi:10.4103/0971-5916.178615.
- Kitagawa, H., Hisatsune, J., Ohge, H., Kustuno, S., Hara, T., Masuda, K., et al. (2021). Implanted Port Catheter System Infection Caused by Methicillin-resistant *Staphylococcus pseudintermedius* ST71-SCCmec type III. *Intern. Med.* doi:10.2169/internalmedicine.5579-20.
- Kosykh, V. G., Schlagman, S. L., and Hattman, S. (1995). Phage T4 DNA [N]-adenine6Methyltransferase. OVEREXPRESSION, PURIFICATION, AND CHARACTERIZATION. *J. Biol. Chem.* 270, 14389–14393.
doi:10.1074/jbc.270.24.14389.
- Koudelakova, T., Bidmanova, S., Dvorak, P., Pavelka, A., Chaloupkova, R., Prokop, Z., et al. (2013). Haloalkane dehalogenases: Biotechnological applications. *Biotechnol. J.* 8, 32–45. doi:10.1002/biot.201100486.
- Kovalskaya, N. Y., Herndon, E. E., Foster-Frey, J. A., Donovan, D. M., and Hammond, R. W. (2019). Antimicrobial activity of bacteriophage derived triple fusion protein against *Staphylococcus aureus*. *AIMS Microbiol.* 5, 158–175. doi:10.3934/microbiol.2019.2.158.
- Kwan, T., Liu, J., DuBow, M., Gros, P., and Pelletier, J. (2005). The complete genomes and proteomes of 27 *Staphylococcus aureus* bacteriophages. *Proc. Natl. Acad. Sci. U. S. A.* 102, 5174–5179.
doi:10.1073/pnas.0501140102.
- Laxminarayan, R., Sridhar, D., Blaser, M., Wang, M., and Woolhouse, M. (2016). Achieving global targets for antimicrobial resistance. *Science* 353, 874–875. doi:10.1126/science.aaf9286.
- Lazar, I., Horvath-Lazar, E., and Lazar, I. (2010). GelAnalyzer. Available at: <http://www.gelanalyzer.com/> [Accessed March 21, 2021].
- Lemoine, F., Correia, D., Lefort, V., Doppelt-Azeroual, O., Mareuil, F., Cohen-Boulakia, S., et al. (2019). NGPhylogeny.fr: new generation phylogenetic services for non-specialists. *Nucleic Acids Res.* 47, W260–W265. doi:10.1093/nar/gkz303.
- Lennon, M., Liao, Y.-T., Salvador, A., Lauzon, C. R., and Wu, V. C. H. (2020). Bacteriophages specific to Shiga toxin-producing *Escherichia coli* exist in goat feces and associated environments on an organic

REFERENCE LIST

- produce farm in Northern California, USA. *PLOS ONE* 15, e0234438. doi:10.1371/journal.pone.0234438.
- Leskinen, K., Tuomala, H., Wicklund, A., Horsma-Heikkinen, J., Kuusela, P., Skurnik, M., et al. (2017). Characterization of vB_SauM-fRuSau02, a Twort-Like Bacteriophage Isolated from a Therapeutic Phage Cocktail. *Viruses* 9, 258. doi:10.3390/v9090258.
- Li, H., and Durbin, R. (2010). Fast and accurate long-read alignment with Burrows-Wheeler transform. *Bioinforma. Oxf. Engl.* 26, 589–595. doi:10.1093/bioinformatics/btp698.
- Lin, D. M., Koskella, B., and Lin, H. C. (2017). Phage therapy: An alternative to antibiotics in the age of multi-drug resistance. *World J. Gastrointest. Pharmacol. Ther.* 8, 162. doi:10.4292/wjgpt.v8.i3.162.
- Litt, P. K., Saha, J., and Jaroni, D. (2018). Characterization of Bacteriophages Targeting Non-O157 Shiga Toxigenic Escherichia coli. *J. Food Prot.* 81, 785–794. doi:10.4315/0362-028X.JFP-17-460.
- Łobocka, M., Hejnowicz, M. S., Dąbrowski, K., Gozdek, A., Kosakowski, J., Witkowska, M., et al. (2012). “Genomics of Staphylococcal Twort-like Phages - Potential Therapeutics of the Post-Antibiotic Era,” in *Advances in Virus Research* (Elsevier), 143–216. doi:10.1016/B978-0-12-394438-2.00005-0.
- Lopes, A., Tavares, P., Petit, M.-A., Guérois, R., and Zinn-Justin, S. (2014). Automated classification of tailed bacteriophages according to their neck organization. *BMC Genomics* 15, 1027. doi:10.1186/1471-2164-15-1027.
- Lozano, C., Rezusta, A., Ferrer, I., Pérez-Laguna, V., Zarazaga, M., Ruiz-Ripa, L., et al. (2017). *Staphylococcus pseudintermedius* Human Infection Cases in Spain: Dog-to-Human Transmission. *Vector-Borne Zoonotic Dis.* 17, 268–270. doi:10.1089/vbz.2016.2048.
- Ma, G. C., Worthing, K. A., Ward, M. P., and Norris, J. M. (2020). Commensal Staphylococci Including Methicillin-Resistant *Staphylococcus aureus* from Dogs and Cats in Remote New South Wales, Australia. *Microb. Ecol.* 79, 164–174. doi:10.1007/s00248-019-01382-y.

- Madeira, F., Park, Y. mi, Lee, J., Buso, N., Gur, T., Madhusoodanan, N., et al. (2019). The EMBL-EBI search and sequence analysis tools APIs in 2019. *Nucleic Acids Res.* 47, W636–W641. doi:10.1093/nar/gkz268.
- Mališová, L., Šafránková, R., Kekláková, J., Petráš, P., Žemličková, H., and Jakubů, V. (2019). Correct species identification (reclassification in CNCTC) of strains of *Staphylococcus intermedius*-group can improve an insight into their evolutionary history. *Folia Microbiol. (Praha)* 64, 231–236. doi:10.1007/s12223-018-0647-7.
- Mašlaňová, I., Doškař, J., Varga, M., Kuntová, L., Mužík, J., Malúšková, D., et al. (2013). Bacteriophages of *Staphylococcus aureus* efficiently package various bacterial genes and mobile genetic elements including SCC *mec* with different frequencies: Quantification of staphylococcal genes in phages. *Environ. Microbiol. Rep.* 5, 66–73. doi:10.1111/j.1758-2229.2012.00378.x.
- Mattila, S., Ruotsalainen, P., and Jalasvuori, M. (2015). On-Demand Isolation of Bacteriophages Against Drug-Resistant Bacteria for Personalized Phage Therapy. *Front. Microbiol.* 6. doi:10.3389/fmicb.2015.01271.
- McMeekin, C., Hill, K., Gibson, I., Bridges, J., and Benschop, J. (2017). Antimicrobial resistance patterns of bacteria isolated from canine urinary samples submitted to a New Zealand veterinary diagnostic laboratory between 2005–2012. *N. Z. Vet. J.* 65, 99–104. doi:10.1080/00480169.2016.1259594.
- Mellmann, A., Becker, K., von Eiff, C., Keckevoet, U., Schumann, P., and Harmsen, D. (2006). Sequencing and Staphylococci Identification. *Emerg. Infect. Dis.* 12, 333–336. doi:10.3201/eid1202.050962.
- Melter, O., Svec, P., Tkadlec, J., Doskar, J., Kinska, H., and Pantucek, R. (2017). Characterisation of methicillin-susceptible *Staphylococcus pseudintermedius* isolates from canine infections and determination of virulence factors using multiplex PCR. *Veterinární Medicína* 62, 81–89. doi:10.17221/105/2016-VETMED.
- Miller, R. W., Skinner, J., Sulakvelidze, A., Mathis, G. F., and Hofacre, C. L. (2010). Bacteriophage Therapy for Control of Necrotic Enteritis of Broiler Chickens Experimentally Infected with *Clostridium perfringens*. *Avian Dis.* 54, 33–40. doi:10.1637/8953-060509-Reg.1.

REFERENCE LIST

- Milne, I., Stephen, G., Bayer, M., Cock, P. J. A., Pritchard, L., Cardle, L., et al. (2013). Using Tablet for visual exploration of second-generation sequencing data. *Brief. Bioinform.* 14, 193–202. doi:10.1093/bib/bbs012.
- Mishra, A. K., Sharma, N., Kumar, A., Kumar, N., Gundallahalli Bayyappa, M. R., Kumar, S., et al. (2014). Isolation, characterization and therapeutic potential assessment of bacteriophages virulent to *Staphylococcus aureus* associated with goat mastitis. *Iran. J. Vet. Res.* 15, 320–325.
- Moodley, A., Kot, W., Nälgård, S., Jakociune, D., Neve, H., Hansen, L. H., et al. (2019). Isolation and characterization of bacteriophages active against methicillin-resistant *Staphylococcus pseudintermedius*. *Res. Vet. Sci.* 122, 81–85. doi:10.1016/j.rvsc.2018.11.008.
- Moraru, C., Varsani, A., and Kropinski, A. M. (2020). VIRIDIC—A Novel Tool to Calculate the Intergenomic Similarities of Prokaryote-Infecting Viruses. *Viruses* 12, 1268. doi:10.3390/v12111268.
- Morris, D. O., Loeffler, A., Davis, M. F., Guardabassi, L., and Weese, J. S. (2017). Recommendations for approaches to methicillin-resistant staphylococcal infections of small animals: diagnosis, therapeutic considerations and preventative measures.: Clinical Consensus Guidelines of the World Association for Veterinary Dermatology. *Vet. Dermatol.* 28, 304-e69. doi:10.1111/vde.12444.
- Murray, A. K., Lee, J., Bendall, R., Zhang, L., Sunde, M., Schau Slettemeås, J., et al. (2018). *Staphylococcus cornubiensis* sp. nov., a member of the *Staphylococcus intermedius* Group (SIG). *Int. J. Syst. Evol. Microbiol.* 68, 3404–3408. doi:10.1099/ijsem.0.002992.
- NCBI Resource Coordinators (2018). Database resources of the National Center for Biotechnology Information. *Nucleic Acids Res.* 46, D8–D13. doi:10.1093/nar/gkx1095.
- Neethirajan, S., and DiCicco, M. (2014). Atomic force microscopy study of the antibacterial effect of fosfomicin on methicillin-resistant *Staphylococcus pseudintermedius*. *Appl. Nanosci.* 4, 703–709. doi:10.1007/s13204-013-0256-3.
- Nemeghaire, S., Argudín, M. A., Feßler, A. T., Hauschild, T., Schwarz, S., and Butaye, P. (2014). The ecological importance of the *Staphylococcus sciuri* species group as a reservoir for resistance and virulence

- genes. *Vet. Microbiol.* 171, 342–356. doi:10.1016/j.vet-mic.2014.02.005.
- Nikkhahi, F., Soltan Dallal, M. M., Alimohammadi, M., Rahimi Foroushani, A., Rajabi, Z., Fardsanei, F., et al. (2017). Phage therapy: assessment of the efficacy of a bacteriophage isolated in the treatment of salmonellosis induced by *Salmonella enteritidis* in mice. *Gastroenterol. Hepatol. Bed Bench* 10, 131–136.
- Niu, Y. D., Stanford, K., Ackermann, H.-W., and McAllister, T. A. (2012). Characterization of 4 T1-like lytic bacteriophages that lyse Shiga-toxin *Escherichia coli* O157:H7. *Can. J. Microbiol.* 58, 923–927. doi:10.1139/w2012-063.
- North, O. I., Sakai, K., Yamashita, E., Nakagawa, A., Iwazaki, T., Büttner, C. R., et al. (2019). Phage tail fibre assembly proteins employ a modular structure to drive the correct folding of diverse fibres. *Nat. Microbiol.* 4, 1645–1653. doi:10.1038/s41564-019-0477-7.
- Nováček, J., Šiborová, M., Benešík, M., Pantůček, R., Doškař, J., and Plevka, P. (2016). Structure and genome release of Twort-like Myoviridae phage with a double-layered baseplate. *Proc. Natl. Acad. Sci. U. S. A.* 113, 9351–9356. doi:10.1073/pnas.1605883113.
- Nováková, D., Švec, P., Zeman, M., Busse, H.-J., Mašlaňová, I., Pantůček, R., et al. (2020). *Pseudomonas leptonychotis* sp. nov., isolated from Weddell seals in Antarctica. *Int. J. Syst. Evol. Microbiol.* 70, 302–308. doi:10.1099/ijsem.0.003753.
- Nowakowski, M., Jaremko, Ł., Wladyka, B., Dubin, G., Ejchart, A., and Mak, P. (2018). Spatial attributes of the four-helix bundle group of bacteriocins – The high-resolution structure of BacSp222 in solution. *Int. J. Biol. Macromol.* 107, 2715–2724. doi:10.1016/j.ijbiomac.2017.10.158.
- Nurk, S., Bankevich, A., Antipov, D., Gurevich, A., Korobeynikov, A., Lapidus, A., et al. (2013). “Assembling Genomes and Mini-metagenomes from Highly Chimeric Reads,” in *Research in Computational Molecular Biology Lecture Notes in Computer Science.*, eds. M. Deng, R. Jiang, F. Sun, and X. Zhang (Berlin, Heidelberg: Springer Berlin Heidelberg), 158–170. doi:10.1007/978-3-642-37195-0_13.

REFERENCE LIST

- Okonechnikov, K., Golosova, O., and Fursov, M. (2012). Unipro UGENE: a unified bioinformatics toolkit. *Bioinformatics* 28, 1166–1167. doi:10.1093/bioinformatics/bts091.
- Oliveira, H., Sampaio, M., Melo, L. D. R., Dias, O., Pope, W. H., Hatfull, G. F., et al. (2019). Staphylococci phages display vast genomic diversity and evolutionary relationships. *BMC Genomics* 20, 357. doi:10.1186/s12864-019-5647-8.
- Overturf, G. D., Talan, D. A., Singer, K., Anderson, N., Miller, J. I., Greene, R. T., et al. (1991). Phage typing of *Staphylococcus intermedius*. *J. Clin. Microbiol.* 29, 373–375. doi:10.1128/JCM.29.2.373-375.1991.
- Park, G. Y., Yu, H. J., Son, J. S., Park, S. J., Cha, H.-J., and Song, K. S. (2020). *Pasteurella multocida* specific bacteriophage suppresses *P. multocida*-induced inflammation: identification of genes related to bacteriophage signaling by *Pasteurella multocida*-infected swine nasal turbinate cells. *Genes Genomics* 42, 235–243. doi:10.1007/s13258-019-00898-4.
- Pedersen, J. S., Kot, W., Plöger, M., Lametsh, R., Neve, H., Franz, C. M. A. P., et al. (2020). A Rare, Virulent *Clostridium perfringens* Bacteriophage Susfortuna Is the First Isolated Bacteriophage in a New Viral Genus. *PHAGE* 1, 230–236. doi:10.1089/phage.2020.0038.
- Perreten, V., Kania, S. A., and Bemis, D. (2020). *Staphylococcus ursi* sp. nov., a new member of the ‘*Staphylococcus intermedius* group’ isolated from healthy black bears. *Int. J. Syst. Evol. Microbiol.* 70, 4637–4645. doi:10.1099/ijsem.0.004324.
- Pirnay, J.-P., Blasdel, B. G., Bretaudeau, L., Buckling, A., Chanishvili, N., Clark, J. R., et al. (2015). Quality and Safety Requirements for Sustainable Phage Therapy Products. *Pharm. Res.* 32, 2173–2179. doi:10.1007/s11095-014-1617-7.
- Pottumarthy, S., Schapiro, J. M., Prentice, J. L., Houze, Y. B., Swanzy, S. R., Fang, F. C., et al. (2004). Clinical Isolates of *Staphylococcus intermedius* Masquerading as Methicillin-Resistant *Staphylococcus aureus*. *J. Clin. Microbiol.* 42, 5881–5884. doi:10.1128/JCM.42.12.5881-5884.2004.
- Qureshi, S., Saxena, H. M., Imam, N., Kashoo, Z., Sharief Banday, M., Alam, A., et al. (2018). Isolation and genome analysis of a lytic *Pasteurella*

- multocida* Bacteriophage PMP-GAD-IND. *Lett. Appl. Microbiol.* 67, 244–253. doi:10.1111/lam.13010.
- Rambaut, A. (2018). *figtree*. Available at: <https://github.com/rambaut/figtree> [Accessed March 21, 2021].
- Rhys-Davies, L., and Ogden, J. (2020). Vets' and Pet Owners' Views About Antibiotics for Companion Animals and the Use of Phages as an Alternative. *Front. Vet. Sci.* 7, 513770. doi:10.3389/fvets.2020.513770.
- Richards, P. J., Connerton, P. L., and Connerton, I. F. (2019). Phage Biocontrol of *Campylobacter jejuni* in Chickens Does Not Produce Collateral Effects on the Gut Microbiota. *Front. Microbiol.* 10. doi:10.3389/fmicb.2019.00476.
- Riegel, P., Jesel-Morel, L., Laventie, B., Boisset, S., Vandenesch, F., and Prévost, G. (2011). Coagulase-positive *Staphylococcus pseudintermedius* from animals causing human endocarditis. *Int. J. Med. Microbiol.* 301, 237–239. doi:10.1016/j.ijmm.2010.09.001.
- Rodríguez-Rubio, L., Gutiérrez, D., Martínez, B., Rodríguez, A., Götz, F., and García, P. (2012). The Tape Measure Protein of the *Staphylococcus aureus* Bacteriophage ν B_SauS-phiPLA35 Has an Active Muramidase Domain. *Appl. Environ. Microbiol.* 78, 6369–6371. doi:10.1128/AEM.01236-12.
- Roucourt, B., and Lavigne, R. (2009). The role of interactions between phage and bacterial proteins within the infected cell: a diverse and puzzling interactome. *Environ. Microbiol.* 11, 2789–2805. doi:10.1111/j.1462-2920.2009.02029.x.
- Ruscher, C., Lübke-Becker, A., Wleklinski, C.-G., Şoba, A., Wieler, L. H., and Walther, B. (2009). Prevalence of Methicillin-resistant *Staphylococcus pseudintermedius* isolated from clinical samples of companion animals and equidae. *Vet. Microbiol.* 136, 197–201. doi:10.1016/j.vetmic.2008.10.023.
- Sambrook, J., Fritsch, E., and Maniatis, T. (1989). *Molecular cloning: A laboratory manual: Vol. 2*. 2. ed. S.l.: Cold Spring Harbor.
- Santos, T. M. A., Ledbetter, E. C., Caixeta, L. S., Bicalho, M. L. S., and Bicalho, R. C. (2011). Isolation and characterization of two bacteriophages with strong in vitro antimicrobial activity against

REFERENCE LIST

- Pseudomonas aeruginosa* isolated from dogs with ocular infections. *Am. J. Vet. Res.* 72, 1079–1086. doi:10.2460/ajvr.72.8.1079.
- Sasaki, A., Shimizu, A., Kawano, J., Wakita, Y., Hayashi, T., and Ootsuki, S. (2005). Characteristics of *Staphylococcus intermedius* Isolates from Diseased and Healthy Dogs. *J. Vet. Med. Sci.* 67, 103–106. doi:10.1292/jvms.67.103.
- Sasaki, T., Kikuchi, K., Tanaka, Y., Takahashi, N., Kamata, S., and Hiramatsu, K. (2007). Reclassification of Phenotypically Identified *Staphylococcus intermedius* Strains. *J. Clin. Microbiol.* 45, 2770–2778. doi:10.1128/JCM.00360-07.
- Sasaki, T., Tsubakishita, S., Tanaka, Y., Sakusabe, A., Ohtsuka, M., Hiro-taki, S., et al. (2010). Multiplex-PCR Method for Species Identification of Coagulase-Positive *Staphylococci*. *J. Clin. Microbiol.* 48, 765–769. doi:10.1128/JCM.01232-09.
- Schade, S. Z., Adler, J., and Ris, H. (1967). How bacteriophage chi attacks motile bacteria. *J. Virol.* 1, 599–609. doi:10.1128/JVI.1.3.599-609.1967.
- Schindelin, J., Arganda-Carreras, I., Frise, E., Kaynig, V., Longair, M., Pietzsch, T., et al. (2012). Fiji: an open-source platform for biological-image analysis. *Nat. Methods* 9, 676–682. doi:10.1038/nmeth.2019.
- Schmelcher, M., Shen, Y., Nelson, D. C., Eugster, M. R., Eichenseher, F., Hanke, D. C., et al. (2015). Evolutionarily distinct bacteriophage endolysins featuring conserved peptidoglycan cleavage sites protect mice from MRSA infection. *J. Antimicrob. Chemother.* 70, 1453–1465. doi:10.1093/jac/dku552.
- Schrödinger LLC (2015). The PyMOL Molecular Graphics System, Version 1.8.
- Schuch, R., and Fischetti, V. A. (2006). Detailed Genomic Analysis of the W β and γ Phages Infecting *Bacillus anthracis*: Implications for Evolution of Environmental Fitness and Antibiotic Resistance. *J. Bacteriol.* 188, 3037–3051. doi:10.1128/JB.188.8.3037-3051.2006.
- Schulz, E. C., Dickmanns, A., Urlaub, H., Schmitt, A., Mühlenhoff, M., Stummeyer, K., et al. (2010). Crystal structure of an intramolecular

- chaperone mediating triple- β -helix folding. *Nat. Struct. Mol. Biol.* 17, 210–215. doi:10.1038/nsmb.1746.
- Seemann, T. (2020). *abricate*. Available at: <https://github.com/tseemann/abricate> [Accessed March 21, 2021].
- Seo, B.-J., Song, E.-T., Lee, K., Kim, J.-W., Jeong, C.-G., Moon, S.-H., et al. (2018). Evaluation of the broad-spectrum lytic capability of bacteriophage cocktails against various *Salmonella* serovars and their effects on weaned pigs infected with *Salmonella* Typhimurium. *J. Vet. Med. Sci.* 80, 851–860. doi:10.1292/jvms.17-0501.
- Silva, Y. J., Moreirinha, C., Pereira, C., Costa, L., Rocha, R. J. M., Cunha, Â., et al. (2016). Biological control of *Aeromonas salmonicida* infection in juvenile Senegalese sole (*Solea senegalensis*) with Phage AS-A. *Aquaculture* 450, 225–233. doi:10.1016/j.aquaculture.2015.07.025.
- Skaradzińska, A., Śliwka, P., Kuźmińska-Bajor, M., Skaradziński, G., Rząsa, A., Friese, A., et al. (2017). The Efficacy of Isolated Bacteriophages from Pig Farms against ESBL/AmpC-Producing *Escherichia coli* from Pig and Turkey Farms. *Front. Microbiol.* 8. doi:10.3389/fmicb.2017.00530.
- Slopek, S., and Krzywy, T. (1985). Morphology and ultrastructure of bacteriophages. An electron microscopic study. *Arch. Immunol. Ther. Exp. (Warsz.)* 33, 1–217.
- Smith, H. W., and Huggins, M. B. (1983). Effectiveness of Phages in Treating Experimental *Escherichia coli* Diarrhoea in Calves, Piglets and Lambs. *Microbiology* 129, 2659–2675. doi:10.1099/00221287-129-8-2659.
- Stejskal, K., Potěšil, D., and Zdráhal, Z. (2013). Suppression of Peptide Sample Losses in Autosampler Vials. *J. Proteome Res.* 12, 3057–3062. doi:10.1021/pr400183v.
- Stewart, C. R., Casjens, S. R., Cresawn, S. G., Houtz, J. M., Smith, A. L., Ford, M. E., et al. (2009). The Genome of *Bacillus subtilis* Bacteriophage SPO1. *J. Mol. Biol.* 388, 48–70. doi:10.1016/j.jmb.2009.03.009.
- Stewart, C. R., Gaslightwala, I., Hinata, K., Krolikowski, K. A., Needleman, D. S., Peng, A. S.-Y., et al. (1998). Genes and Regulatory Sites of the “Host-Takeover Module” in the Terminal Redundancy of *Bacillus*

REFERENCE LIST

- subtilisBacteriophage SPO1. *Virology* 246, 329–340.
doi:10.1006/viro.1998.9197.
- Švec, P., Kosina, M., Zeman, M., Holočová, P., Králová, S., Němcová, E., et al. (2020). *Pseudomonas karstica* sp. nov. and *Pseudomonas spelaei* sp. nov., isolated from calcite moonmilk deposits from caves. *Int. J. Syst. Evol. Microbiol.* 70, 5131–5140. doi:10.1099/ijsem.0.004393.
- Švec, P., Pantůček, R., Petráš, P., Sedláček, I., and Nováková, D. (2010). Identification of *Staphylococcus* spp. using (GTG)₅-PCR fingerprinting. *Syst. Appl. Microbiol.* 33, 451–456. doi:10.1016/j.syapm.2010.09.004.
- The UniProt Consortium, Bateman, A., Martin, M.-J., Orchard, S., Magrane, M., Agivetova, R., et al. (2021). UniProt: the universal protein knowledgebase in 2021. *Nucleic Acids Res.* 49, D480–D489. doi:10.1093/nar/gkaa1100.
- Tsai, R., Corrêa, I. R., Xu, M. Y., and Xu, S. (2017). Restriction and modification of deoxyarchaeosine (dG⁺)-containing phage 9 g DNA. *Sci. Rep.* 7, 8348. doi:10.1038/s41598-017-08864-4.
- Twort, F. W. (1915). An investigation on the nature of ultra-microscopic viruses. *The Lancet* 186, 1241–1243. doi:10.1016/S0140-6736(01)20383-3.
- van Duijkeren, E., Catry, B., Greko, C., Moreno, M. A., Pomba, M. C., Pyorala, S., et al. (2011). Review on methicillin-resistant *Staphylococcus pseudintermedius*. *J. Antimicrob. Chemother.* 66, 2705–2714. doi:10.1093/jac/dkr367.
- Verstappen, K. M., Huijbregts, L., Spaninks, M., Wagenaar, J. A., Fluit, A. C., and Duim, B. (2017). Development of a real-time PCR for detection of *Staphylococcus pseudintermedius* using a novel automated comparison of whole-genome sequences. *PLOS ONE* 12, e0183925. doi:10.1371/journal.pone.0183925.
- Verstappen, K. M., Tulinski, P., Duim, B., Fluit, A. C., Carney, J., van Nes, A., et al. (2016). The Effectiveness of Bacteriophages against Methicillin-Resistant *Staphylococcus aureus* ST398 Nasal Colonization in Pigs. *PLOS ONE* 11, e0160242. doi:10.1371/journal.pone.0160242.
- Voelker, R. (2019). FDA Approves Bacteriophage Trial. *JAMA* 321, 638. doi:10.1001/jama.2019.0510.

- Vrbovská, V., Sedláček, I., Zeman, M., Švec, P., Kovařovic, V., Šedo, O., et al. (2020). Characterization of *Staphylococcus intermedius* group isolates associated with animals from Antarctica and emended description of *Staphylococcus delphini*. *Microorganisms* 8, 204. doi:10.3390/microorganisms8020204.
- Wakita, Y., Shimizu, A., Hájek, V., Kawano, J., and Yamashita, K. (2002). Characterization of *Staphylococcus intermedius* from Pigeons, Dogs, Foxes, Mink, and Horses by Pulsed-Field Gel Electrophoresis. *J. Vet. Med. Sci.* 64, 237–243. doi:10.1292/jvms.64.237.
- Walker, B. J., Abeel, T., Shea, T., Priest, M., Abouelliel, A., Sakthikumar, S., et al. (2014). Pilon: An Integrated Tool for Comprehensive Microbial Variant Detection and Genome Assembly Improvement. *PLoS ONE* 9, e112963. doi:10.1371/journal.pone.0112963.
- Wall, S. K., Zhang, J., Rostagno, M. H., and Ebner, P. D. (2010). Phage Therapy To Reduce Preprocessing Salmonella Infections in Market-Weight Swine. *Appl. Environ. Microbiol.* 76, 48–53. doi:10.1128/AEM.00785-09.
- Wegener, A., Damborg, P., Guardabassi, L., Moodley, A., Mughini-Gras, L., Duim, B., et al. (2020). Specific staphylococcal cassette chromosome mec (SCCmec) types and clonal complexes are associated with low-level amoxicillin/clavulanic acid and cefalotin resistance in methicillin-resistant *Staphylococcus pseudintermedius*. *J. Antimicrob. Chemother.* 75, 508–511. doi:10.1093/jac/dkz509.
- Wick, R. R., Judd, L. M., Gorrie, C. L., and Holt, K. E. (2017). Unicycler: Resolving bacterial genome assemblies from short and long sequencing reads. *PLoS Comput. Biol.* 13, e1005595. doi:10.1371/journal.pcbi.1005595.
- Wipf, J. R. K., Deutsch, D. R., Westblade, L. F., and Fischetti, V. A. (2019). Genome Sequences of Six Prophages Isolated from *Staphylococcus pseudintermedius* Strains Recovered from Human and Animal Clinical Specimens. *Microbiol. Resour. Announc.* 8, MRA.00387-19, e00387-19. doi:10.1128/MRA.00387-19.
- Wiśniewski, J. R., Ostasiewicz, P., and Mann, M. (2011). High Recovery FASP Applied to the Proteomic Analysis of Microdissected Formalin Fixed Paraffin Embedded Cancer Tissues Retrieves Known Colon

REFERENCE LIST

- Cancer Markers. *J. Proteome Res.* 10, 3040–3049.
doi:10.1021/pr200019m.
- Xia, G., and Wolz, C. (2014). Phages of *Staphylococcus aureus* and their impact on host evolution. *Infect. Genet. Evol.* 21, 593–601.
doi:10.1016/j.meegid.2013.04.022.
- Xu, J., Hendrix, R. W., and Duda, R. L. (2014). Chaperone–Protein Interactions That Mediate Assembly of the Bacteriophage Lambda Tail to the Correct Length. *J. Mol. Biol.* 426, 1004–1018.
doi:10.1016/j.jmb.2013.06.040.
- Yan, L., Hong, S. M., and Kim, I. H. (2012). Effect of Bacteriophage Supplementation on the Growth Performance, Nutrient Digestibility, Blood Characteristics, and Fecal Microbial Shedding in Growing Pigs. *Asian-Australas. J. Anim. Sci.* 25, 1451–1456.
doi:10.5713/ajas.2012.12253.
- Yang, J., and Zhang, Y. (2015). I-TASSER server: new development for protein structure and function predictions. *Nucleic Acids Res.* 43, W174–W181. doi:10.1093/nar/gkv342.
- Yarbrough, M. L., Lainhart, W., and Burnham, C.-A. D. (2018). Epidemiology, Clinical Characteristics, and Antimicrobial Susceptibility Profiles of Human Clinical Isolates of *Staphylococcus intermedius* Group. *J. Clin. Microbiol.* 56, e01788-17. doi:10.1128/JCM.01788-17.
- Yen, M., Cairns, L. S., and Camilli, A. (2017). A cocktail of three virulent bacteriophages prevents *Vibrio cholerae* infection in animal models. *Nat. Commun.* 8, 14187. doi:10.1038/ncomms14187.
- Yost, D. G., Tsourkas, P., and Amy, P. S. (2016). Experimental bacteriophage treatment of honeybees (*Apis mellifera*) infected with *Paenibacillus larvae*, the causative agent of American Foulbrood Disease. *Bacteriophage* 6, e1122698. doi:10.1080/21597081.2015.1122698.
- Zankari, E., Hasman, H., Cosentino, S., Vestergaard, M., Rasmussen, S., Lund, O., et al. (2012). Identification of acquired antimicrobial resistance genes. *J. Antimicrob. Chemother.* 67, 2640–2644.
doi:10.1093/jac/dks261.

- Žbikowska, K., Michalczuk, M., and Dolka, B. (2020). The Use of Bacteriophages in the Poultry Industry. *Animals* 10, 872. doi:10.3390/ani10050872.
- Zeman, M., Bárdy, P., Vrbovska, V., Roudnický, P., Zdráhal, Z., Růžičková, V., et al. (2019). New genus Fibralongavirus in Siphoviridae phages of *Staphylococcus pseudintermedius*. *Viruses* 11, 1143. doi:10.3390/v11121143.
- Zeman, M., Mašlaňová, I., Indráková, A., Šiborová, M., Mikulášek, K., Bendíčková, K., et al. (2017). *Staphylococcus sciuri* bacteriophages double-convert for staphylokinase and phospholipase, mediate inter-species plasmid transduction, and package *mecA* gene. *Sci. Rep.* 7, 46319. doi:10.1038/srep46319.
- Zhao, J., Liu, Y., Xiao, C., He, S., Yao, H., and Bao, G. (2017). Efficacy of Phage Therapy in Controlling Rabbit Colibacillosis and Changes in Cecal Microbiota. *Front. Microbiol.* 8. doi:10.3389/fmicb.2017.00957.

9 Author's publications

Original research articles including supplementary information:

New genus *Fibralongavirus* in *Siphoviridae* phages of *Staphylococcus pseudintermedius*

Staphylococcus sciuri bacteriophages double-convert for staphylokinase and phospholipase, mediate interspecies plasmid transduction and package *mecA* gene

Characterization of *Staphylococcus intermedius* group isolates associated with animals from Antarctica and emended description of *Staphylococcus delphini*

Pseudomonas leptonychotis sp. nov., isolated from Weddell seals in Antarctica


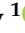


Other publications:

Pseudomonas karstica sp. nov. and *Pseudomonas spelaei* sp. nov., isolated from calcite moonmilk deposits from caves

Hymenobacter terrestris sp. nov. and *Hymenobacter lapidiphilus* sp. nov., isolated from regoliths in Antarctica

Article

New Genus *Fibralongavirus* in Siphoviridae Phages of *Staphylococcus pseudintermedius*

Michal Zeman ¹, Pavol Bárdy ¹, Veronika Vrbovska ¹, Pavel Roudnický ²,
Zbyněk Zdráhal ^{2,3}, Vladislava Růžičková ¹, Jiří Doškař ¹ and Roman Pantůček ^{1,*}

¹ Department of Experimental Biology, Faculty of Science, Masaryk University, Kotlářská 2, 611 37 Brno, Czech Republic; michal.zeman91@gmail.com (M.Z.); bardy.pavol@mail.muni.cz (P.B.); veronika.vrbovska@gmail.com (V.V.); vladkar@sci.muni.cz (V.R.); doskar@sci.muni.cz (J.D.)

² Central European Institute of Technology, Masaryk University, Kamenice 5, 625 00 Brno, Czech Republic; p.roudnický@mail.muni.cz (P.R.); zdrahal@sci.muni.cz (Z.Z.)

³ National Centre for Biomolecular Research, Faculty of Science, Masaryk University, Kamenice 5, 625 00 Brno, Czech Republic

* Correspondence: pantucek@sci.muni.cz; Tel.: +420-549-49-6379

Received: 18 November 2019; Accepted: 4 December 2019; Published: 10 December 2019



Abstract: Bacteriophages of the significant veterinary pathogen *Staphylococcus pseudintermedius* are rarely described morphologically and genomically in detail, and mostly include phages of the Siphoviridae family. There is currently no taxonomical classification for phages of this bacterial species. Here we describe a new phage designated vB_SpsS_QT1, which is related to phage 2638A originally described as a *Staphylococcus aureus* phage. Propagating strain *S. aureus* 2854 of the latter was reclassified by *rpoB* gene sequencing as *S. pseudintermedius* 2854 in this work. Both phages have a narrow but different host range determined on 54 strains. Morphologically, both of them belong to the family Siphoviridae, share the B1 morphotype, and differ from other staphylococcal phage genera by a single long fibre at the terminus of the tail. The complete genome of phage vB_SpsS_QT1 was sequenced with the IonTorrent platform and expertly annotated. Its linear genome with cohesive ends is 43,029 bp long and encodes 60 predicted genes with the typical modular structure of staphylococcal siphophages. A global alignment found the genomes of vB_SpsS_QT1 and 2638A to share 84% nucleotide identity, but they have no significant similarity of nucleotide sequences with other phage genomes available in public databases. Based on the morphological, phylogenetic, and genomic analyses, a novel genus *Fibralongavirus* in the family Siphoviridae is described with phage species vB_SpsS_QT1 and 2638A.

Keywords: bacteriophages; *Staphylococcus pseudintermedius*; viral taxonomy; Siphoviridae; comparative genomics

1. Introduction

Staphylococcus pseudintermedius is a member of the *Staphylococcus intermedius* group (SIG), which is mostly associated with veterinary pathogens. Staphylococcal isolates from dogs previously identified as *Staphylococcus intermedius* belong almost exclusively to the species *S. pseudintermedius* [1]. Differentiation between species was made possible by modern molecular diagnostic methods based on polymerase chain reaction-restriction fragment length polymorphism [2], repetitive element sequence-based PCR fingerprinting [3] and multi-locus sequence analysis [4]. *S. pseudintermedius* is recognised as an important causative agent of pyoderma and dermatitis in canines, felines, and other animals [5]. Its host range is not restricted to animals, but also has the potential to cause zoonotic infections [6] or endocarditis in humans [7]. Similar to *Staphylococcus aureus*, there is a threat of

antimicrobial resistance and the emergence of methicillin-resistant *S. pseudintermedius* (MRSP) strains [8]. The importance of this problem is underlined by the “Reflection Paper on Methicillin-Resistant *S. pseudintermedius*” from the European Medicines Agency [9]. The European Medicines Agency even suggests phage therapy as a possible way to control MRSP.

Most of the phage studies were performed before their subdivision into SIG members and focused on the phage typing of *Staphylococcus intermedius* [10–12]. There are only rare reports of staphylococcal Myoviridae phages that act against *S. pseudintermedius* [13]. A group of Siphoviridae phages active against *S. pseudintermedius* was characterized with the aim of therapeutically using them against MRSP [14]. In this paper, we report the description of the new morphologically distinctive genus, *Fibralongavirus*, and a new representative of this genus, the phage vB_SpsS_QT1 (abbreviated as QT1). This proposition was already accepted by the International Committee on the Taxonomy of Viruses (ICTV) but has not been ratified yet.

2. Materials and Methods

2.1. Bacterial Strains and Bacteriophages

Phage 2638A (= HER 283) and its propagation strain *S. pseudintermedius* 2854 (= HER 1283) were purchased from the Félix d’Hérelle Reference Center for Bacterial Viruses (Quebec City, QC, Canada). Fifty-two *S. pseudintermedius* and two *S. intermedius* strains characterized previously [15,16] and reference strains of SIG group obtained from the Czech Collection of Microorganisms (Masaryk University, Brno, Czech Republic) were used to determine the host range (Table S1). Phage QT1 and its propagating strain *S. pseudintermedius* 625 were deposited in the Czech Collection of Microorganisms under numbers CCM 9019 (= QT1) and CCM 9018 (= strain 625).

2.2. Growth Properties

Phage host range was determined by spotting serial dilutions on double-layer agar plates with tryptone soya agar (TSA) bottom agar (CM0131, Oxoid, Basingstoke, United Kingdom) and 0.6% (*w/v*) top Agar No. 1 (LP0011, Oxoid) with the addition of CaCl₂ to a concentration of 2 mM. The growth properties and adsorption efficiency of phages were determined in tryptone soya broth (TSB) (CM0129, Oxoid), with 2 mM CaCl₂ as described previously [17] with minor modification for staphylococci [18]. The ability to grow on different media was further tested on meat peptone agar (MPA) and double-concentrated yeast extract-tryptone (2× YT) agar composed of 1.6% (*w/v*) tryptone (LP0042, Oxoid), 1.0% (*w/v*) yeast extract (LP0021, Oxoid), 0.5% (*w/v*) NaCl, and 1.5% (*w/v*) agar (LP0013, Oxoid), pH 7.0. A one-step growth curve and phage burst size were determined by the procedure described previously [17]. Free plasmacoagulase and clumping factor tests were performed as described previously [19,20].

2.3. Phage Propagation and Purification

Phages were propagated using a TSB liquid broth incubation technique with the addition of CaCl₂ to a final concentration of 2 mM. The phage lysate was centrifuged twice for 30 min at 3100 g and filtered through a 0.45 µm polyethersulfone filter (Techno Plastic Products, Trasadingen, Switzerland). Phage particles were purified in a CsCl density gradient as described previously [21].

2.4. Electron and Cryo-Electron Microscopy

Purified phage was diluted to the density $A_{280\text{ nm}} = 1.0$ and incubated with 1 µg mL⁻¹ DNase I (Sigma-Aldrich, St. Louis, MO, USA) for 30 min at room temperature. For the negative stain, 4 µL of sample was applied onto glow-discharged carbon-coated 400 mesh copper Quantifoil® grids (Quantifoil Micro Tools, Großlöbichau, Germany) for 1 min. The grids were then washed twice on a drop of deionized water and stained with 2% (*w/v*) uranyl acetate. For cryo-EM, 3.9 µL of sample was applied onto glow-discharged R2/1 300 mesh holey carbon Quantifoil® grids, blotted and plunge-frozen

in liquid ethane using a Vitrobot Mark IV (Thermo Fisher Scientific, Waltham, MA, USA). The samples were analyzed with a Tecnai F20 TEM (Thermo Fisher Scientific) operated at 200 kV.

2.5. DNA Extraction from the Phage Particles

DNase I (Sigma-Aldrich) and RNase A (Sigma-Aldrich) treatment was performed to remove any exogenous host genomic DNA and RNA from purified phage particles as previously described [21]. DNA from the viral particles for sequencing was purified by phenol-chloroform extraction [21]. The concentration and purity of phage DNA was determined using a NanoDrop spectrophotometer (Thermo Fisher Scientific).

2.6. Partial *rpoB* Gene Sequencing and Phylogenetic Analysis

Partial *rpoB* gene amplification was performed as described previously [22]. PCR amplicons were sequenced by Sanger sequencing with the primers 1418F and 1876R in the Eurofins Genomics sequencing facility (Ebersberg, Germany).

2.7. Genome Sequencing and Bioinformatic Analyses

Phage genome and bacterial whole-genome shotgun (WGS) sequencing was performed using an Ion Torrent™ Personal Genome Machine (Ion PGM™, Thermo Fisher Scientific). Bacterial genomic DNA was extracted using a High Pure PCR Template Preparation Kit (Roche Diagnostics, Mannheim, Germany) with 5 mg mL⁻¹ lysostaphin (Ambi Products, Lawrence, NY, USA) added to the suspension buffer. The purified genomic DNA was used for preparing a 400-bp sequencing library with an Ion Plus Fragment Library Kit (Thermo Fisher Scientific). The sample was loaded onto a 316v2 chip and sequenced using an Ion PGM Hi-Q sequencing kit (Thermo Fisher Scientific). The physical ends of the phage genome were resolved by the primer walking strategy using ligated QT1 DNA concatemers with T4 DNA ligase (New England Biolabs, Ipswich, MA, USA) as the template for a 597 bp fragment amplified with the primers QT1end_FW (AAAGCACGGCAGATTTGAAC) and QT1end_RV (CGTCACGTATTTTGGGGTCT) and sequenced in Eurofins Genomics (Ebersberg, Germany).

The quality of sequencing reads was analysed by FastQC v0.11.8 [23]. De novo assembly and error correction of raw reads was performed by SPAdes v3.12 [24] with all k-mers 21-127 and follow-up mismatch correction. Genome assembly evaluation was performed by QUAST v5.0.1 [25].

Sequences were manipulated and inspected in the cross-platform bioinformatics software Ugene v1.31.1 [26]. Pairwise global alignments of protein sequences were computed using Emboss stretcher [27]. The primal analysis of sequences was combined from open reading frames (ORFs) prediction using GeneMark.hmm [28] and automatic annotation by RAST v2.0 (genetic code 11, RASTtk annotation scheme) [29]. Gene content was further examined by BLASTp searches in protein sequence databases, pVOGs [30], CD-Search [31], and InterPro v.59 [32]. Then, tRNAscan-SE [33], RNAmmer v.1.2 [34], and hmmsearch v.3.0 [35] were used to analyse functional RNAs. Virulence genes were detected with Abricate v0.8.10 [36] using the databases CARD [37], Resfinder [38], NCBI [39], ARG-ANNOT [40] and VFDB [41]. The protein secondary structure was predicted with Jpred4 [42]. HeliQuest [43] and I-TASSER [44] were used for further structural predictions. Multiple sequence alignments were visualized using EasyFig v.2.1 [45].

Phylogenetic analyses of the β subunit of bacterial RNA polymerase, large subunit of terminase, and major capsid protein were done on the NGPhylogeny.fr server using “PhyML+SMS/OneClick” mode [46] and visualized in FigTree v1.4.3 [47]. The whole-genome comparison of phage genomes was calculated using Gegenees v3.0beta [48] with the blastn algorithm on fragment size = 50 and step size = 25 and genomes were sorted by an internal automatic algorithm.

2.8. Pulsed-Field Gel Electrophoresis.

One μ g of phage DNA was loaded onto 1.5% (*w/v*) agarose gel (Serva, Heidelberg, Germany) and separated with Cheff Mapper (Bio-Rad, Hercules, CA, USA) to detect concatemerised cohesive ends.

A constant voltage of 5 V cm⁻¹ and pulse times of 2–20 s with linear ramping were applied for 20 h. Lambda DNA concatemers (Sigma-Aldrich) were used as molecular weight marker.

2.9. SDS-PAGE of Structural Proteins

Vertical one-dimensional electrophoresis (1-DE) was performed in discontinuous 12% acrylamide SDS-PAGE gel using a Protean II xi Cell (Bio-Rad). Blue Prestained Protein Standard, Broad Range (11–190 kDa) (New England Biolabs) was applied as the molecular weight marker. Proteins were stained with a homemade BlueSilver (100 g ammonium sulphate, 117.6 mL 85% (w/w) H₃PO₄, 200 mL methanol, and 1.2 g Coomassie blue G 250 filled with distilled water to 1 L) [49].

2.10. Filter-Aided Sample Preparation for Mass Spectrometry and LC-MS/MS Analysis

The protein solution was processed by the filter-aided sample preparation (FASP) method [50], using trypsin (1 µL, 0.5 µg µL⁻¹, sequencing grade, Promega, Madison, WI, USA) for digestion (incubated for 18 h at 37 °C, enzyme: protein ratio 1:50). The resulting peptides were directly extracted into LC-MS vials with 2.5% formic acid in 50% acetonitrile (ACN) and 100% ACN with the addition of polyethylene glycol (20,000; final concentration 0.001%) [51] and concentrated in a SpeedVac concentrator (Thermo Fisher Scientific) prior to LC-MS analyses.

Liquid chromatography–mass spectrometry (LC-MS/MS) analysis of the peptide mixture was done using an RSLCnano system (Thermo Fisher Scientific) online connected to an Impact II Ultra-High Resolution Qq-Time-Of-Flight mass spectrometer (Bruker, Billerica, MA, USA). Peptides were concentrated in a trapping column (100 µm × 30 mm; 3.5-µm X-Bridge BEH 130 C18 sorbent, Waters, Milford, MA, USA) and separated in an Acclaim Pepmap100 C18 analytical column (3 µm particles, 75 µm × 500 mm; Thermo Fisher Scientific). MS data were acquired in a data-dependent strategy with a 3-s cycle time. The mass range was set to 150–2200 m/z and precursors were selected from 300–2000 m/z.

The obtained MS/MS spectra were analyzed in Proteome Discoverer software v1.4 (Thermo Fisher Scientific) using In-house Mascot v2.5.1 (Matrix Science, London, UK) search engine. Mascot MS/MS ion searches were done separately against the provided databases—the QT1 proteome (60 protein sequences), *S. pseudintermedius* 625 prophages (182 protein sequences) and the *Staphylococcus* spp. database UniRef100_Staphylococcus (339,865 protein sequences). The cRAP contaminant database (downloaded from <http://www.thegpm.org/crap/>) was searched in advance to exclude contaminant spectra prior to the main database search. The mass tolerances for peptides and MS/MS fragments were 25 ppm and 0.05 Da, respectively. The oxidation of methionine, carbamidomethylation (C), and deamidation (N, Q) were set as variable modifications, and two enzyme miscleavages were allowed for all searches. Rank 1 peptides with a minimum length of 6 amino acids and Mascot expectation value < 0.01 were used for protein list generation. Proteins identified based on at least two peptides are reported.

2.11. Nucleotide Sequence Accession Numbers

The complete genome of the *S. pseudintermedius* phage vB_SpsS_QT1 was deposited in the GenBank database under the accession number MK450538. A partial sequence of the *rpoB* gene from *S. pseudintermedius* HER 1283 was deposited in GenBank with the accession number MN564940. The data from the WGS of the bacterial propagating strain *S. pseudintermedius* 625 were recorded in the GenBank WGS project under the accession number WJOJ00000000. The sequence of p222-like_Sps625 plasmid was deposited in GenBank under the accession number WJOJ01000027.

3. Results

3.1. Growth Characteristics of Phage QT1

Phage QT1 was isolated from rare plaques found in a culture of *S. pseudintermedius* strain 625 on an agar plate. The phage-containing material was transferred to TSB and further propagated on strain 625. Phage QT1 was able to grow on TSA, MPA and 2× YT agar, and formed clear plaques with a diameter of 1.15 ± 0.077 mm ($n = 30$) on TSA with soft agar. Phage QT1 was able to propagate both in liquid broth and on the agar plates using the double-layer agar technique. About 5%–10% of plaques were turbid, but we were unable to derive lysogens of phage QT1 on its propagating strain. The adsorption of the phage was determined on three strains (Figure S1), namely propagating strain *S. pseudintermedius* 625, phage-resistant *S. pseudintermedius* 408, and *S. pseudintermedius* 73, which exhibited an inhibition of growth with no plaques at higher dilutions. The adsorption constant for system phage QT1 and propagating strain *S. pseudintermedius* 625 was calculated as $k = 2.98 \times 10^{-9}$ mL min⁻¹. One minute after the inoculation of the host bacteria, about 20% of the phage particles remained unadsorbed in supernatants in all strains. After 10 min 97%, 91% and 77% of phages were adsorbed on *S. pseudintermedius* strains 625, 73 and 408, respectively (Figure S1). The latent period until the release of new progeny was 55 min. The burst size determined on the propagating strain was 76 phages per cell.

3.2. Virion Morphology of Phages QT1 and 2638A

Micrographs from negative stain transmission electron microscopy show that phage QT1 belongs to the family Siphoviridae and has the B1 morphotype (Figure 1). Due to artefacts caused by staining, the dimensions of virion were determined from native cryo-EM samples (Figure S2). The phage head has a diameter of 61 ± 2.3 nm ($n = 10$), its long non-contractile tail has a length of 320 ± 7.4 nm ($n = 10$) and ends with a single tail fibre from the bottom of the tail with a length of about 70 ± 2.0 nm ($n = 9$). The tail has a width of about 10 nm. The length of the whole virion is about 445 nm. The morphologically most similar phage to QT1 is phage 2638A. The tail fibre of phage 2638A is shorter than that of QT1, with a length of 53 ± 3.1 nm ($n = 11$) (Figure 1).

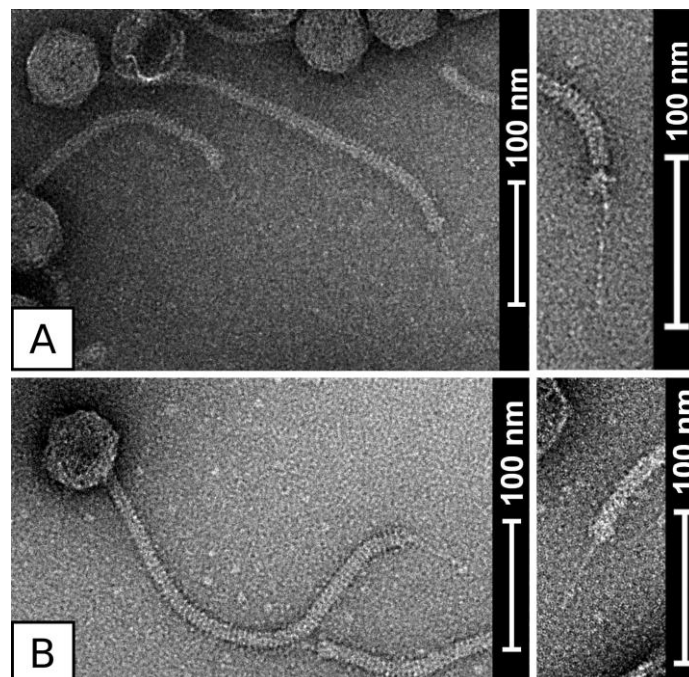


Figure 1. Micrographs of negatively stained phages QT1 (A) and 2638A (B), with detail on the tail fibre on the right side. The phage suspension was treated with DNase I.

3.3. Reclassification of the Propagating Strain *Staphylococcus aureus* 2854 for Phage 2638A as *Staphylococcus pseudintermedius* and Phage Host Range

Phage 2638A was originally described as a phage of *Staphylococcus aureus* [52,53], however phylogenetic analysis based on partial *rpoB* sequencing, which was previously shown to be suitable for the identification of staphylococcal species [22], classified its propagating strain as *S. pseudintermedius* (Figure 2).

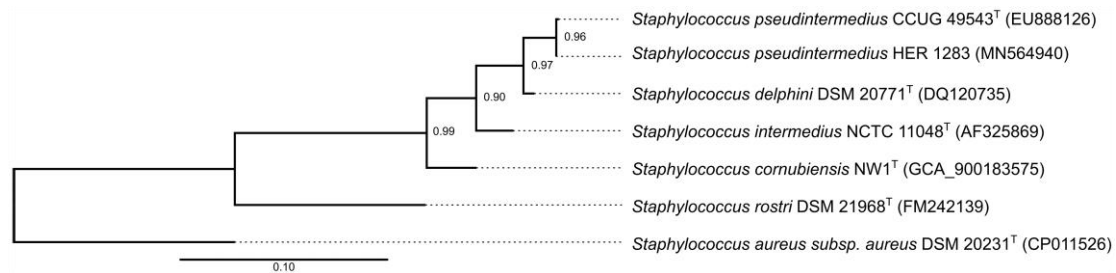


Figure 2. Maximum-likelihood phylogenetic tree based on partial *rpoB* gene sequences of type species of *Staphylococcus intermedius* group and propagating strain for phage 2638A (*S. pseudintermedius* HER 1283). *S. aureus* was used as a reference. GenBank accession numbers to partial *rpoB* gene sequences are in brackets except for *S. cornubiensis*, where the GenBank assembly accession number is indicated. Shimodaira-Hasegawa-like support values from approximate likelihood-ratio test are indicated at the branching points. The scale represents nucleic acid substitutions per site.

The host range of both phages QT1 and 2638A was determined on a set of 54 SIG strains (Table S1). Only 13 strains (24%) exhibited sensitivity to QT1 and/or 2638A. About 27% of insensitive strains exhibited inhibition of growth, when undiluted or 10× diluted phage lysate was used, with no plaques at higher dilutions.

3.4. Phage Structural Proteins

Structural proteins of both phages have similar patterns visible on 1D SDS-PAGE, with the only difference being in the putative tail fibre protein (Figure 3). A significant difference is apparent in the molecular weight of the tail fibre, estimated to be 162 kDa and 132 kDa for phages QT1 and 2638A, respectively.

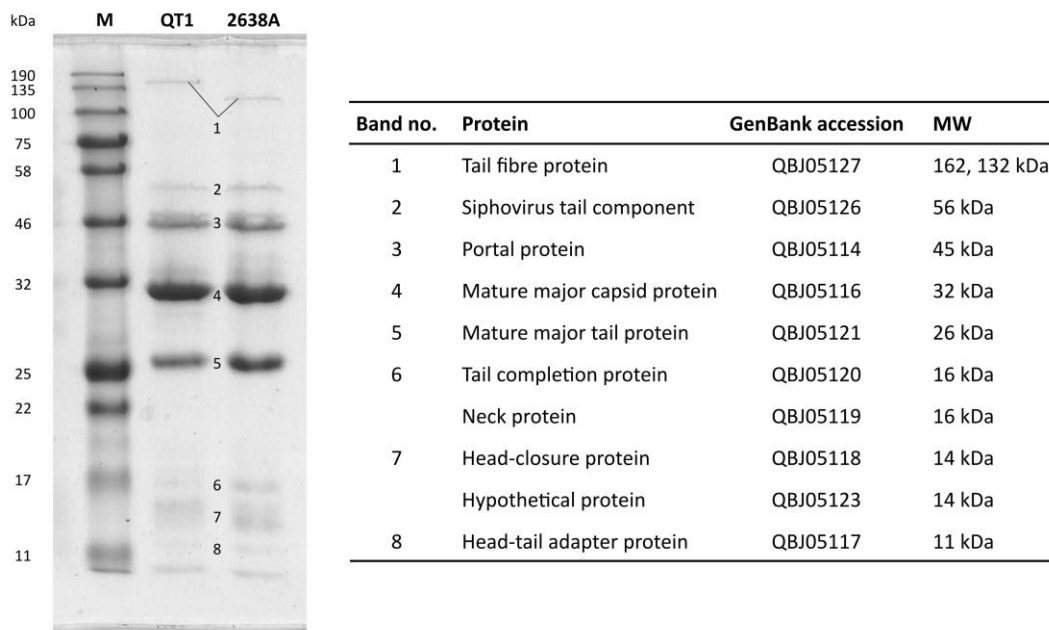


Figure 3. Coomassie brilliant blue-stained 1D SDS-PAGE gel with QT1 and 2638A virion structural proteins. Proteins were extracted from phage particles purified in a CsCl density gradient. All described proteins were confirmed by liquid chromatography-mass spectrometry for phage QT1. GenBank accession numbers for phage QT1 proteins are shown. M, Blue Prestained Protein Standard-Broad Range (New England Biolabs); MW, molecular weight.

3.5. QT1 Genome Description

The genome of phage QT1 consists of dsDNA and has a length of 43,029 bp and G+C content of 36.9%. The physical ends of its genome are 10-nt-long 5' end overhangs (CGGCGCTTGG). These cohesive ends allow the formation of concatemers, confirmed by pulsed-field gel electrophoresis (Figure S3). Sixty genes were predicted in the QT1 genome, and no genes for tRNA were found. Its genes are organized into modules typical for staphylococcal Siphoviridae phages (Figure 4). Phages QT1 and 2638A [52] share 84% global nucleotide identity and 7% gaps in a 43,585-nt space (Figure 4). According to CD-HIT and a 40% aa identity threshold, forty-one proteins (68%) are similar between phage QT1 and 2638A. The DNA sequence of the packaging module has 99% identity to that of phage 2638A. Both phages QT1 and 2638A belong to the Type1 (Cluster 2) category of Siphoviridae according to a Virfam [54] analysis of the neck module and part of the head and tail proteins. The module for the morphogenesis of the head and tail is identical except for the tail length tape-measure protein (Tmp). Tmp proteins of QT1 and 2638A have a different COG5412 super family domain in the distinctive protein region. The Tmp of QT1 contains the same type of peptidase M23 domain that is present in QT1 endolysin (29.6% aa identity, 40.8% similarity) and might act as a tail hydrolase. The tail appendices (baseplate) module also shares high identity in both phages, except for the tail fibre protein (Tfi). The tail fibre protein consists of an N-terminal conserved domain that is approximately 300 amino-acids long and there is a 90-aa-long intra-molecular chaperone auto-processing domain at the C terminus of the protein [55]. The rest of the protein does not have any predicted (known) domains and contributes to the majority of the overall protein length. The tail fibre protein in phage 2638A is shorter than the tail fibre in QT1 because of a deletion in the middle of the gene corresponding to 265 aa. The whole structural module shares a high degree of nucleotide identity (88.1%) except for the last gene encoding a DUF2951 domain-containing protein (GenBank accession QBJ05130) adjacent to the holin gene. This protein is just distantly related to its homologue in 2638A (39% identity, 53% similarity).

In the lytic module, endolysins of both phages share a high degree of similarity (96% aa identity, 97% similarity). The region between the phage endolysin and integrase genes that frequently harbours

virulence factors in *S. aureus* temperate phages contains a 650-bp long region with 3 hypothetical genes that share 97% nucleotide identity to phage 2638A. The rest of the region is not conserved.

An integration and lysogeny regulation module encoding a tyrosine-based XerC integrase is completely different in the QT1 and 2638A phages. The region transcribed from the negative strand is visible in the AT-skew plot (Figure 4) as a significant drop in the AT deviation $(A-T)/(A+T)$ value compared to the rest of the genome (window 1000 bp, with 1000 steps per window).

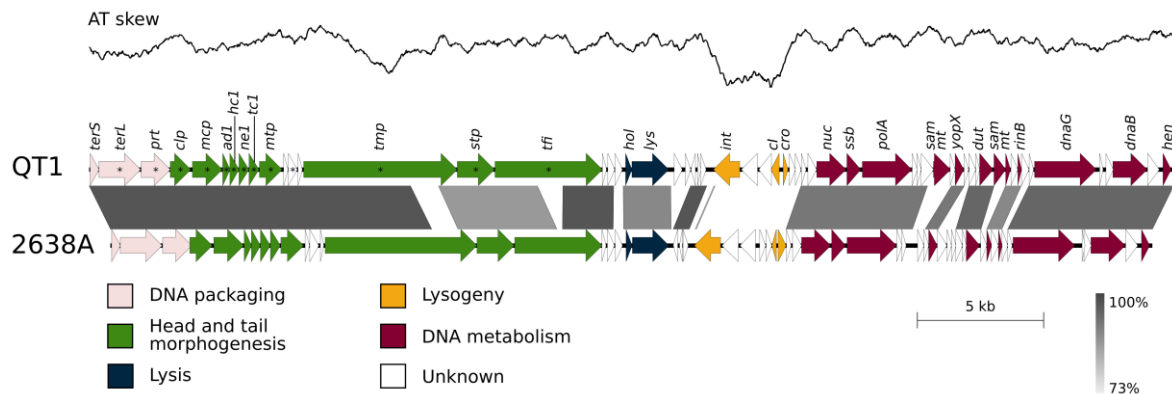


Figure 4. Genome comparison of *S. pseudintermedius* phages QT1 (GenBank accession number MK450538) and 2638A (GenBank accession number NC_007051). The genomes were aligned using the blastn algorithm and similar regions with more than 73% identity are indicated. The position and orientation of predicted genes is represented by arrows. Genome modules are colour coded according to the legend. AT skew for phage QT1 was drawn over a 1000 bp-long window with a step every 1 nt. * denotes proteins from the DNA packaging and head and tail morphogenesis modules of QT1 detected by mass spectrometry.

Four genes are different in the DNA metabolism module when comparing the genome of phage QT1 to the genome of phage 2638A. Two of them are hypothetical, but the other two in the QT1 genome were predicted to be SAM methyltransferase genes. However, the DNA of phage QT1 was digested with two methylation-sensitive restriction enzymes, MboI and AvaII (Dam and Dcm sensitive restriction).

Most of the proteins from the packaging module and the head-tail morphogenesis module were detected in virions using LC-MS analyses (Table S2). No small subunit of terminase was observed, and one hypothetical protein (GenBank QBJ05123) encoded by a gene located between the major tail protein and the tail length tape measure protein was observed. The major tail protein is probably proteolytically cleaved and its C-terminal bacterial Ig-like domain is missing in mature virions, revealed as the lack of peptide coverage in MS data. Due to the high sensitivity of mass spectrometry, some proteins from other modules were detected at low quantities even after purification in a CsCl density gradient (Table S2).

3.6. Taxonomical Classification and Proposal of New Genus Fibralongavirus

Phylogenetic analysis of the major capsid protein (Mcp) and large subunit of terminase (TerL) confirmed that phages QT1 and 2638A form a distinct group from members of known staphylococcal phage genera (Figure 5). The closest relative to QT1 and 2638A of other genera is *Staphylococcus aureus* phage 77, a representative of the *Biseptimavirus* genus.

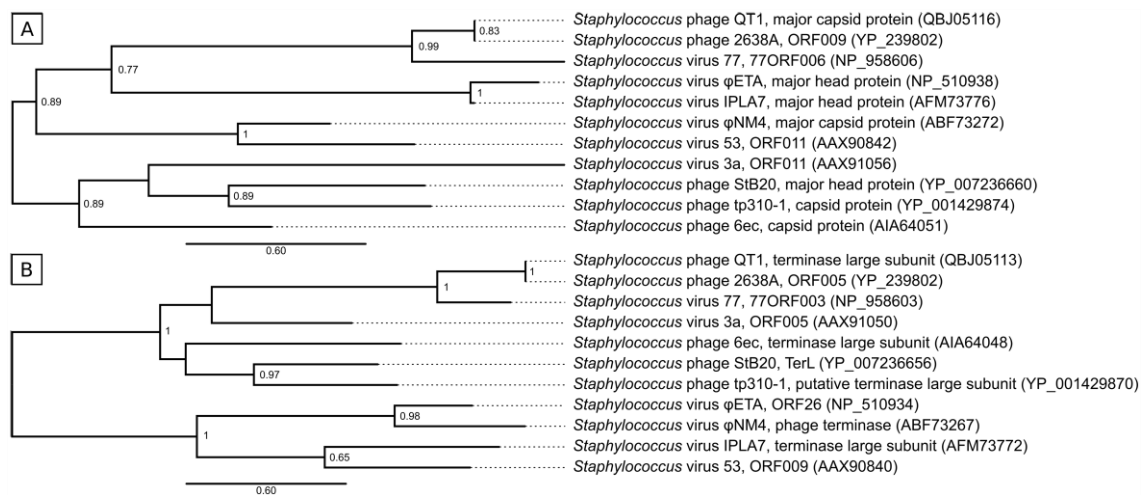


Figure 5. Maximum-likelihood phylogenetic tree based on amino acid sequences of major capsid proteins (A) and large subunits of terminase (B) of phages QT1 and 2638A and representatives of other *Staphylococcus* phage genera. Phage names were adopted from NCBI, GenBank accession numbers are in brackets. Shimodaira-Hasegawa-like support values from approximate likelihood-ratio test are indicated at the branching points. Scales represent amino acid residue substitution per site.

Genomes of staphylococcal siphophages classified by ICTV and phages QT1 and 2638A were compared in Gegenees fragmented aligner (Figure 6). The phages formed clusters that agreed with their classification to viral genera, although some sub-clustering inside known genera was visible. Phages QT1 and 2638A formed a cluster with an overall similarity of 58%–60%, which was separated from other already described genera. On the other hand, they shared less than 1% overall similarity with members of known phage genera. When the phage QT1 genome was compared to all *S. pseudintermedius* Siphoviridae phages and prophages that are publicly available in NCBI databases, prophage φSP119-1 (GenBank accession MK075004) [56] is clustered together with phages QT1 and 2638A (Figure S4). The prophage φSP119-1 genome contains a gene for a tail fibre protein with an expected length of 64 nm calculated from protein sequence data. The integrase of prophage φSP119-1 is only one amino acid different (K241R) from QT1's integrase, and the prophage is integrated into the tRNA^{Ser} gene.

All the results support the proposal of a new genus in the family Siphoviridae, for which we suggest the name *Fibralongavirus* with regard to the long terminal tail fibre. Phages QT1 (vB_SpsS_QT1) and 2638A (vB_SpsS_2638A) represent two phage species with 95% genome sequence identity as the criterion for demarcation of the species in this new genus. The major differences between the two species are in the integration module and minor ones in the DNA metabolism module. We propose phage 2638A as the type species for the genus *Fibralongavirus*.

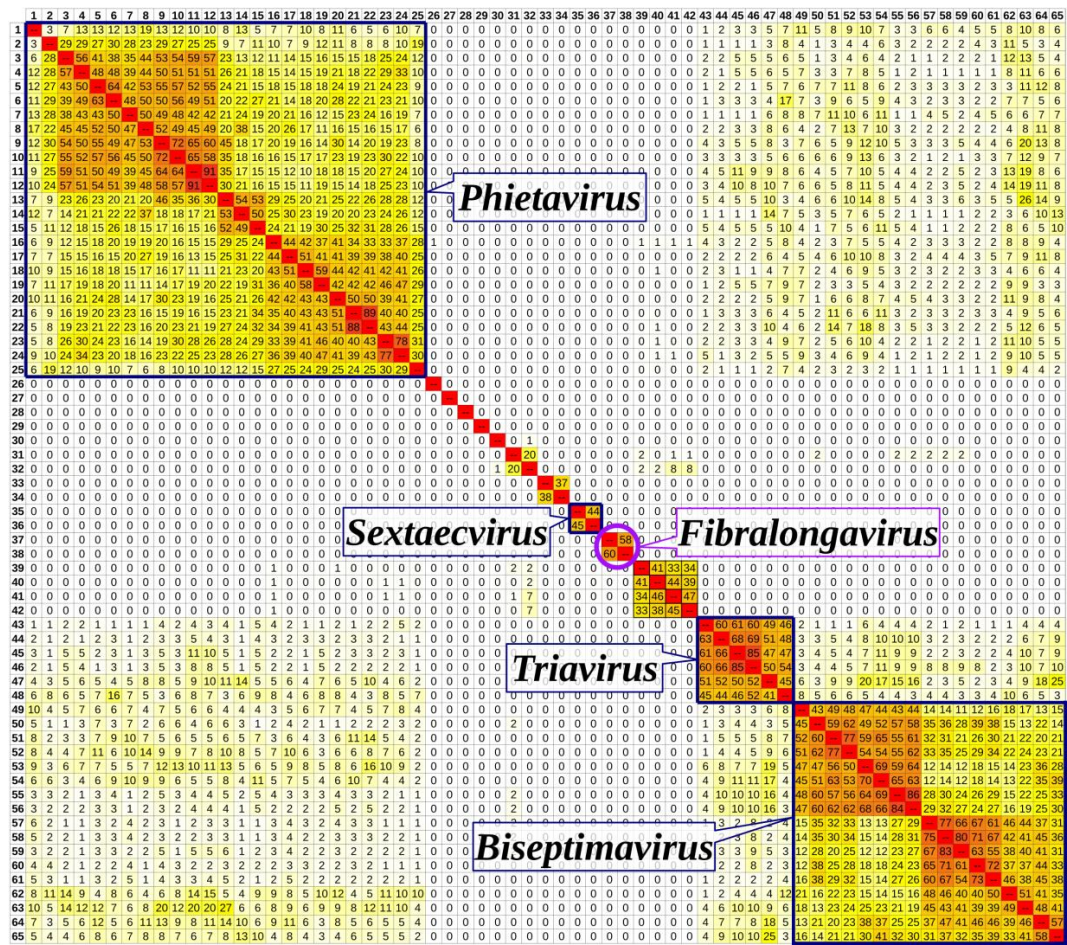


Figure 6. Heat map showing the percent nucleotide similarity of bacteriophage genomes classified by ICTV. Clustering to accepted phage genera according to fragmented nucleotide sequence alignment is indicated in text boxes. Phage names and GenBank accession numbers of used phages labelled as in NCBI are as follows: 1—187, AY954950; 2—φSauS-IPLA88, EU861004; 3—85, AY954953; 4—φMR25, AB370205; 5—69, AY954951; 6—φ11, AF424781; 7—SAP-26, GU477322; 8—φETA2, AP008953; 9—φNM1, NC_008583; 10—φNM2, DQ530360; 11—53, AY954952; 12—80α, DQ517338; 13—φNM4, DQ530362; 14—φETA3, AP008954; 15—96, AY954960; 16—71, AY954962; 17—φETA, AP001553; 18—55, AY954963; 19—φMR11, AB370268; 20—29, AY954964; 21—52A, AY954965; 22—80, DQ908929; 23—92, AY954967; 24—88, AY954966; 25—X2, AY954968; 26—EW, AY954959; 27—φRS7, NC_022914; 28—SpaA1, NC_018277; 29—37, AY954958; 30—IME-SA4, NC_029025; 31—StB20-like, NC_028821; 32—StB20, NC_019915; 33—φ575, KY389063; 34—φ879, KY389064; 35—6ec, KJ804259; 36—vB_SepS_SEP9, KF929199; 37—vB_SpsS_QT1, MK450538; 38—2638A, NC_007051; 39—vB_SepiS-φIPLA5, JN192400; 40—CNPH82, DQ831957; 41—vB_SepiS-φIPLA7 JN192401; 42—PH15 DQ834250; 43—vB_SauS-φIPLA35 EU861005; 44—3A AY954956; 45—47, AY954957; 46—φ12, AF424782; 47—φSLT, AB045978; 48—42E, AY954955; 49—φPV83, NC_002486; 50—JS01 NC_021773; 51—tp310-3, NC_009763; 52—φ13, AF424783; 53—φPVL108, AB243556; 54—φPVL-CN125, NC_012784; 55—PVL, NC_002321; 56—tp310-1, NC_009761; 57—23MRA, NC_028775; 58—φNM3, NC_008617; 59—StauST398-4, NC_023499; 60—φN315, NC_004740; 61—φBU01, NC_026016; 62—P954, NC_013195; 63—77, AY508486; 64—φSa119, NC_025460; 65—φ5967PVL, NC_019921.

3.7. Genome Description of Propagating Strain for Phage QT1

The whole-genome sequencing of propagating strain *S. pseudintermedius* 625 confirmed that phage QT1 was not induced from this strain and was probably free in the mixture with stock culture. However, two prophages other than QT1 are present in the genome of *S. pseudintermedius* 625. The genome of

S. pseudintermedius strain 625 contains several virulence genes (Table S3). Strain 625 harbours a p222-like plasmid designated as p222-like_Sps625, which is 346 bp longer than p222 and similarly encodes the inducible bacteriocin BacSp222, which is cytotoxic for both gram-positive bacteria and mammalian cells [57]. Six contigs no. 25, 30, 31, 38, 39 and 47 are aligned to a pRE25-like element, described as a mobile genetic element that confers resistance to multiple antibiotics in *S. pseudintermedius* and originating from *Enterococcus* spp. [58].

4. Discussion

Many *S. pseudintermedius* isolates predating the description of SIG members are misclassified as *S. aureus* due to the positive plasma coagulase reaction. Also, in propagation strains for *Fibralongavirus* phages, the test for the activity of a clumping factor was positive and the plasmacoagulase test was positive but delayed. Therefore, molecular techniques or MALDI-TOF MS are crucial for the correct differentiation between *S. aureus* and *S. pseudintermedius* [2]. Here, we document a similar case for the host strain HER1283 for phage 2638A, which was described as *S. aureus* prior to the description of *S. pseudintermedius* species, and based on the *rpoB* gene sequencing [59], we confirmed that phage 2638A isolated in the 1980s is a *S. pseudintermedius* phage (Figure 2). Recent advances in diagnostic techniques enable the correct classification of propagating strains, and there is a good chance that hosts of the original phage isolates would belong to different species than those formerly reported.

The host range of the two members of *Fibralongavirus* is different, but narrow (Table S1). Their adsorption kinetics (Figure S1) show that the phages also adsorb onto a resistant strain, suggesting that bacterial resistance is not caused by the absence of a receptor. CRISPR spacers targeting both 2638A and QT1 were found in published *S. pseudintermedius* genomes SP079 and ED99 [60,61], which may be the reason for bacterial resistance to the phages. The CRISPR spacer is identical in both strains and targets the DNA primase gene of *Fibralongavirus*.

When testing lytic activity using high phage titers 10^8 – 10^{10} PFU mL⁻¹ inhibition of growth was observed, which could mean the presence of tail-associated hydrolases or an abortive infection system [62], although no further experiments were conducted to analyse the mechanism of non-productive phage infection. This phenomenon was not caused by bacteriocin production, as confirmed by testing the antimicrobial activity of the supernatant from the bacterial culture and filtered phage lysate.

There are different approaches to describing the structure of staphylococcal phage genomes [63]. One way to classify phages without comparing modules is by describing the physical ends of the genome. The structure of the DNA packaging and head morphogenesis module was used to discriminate *cos* (Sfi21-like phages) from *pac* (Sfi11-like phages) phages [64]. The presence of a gene for homing endonuclease close to the gene for the small terminase is important for *cos* phages [65]. Phages QT1 and 2638A both support these characteristics for *cos* phages. It is similarly true for *Staphylococcus aureus* phage 77, which is their closest neighbour according to the phylogeny of Mcp and TerL (Figure 5). Siphophages mediate generalized transduction even to phage-resistant strains, [18] however we have not observed any bacterial sequences in phage sequencing reads in agreement with previous studies showing that *cos* phages transduce at low frequencies [21].

There is a major difference between phages QT1 and 2638A in the integration module (Figure 4). Although the domain structure of the integrases is identical (AP2 binding, SAM-like and catalytic domains), the amino acid sequence is dissimilar, and prophages integrate into different loci in the genome. A prophage that contains an identical integrase to phage QT1 is integrated into tRNA^{Ser} between the genes encoding for the ComK and SdrD proteins in the genome of *S. pseudintermedius* SL/154 [66]. In contrast, an integrase identical to that of phage 2638A is inserted into the gene for tRNA^{Arg} between genes encoding for the ClpP and WhiA proteins in the genome of *S. pseudintermedius* 104N (GenBank assembly accession number GCF_002847235).

The replication module is similar for both phages. The single-strand binding protein QBJ05148 was originally predicted to be a DUF2815-containing protein, but after tertiary structural prediction the

model fitted the solved structure of an *Enterobacter* phage Enc34 single-strand binding protein [67] (PDB accession 5ODK). The domain of unknown function DUF2815 might become obsolete. There are minor differences between QT1 and 2638A in their DNA metabolism modules, especially in the presence of two predicted methyltransferases in the genome of phage QT1. The existence of methylases in staphylococcal phage genomes was observed at phages 80 or ϕ 42 [68,69], however methylases are not widely distributed among staphylococcal phages. The role of methyltransferases in the phage genome is unknown. It is expected that methyltransferases protect the phage DNA from host restriction [70] or when the phage undergo lysogenic cycle, the lysogenic bacteria might become resistant to the infection by next phages [68]. Experiments with methylation-sensitive restriction endonucleases showed that DNA was cleaved. The reason might be that either different sites are methylated, the methyltransferases are dysfunctional, or methyltransferases process a different substrate than genomic DNA

Structural proteins were confirmed by both SDS-PAGE analysis and mass spectrometry (Figure 3; Table S2). The major capsid protein of QT1 is similar to the HK97 family of major capsid proteins but has a shorter Δ -domain consisting of approximately 60 residues. This domain is proteolytically cleaved by the adjacent protease and is not present in the mature virion. A hypothetical protein (GenBank accession QBJ05123) was detected via LC-MS/MS analysis. The position of this gene close to the tail length tape-measure protein (Tmp) was expected to act as a chaperone for Tmp during the assembly of the tail [71], but it seems that this protein might be somehow included in the structure of the tail itself.

The gene for the tail length tape-measure protein is the longest gene in the genome and Tmp is expected to work as a ruler to determine the length of the phage tail. With uniform coverage from the mass spectrometer, all domains are present in the virus particle. Thus, domains predicted to be a lysozyme-like domain and M23 peptidase domain may degrade peptidoglycan in a similar way as in phage ν B_SauS- ϕ IPLA35 [72] and could be a possible candidate protein for enzymatics.

The central long tail fibre is distinctive for *Fibralongavirus* morphology (Figure 1). The full length of the tail fibre in the mature virion is supported by SDS-PAGE, where the corresponding band is visible in the untruncated length (162 kDa) corresponding to 1419 residues (Figure 3). The tail fibre from phage 2638A is 265 residues shorter (132 kDa) than the tail fibre from QT1, which manifests as a 17 nm shorter fibre under electron microscopy. With internal chaperon domain, there is probably no need for next tail fibre assembly protein as is the case with many other phages [73]. This long tail fibre might play a role in fast adsorption that was observed even on a phage resistant strain, or its length is required to attach to a membrane receptor under thick *S. pseudintermedius* cell wall [74]. Long tail fibres were described in *Bacillus* viruses γ and $W\beta$, *Escherichia* virus T5, *Salmonella* virus χ , and similar phages. Genetic analysis of *Bacillus* viruses γ and $W\beta$ observed the tail fibre gene to be a mutation hotspot for host tropism and tail fibre mutations leading to larger plaque size [75]. In *Salmonella* virus χ , the long tail fibre serves for reversible adsorption to the flagellum of bacteria [76]. *Staphylococcus* lacks flagella, but this tail fibre might serve as an initial reversible binding receptor. After initial adsorption, a second unidentified receptor at the base of the tail might irreversibly bind to the host cell and mediate DNA ejection. The C terminal end of the tail fibre protein contains an intramolecular chaperone auto-processing domain. This domain mediates auto-proteolysis when is in trimeric form [55]. This might suggest another mechanism of adsorption. A change in the conformation after the initial contact of the tail fibre with the target molecule might activate the auto-processing domain and cleave the tail fibre, releasing another binding site that would irreversibly bind to bacteria. This approach would not require the presence of another protein in the genome of the phage.

The holins of both phages are almost identical. A major work that described phage 2638A was predominantly focused on the endolysin from this phage, because of its dissimilarity to other *S. aureus* endolysins [77–80]. The high amino-acid identity (95.7%–97.1%) of endolysins of phages 2638A, QT1, and the ϕ SP119-1 prophage [56] indicate that endolysins of *Fibralongavirus* have similar properties. The endolysin of 2638A has a secondary translational start [77] mediated by a leucine codon (TTG) at position 180, which is common in the *Fibralongavirus* genus. We assume that two variants of endolysin are produced. The secondary translational start of QT1 has an identical sequence 18 nt prior and

after the secondary starting codon. One endolysin variant contains the M23 peptidase, amidase and SH3 binding domains, and the other one is composed only of the amidase and SH3 binding domains. Although the endolysin of phage 2638A comes from *S. pseudintermedius*, it was used to protect mice from methicillin-resistant *S. aureus* and performed exceptionally well, protecting up to 100% of infected mice [79]. Applied research of the endolysin from QT1 would be beneficial for the further improvement of enzybiotics.

Most of the work on the classification of staphylococcal siphoviruses focuses on *S. aureus*, and the only non-*S. aureus* phage genus in ICTV taxonomy is *Sextaevirus* of *Staphylococcus epidermidis*. However, further work is needed on the taxonomical position of non-*S. aureus* phages such as vB_SepiS-φIPLA5, vB_SepiS-φIPLA7, CNPH82 and PH15 that infect *S. epidermidis* [81,82] and are visible as a separate cluster (Figure 6). The description of the genus *Fibralongavirus* increases the number of known non-*S. aureus* genera and expands the current knowledge about the diversity of medically important non-*S. aureus* phages. The next member of genus *Fibralongavirus* could be prophage φSP119-1 (GenBank accession MK075004), if it can be induced. Along with the genus *Fibralongavirus*, there are at least two other clusters in *S. pseudintermedius* phages available in GenBank (Figure S4) and more research should be focused on those genera.

Considering the clinical background and presence of virulence factors in the genome of propagating strain 625, a different, safer propagating strain would be needed for the application of phages in therapy. The use of phages that contain integrase for phage therapy is unfavourable [83], however the described phage QT1 is active against clinical strains of *S. pseudintermedius* and could be used until a polyvalent phage is described and can be used as a gene source for enzybiotics.

Supplementary Materials: The following are available online at <http://www.mdpi.com/1999-4915/11/12/1143/s1>: Figure S1: Adsorption curves for phage QT1 on different *Staphylococcus pseudintermedius* strains; Figure S2: Cryo-EM micrograph of phage QT1; Figure S3: Pulsed-field gel electrophoresis image of separated concatemers of phage QT1 genome; Figure S4: Heatmap of phages and prophages of *Staphylococcus pseudintermedius*; Table S1: Host range of phages QT1 and 2638A, and strain isolation source; Table S2: Proteomic report of proteins detected in LC-MS/MS; Table S3: Virulence factors detected in the genome of *Staphylococcus pseudintermedius* strain 625.

Author Contributions: M.Z. and R.P. isolated phage and designed the study. M.Z. performed the microbiological characterization of phages. Whole-genome sequencing was performed by M.Z. and V.V., P.R., Z.Z. and M.Z. did the proteomic analysis. V.R. did the phenotypic tests of the propagation strain. P.B. and M.Z. did the electron microscopy. All the authors analysed data. M.Z. and R.P. wrote the manuscript. All the authors reviewed and approved the final manuscript.

Funding: The study was supported by the Ministry of Health of the Czech Republic (16-29916A). CIISB research infrastructure project (LM2015043) and the project CEITEC 2020 (LQ1601), funded by MEYS CR, are gratefully acknowledged for the financial support of the measurements at the Cryo-electron Microscopy and Tomography CF and the LC-MS/MS measurements at the Proteomics Core Facility. Students participating in this work were supported by the Grant Agency of Masaryk University (MUNI/A/0958/2018).

Conflicts of Interest: The authors declare no conflict of interest.

References

1. Sasaki, T.; Kikuchi, K.; Tanaka, Y.; Takahashi, N.; Kamata, S.; Hiramatsu, K. Reclassification of phenotypically identified *Staphylococcus intermedius* strains. *J. Clin. Microbiol.* **2007**, *45*, 2770–2778. [[CrossRef](#)] [[PubMed](#)]
2. Bannoehr, J.; Franco, A.; Iurescia, M.; Battisti, A.; Fitzgerald, J.R. Molecular diagnostic identification of *Staphylococcus pseudintermedius*. *J. Clin. Microbiol.* **2009**, *47*, 469–471. [[CrossRef](#)] [[PubMed](#)]
3. Švec, P.; Pantůček, R.; Petráš, P.; Sedláček, I.; Nováková, D. Identification of *Staphylococcus* spp. using (GTG)₅-PCR fingerprinting. *Syst. Appl. Microbiol.* **2010**, *33*, 451–456. [[CrossRef](#)] [[PubMed](#)]
4. Bannoehr, J.; Ben Zakour, N.L.; Waller, A.S.; Guardabassi, L.; Thoday, K.L.; van den Broek, A.H.; Fitzgerald, J.R. Population genetic structure of the *Staphylococcus intermedius* group: Insights into *agr* diversification and the emergence of methicillin-resistant strains. *J. Bacteriol.* **2007**, *189*, 8685–8692. [[CrossRef](#)] [[PubMed](#)]
5. Bannoehr, J.; Guardabassi, L. *Staphylococcus pseudintermedius* in the dog: Taxonomy, diagnostics, ecology, epidemiology and pathogenicity. *Vet. Dermatol.* **2012**, *23*, 253–e52. [[CrossRef](#)] [[PubMed](#)]

6. Börjesson, S.; Gómez-Sanz, E.; Ekström, K.; Torres, C.; Grönlund, U. *Staphylococcus pseudintermedius* can be misdiagnosed as *Staphylococcus aureus* in humans with dog bite wounds. *Eur. J. Clin. Microbiol. Infect. Dis.* **2014**, *34*, 839–844. [CrossRef] [PubMed]
7. Riegel, P.; Jesel-Morel, L.; Laventie, B.; Boisset, S.; Vandenesch, F.; Prévost, G. Coagulase-positive *Staphylococcus pseudintermedius* from animals causing human endocarditis. *Int. J. Med. Microbiol.* **2011**, *301*, 237–239. [CrossRef]
8. Van Duijkeren, E.; Catry, B.; Greko, C.; Moreno, M.A.; Pomba, M.C.; Pyoral, S.; Ruzauskas, M.; Sanders, P.; Threlfall, E.J.; Torren-Edo, J.; et al. Review on methicillin-resistant *Staphylococcus pseudintermedius*. *J. Antimicrob. Chemother.* **2011**, *66*, 2705–2714. [CrossRef]
9. European Medicines Agency (EMA). Reflection Paper on Methicillin-Resistant *Staphylococcus pseudintermedius* EMEA/CVMP/SAGAM/736964/2009. Available online: <https://www.ema.europa.eu/en/methicillin-resistant-staphylococcus-pseudintermedius> (accessed on 13 November 2019).
10. Kawano, J.; Shimizu, A.; Kimura, S.; Blouse, L. Experimental bacteriophage set for typing *Staphylococcus intermedius*. *Zentralbl. Bakteriolog. Mikrobiol. Hyg. A* **1982**, *253*, 321–330. [CrossRef]
11. Overturf, G.D.; Talan, D.A.; Singer, K.; Anderson, N.; Miller, J.I.; Greene, R.T.; Froman, S. Phage typing of *Staphylococcus intermedius*. *J. Clin. Microbiol.* **1991**, *29*, 373–375.
12. Wakita, Y.; Shimizu, A.; Hájek, V.; Kawano, J.; Yamashita, K. Characterization of *Staphylococcus intermedius* from pigeons, dogs, foxes, mink, and horses by pulsed-field gel electrophoresis. *J. Vet. Med. Sci.* **2002**, *64*, 237–243. [CrossRef] [PubMed]
13. Leskinen, K.; Tuomala, H.; Wicklund, A.; Horsma-Heikkinen, J.; Kuusela, P.; Skurnik, M.; Kiljunen, S. Characterization of vB_SauM-fRuSau02, a Twort-like bacteriophage isolated from a therapeutic phage cocktail. *Viruses* **2017**, *9*, 258. [CrossRef] [PubMed]
14. Moodley, A.; Kot, W.; Nälgård, S.; Jakociune, D.; Neve, H.; Hansen, L.H.; Guardabassi, L.; Vogensen, F.K. Isolation and characterization of bacteriophages active against methicillin-resistant *Staphylococcus pseudintermedius*. *Res. Vet. Sci.* **2019**, *122*, 81–85. [CrossRef] [PubMed]
15. Melter, O.; Švec, P.; Tkadlec, J.; Doškař, J.; Kinská, H.; Pantůček, R. Characterisation of methicillin-susceptible *Staphylococcus pseudintermedius* isolates from canine infections and determination of virulence factors using multiplex PCR. *Vet. Med.* **2017**, *62*, 81–89. [CrossRef]
16. Mališová, L.; Šafránková, R.; Kečliková, J.; Petráš, P.; Žemličková, H.; Jakubů, V. Correct species identification (reclassification in CNCTC) of strains of *Staphylococcus intermedius*-group can improve an insight into their evolutionary history. *Folia Microbiol.* **2018**, *64*, 231–236. [CrossRef] [PubMed]
17. Hyman, P.; Abedon, S.T. Practical Methods for Determining Phage Growth Parameters. In *Bacteriophages. Methods in Molecular Biology*; Clokie, M.R., Kropinski, A.M., Eds.; Humana Press: New York, NY, USA, 2009; Volume 501, pp. 175–202. [CrossRef]
18. Mašlaňová, I.; Stříbná, S.; Doškař, J.; Pantůček, R. Efficient plasmid transduction to *Staphylococcus aureus* strains insensitive to the lytic action of transducing phage. *FEMS Microbiol. Lett.* **2016**, *363*, fnw211. [CrossRef] [PubMed]
19. Subcommittee on Taxonomy of Staphylococci and Micrococci. Recommendations. *Int. Bull. Bacteriol. Nomencl. Taxon.* **1965**, *15*, 109–110. [CrossRef]
20. Cadness-Graves, B.; Williams, R.; Harper, G.J.; Miles, A.A. Slide-test for coagulase-positive staphylococci. *Lancet* **1943**, *241*, 736–738. [CrossRef]
21. Mašlaňová, I.; Doškař, J.; Varga, M.; Kuntová, L.; Mužík, J.; Malúšková, D.; Růžičková, V.; Pantůček, R. Bacteriophages of *Staphylococcus aureus* efficiently package various bacterial genes and mobile genetic elements including SCC_{mec} with different frequencies. *Environ. Microbiol. Rep.* **2013**, *5*, 66–73. [CrossRef]
22. Mellmann, A.; Becker, K.; von Eiff, C.; Keckevoet, U.; Schumann, P.; Harmsen, D. Sequencing and staphylococci identification. *Emerging Infect. Dis.* **2006**, *12*, 333–336. [CrossRef]
23. Andrews, S. FastQC: A Quality Control Tool for High Throughput Sequence Data. Babraham Bioinformatics, Babraham Institute, Cambridge, UK. Available online: <https://www.bioinformatics.babraham.ac.uk/projects/fastqc/> (accessed on 3 June 2018).
24. Nurk, S.; Bankevich, A.; Antipov, D.; Gurevich, A.; Korobeynikov, A.; Lapidus, A.; Prjibelsky, A.; Pyshkin, A.; Sirotkin, A.; Sirotkin, Y.; et al. Assembling Genomes and Mini-Metagenomes from Highly Chimeric Reads. In *Research in Computational Molecular Biology*; Minghua, D., Rui, J., Fengzhu, S., Xuegong, Z., Eds.; Springer: Berlin, Germany, 2013; Volume 7821, pp. 158–170. [CrossRef]

25. Gurevich, A.; Saveliev, V.; Vyahhi, N.; Tesler, G. QUAST: Quality assessment tool for genome assemblies. *Bioinformatics* **2013**, *29*, 1072–1075. [[CrossRef](#)] [[PubMed](#)]
26. Okonechnikov, K.; Golosova, O.; Fursov, M. Unipro UGENE: A unified bioinformatics toolkit. *Bioinformatics* **2012**, *28*, 1166–1167. [[CrossRef](#)] [[PubMed](#)]
27. Myers, E.W.; Miller, W. Optimal alignments in linear space. *Comput. Appl. Biosci.* **1988**, *4*, 11–17. [[CrossRef](#)] [[PubMed](#)]
28. Besemer, J. Heuristic approach to deriving models for gene finding. *Nucleic Acids Res.* **1999**, *27*, 3911–3920. [[CrossRef](#)]
29. Brettin, T.; Davis, J.J.; Disz, T.; Edwards, R.A.; Gerdes, S.; Olsen, G.J.; Olson, R.; Overbeek, R.; Parrello, B.; Pusch, G.D.; et al. RASTtk: A modular and extensible implementation of the RAST algorithm for building custom annotation pipelines and annotating batches of genomes. *Sci. Rep.* **2015**, *5*, 8365. [[CrossRef](#)]
30. Grazziotin, A.L.; Koonin, E.V.; Kristensen, D.M. Prokaryotic Virus Orthologous Groups (pVOGs): A resource for comparative genomics and protein family annotation. *Nucleic Acids Res.* **2017**, *45*, D491–D498. [[CrossRef](#)]
31. Marchler-Bauer, A.; Bo, Y.; Han, L.; He, J.; Lanczycki, C.J.; Lu, S.; Chitsaz, F.; Derbyshire, M.K.; Geer, R.C.; Gonzales, N.R.; et al. CDD/SPARCLE: Functional classification of proteins via subfamily domain architectures. *Nucleic Acids Res.* **2017**, *45*, D200–D203. [[CrossRef](#)]
32. Mitchell, A.L.; Attwood, T.K.; Babbitt, P.C.; Blum, M.; Bork, P.; Bridge, A.; Brown, S.D.; Chang, H.-Y.; El-Gebali, S.; Fraser, M.I.; et al. InterPro in 2019: Improving coverage, classification and access to protein sequence annotations. *Nucleic Acids Res.* **2019**, *47*, D351–D360. [[CrossRef](#)]
33. Lowe, T.M.; Chan, P.P. tRNAscan-SE on-line: Integrating search and context for analysis of transfer RNA genes. *Nucleic Acids Res.* **2016**, *44*, W54–W57. [[CrossRef](#)]
34. Lagesen, K.; Hallin, P.; Rødland, E.A.; Stærfeldt, H.H.; Rognes, T.; Ussery, D.W. RNAmmer: Consistent and rapid annotation of ribosomal RNA genes. *Nucleic Acids Res.* **2007**, *35*, 3100–3108. [[CrossRef](#)]
35. Finn, R.D.; Clements, J.; Eddy, S.R. HMMER web server: Interactive sequence similarity searching. *Nucleic Acids Res.* **2011**, *39*, W29–W37. [[CrossRef](#)] [[PubMed](#)]
36. Seemann, T. Abricate: Mass Screening of Contigs for Antimicrobial and Virulence Genes. Department of Microbiology and Immunology, The University of Melbourne, Melbourne, Australia. Available online: <https://github.com/tseemann/abicate> (accessed on 28 February 2019).
37. Jia, B.; Raphenya, A.R.; Alcock, B.; Waglechner, N.; Guo, P.; Tsang, K.K.; Lago, B.A.; Dave, B.M.; Pereira, S.; Sharma, A.N.; et al. CARD 2017: Expansion and model-centric curation of the comprehensive antibiotic resistance database. *Nucleic Acids Res.* **2017**, *45*, D566–D573. [[CrossRef](#)] [[PubMed](#)]
38. Zankari, E.; Hasman, H.; Cosentino, S.; Vestergaard, M.; Rasmussen, S.; Lund, O.; Aarestrup, F.M.; Larsen, M.V. Identification of acquired antimicrobial resistance genes. *J. Antimicrob. Chemother.* **2012**, *67*, 2640–2644. [[CrossRef](#)] [[PubMed](#)]
39. Feldgarden, M.; Brover, V.; Haft, D.H.; Prasad, A.B.; Slotta, D.J.; Tolstoy, I.; Tyson, G.H.; Zhao, S.; Hsu, C.-H.; McDermott, P.F.; et al. Validating the AMRFinder tool and resistance gene database by using antimicrobial resistance genotype-phenotype correlations in a collection of isolates. *Antimicrob. Agents Chemother.* **2019**, *63*, e00483-19. [[CrossRef](#)] [[PubMed](#)]
40. Gupta, S.K.; Padmanabhan, B.R.; Diene, S.M.; Lopez-Rojas, R.; Kempf, M.; Landraud, L.; Rolain, J.M. ARG-ANNOT, a new bioinformatic tool to discover antibiotic resistance genes in bacterial genomes. *Antimicrob. Agents Chemother.* **2014**, *58*, 212–220. [[CrossRef](#)]
41. Chen, L.; Zheng, D.; Liu, B.; Yang, J.; Jin, Q. VFDB 2016: Hierarchical and refined dataset for big data analysis—10 years on. *Nucleic Acids Res.* **2016**, *44*, D694–D697. [[CrossRef](#)]
42. Drozdetskiy, A.; Cole, C.; Procter, J.; Barton, G.J. JPred4: A protein secondary structure prediction server. *Nucleic Acids Res.* **2015**, *43*, W389–W394. [[CrossRef](#)]
43. Gautier, R.; Douguet, D.; Antonny, B.; Drin, G. HELIQUEST: A web server to screen sequences with specific α -helical properties. *Bioinformatics* **2008**, *24*, 2101–2102. [[CrossRef](#)]
44. Yang, J.; Yan, R.; Roy, A.; Xu, D.; Poisson, J.; Zhang, Y. The I-TASSER Suite: Protein structure and function prediction. *Nat. Methods* **2014**, *12*, 7–8. [[CrossRef](#)]
45. Sullivan, M.J.; Petty, N.K.; Beatson, S.A. Easyfig: A genome comparison visualizer. *Bioinformatics* **2011**, *27*, 1009–1010. [[CrossRef](#)]

46. Lemoine, F.; Correia, D.; Lefort, V.; Doppelt-Azeroual, O.; Mareuil, F.; Cohen-Boulakia, S.; Gascuel, O. NGPhylogeny.fr: New generation phylogenetic services for non-specialists. *Nucleic Acids Res.* **2019**, *47*, W260–W265. [[CrossRef](#)] [[PubMed](#)]
47. Rambaut, A. FigTree: Produce High-Quality Figures of Phylogenetic Trees. Institute of Evolutionary Biology, University of Edinburgh, Edinburgh, UK. Available online: <http://tree.bio.ed.ac.uk/software/figtree/> (accessed on 9 August 2019).
48. Ahmed, N.; Ågren, J.; Sundström, A.; Häfström, T.; Segerman, B. Gegenees: Fragmented alignment of multiple genomes for determining phylogenomic distances and genetic signatures unique for specified target groups. *PLoS ONE* **2012**, *7*, e39107. [[CrossRef](#)]
49. Candiano, G.; Bruschi, M.; Musante, L.; Santucci, L.; Ghiggeri, G.M.; Carnemolla, B.; Orecchia, P.; Zardi, L.; Righetti, P.G. Blue silver: A very sensitive colloidal Coomassie G-250 staining for proteome analysis. *Electrophoresis* **2004**, *25*, 1327–1333. [[CrossRef](#)] [[PubMed](#)]
50. Wiśniewski, J.R.; Ostasiewicz, P.; Mann, M. High recovery FASP applied to the proteomic analysis of microdissected formalin fixed paraffin embedded cancer tissues retrieves known colon cancer markers. *J. Proteome Res.* **2011**, *10*, 3040–3049. [[CrossRef](#)]
51. Stejskal, K.; Potěšil, D.; Zdráhal, Z. Suppression of peptide sample losses in autosampler vials. *J. Proteome Res.* **2013**, *12*, 3057–3062. [[CrossRef](#)]
52. Kwan, T.; Liu, J.; DuBow, M.; Gros, P.; Pelletier, J. The complete genomes and proteomes of 27 *Staphylococcus aureus* bacteriophages. *Proc. Natl Acad. Sci. USA* **2005**, *102*, 5174–5179. [[CrossRef](#)]
53. Slopek, S.; Krzywy, T. Morphology and ultrastructure of bacteriophages. An electron microscopic study. *Arch. Immunol. Ther. Exp.* **1985**, *33*, 12–17.
54. Lopes, A.; Tavares, P.; Petit, M.A.; Guérois, R.; Zinn-Justin, S. Automated classification of tailed bacteriophages according to their neck organization. *BMC Genom.* **2014**, *15*, 1027. [[CrossRef](#)]
55. Schulz, E.C.; Dickmanns, A.; Urlaub, H.; Schmitt, A.; Mühlhoff, M.; Stummeyer, K.; Schwarzer, D.; Gerardy-Schahn, R.; Ficner, R. Crystal structure of an intramolecular chaperone mediating triple- β -helix folding. *Nat. Struct. Mol. Biol.* **2010**, *17*, 210–215. [[CrossRef](#)]
56. Wipf, J.R.K.; Deutsch, D.R.; Westblade, L.F.; Fischetti, V.A.; Putonti, C. Genome sequences of six prophages isolated from *Staphylococcus pseudintermedius* strains recovered from human and animal clinical specimens. *Microbiol. Res. Announc.* **2019**, *8*, e00387-19. [[CrossRef](#)]
57. Nowakowski, M.; Jaremko, Ł.; Wladyka, B.; Dubin, G.; Ejchart, A.; Mak, P. Spatial attributes of the four-helix bundle group of bacteriocins – The high-resolution structure of BacSp222 in solution. *Int. J. Biol. Macromol.* **2018**, *107*, 2715–2724. [[CrossRef](#)] [[PubMed](#)]
58. Kang, J.H.; Hwang, C.Y. First detection of multiresistance pRE25-like elements from *Enterococcus* spp. in *Staphylococcus pseudintermedius* isolated from canine pyoderma. *J. Glob. Antimicrob. Resist.* **2020**, in press. [[CrossRef](#)] [[PubMed](#)]
59. Drancourt, M.; Raoult, D. *rpoB* gene sequence-based identification of *Staphylococcus* species. *J. Clin. Microbiol.* **2002**, *40*, 1333–1338. [[CrossRef](#)] [[PubMed](#)]
60. Azam, A.H.; Kadoi, K.; Miyanaga, K.; Usui, M.; Tamura, Y.; Cui, L.; Tanji, Y. Analysis host-recognition mechanism of staphylococcal kayvirus ϕ SA039 reveals a novel strategy that protects *Staphylococcus aureus* against infection by *Staphylococcus pseudintermedius* Siphoviridae phages. *Appl. Microbiol. Biotechnol.* **2019**, *103*, 6809–6823. [[CrossRef](#)] [[PubMed](#)]
61. Ben Zakour, N.L.; Beatson, S.A.; van den Broek, A.H.M.; Thoday, K.L.; Fitzgerald, J.R. Comparative genomics of the *Staphylococcus intermedius* group of animal pathogens. *Front. Cell. Infect. Microbiol.* **2012**, *2*, 44. [[CrossRef](#)]
62. Abedon, S.T. Lysis from without. *Bacteriophage* **2014**, *1*, 46–49. [[CrossRef](#)]
63. Ingmer, H.; Gerlach, D.; Wolz, C. Temperate phages of *Staphylococcus aureus*. *Microbiol. Spectrum* **2019**, *7*. [[CrossRef](#)]
64. Brüssow, H.; Desiere, F. Comparative phage genomics and the evolution of Siphoviridae: Insights from dairy phages. *Mol. Microbiol.* **2001**, *39*, 213–223. [[CrossRef](#)]
65. Quiles-Puchalt, N.; Carpena, N.; Alonso, J.C.; Novick, R.P.; Marina, A.; Penadés, J.R. Staphylococcal pathogenicity island DNA packaging system involving *cos*-site packaging and phage-encoded HNH endonucleases. *Proc. Natl Acad. Sci. USA* **2014**, *111*, 6016–6021. [[CrossRef](#)]

66. Becker, K.; Verstappen, K.M.; Huijbregts, L.; Spaninks, M.; Wagenaar, J.A.; Fluit, A.C.; Duim, B. Development of a real-time PCR for detection of *Staphylococcus pseudintermedius* using a novel automated comparison of whole-genome sequences. *PLoS ONE* **2017**, *12*, e0183925. [[CrossRef](#)]
67. Cernooka, E.; Rumnieks, J.; Tars, K.; Kazaks, A. Structural basis for DNA recognition of a single-stranded DNA-binding protein from *Enterobacter* phage Enc34. *Sci. Rep.* **2017**, *7*, 15529. [[CrossRef](#)] [[PubMed](#)]
68. Dempsey, R.M. *Sau42I*, a II-like restriction-modification system encoded by the *Staphylococcus aureus* quadruple-converting phage $\phi 42$. *Microbiology* **2005**, *151*, 1301–1311. [[CrossRef](#)] [[PubMed](#)]
69. Christie, G.E.; Matthews, A.M.; King, D.G.; Lane, K.D.; Olivarez, N.P.; Tallent, S.M.; Gill, S.R.; Novick, R.P. The complete genomes of *Staphylococcus aureus* bacteriophages 80 and 80 α —Implications for the specificity of SaPI mobilization. *Virology* **2010**, *407*, 381–390. [[CrossRef](#)] [[PubMed](#)]
70. Kossykh, V.G.; Schlagman, S.L.; Hattman, S. Phage T4 DNA [N]-adenine⁶ methyltransferase. Overexpression, purification, and characterization. *J. Biol. Chem.* **1995**, *270*, 14389–14393. [[CrossRef](#)]
71. Xu, J.; Hendrix, R.W.; Duda, R.L. Chaperone–protein interactions that mediate assembly of the bacteriophage λ tail to the correct length. *J. Mol. Biol.* **2014**, *426*, 1004–1018. [[CrossRef](#)]
72. Rodríguez-Rubio, L.; Gutiérrez, D.; Martínez, B.; Rodríguez, A.; Götz, F.; García, P. The tape measure protein of the *Staphylococcus aureus* bacteriophage $\nu B_{\text{SauS-}\phi\text{IPLA35}}$ has an active muramidase domain. *Appl. Environ. Microbiol.* **2012**, *78*, 6369–6371. [[CrossRef](#)]
73. North, O.I.; Sakai, K.; Yamashita, E.; Nakagawa, A.; Iwazaki, T.; Buttner, C.R.; Takeda, S.; Davidson, A.R. Phage tail fibre assembly proteins employ a modular structure to drive the correct folding of diverse fibres. *Nat. Microbiol.* **2019**, *4*, 1645–1653. [[CrossRef](#)]
74. Neethirajan, S.; DiCicco, M. Atomic force microscopy study of the antibacterial effect of fosfomycin on methicillin-resistant *Staphylococcus pseudintermedius*. *Appl. Nanosci.* **2013**, *4*, 703–709. [[CrossRef](#)]
75. Schuch, R.; Fischetti, V.A. Detailed genomic analysis of the W β and γ phages infecting *Bacillus anthracis*: Implications for evolution of environmental fitness and antibiotic resistance. *J. Bacteriol.* **2006**, *188*, 3037–3051. [[CrossRef](#)]
76. Schade, S.Z.; Adler, J.; Ris, H. How bacteriophage χ attacks motile bacteria. *J. Virol.* **1967**, *1*, 599–609.
77. Abaev, I.; Foster-Frey, J.; Korobova, O.; Shishkova, N.; Kiseleva, N.; Kopylov, P.; Pryamchuk, S.; Schmelcher, M.; Becker, S.C.; Donovan, D.M. Staphylococcal phage 2638A endolysin is lytic for *Staphylococcus aureus* and harbors an inter-lytic-domain secondary translational start site. *Appl. Microbiol. Biotechnol.* **2012**, *97*, 3449–3456. [[CrossRef](#)] [[PubMed](#)]
78. Becker, S.C.; Foster-Frey, J.; Stodola, A.J.; Anacker, D.; Donovan, D.M. Differentially conserved staphylococcal SH3b_5 cell wall binding domains confer increased staphylolytic and streptolytic activity to a streptococcal prophage endolysin domain. *Gene* **2009**, *443*, 32–41. [[CrossRef](#)] [[PubMed](#)]
79. Schmelcher, M.; Shen, Y.; Nelson, D.C.; Eugster, M.R.; Eichenseher, F.; Hanke, D.C.; Loessner, M.J.; Dong, S.; Pritchard, D.G.; Lee, J.C.; et al. Evolutionarily distinct bacteriophage endolysins featuring conserved peptidoglycan cleavage sites protect mice from MRSA infection. *J. Antimicrob. Chemother.* **2015**, *70*, 1453–1465. [[CrossRef](#)] [[PubMed](#)]
80. Kovalskaya, N.Y.; Herndon, E.E.; Foster-Frey, J.A.; Donovan, D.M.; Hammond, R.W. Antimicrobial activity of bacteriophage derived triple fusion protein against *Staphylococcus aureus*. *AIMS Microbiol.* **2019**, *5*, 158–175. [[CrossRef](#)] [[PubMed](#)]
81. Daniel, A.; Bonnen, P.E.; Fischetti, V.A. First complete genome sequence of two *Staphylococcus epidermidis* bacteriophages. *J. Bacteriol.* **2006**, *189*, 2086–2100. [[CrossRef](#)]
82. Gutiérrez, D.; Martínez, B.; Rodríguez, A.; García, P. Genomic characterization of two *Staphylococcus epidermidis* bacteriophages with anti-biofilm potential. *BMC Genom.* **2012**, *13*, 228. [[CrossRef](#)]
83. Fernández, L.; Gutiérrez, D.; García, P.; Rodríguez, A. The perfect bacteriophage for therapeutic applications—A quick guide. *Antibiotics* **2019**, *8*, 126. [[CrossRef](#)]



Supplementary materials

New genus *Fibralongavirus* in Siphoviridae phages of *Staphylococcus pseudintermedius*

Michal Zeman ¹, Pavol Bárdy ¹, Veronika Vrbovská ¹, Pavel Roudnický ², Zbyněk Zdráhal ^{2,3}, Vladislava Růžičková ¹, Jiří Doškař ¹ and Roman Pantůček ^{1,*}

¹ Department of Experimental Biology, Faculty of Science, Masaryk University, Kotlářská 2, 611 37 Brno, Czech Republic; michal.zeman91@gmail.com (M.Z.); bardy.pavol@mail.muni.cz (P.B.); veronika.vrbovska@gmail.com (V.V.); vladkar@sci.muni.cz (V.R.); doskar@sci.muni.cz (J.D.)

² Central European Institute of Technology, Masaryk University, Kamenice 5, 625 00 Brno, Czech Republic; p.roudnický@mail.muni.cz (P.R.); zdrahal@sci.muni.cz (Z.Z.)

³ National Centre for Biomolecular Research, Faculty of Science, Masaryk University, Kamenice 5, 625 00 Brno, Czech Republic

* Correspondence: pantucek@sci.muni.cz; Tel.: +420-549-49-6379 (R.P.)

This document contains supplementary materials:

Figure S1. Adsorption curves for phage QT1 on different *Staphylococcus pseudintermedius* strains.

Figure S2. Cryo-EM micrograph of phage QT1.

Figure S3. Pulsed-field gel electrophoresis image of separated concatemers of phage QT1 genome.

Figure S4. Heatmap of phages and prophages of *Staphylococcus pseudintermedius*.

Table S1. Host range of phages QT1 and 2638A, and strain isolation source.

Table S2. Proteomic report of proteins detected in LC-MS/MS.

Table S3. Virulence factors detected in the genome of *Staphylococcus pseudintermedius* strain 625.

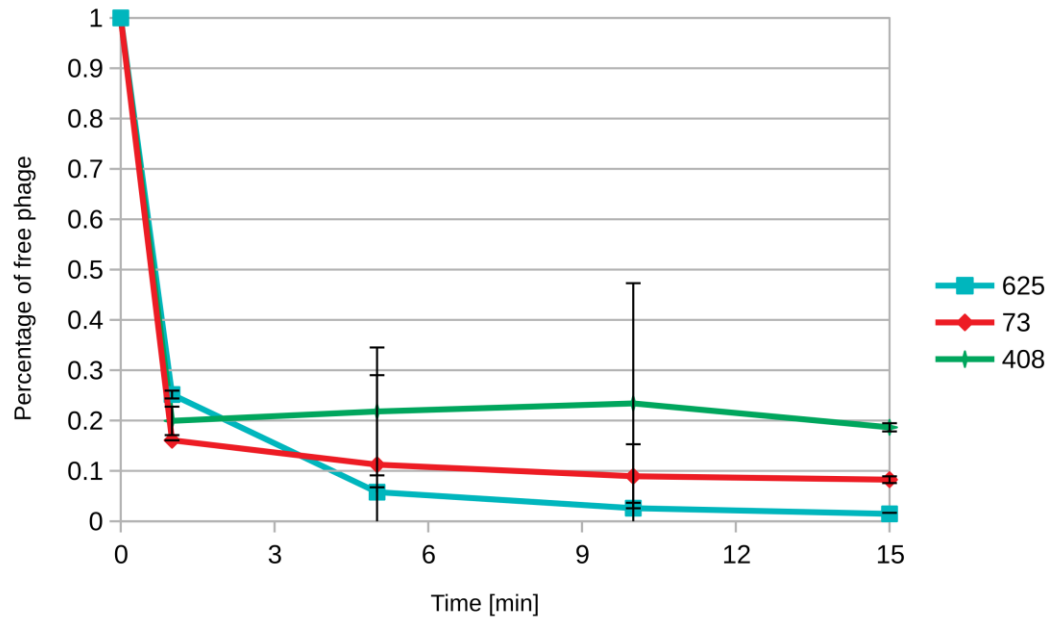


Figure S1. Adsorption curves for phage QT1 on different *Staphylococcus pseudintermedius* strains. Strain 625 is susceptible, strain 73 exhibited lysis from without, strain 408 was resistant to QT1. Points on the graph are mean values and the error bars correspond to standard deviations, based on three independent experiments.

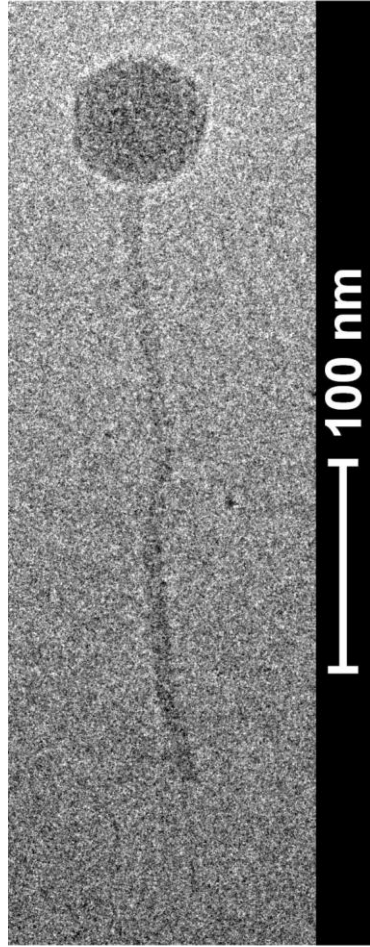


Figure S2. Cryo-EM micrograph of phage QT1. Tail fibre is barely visible on native phage.

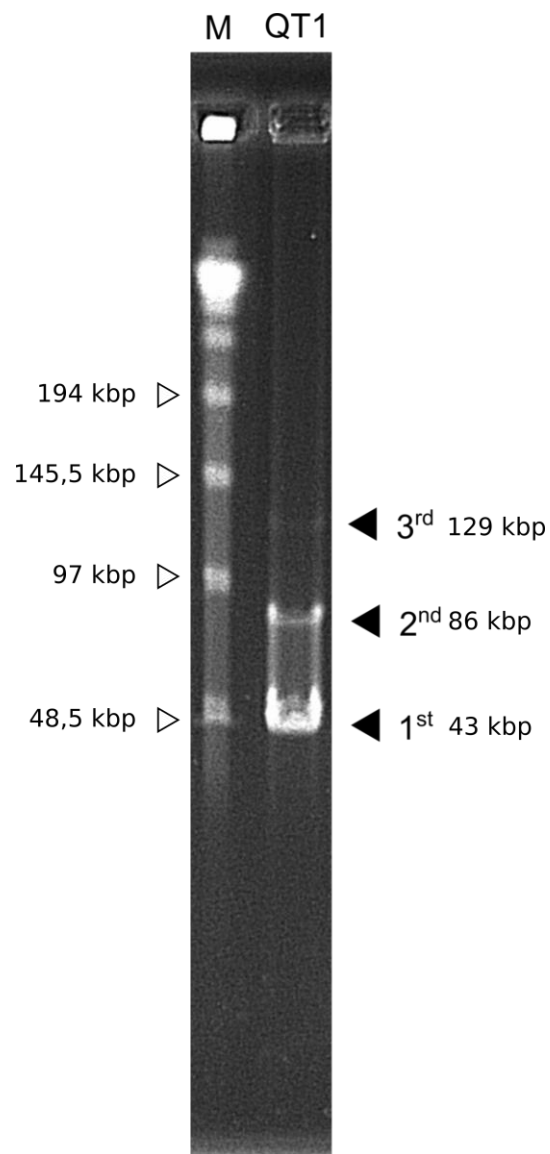


Figure S3. Pulsed-field gel electrophoresis image of separated concatemers of phage QT1 genome. At least trimers of the whole genome are visible. Lambda DNA concatemers were used as a marker (M).

	1	2	3	4	5	6	7	8	9	10	11	12	13	14	15	16	17	18	19	
1. AP019560 <i>Staphylococcus</i> phage SP120	100	62	56	49	58	57	54	56	57	57	57	43	12	9	3	1	3	1	1	
2. AP019562 <i>Staphylococcus</i> phage SP276	63	100	58	45	53	55	53	54	54	55	55	39	17	8	2	1	3	1	1	
3. KX827369 <i>Staphylococcus</i> phage SpT152	55	56	100	52	55	60	58	60	59	59	59	40	12	7	1	2	3	3	1	
4. MK075003 <i>Staphylococcus</i> phage phiSP44-1	46	42	50	100	47	53	52	55	53	53	53	45	9	4	1	2	1	1	0	
5. AP019561 <i>Staphylococcus</i> phage SP197	57	52	55	49	100	71	74	73	71	70	71	39	9	5	3	3	3	2	1	
6. KX827370 <i>Staphylococcus</i> phage SpT252	57	55	62	56	73	100	90	83	85	84	84	40	11	4	3	1	2	1	1	
7. MF428479 <i>Staphylococcus</i> phage SN11	55	53	61	56	76	90	100	90	88	87	87	40	9	3	2	1	2	2	1	
8. MF428478 <i>Staphylococcus</i> phage SN13	56	54	62	58	74	82	89	100	96	95	95	38	10	5	3	3	2	2	0	
9. MF428480 <i>Staphylococcus</i> phage SN10	58	54	62	56	73	86	89	97	100	99	99	38	9	4	3	1	2	2	0	
10. MF428481 <i>Staphylococcus</i> phage SN8	59	55	62	56	72	85	88	96	99	100	100	38	9	4	3	1	2	2	0	
11. KX827368 <i>Staphylococcus</i> phage SpT5	59	55	61	56	73	85	88	96	99	100	100	38	9	4	3	1	2	2	0	
12. MK075006 <i>Staphylococcus</i> phage phiSP119-3	39	35	37	43	37	36	37	35	35	34	34	100	11	4	6	1	10	6	1	
13. MK075002 <i>Staphylococcus</i> phage phiSP38-1	11	15	11	9	8	11	9	9	8	8	8	12	100	41	11	6	11	7	4	
14. KX827371 <i>Staphylococcus</i> phage SpT99F3	10	7	8	4	5	4	3	5	4	4	4	4	44	100	11	17	20	15	1	
15. NC_007051 <i>Staphylococcus</i> phage 2638A	2	2	1	1	3	2	2	3	3	3	3	6	11	10	100	60	55	14	1	
16. MK450538 <i>Staphylococcus</i> phage vB_SpsS_QT1	1	1	2	2	3	1	1	3	1	1	1	1	6	16	58	100	62	14	1	
17. MK075004 <i>Staphylococcus</i> phage phiSP119-1	3	3	3	1	3	2							11	18	51	60	100	13	0	
18. MK075001 <i>Staphylococcus</i> phage phiSP15-1	1	1	3	1	2	1	Fibralongavirus							14	13	13	13	100	1	
19. MK075005 <i>Staphylococcus</i> phage phiSP119-2	1	1	1	0	1	1	1	0	0	0	0	1	4	1	1	1	1	1	1	100

Figure S4. Heatmap of phages and prophages of *Staphylococcus pseudintermedius* with cluster around phage QT1 based on fragmented nucleotide sequence alignment. The proposed genus *Fibralongavirus* is highlighted in text box. Phage names and GenBank accession numbers of used phages are labelled as in NCBI.

Table S1. Host range of phages QT1 and 2638A, and strain isolation source.

Strain	Sensitivity to QT1	Sensitivity to 2638A	Source	Species	Reference or culture collection
625 [#]	+	+	Dog	<i>S. pseudintermedius</i>	Melter <i>et al.</i> , 2017
2854 (=HER 1283)	+	+	not available	<i>S. pseudintermedius</i>	HER, Slopek and Krzywy, 1985
CCM 2885	(+)	-	Healthy fox	<i>S. pseudintermedius</i>	CCM
CCM 4539	-	-	Human throat	<i>S. pseudintermedius</i>	CCM
CCM 4710	-	-	Human wound	<i>S. pseudintermedius</i>	CCM
CCM 7315 ^T	(+)	-	Cat lung	<i>S. pseudintermedius</i>	CCM
CCM 7532	-	-	Dog dermatitis	<i>S. pseudintermedius</i>	CCM
CCM 7829	(+)	-	Dog adenitis	<i>S. pseudintermedius</i>	CCM
CCM 7830	(+)	-	Dog skin	<i>S. pseudintermedius</i>	CCM
CCM 7843	-	-	Human conjunctiva	<i>S. intermedius</i>	CCM
CCM 5739 ^T	-	-	Pigeon	<i>S. intermedius</i>	CCM
29	-	-	Dog	<i>S. pseudintermedius</i>	Melter <i>et al.</i> , 2017
30	-	-	Dog	<i>S. pseudintermedius</i>	Melter <i>et al.</i> , 2017
33	(+)	-	Dog	<i>S. pseudintermedius</i>	Melter <i>et al.</i> , 2017
35	+	-	Dog	<i>S. pseudintermedius</i>	Melter <i>et al.</i> , 2017
73	-	-	Dog	<i>S. pseudintermedius</i>	Melter <i>et al.</i> , 2017
86	-	-	Dog	<i>S. pseudintermedius</i>	Melter <i>et al.</i> , 2017
105	-	-	Dog	<i>S. pseudintermedius</i>	Melter <i>et al.</i> , 2017
153	-	-	Dog	<i>S. pseudintermedius</i>	Melter <i>et al.</i> , 2017
156	-	-	Dog	<i>S. pseudintermedius</i>	Melter <i>et al.</i> , 2017
193	-	-	Dog	<i>S. pseudintermedius</i>	Melter <i>et al.</i> , 2017
236	-	-	Dog	<i>S. pseudintermedius</i>	Melter <i>et al.</i> , 2017
239	-	-	Dog	<i>S. pseudintermedius</i>	Melter <i>et al.</i> , 2017
252	-	-	Dog	<i>S. pseudintermedius</i>	Melter <i>et al.</i> , 2017
259	+	-	Dog	<i>S. pseudintermedius</i>	Melter <i>et al.</i> , 2017
279	-	-	Dog	<i>S. pseudintermedius</i>	Melter <i>et al.</i> , 2017
293	-	-	Dog	<i>S. pseudintermedius</i>	Melter <i>et al.</i> , 2017
297	-	-	Dog	<i>S. pseudintermedius</i>	Melter <i>et al.</i> , 2017
313	-	-	Dog	<i>S. pseudintermedius</i>	Melter <i>et al.</i> , 2017
383	-	-	Dog	<i>S. pseudintermedius</i>	Melter <i>et al.</i> , 2017
408	-	-	Dog	<i>S. pseudintermedius</i>	Melter <i>et al.</i> , 2017
497	-	-	Dog	<i>S. pseudintermedius</i>	Melter <i>et al.</i> , 2017
550	-	-	Dog	<i>S. pseudintermedius</i>	Melter <i>et al.</i> , 2017
552	-	-	Dog	<i>S. pseudintermedius</i>	Melter <i>et al.</i> , 2017
558	-	-	Dog	<i>S. pseudintermedius</i>	Melter <i>et al.</i> , 2017
571	-	-	Dog	<i>S. pseudintermedius</i>	Melter <i>et al.</i> , 2017
612	-	-	Dog	<i>S. pseudintermedius</i>	Melter <i>et al.</i> , 2017
621	(+)	-	Dog	<i>S. pseudintermedius</i>	Melter <i>et al.</i> , 2017
630	-	-	Dog	<i>S. pseudintermedius</i>	Melter <i>et al.</i> , 2017
666	-	-	Dog	<i>S. pseudintermedius</i>	Melter <i>et al.</i> , 2017
679	-	-	Dog	<i>S. pseudintermedius</i>	Melter <i>et al.</i> , 2017
748	-	-	Dog	<i>S. pseudintermedius</i>	Melter <i>et al.</i> , 2017
778	-	-	Dog	<i>S. pseudintermedius</i>	Melter <i>et al.</i> , 2017
802	-	-	Dog	<i>S. pseudintermedius</i>	Melter <i>et al.</i> , 2017
00/470	-	(+)	Human	<i>S. pseudintermedius</i>	Mališová <i>et al.</i> , 2019
02/172	-	-	Human	<i>S. pseudintermedius</i>	Mališová <i>et al.</i> , 2019
02/179	-	-	Human	<i>S. pseudintermedius</i>	Mališová <i>et al.</i> , 2019
02/264	-	(+)	Dog	<i>S. pseudintermedius</i>	Mališová <i>et al.</i> , 2019
02/438	-	-	Human	<i>S. pseudintermedius</i>	Mališová <i>et al.</i> , 2019
02/589	-	-	Human	<i>S. pseudintermedius</i>	Mališová <i>et al.</i> , 2019
02/682	-	(+)	Human	<i>S. pseudintermedius</i>	Mališová <i>et al.</i> , 2019
02/718	-	-	Human	<i>S. pseudintermedius</i>	Mališová <i>et al.</i> , 2019
14/858*	-	-	Tomcat wound	<i>S. pseudintermedius</i>	NRL/St
15/646*	-	-	Human skin abscess	<i>S. pseudintermedius</i>	NRL/St

+ sensitive at routine test dilution (RTD, 10⁸ PFU mL⁻¹); (+) sensitive at RTD × 100, presence of plaques was considered as positive result; - resistant; [#] propagation strain for phage QT1; * *mecA* positive isolate

CCM – Czech Collection of Microorganisms, Masaryk University, Faculty of Science, Czech Republic

NRL/St – National Reference Laboratory for Staphylococci, National Institute of Public Health, Czech Republic

HER – Félix d'Hérelle Reference Center for Bacterial Viruses, Université Laval, Canada

Table S2. Proteomic report of proteins detected in LC-MS/MS. The proteome of phage QT1 was used as a reference database.

GenBank Accession	Description	MW [kDa]	# AAs	SAF	NSAF (%)	Sum (Coverage)	Sum (# Unique Peptides)	Sum(# PSMs)
QBJ05121.1	major tail protein with YjdB Ig-like domain [vB_SpsS_QT1]	32.8	301	1.16	25.23	0.82	14	348
QBJ05114.1	portal protein [vB_SpsS_QT1]	44.6	385	0.73	15.93	0.85	34	281
QBJ05117.1	head-tail adapter protein [vB_SpsS_QT1]	11.2	96	0.59	12.96	0.85	7	57
QBJ05116.1	major capsid protein [vB_SpsS_QT1]	43.2	395	0.58	12.59	0.81	33	228
QBJ05126.1	tail component [vB_SpsS_QT1]	56.1	494	0.25	5.52	0.72	32	125
QBJ05120.1	tail completion protein [vB_SpsS_QT1]	16.1	133	0.21	4.59	0.72	9	28
QBJ05118.1	head-closure protein [vB_SpsS_QT1]	14.2	120	0.21	4.55	0.78	7	25
QBJ05127.1	structural protein [vB_SpsS_QT1]	161.5	1419	0.20	4.31	0.64	78	280
QBJ05125.1	tail length tape-measure protein [vB_SpsS_QT1]	222.1	2031	0.14	2.98	0.56	101	277
QBJ05165.1	hypothetical protein [vB_SpsS_QT1]	6.9	58	0.07	1.50	0.36	2	4
QBJ05143.1	hypothetical protein [vB_SpsS_QT1]	9.6	80	0.06	1.36	0.36	3	5
QBJ05164.1	hypothetical protein [vB_SpsS_QT1]	11.7	100	0.06	1.31	0.52	4	6
QBJ05160.1	putative methyltransferase [vB_SpsS_QT1]	18.2	154	0.05	1.13	0.32	6	8
QBJ05123.1	hypothetical protein [vB_SpsS_QT1]	13.7	119	0.04	0.92	0.45	5	5
QBJ05113.1	terminase large subunit [vB_SpsS_QT1]	64.3	553	0.04	0.87	0.34	16	22
QBJ05115.1	Clp protease [vB_SpsS_QT1]	30.4	274	0.04	0.80	0.37	7	10
QBJ05139.1	immunoprotective extracellular protein [vB_SpsS_QT1]	24.3	215	0.03	0.71	0.62	7	7
QBJ05119.1	neck protein [vB_SpsS_QT1]	15.7	133	0.03	0.66	0.24	3	4
QBJ05153.1	S-adenosyl-L-methionine-dependent methyltransferase [vB_SpsS_QT1]	26.6	225	0.02	0.48	0.14	3	5
QBJ05148.1	nucleic acid-binding protein [vB_SpsS_QT1]	19.8	184	0.02	0.36	0.21	3	3
QBJ05132.1	N-acetylmuramoyl-L-alanine amidase [vB_SpsS_QT1]	55.3	486	0.01	0.31	0.16	6	7
QBJ05149.1	DNA polymerase A with ribonuclease H-like domain [vB_SpsS_QT1]	73.8	653	0.01	0.30	0.16	9	9
QBJ05147.1	putative DNA replication ATP dependent nuclease [vB_SpsS_QT1]	44.2	388	0.01	0.28	0.12	4	5
QBJ05166.1	DNA primase [vB_SpsS_QT1]	94.2	816	0.01	0.21	0.11	7	8
QBJ05169.1	DNA helicase [vB_SpsS_QT1]	52.6	452	0.01	0.14	0.08	3	3


MW – calculated molecular weight; SAF – Spectral Abundance Factor; NSAF – Normalized Spectral Abundance Factor; PSM - peptide spectrum match

Table S3. Virulence factors detected in the genome of *Staphylococcus pseudintermedius* strain 625.

Product	Abbreviation	Locus tag	Coverage	E value	Identity	Predicted function	Best hit*
Major factors							
Leukocidin S-I, gamma-hemolysin	LukS-I	GB868_01705	100	0	100	pore forming	WP_014613568
Leukocidin F-I, gamma-hemolysin	LukF-I	GB868_01700	100	0	99.7	pore forming	WP_014613567
Phospholipase C, beta-hemolysin	Hlb	GB868_04675	90	0	74.58	pore forming	P09978
Delta-hemolysin	Hld	GB868_08280	100	2E-7	65.38	pore forming	P0A0M1
Hemolysin <i>S. pseudintermedius</i>	HISp	GB868_01530	93	4E-7	42.86	pore forming	P85219
Alpha-class phenol soluble modulins	PSM α	GB868_09320 [#]	100	2E-17	95.65	pore forming	WP_103214038
Beta-class phenol soluble modulins	PSM β	GB868_09315	100	6E-23	100	pore forming	WP_014614190
Enterotoxin C2 – bovine	SECb	GB868_07230	100	3E-122	57.6	superantigen	P34071
Enzymatic function							
Exfoliative toxin B	Etb	GB868_07225	98	7E-112	56.3	skin scalding	P09332
ATP-dependent Clp protease proteolytic subunit ClpP	ClpP	GB868_07115	99	2E-145	94.85	protease	Q5HQW0
ATP-dependent Clp protease proteolytic subunit clpB	ClpB	GB868_05635	99	0	83.37	chaperone heatshock	Q6GIB2
ATP-dependent Clp protease proteolytic subunit clpC	ClpC	GB868_04880	100	0	90.48	chaperone heatshock	Q5HRM8
ATP-dependent Clp protease proteolytic subunit clpX	ClpX	GB868_02335	100	0	90.24	protease subunit	A5ITJ9
Aureolysin	Aur	GB868_05855	100	0	62.4	immune evasion	P81177
Staphylocoagulase precursor	Coa	GB868_10500	49	5E-19	30.01	blood clotting	P07767
Biofilm							
Intercellular adhesin protein A	IcaA	GB868_03145	99	0	61.61	biofilm production	Q6G608
Intercellular adhesin protein B	IcaB	GB868_03155	84	5E-113	56.73	biofilm production	Q5HCM9
Intercellular adhesin protein C	IcaC	GB868_03160	98	2E-131	55.76	biofilm production	P69518
Intercellular adhesin protein D	IcaD	GB868_03150	88	9E-14	33.33	biofilm production	P69519
Veg protein	Veg	GB868_10350	89	4E-37	63.29	biofilm regulation	P37466
Quorum sensing							
Accessory gene regulator protein A	AgrA	GB868_08300	100	1E-160	83.61	quorum sensing	P0A0I5
Accessory gene regulator protein B	AgrB	GB868_08285	100	1E-122	89.36	quorum sensing	P61649
Accessory gene regulator protein C	AgrC	GB868_08295	99	0	93.49	quorum sensing	WP_096636795
Accessory gene regulator protein D	AgrD	GB868_08290	100	8E-24	95.56	quorum sensing	WP_063278585
Immune evasion, mscram							
Super-antigen protein	Ssl11	GB868_10495	100	4E-54	44.26	superantigen	WP_031788342
Secretory antigen ssaA protein	SsaA1	GB868_08840	100	2E-76	56.8	immune evasion	Q5HLV2
Secretory antigen ssaA protein	SsaA2	GB868_08860	89	3E-41	63.39	immune evasion	Q2G2J2
Immunoglobulin G-binding protein SBI	Sbi	GB868_03995	68	3E-51	48.22	immune evasion	A7X659
Major histocompatibility complex II analog	Map	GB868_02100	98	9E-42	42.29	immune evasion	P69775
Fibronectin binding protein A	SpsL	GB868_03575	100	0	89.4	mscramm	ADX75396
Fibronectin-binding protein and Serine-aspartate repeat-containing protein	SpsD	GB868_00855	90	0	87.9	mscramm	ADX76659
Fibronectin/fibrinogen and RNA binding protein	Frbp	GB868_10105	99	0	47.1	mscramm	O34693
Serine-aspartate repeat-containing protein E	SdrD	GB868_05385	88	2E-149	36.46	mscramm	Q6GBS4
Adhesion lipoprotein	EfaA	GB868_04210	97	1E-98	47.52	mscramm	NP_815739
Cell surface elastin binding protein	EpbS	GB868_00450	99	8E-44	33.66	mscramm	NP_646186
Bacteriocins							
Microcin C7 self-immunity protein MccF	MccF	GB868_01200	96	5E-34	29.25	bacteriocin resistance	Q47511
Colicin V production protein	CvpA	GB868_09450	100	0	100	bacteriocin	WP_037543270
Four-helix bundle bacteriocin BacSp222	BacSp222	GB868_11725	100	2E-31	100	bacteriocin / immuno-modulation	A0A0P0C3P7

*swiss-prot as a reference database, otherwise well documented protein; mscramm - microbial surface components recognizing adhesive matrix molecules; # correct coordinates are contig WJOJ01000014 - nucleotide 16837..16908

SCIENTIFIC REPORTS



OPEN

Staphylococcus sciuri bacteriophages double-convert for staphylokinase and phospholipase, mediate interspecies plasmid transduction, and package *mecA* gene

Received: 04 January 2017

Accepted: 14 March 2017

Published: 13 April 2017

M. Zeman¹, I. Mašlaňová¹, A. Indráková¹, M. Šiborová², K. Mikulášek², K. Bendíčková³, P. Plevka², V. Vrbovská^{1,3}, Z. Zdráhal², J. Doškař¹ & R. Pantůček¹

Staphylococcus sciuri is a bacterial pathogen associated with infections in animals and humans, and represents a reservoir for the *mecA* gene encoding methicillin-resistance in staphylococci. No *S. sciuri* siphophages were known. Here the identification and characterization of two temperate *S. sciuri* phages from the *Siphoviridae* family designated ϕ 575 and ϕ 879 are presented. The phages have icosahedral heads and flexible noncontractile tails that end with a tail spike. The genomes of the phages are 42,160 and 41,448 bp long and encode 58 and 55 ORFs, respectively, arranged in functional modules. Their head-tail morphogenesis modules are similar to those of *Staphylococcus aureus* ϕ 13-like serogroup F phages, suggesting their common evolutionary origin. The genome of phage ϕ 575 harbours genes for staphylokinase and phospholipase that might enhance the virulence of the bacterial hosts. In addition both of the phages package a homologue of the *mecA* gene, which is a requirement for its lateral transfer. Phage ϕ 879 transduces tetracycline and aminoglycoside pSTS7-like resistance plasmids from its host to other *S. sciuri* strains and to *S. aureus*. Furthermore, both of the phages efficiently adsorb to numerous staphylococcal species, indicating that they may contribute to interspecies horizontal gene transfer.

Coagulase-negative and novobiocin-resistant *Staphylococcus sciuri* is mainly considered to be a commensal, animal-associated species with a broad range of habitats including domestic and wild animals, humans and the environment^{1,2}. The presence of the bacteria correlates with animal diseases including dog dermatitis³, exudative epidermitis in pigs⁴, and with a number of nosocomial diseases of humans, namely endocarditis, pelvic inflammation, and wound infections^{5–8}. It was speculated that the *S. sciuri* species group is a potential reservoir of virulence and antimicrobial resistance genes for other staphylococci⁹. Homologues of the *mecA* gene coding for a PBP2a-like protein responsible for methicillin resistance carried on the staphylococcal cassette chromosome *mec* (SCC*mec*) are often found in bacteria from the *S. sciuri* group^{10–12}. The protein PBP2a of *S. sciuri* has 88% amino acid sequence identity to the PBP2a of methicillin-resistant *S. aureus*¹³. The acquisition of the SCC*mec* element by methicillin-susceptible *S. aureus* was crucial for the bacterium to become a successful pathogen¹⁴. It is hypothesized that *S. aureus* acquired this element directly from coagulase-negative staphylococci by transduction¹⁵. Transduction by temperate bacteriophages is a major path for the horizontal gene transfer of

¹Department of Experimental Biology, Faculty of Science, Masaryk University, Kotlářská 2, 611 37 Brno, Czech Republic. ²Central European Institute of Technology, Masaryk University, Kamenice 5, 625 00 Brno, Czech Republic.

³Czech Collection of Microorganisms, Department of Experimental Biology, Faculty of Science, Masaryk University, Kamenice 5, 625 00 Brno, Czech Republic. Correspondence and requests for materials should be addressed to R.P. (email: pantucek@sci.muni.cz)

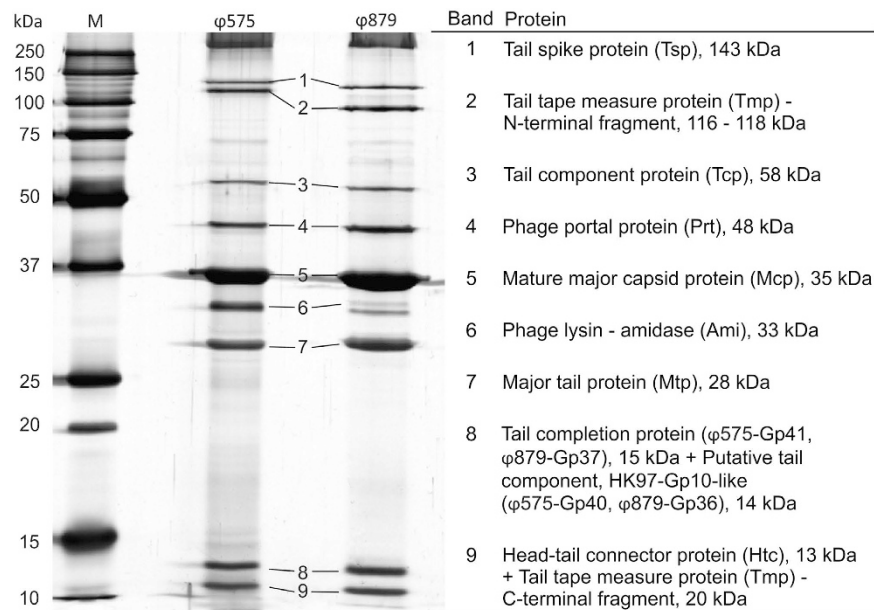


Figure 1. Analysis of ϕ 575 and ϕ 879 virion structural proteins. Left: silver-stained 1D SDS-PAGE gel with proteins extracted from purified phage particles. Selected bands were excised from the gel, digested with trypsin and subsequently analysed by mass spectrometry. Right: proteins identified by mass spectrometry with their theoretical molecular weight. M - molecular weight marker.

virulence and resistance determinants in staphylococci^{16–20}. In recent years, the siphovirus genomic sequences of coagulase-negative staphylococci, which are important nosocomial pathogens, have been described in detail^{21–24}.

Here the characterization of two newly discovered *S. sciuri* bacteriophages is presented and their potential for horizontal gene transfer of the SCC elements and antibiotic resistance plasmids is analysed.

Results

Identification of temperate phages in *S. sciuri* species and their host range. A screening method based on the UV-induction of prophages on a 96-well tissue culture plate was applied for rapid phage detection. From the set of 15 *S. sciuri* strains, only three temperate phages from strains P575, P879 and P581 were induced and were able to propagate on the suitable host strains P612, P723 and P583, respectively (Supplementary Table S1). Phages ϕ 575 and ϕ 879 lysed three and five strains, respectively, out of the 36 *S. sciuri* group strains tested (Supplementary Table S2). The third phage ϕ 581 induced from *S. sciuri* P581, as well as phage ϕ 879, also lysed a *Staphylococcus lentus* strain, thus demonstrating an interspecies host range in oxidase-positive and novobiocin-resistant staphylococci. However, a high-titre lysate of ϕ 581 could not be obtained for further analyses.

Phage morphology and biological features. Both phages were able to propagate using the double-layer agar method, but not in liquid broth. They produced predominantly turbid plaques surrounded by a clear ring that indicates a high frequency of lysogenisation (Supplementary Fig. S1). Plaque diameter was variable from 0.8 to 1.4 mm. The indistinct edges of plaques that were similar for both phages may have been produced by the diffusion of lytic enzymes. The presence of endolysins in the phage lysate was confirmed by 1D SDS PAGE and subsequent mass spectrometry analysis (Fig. 1).

Morphological analysis by transmission electron microscopy (TEM) with negative staining and cryo-conditions (cryo-EM) revealed that both *S. sciuri* bacteriophages ϕ 575 and ϕ 879 belong to the *Siphoviridae* family. The phages consist of an icosahedral head (B1 morphology) with flexible, non-contractile tails ending with a tail spike (Fig. 2A and B). The diameters of the phage heads are 66 and 70 nm for ϕ 575 and ϕ 879, respectively (Supplementary Table S3). The electron density at the end of the tail spike suggests the presence of a metal ion (Fig. 2C).

The adsorption kinetics of the phages were determined on various staphylococcal species including several *S. aureus* derivatives of laboratory isolates^{25–28} (Supplementary Table S1). Although both phages efficiently adsorbed onto other staphylococcal species (Fig. 3), they were unable to propagate on non-*S. sciuri* strains. The phages also adsorbed onto *S. aureus* RN4220 Δ tagO, which *S. aureus* siphoviruses are unable to adsorb onto due to the absence of wall teichoic acid (WTA). Phage ϕ 575 adsorbed reversibly onto *S. aureus* PS 187. Both phages did not adsorb onto *S. epidermidis* CCM 2124 nor onto the *S. aureus* SA113 Δ oat::Km mutant, which lacks the O-acetylation of the C⁶-OH of the muramic acid of peptidoglycan.

Genome structure. The phage genome sequences aligned with 100% identity to the prophage sequences of their lysogenic hosts. The genomes of ϕ 575 and ϕ 879 are arranged in functional modules and consist of 42,160 bp and 41,448 bp of dsDNA with a GC content of 31.8 and 32.1%, which is similar to the GC content of the host

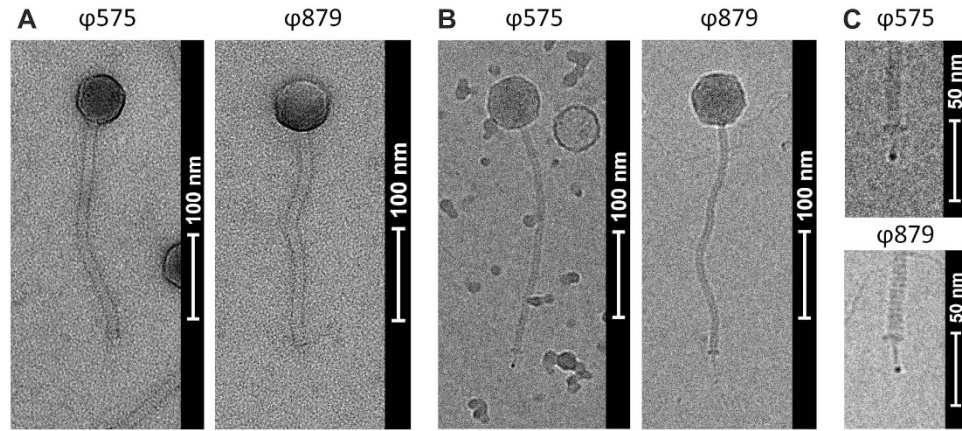


Figure 2. Morphology of phages ϕ 575 and ϕ 879. (A) Transmission electron microscopy images of negatively stained particles. (B) Cryo-electron micrographs of the phages. (C) Tail spike with electron-dense tip.

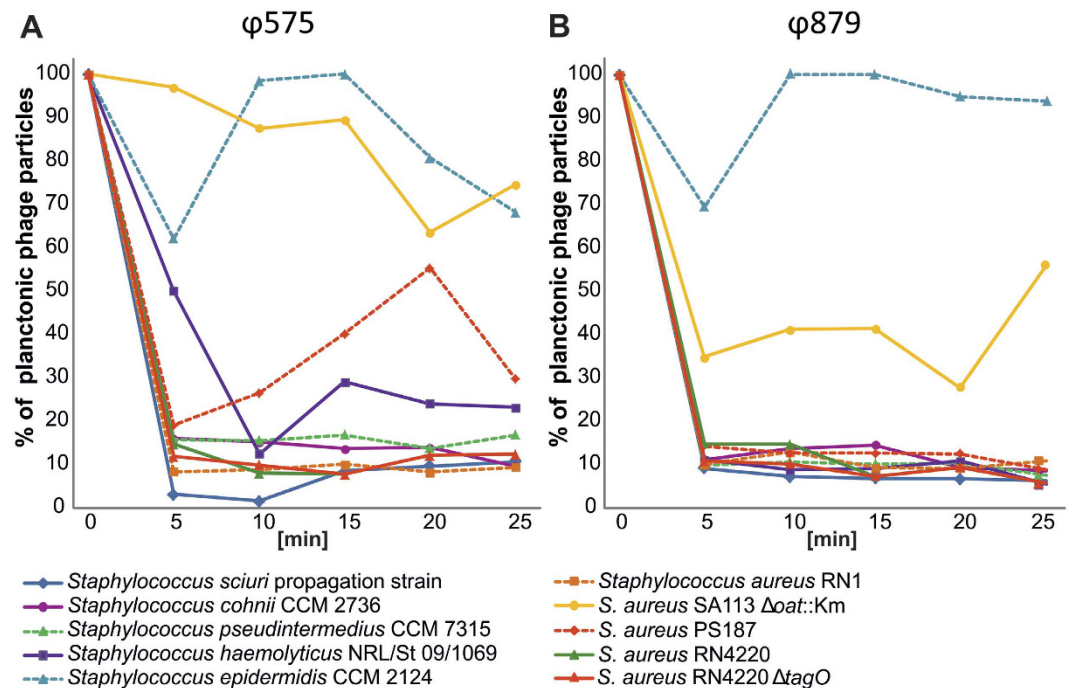


Figure 3. Adsorption kinetics of *Staphylococcus sciuri* bacteriophages. The adsorption rate of ϕ 575 (A) and ϕ 879 (B) was calculated by determining the number of unbound phage particles in the supernatant and subtracting it from the total number of input PFU. The results were expressed as a percentage of the initial phage count.

strains (32.4 and 32.3%). Both phage genomes have cohesive ends resulting in the formation of concatemers detected by pulsed-field gel electrophoresis (Supplementary Fig. S2). The physical ends of the phage DNA were not determined, but a significant decrease in DNA flexibility suggests that the physical ends of phage DNA are located in the region close to the 5' end of the terminase small subunit (*terS*) gene.

Two additional prophages were identified in the strain *S. sciuri* P879. Their genomes are 43.3 and 51.0 kb in size and, like the characterized phages, have tyrosine integrase with a predicted XerC domain. Their genes encoding head proteins are arranged in a similar way to those in Mu-like phages²⁹, however, attempts to induce these phages were unsuccessful.

Fifty-eight ORFs ranging from 156 bp to 4,971 bp were found in the ϕ 575 genome, of which 37 have homologues in GenBank and the function was predicted for 33 of them (Supplementary Table S4). The gene density in this phage genome is 1.38 genes per kbp. The phage *att* site sequence 'ATTCATCATAAAGTCAATACAGAACATTTGTACTTGTGCACAA' was identified in the host strain P575 as a direct repeat between the ABC transporter *uup* gene (GenBank accession no. OFV61085.1) and a hypothetical

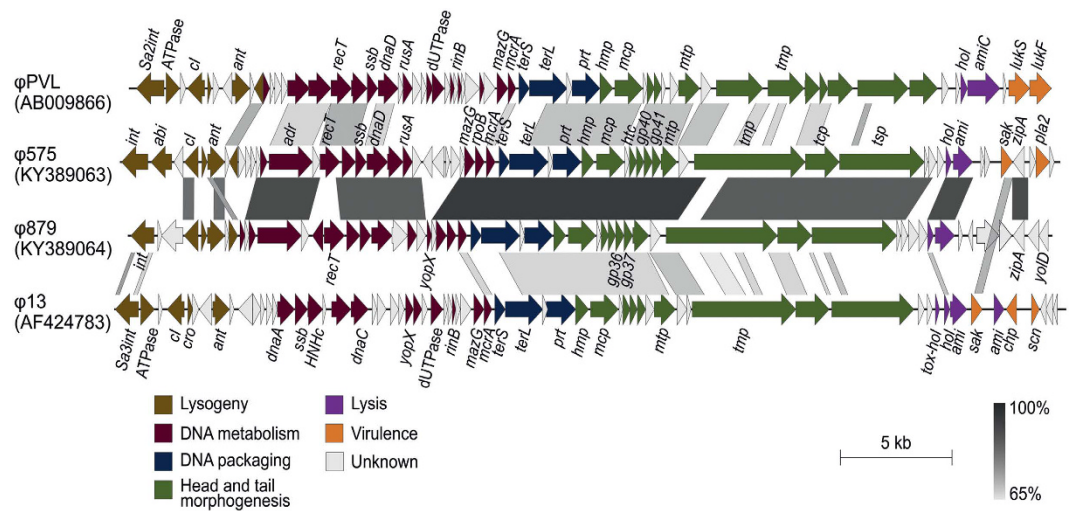


Figure 4. Genome comparison of *Staphylococcus sciuri* phages ϕ 575 and ϕ 879 and *Staphylococcus aureus* phages ϕ PVL and ϕ 13. The GenBank accession number for each sequence is given in brackets. Genomes were aligned using the blastn algorithm and similar regions with more than 65% identity are indicated. The positions and orientations of the coding regions are represented by arrows. Genome modules are color-coded according to the legend.

protein gene (OFV61133.1). In the ϕ 575 genome, downstream of the lytic module, the presence of virulence genes for staphylokinase (*sak*) and phospholipase (*pla2*) was detected.

The ϕ 879 genome has 55 predicted ORFs ranging from 162 bp to 4,998 bp, of which 36 have homologues in GenBank and the function was predicted for 32 of them (Supplementary Table S4). Its gene density is 1.33 genes per kbp. The sequence of the phage *att* site is 'GAATCCCTCCCAGGACGTAAATTACCAATATCCCGTTGTATCT' and it is located between the genes for a hypothetical protein and the acetyltransferase from the GNAT family (OFV64881.1 and OFV64929.1), and overlaps with the tRNA^{Arg} gene by 17 nt (BFX02_03905). The integration module of both *S. sciuri* phages starts with the site-specific tyrosine recombinase XerC with an AP2-like DNA-binding integrase domain. The integrases themselves are dissimilar, with just 24% amino acid sequence identity.

Both phages have a σ -subunit of the RNA polymerase gene in their transcription regulation module. The presence of the sigma factor implies that both phages use their own promoters. The last protein in the DNA metabolism module is a 5-methylcytosine-specific restriction McrA-like protein that contains an HNHc endonuclease domain and is expected to provide higher resistance of their bacterial host to infection by other phages³⁰. The presence of the HNH gene near the genes for the terminase subunits and portal protein is conserved in HK97-like phages³¹. The gene cluster responsible for replication exhibited similarities (66–73% nucleotide identity) to the genomes of *S. aureus* serogroup F phages such as ϕ PVL or ϕ N315. No predicted genes coding for functional RNAs were found in the ϕ 575 and ϕ 879 genomes.

The DNA packaging module follows the DNA metabolism module, and the two phages share 97% nucleotide identity in this module. The highest similarity (65–73% and 61–74% nucleotide identity) in the packaging and head module of the ϕ 575 and ϕ 879 phages was found to the *S. aureus* triple-converting phage ϕ 13 from serological group F³² from the Sa3 integrase family, and the *S. aureus* Panton-Valentine converting phage ϕ PVL³³ from the Sa2 integrase family (Fig. 4). The module for head-tail morphogenesis encodes structural virion proteins and is also highly similar in both of the described phages (90% nucleotide identity).

Structural proteins were analysed by SDS-PAGE in combination with mass spectrometry (Fig. 1). The major capsid protein (Mcp) belongs to the HK97 family. Its 120-amino acid-long N-terminal δ domain is cleaved by prohead protease and is not present in mature virions of the analysed phages. Mass spectrometry showed a 94% coverage of mature Mcp (Supplementary Fig. S3). The molecular weight of Mcp determined from SDS-PAGE gel is ~35 kDa (Fig. 1). Tail tape measure protein (Tmp), which determines the length of the tail, tends to be proteolytically cleaved³⁴. The C-terminal end of Tmp contains a lysozyme-like domain involved in the hydrolysis of beta-1,4-linked polysaccharides of the bacterial cell wall and was detected in mature phages (Fig. 1). The function of the second largest protein in this module was predicted to be a tail spike protein determined on the basis of its position, length and secondary structure forming numerous beta sheets. No other tail-associated cell wall hydrolases were detected in the phage proteomes.

The module responsible for lysis of the bacterial cell is almost identical for both phages (Fig. 4). The holins of ϕ 575 and ϕ 879 are conserved in both phages and share over 90% amino acid identity. They exhibit more than 60% amino acid identity to *S. aureus* and *Staphylococcus pseudintermedius* prophage holins. The endolysins of ϕ 575 and ϕ 879 exhibit a low similarity to well-characterized staphylococcal endolysins and lack a cell-wall binding domain.

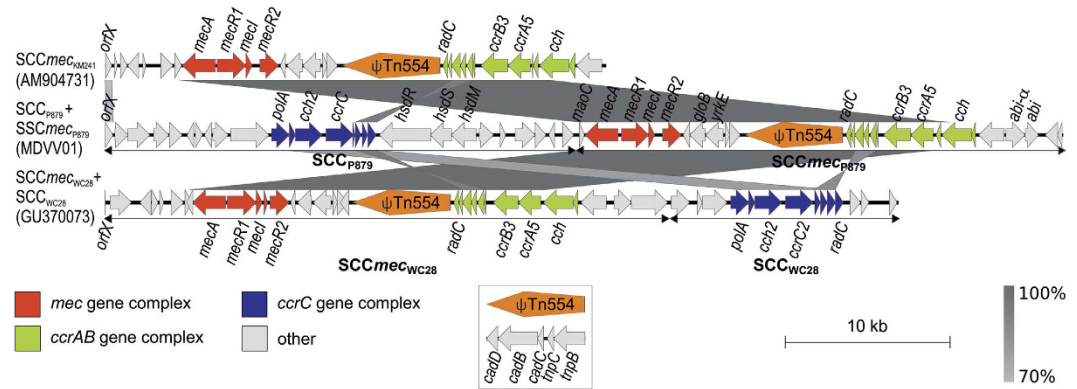


Figure 5. Visualization of *SCCmec*_{P879} element nucleotide sequence alignment to related SCCs. Sequences of SCC elements from *Staphylococcus pseudintermedius* KM241, *Staphylococcus sciuri* P879 and *Staphylococcus cohnii* WC28 were aligned using the blastn algorithm and similar regions with more than 70% identity are indicated. The GenBank accession number for each sequence is given in brackets. The positions and orientations of coding regions are represented by arrows.

Horizontal transfer of pSTS7-like plasmid between *S. sciuri* and *S. aureus* strains. While analysing the sequencing data from purified phages, reads that map to bacterial and plasmid DNA sequences were found. These findings implied that phages are able to package non-phage DNA. Phage ϕ 879 was able to package a 5,667-bp-long pSTS7-like plasmid designated pSSC723 from propagation strain P723. This plasmid encodes tetracycline efflux protein (TetL) and aminoglycoside adenylyltransferase (AadD). The ratio between the plasmid-borne *aadD* gene and the reference tail protein gene determined by qPCR was 5.7×10^{-3} . Plasmid pSSC723 belongs to the pC194 family and exhibits almost 100% nucleotide identity to the intergene spacer from the previously described *S. epidermidis* plasmid pSTS7. Plasmid pSTS7 originated from the interplasmid recombination of *Bacillus subtilis* plasmid pNS1981 and *S. aureus* plasmid pUB110³⁵.

The transducing abilities of phage ϕ 879 were verified by the transfer of pSSC723 to *S. sciuri* strains P600 and P574, and *S. aureus* strain RN4220. The donor strain P723 with plasmid pSSC723 grew on selective plates with tetracycline and kanamycin, whereas the recipients did not. Rare transductants with a frequency of about 10^{-11} were obtained in two intraspecies and one interspecies transduction to *S. aureus*. Plasmid identity in the donor strain and in transductants was confirmed by sequencing, and the genetic background of transductants was confirmed by macrorestriction analysis with *Sma*I by PFGE (Supplementary Fig. S4).

Packaging of *S. sciuri* *SCCmec* element. Both sequencing reads and quantification using real-time PCR proved the ability of phage ϕ 879 to package *mecA* and plasmid genes from its bacterial host into virions. The packaging frequency of the *mecA* part of *SCCmec* was 3×10^{-5} as determined by qPCR analysis. Cassette chromosome recombinase (*ccr*) genes A, B and C were detected in phage ϕ 879 particles using endpoint PCR. However, the successful transduction of *SCCmec* into recipient *S. aureus* strains was not observed.

A novel *SCCmec*_{P879} element whose parts packaged to phage ϕ 879 virions was identified in methicillin-resistant prophage host *S. sciuri* strain P879. The *SCCmec*_{P879} element is 29,546 bp long, harbouring a *mec* A-class complex and *ccrB3* and *ccrA5* recombinases, and was integrated into the consensus insertion sequence site for SCC elements (GAAGCTTATCATAAGTAA). The major part (21 kb) of the *SCCmec*_{P879} shared 98% nucleotide identity with the *SCCmec* element of *S. pseudintermedius* strain KM241³⁶ and the *SCCmec* element of *Staphylococcus cohnii* strain WC28³⁷. However their J1 and J3 regions were different (Fig. 5). *Ccr* recombinases in *SCCmec*_{P879} exhibited 90–96% amino acid identity to recombinase complexes identified previously in *S. sciuri*^{38,39} or *S. cohnii*³⁷. A cluster of genes including the *cch* gene for MCM-like helicase, which is conserved in a number of other SCC elements, was identified downstream of the recombinase genes *ccrB3* and *ccrA5*. In addition, a non-*mec* SCC element designated *SCC*_{P879}, which is 21,844 bp long, was identified adjacent to *SCCmec*_{P879}. *SCC*_{P879} carries the *ccrC* recombinase gene, genes for a restriction-modification type I system and heavy metal resistance genes (Fig. 5).

In methicillin-susceptible *S. sciuri* P575, a non-SCC homologue of the *mecA* gene (WP_070369365.1) was identified, coding for a PBP2a-like protein with 95% amino acid identity to PBP2a from *S. aureus*. This gene is located between a hypothetical protein gene (WP_058611716.1) and an amino acid permease gene (WP_070369378.1) and was also quantified in phage particles. The relative ratio between *mecA* and the reference tail protein gene copy numbers in phage particles was 8.2×10^{-4} , which is higher than for phage ϕ 879.

Discussion

Many prophages reside in the bacterial genomes and contribute to bacterial evolutionary processes via the horizontal exchange of genetic information⁴⁰. Some prophages confer novel biological properties to their host strains, enabling them to adapt to new environments or obtain virulence determinants by lysogenic conversion, thereby driving bacterial adaptation and evolution. Typically, 1–4 prophages are found in each *S. aureus* genome⁴¹. Similarly, putative prophages often reside in the genomes of some coagulase-negative staphylococci⁴² and *Macroccoccus caseolyticus* related to *S. sciuri*⁴³, but only a few *S. epidermidis*, *Staphylococcus hominis* and

Staphylococcus capitis viable phages have been genetically characterized in detail^{21–23}. Recently, *S. sciuri* myoviruses isolated from urban sewage were described⁴⁴, however no *S. sciuri* siphoviruses have been morphologically and genetically characterized to date.

The genomes of *S. sciuri* phages ϕ 575 and ϕ 879 have modular structures and sizes that are similar to those of other staphylococcal siphoviruses^{21,32,45,46}. The phage genomes share 76% overall nucleotide identity, as calculated by a global alignment algorithm. Since they are related to *S. aureus* serogroup F phages belonging to integrase type Sa3, it is suggested that both bacteriophages belong to the *Biseptimavirus* genus⁴⁷. Additional similarities with putative prophages across the genus *Staphylococcus* were identified in a Blast search of the microbial genome database. ϕ 575 and ϕ 879 exhibit 66–72% and 73–80% nucleotide identity, respectively, in their head-tail modules with prophages present in the genomes of *S. pseudintermedius* strains 063228 and NA45⁴⁸ and *Staphylococcus schleiferi* strains 5909–02 and 2317–03⁴⁹.

Even though the phages are similar, each integrates to different *att* sites in the host chromosome. This is because of differences in their integration modules. The integrase from ϕ 879 has 51% amino acid identity to the Sa3 integrase from related *S. aureus* phage ϕ 13, mainly in the C-terminal catalytic domain. The phage integrase from ϕ 575 has 34% amino acid identity to the integrases from the *Lysinibacillus* and *Bacillus* spp. phages^{50,51}.

Virulence factor-converting phages have not been detected in coagulase-negative staphylococci yet. Staphylokinase is a plasminogen activator protein secreted by most human lysogenic *S. aureus* strains. A secondary function of staphylokinase is its ability to neutralize host antimicrobial peptides whose binding may control its plasminogen activation properties⁵². The staphylokinase of ϕ 575 exhibits a 52% amino acid sequence identity to that of *S. aureus* phages encoded by the immune evasion cluster associated with Sa3 integrase family phages^{53,54}.

Phospholipase homologues can influence the innate and adaptive immune response and damage the membranes of host cells⁵⁵. Phages carrying a gene for phospholipase were identified in streptococci⁵⁶. Both virulence factors Sak and Pla2 contain an approximately 30-amino acid-long signal peptide that is required for protein secretion. The lysogenic hosts carrying phospholipase or staphylokinase are more likely to become virulent. There are two ORFs with opposite orientation between the *sak* and *pla2* genes in the ϕ 575 phage genome. The first, *zipA*-like gene was located on the complementary strand and the second gene has unknown function but was predicted to contain a transmembrane domain. The organisation of virulence factors in this region is similar to that of the immune evasion cluster, which harbours the *sea*, *sak*, *scn*, and *chp* genes⁵⁴. Therefore the cluster of genes following the lysis module in ϕ 575 could include other potential virulence factors.

Bacteriophages with a tail spike structure bind to proteinaceous receptors⁵⁷. Prototypical phages with a tail spike are lactococcal bacteriophage p2⁵⁸ and *B. subtilis* phage SPP1⁵⁹. The high electron density observed at the end of the tail spike of ϕ 575 and ϕ 879 might be due to the presence of metal ions as was previously shown for the tail of bacteriophage p2, where iron, calcium and chloride ions were identified in the spike's trimeric metal-binding structure^{60,61}.

It is generally assumed that *pac* phages, which include the *S. aureus* phages of serogroup B, are responsible for generalized transduction⁶². In contrast, here it was shown that *cos* phages ϕ 575 and ϕ 879 package host genes in their virions. This finding corroborates previous observations of the transmission of pathogenicity islands via *cos* phages^{63,64}.

Two types of mobile genetic elements, SCC*mec* and an pSTS7-like plasmid, were detected by qPCR in the phage ϕ 879 particles. The SCC*mec*_{p879} core genes detected in ϕ 879 virions are highly similar to SCC elements from other staphylococcal species such as *S. pseudintermedius* and *S. cohnii*. This indicates a possible horizontal interspecies transfer of this element. The MCM-like helicase identified in SCC*mec*_{p879} possibly participates in the extrachromosomal replication of this element⁶⁵. This may increase the probability of SCC*mec* packaging into the phage virions. The relative quantity of packaged plasmid DNA in phage ϕ 879 particles was higher than the relative quantity of the *mecA* gene from the SCC*mec* region. This implies that the pSSC723 plasmid is packaged as a multimer, as was suggested for other small plasmids⁶⁶. In addition, plasmid interspecies and intraspecies transfer was proved at low frequencies, although the effective infection of *S. sciuri* phage ϕ 879 has not been observed in the recipient strains. Two recent studies, it was confirmed that phage adsorption on the recipient cell wall is sufficient for successful transduction, and effective infection is not necessary^{18,20}.

The effective adsorption of analysed phages on the cells of non-*S. sciuri* species (Fig. 3) supports the speculated interspecies horizontal transfer of mobile elements or their parts by phages. A reversible adsorption of both phages was observed in *S. aureus* PS 187 that has a distinct structure of WTA²⁸, suggesting the possibility of a two-stage adsorption. This type of adsorption has been described for the *B. subtilis* SPP1 phage as a result of a missing YueB membrane receptor on mutant host cells, where the glucosylated poly (glycerol-phosphate) of cell WTA proved to be a major target for SPP1 reversible binding⁶⁷. A homologue of the YueB receptor described in *B. subtilis* was not found in staphylococci, however membrane proteins homologous to the phage infection proteins of the PIP family (e.g. YhgE) may act as possible receptors. The successful adsorption of ϕ 575 and ϕ 879 to *S. aureus* knockout mutant RN4220 Δ *tagO* and also the inability of both phages to adsorb onto *S. aureus* SA113 Δ *oat* suggests that teichoic acids are not their only receptors, as with *S. aureus* phages⁶⁸, but that O-acetyl groups at the 6-position of muramic acid play a role in the process of adsorption.

Conclusions

The identification of bacterial virulence factors encoded by *S. sciuri* phages, their ability to package and transmit mobile elements and to adsorb onto the cells of other staphylococcal species show that *S. sciuri* siphoviruses may contribute to the horizontal gene transfer within the *Staphylococcus* genus. Additionally, phages ϕ 575 and ϕ 879 exhibit evolutionary relationships to phages of the coagulase-positive species *S. aureus* and *S. pseudintermedius*, indicating a possible common gene pool of the phage genomes of these pathogens.

Material and Methods

Bacterial strains and Bacteriophages. Fifteen *S. sciuri* strains were selected for the screening of temperate phages and an additional 21 strains from the *S. sciuri* species group were used for the host-range determination. All *S. sciuri* strains were obtained from the National Reference Laboratory for Staphylococci (NRL/St), National Institute of Public Health (Prague, Czech Republic) and characterized previously². The presence of the phages and their host range were tested on the set of *S. sciuri* strains by soft agar spot assay. The phage host strains, propagation strains, and strains used in the characterization of phage biological properties are listed in Supplementary Tables S1 and S2. The adsorption efficiencies of the phages were determined as described previously¹⁸. The antibiotic resistance pattern of selected *S. sciuri* strains was tested by the disc diffusion method on Mueller-Hinton agar (Oxoid) with discs (Oxoid) generally used for Gram-positive cocci (Supplementary Table S5).

High-throughput detection of UV-inducible prophages. A modified protocol designed for prophage induction on 96-well plates was used in this study⁶⁹. Twenty μl of the overnight cultures were dispensed in a 96-well culture plate with 180 μl of CM1 nutrient broth (Oxoid, United Kingdom). The plates were incubated for 2 hours at 37 °C with shaking (120 rpm). After centrifugation at 1,100 g for 15 min, the pellet was resuspended in 200 μl of physiological solution and the plates were UV-irradiated for 25 s or 35 s using a 15 W UV-lamp (340 nm) at a distance of 60 cm. Forty μl of the irradiated suspension was transferred to a new plate together with 120 μl of physiological solution and 40 μl of 10 \times concentrated prophage broth per well, consisting of 10 g Trypton L42 (Oxoid), 2 g Yeast extract powder L21 (Oxoid), 2 g NaCl and 13 g Nutrient broth CM1 (Oxoid) dissolved in 100 ml of distilled water. The plates were protected from daylight and incubated at 37 °C for 2 hours. The plates were then centrifuged at 2,000 g for 10 min and the supernatants were passed through a 0.45 μm filter (TPP Techno Plastic Products, Switzerland) into a sterile microtube. If the screening resulted in lysis of the indicator strains, the presence of viable phages was proved by large-scale UV or mitomycin C induction.

Phage propagation and purification. Phages obtained from a single plaque were propagated using a double-layer agar technique with 1.5% 2YT bottom agar and 0.7% top Agar No. 1 L11 (Oxoid) with the addition of CaCl_2 to a concentration of 2 mM. After overnight incubation, the top layer was disrupted and the phage was washed down with broth, centrifuged twice for 30 min at 3,100 g and filtered through a 0.45- μm filter. Phage particles were purified in a CsCl density gradient⁷⁰.

Electron and Cryo-electron microscopy. Negative-stained samples were prepared by double staining in 2% uranyl acetate. Cryo samples were prepared by vitrification of the bacteriophage solution (at a concentration of 10¹⁰ PFU ml⁻¹) on Quantifoil grids by plunging into liquid ethane using an FEI Vitrobot Mark IV. All samples were observed with an FEI Tecnai F20 electron microscope operated at 200 kV at a magnification of 29,000 \times .

Plasmid transduction. Intraspecies and interspecies transduction experiments were performed as described previously¹⁸. Transductants were selected on plates with kanamycin and tetracycline (both at concentration 8 $\mu\text{g ml}^{-1}$), where the recipient strains *S. sciuri* P600, P574 and *S. aureus* RN4220 were unable to grow.

DNA extraction from the phage particles. DNase I (Sigma-Aldrich, Germany) and RNase A (Sigma-Aldrich) treatment was performed to remove any exogenous host genomic DNA and RNA from purified phage particles as described previously⁷⁰. The DNA was isolated with a Phage DNA Isolation Kit (Norgen Biotek Corporation, Canada) according to the manufacturer's recommendations. DNA from the viral particles for sequencing was isolated by phenol-chloroform extraction⁶². The concentration and purity of the phage DNA was determined using a NanoDrop spectrophotometer (Thermo Fisher Scientific, USA).

Pulsed-field gel electrophoresis. One μg of phage DNA was loaded onto 1.5% agarose gel and separated by PFGE (Cheff Mapper, Bio-Rad, USA) to detect concatemered cohesive ends. A constant voltage of 5 V cm⁻¹ and switch times of 2–20 s with linear ramping were applied. Lambda DNA concatemers and a 5 kb DNA ladder (Bio-Rad) were used as molecular weight markers.

Genome sequencing and bioinformatic analysis. Phage genome and bacterial whole-genome shotgun (WGS) sequencing was performed using an Ion Torrent™ Personal Genome Machine (Ion PGM™). The purified genomic DNA was used for preparing a 400-bp sequencing library with an Ion Plus Fragment Library Kit (Thermo Fisher Scientific). The sample was loaded on a 316v2 chip and sequenced using an Ion PGM Hi-Q sequencing kit (Thermo Fisher Scientific). Quality trimming and error correction of the reads were performed with the Ion Torrent Suite Software (version 5.0.2). The assembly computation was performed using the implemented Assembler SPAdes (v.3.1.0) with default parameters for Ion Torrent data.

Sequences were manipulated and inspected in the cross-platform bioinformatics software Ugene v.1.23.171. The primal analysis of sequences was a combination of open reading frames (ORFs) prediction using GeneMark.hmm⁷² and automatic annotation by RAST⁷³. Gene content was further examined via a BLASTp search on protein sequence databases⁷⁴, CD-Search⁷⁵ and InterPro v.59⁷⁶. tRNAscan-SE⁷⁷, RNAmmer v.1.2⁷⁸, and hmmssearch v.3.0⁷⁹ were used to analyse functional RNAs. Protein secondary structure was predicted with JPred4⁸⁰. Multiple sequence alignments were visualized using EasyFig v.2.1⁸¹.

Nucleotide sequence accession numbers. The complete genomes of the *S. sciuri* phages ϕ 575 and ϕ 879 were deposited in GenBank under the accession numbers KY389063 and KY389064, respectively. The data from the WGS of bacterial host strains P575 and P879 were recorded in the GenBank WGS project under the accession

numbers MDVU01 and MDVV01, respectively. The sequence of the pSSC723 plasmid was deposited in GenBank under the accession number KY389065.

SDS-PAGE and Mass Spectrometry. Vertical one-dimensional electrophoresis (1-DE), using Bio-Rad equipment, was performed in a Protean II xi Cell (discontinuous 12% T SDS-PAGE). Precision Plus Protein Standard (Bio-Rad) was applied as the molecular weight marker. Proteins were stained with a ProteoSilver Plus kit (Sigma Aldrich). Protein bands were excised, destained and subjected to tryptic digestion (40 °C, 2 h) without the reduction and alkylation of cysteine residues. Digested peptides were extracted from gels using 50% acetonitrile solution with 2.5% formic acid and concentrated in a SpeedVac concentrator (Thermo Fisher Scientific). LC-MS/MS analyses of the peptide mixture were done using an RSLCnano system (Thermo Fisher Scientific) on-line connected to an Impact II Ultra-High Resolution Qq-Time-Of-Flight mass spectrometer (Bruker, Bremen, Germany). Prior to LC separation, tryptic digests were on-line concentrated in a trap column. The peptides were separated using an Acclaim Pepmap100 C18 column (3 µm particles, 75 µm × 500 mm; Thermo Fisher Scientific, 300 nl min⁻¹) and a 0.1% FA/acetonitrile gradient. MS data were acquired in a data-dependent strategy with a 3 s cycle time. Mass range was set to 150–2,200 m/z and precursors were selected from 300 to 2,000 m/z. Mascot (version 2.4.1) MS/MS ion searches were done against a local database containing translated phage insert sequences. Mass tolerance for precursors and MS/MS fragments were 15 ppm and 0.05 Da, respectively. The oxidation of methionine, deamidation (N, Q) and propionamide (C) were set as variable modifications for all searches.

The relative quantification analysis of bacterial genes in phage particles. The target genes for qPCR were first detected by conventional end-point PCR and the amplicons verified by sequencing. A LightCycler 490 Real-Time PCR Instrument (Roche Diagnostics, USA) was used for relative quantification analysis. Reactions were carried out in triplicates in MicroAmp[®] optical 96-well reaction plates sealed with optical adhesive covers (Roche Diagnostics). Each reaction mixture (10 µl) contained 7.5 µl FastStart[®] TaqMan Probe Master (Roche Diagnostics), 900 nM of each primer, 250 nM of hydrolysis probe (Supplementary Table S6), and 50 ng of template DNA. An initial denaturation of DNA at 95 °C for 10 min was followed by 40 cycles of amplification (95 °C for 15 s and 60 °C for 45 s).

The relative quantification analysis was performed as a dual-colour experiment. The FAM probes were used to target *mecA* and aminoglycoside acetyltransferase genes, the Cy5 probe was used for reference phage gene coding for the head-tail connector protein. The results were generated by the Light-Cycler software using the maximum of the second derivative, and a target gene was paired with the reference by a one-to-one pairing analysis. The reaction efficiency was calculated for each analysed gene, and the results were normalized according to the efficiencies from the relative quantification. The calculated ratio between the number of target gene copies and reference gene copies was estimated.

References

- Kloos, W. E., Schleifer, K. H. & Smith, R. F. Characterization of *Staphylococcus sciuri* sp. nov. and its subspecies. *International Journal of Systematic Bacteriology* **26**, 22–37, doi: 10.1099/00207713-26-1-22 (1976).
- Švec, P., Petráš, P., Pantůček, R., Doškař, J. & Sedláček, I. High intraspecies heterogeneity within *Staphylococcus sciuri* and rejection of its classification into *S. sciuri* subsp. *sciuri*, *S. sciuri* subsp. *carnaticus* and *S. sciuri* subsp. *rodentium*. *International Journal of Systematic and Evolutionary Microbiology* **66**, 5181–5186, doi: 10.1099/ijsem.0.001493 (2016).
- Hauschild, T. & Wojcik, A. Species distribution and properties of staphylococci from canine dermatitis. *Research in Veterinary Science* **82**, 1–6, doi: 10.1016/j.rvsc.2006.04.004 (2007).
- Chen, S. *et al.* A highly pathogenic strain of *Staphylococcus sciuri* caused fatal exudative epidermitis in piglets. *PLoS One* **2**, e147, doi: 10.1371/journal.pone.0000147 (2007).
- Hedin, G. & Widerstrom, M. Endocarditis due to *Staphylococcus sciuri*. *European Journal of Clinical Microbiology and Infectious Diseases* **17**, 673–675, doi: 10.1007/BF01708356 (1998).
- Stepanović, S., Dakić, I., Djukić, S., Ložuk, B. & Svabic-Vlahović, M. Surgical wound infection associated with *Staphylococcus sciuri*. *Scandinavian Journal of Infectious Diseases* **34**, 685–686, doi: 10.1080/00365540110076949a (2002).
- Dakić, I. *et al.* Isolation and molecular characterization of *Staphylococcus sciuri* in the hospital environment. *Journal of Clinical Microbiology* **43**, 2782–2785, doi: 10.1128/JCM.43.6.2782-2785.2005 (2005).
- Stepanović, S., Ježek, P., Dakić, I., Vučković, D. & Seifert, L. *Staphylococcus sciuri*: an unusual cause of pelvic inflammatory disease. *International Journal of STD & AIDS* **16**, 452–453, doi: 10.1258/0956462054093999 (2005).
- Nemeghaire, S. *et al.* The ecological importance of the *Staphylococcus sciuri* species group as a reservoir for resistance and virulence genes. *Veterinary Microbiology* **171**, 342–356, doi: 10.1016/j.vetmic.2014.02.005 (2014).
- Couto, I., Wu, S. W., Tomasz, A. & de Lencastre, H. Development of methicillin resistance in clinical isolates of *Staphylococcus sciuri* by transcriptional activation of the *mecA* homologue native to the species. *Journal of Bacteriology* **185**, 645–653, doi: 10.1128/JB.185.2.645-653.2003 (2003).
- Rolo, J., de Lencastre, H. & Miragaia, M. High frequency and diversity of cassette chromosome recombinases (*ccr*) in methicillin-susceptible *Staphylococcus sciuri*. *Journal of Antimicrobial Chemotherapy* **69**, 1461–1469, doi: 10.1093/jac/dku028 (2014).
- Zhou, Y., Antignac, A., Wu, S. W. & Tomasz, A. Penicillin-binding proteins and cell wall composition in beta-lactam-sensitive and -resistant strains of *Staphylococcus sciuri*. *Journal of Bacteriology* **190**, 508–514, doi: 10.1128/JB.01549-07 (2008).
- Wu, S., de Lencastre, H. & Tomasz, A. Genetic organization of the *mecA* region in methicillin-susceptible and methicillin-resistant strains of *Staphylococcus sciuri*. *Journal of Bacteriology* **180**, 236–242, doi: 10.1128/JB.180.2.236-242.1998 (1998).
- Robinson, D. A. & Enright, M. C. Evolutionary models of the emergence of methicillin-resistant *Staphylococcus aureus*. *Antimicrobial Agents and Chemotherapy* **47**, 3926–3934, doi: 10.1128/AAC.47.12.3926-3934.2003 (2003).
- Otto, M. Coagulase-negative staphylococci as reservoirs of genes facilitating MRSA infection. *Bioessays* **35**, 4–11, doi: 10.1002/bies.201200112 (2013).
- Varga, M. *et al.* Efficient transfer of antibiotic resistance plasmids by transduction within methicillin-resistant *Staphylococcus aureus* USA300 clone. *FEMS Microbiology Letters* **332**, 146–152, doi: 10.1111/j.1574-6968.2012.02589.x (2012).
- Scharn, C. R., Tenover, F. C. & Goering, R. V. Transduction of staphylococcal cassette chromosome *mec* elements between strains of *Staphylococcus aureus*. *Antimicrobial Agents and Chemotherapy* **57**, 5233–5238, doi: 10.1128/AAC.01058-13 (2013).
- Mašláňová, I., Stríbná, S., Doškař, J. & Pantůček, R. Efficient plasmid transduction to *Staphylococcus aureus* strains insensitive to the lytic action of transducing phage. *FEMS Microbiology Letters* **363**, fnw211, doi: 10.1093/femsle/fnw211 (2016).

19. Stanczak-Mrozek, K. I. *et al.* Within-host diversity of MRSA antimicrobial resistances. *Journal of Antimicrobial Chemotherapy* **70**, 2191–2198, doi: 10.1093/jac/dkv119 (2015).
20. Haaber, J. *et al.* Bacterial viruses enable their host to acquire antibiotic resistance genes from neighbouring cells. *Nature Communications* **7**, 13333, doi: 10.1038/ncomms13333 (2016).
21. Deghoroain, M. *et al.* Characterization of novel phages isolated in coagulase-negative staphylococci reveals evolutionary relationships with *Staphylococcus aureus* phages. *Journal of Bacteriology* **194**, 5829–5839, doi: 10.1128/JB.01085-12 (2012).
22. Daniel, A., Bonnen, P. E. & Fischetti, V. A. First complete genome sequence of two *Staphylococcus epidermidis* bacteriophages. *Journal of Bacteriology* **189**, 2086–2100, doi: 10.1128/JB.01637-06 (2007).
23. Gutiérrez, D., Martínez, B., Rodríguez, A. & García, P. Genomic characterization of two *Staphylococcus epidermidis* bacteriophages with anti-biofilm potential. *BMC Genomics* **13**, 228, doi: 10.1186/1471-2164-13-228 (2012).
24. Melo, L. D. *et al.* Characterization of *Staphylococcus epidermidis* phage vB_SepS_SEP9 - a unique member of the *Siphoviridae* family. *Research in Microbiology* **165**, 679–685, doi: 10.1016/j.resmic.2014.09.012 (2014).
25. Kreiswirth, B. N. *et al.* The toxic shock syndrome exotoxin structural gene is not detectably transmitted by a prophage. *Nature* **305**, 709–712, doi: 10.1038/305709a0 (1983).
26. Xia, G. *et al.* Wall teichoic acid-dependent adsorption of staphylococcal siphovirus and myovirus. *Journal of Bacteriology* **193**, 4006–4009, doi: 10.1128/JB.01412-10 (2011).
27. Bera, A., Herbert, S., Jakob, A., Vollmer, W. & Götz, F. Why are pathogenic staphylococci so lysozyme resistant? The peptidoglycan O-acetyltransferase OatA is the major determinant for lysozyme resistance of *Staphylococcus aureus*. *Molecular Microbiology* **55**, 778–787, doi: 10.1111/j.1365-2958.2004.04446.x (2005).
28. Winstel, V., Sanchez-Carballo, P., Holst, O., Xia, G. & Peschel, A. Biosynthesis of the unique wall teichoic acid of *Staphylococcus aureus* lineage ST395. *mBio* **5**, e00869, doi: 10.1128/mBio.00869-14 (2014).
29. Morgan, G. J., Hatfull, G. F., Casjens, S. & Hendrix, R. W. Bacteriophage Mu genome sequence: analysis and comparison with Mu-like prophages in *Haemophilus*, *Neisseria* and *Deinococcus*. *Journal of Molecular Biology* **317**, 337–359, doi: 10.1006/jmbi.2002.5437 (2002).
30. Campbell, A. M. In *Bacterial Genomes: Physical Structure and Analysis* (eds F. J. de Bruijn, J. R. Lupski & G. M. Weinstock) Ch. Prophages and Cryptic Prophages 23–29 (Springer, 1998).
31. Moodley, S., Maxwell, K. L. & Kanelis, V. The protein gp74 from the bacteriophage HK97 functions as a HNH endonuclease. *Protein Science* **21**, 809–818, doi: 10.1002/pro.2064 (2012).
32. Iandolo, J. J. *et al.* Comparative analysis of the genomes of the temperate bacteriophages phi 11, phi 12 and phi 13 of *Staphylococcus aureus* 8325. *Gene* **289**, 109–118, doi: 10.1016/S0378-1119(02)00481-X (2002).
33. Kaneko, J., Kimura, T., Kawakami, Y., Tomita, T. & Kamio, Y. Panton-valentine leukocidin genes in a phage-like particle isolated from mitomycin C-treated *Staphylococcus aureus* V8 (ATCC 49775). *Bioscience Biotechnology and Biochemistry* **61**, 1960–1962, doi: 10.1271/bbb.61.1960 (1997).
34. Tsui, L. C. & Hendrix, R. W. Proteolytic processing of phage lambda tail protein gpH: timing of the cleavage. *Virology* **125**, 257–264, doi: 10.1016/0042-6822(83)90199-X (1983).
35. Schwarz, S., Gregory, P. D., Werckenthin, C., Curnock, S. & Dyke, K. G. A novel plasmid from *Staphylococcus epidermidis* specifying resistance to kanamycin, neomycin and tetracycline. *Journal of Medical Microbiology* **45**, 57–63, doi: 10.1099/00222615-45-1-57 (1996).
36. Descloux, S., Rossano, A. & Perreten, V. Characterization of new staphylococcal cassette chromosome *mec* (SCC*mec*) and topoisomerase genes in fluoroquinolone- and methicillin-resistant *Staphylococcus pseudintermedius*. *Journal of Clinical Microbiology* **46**, 1818–1823, doi: 10.1128/JCM.02255-07 (2008).
37. Zong, Z. & Lu, X. Characterization of a new SCC*mec* element in *Staphylococcus cohnii*. *PLoS One* **5**, e14016, doi: 10.1371/journal.pone.0014016 (2010).
38. Urushibara, N., Paul, S. K., Hossain, M. A., Kawaguchiya, M. & Kobayashi, N. Analysis of Staphylococcal cassette chromosome *mec* in *Staphylococcus haemolyticus* and *Staphylococcus sciuri*: identification of a novel *ccrA* gene complex with a newly identified *ccrA* allotype (*ccrA7*). *Microbial Drug Resistance* **17**, 291–297, doi: 10.1089/mdr.2010.0144 (2011).
39. Harrison, E. M. *et al.* A novel hybrid SCC*mec*-*mecC* region in *Staphylococcus sciuri*. *Journal of Antimicrobial Chemotherapy* **69**, 911–918, doi: 10.1093/jac/dkt452 (2014).
40. Casjens, S. Prophages and bacterial genomics: what have we learned so far? *Molecular Microbiology* **49**, 277–300, doi: 10.1046/j.1365-2958.2003.03580.x (2003).
41. Goerke, C. *et al.* Diversity of prophages in dominant *Staphylococcus aureus* clonal lineages. *Journal of Bacteriology* **191**, 3462–3468, doi: 10.1128/JB.01804-08 (2009).
42. Takeuchi, F. *et al.* Whole-genome sequencing of *Staphylococcus haemolyticus* uncovers the extreme plasticity of its genome and the evolution of human-colonizing staphylococcal species. *Journal of Bacteriology* **187**, 7292–7308, doi: 10.1128/JB.187.21.7292-7308.2005 (2005).
43. Baba, T. *et al.* Complete genome sequence of *Macrococcus caseolyticus* strain JCS5402, reflecting the ancestral genome of the human-pathogenic staphylococci. *Journal of Bacteriology* **191**, 1180–1190, doi: 10.1128/JB.01058-08 (2009).
44. Jurczak-Kurek, A. *et al.* Biodiversity of bacteriophages: morphological and biological properties of a large group of phages isolated from urban sewage. *Scientific Reports* **6**, 34338, doi: 10.1038/srep34338 (2016).
45. Kwan, T., Liu, J., DuBow, M., Gros, P. & Pelletier, J. The complete genomes and proteomes of 27 *Staphylococcus aureus* bacteriophages. *Proceedings of the National Academy of Sciences of the USA* **102**, 5174–5179, doi: 10.1073/pnas.0501140102 (2005).
46. Kahánková, J. *et al.* Multilocus PCR typing strategy for differentiation of *Staphylococcus aureus* siphoviruses reflecting their modular genome structure. *Environmental Microbiology* **12**, 2527–2538, doi: 10.1111/j.1462-2920.2010.02226.x (2010).
47. Gutiérrez, D. *et al.* Three proposed new bacteriophage genera of staphylococcal phages: “3Alikevirus”, “77likevirus” and “Phietalikevirus”. *Archives of Virology* **159**, 389–398, doi: 10.1007/s00705-013-1833-1 (2014).
48. Riley, M. C., Perreten, V., Bemis, D. A. & Kania, S. A. Complete genome sequences of three important methicillin-resistant clinical isolates of *Staphylococcus pseudintermedius*. *Genome Announcements* **4**, e01194-16, doi: 10.1128/genomeA.01194-16 (2016).
49. Misić, A. M., Cain, C. L., Morris, D. O., Rankin, S. C. & Beiting, D. P. Complete genome sequence and methylome of *Staphylococcus schleiferi*, an important cause of skin and ear infections in veterinary medicine. *Genome Announcements* **3**, e01011-15, doi: 10.1128/genomeA.01011-15 (2015).
50. Xu, K., Yuan, Z., Rayner, S. & Hu, X. Genome comparison provides molecular insights into the phylogeny of the reassigned new genus *Lysinibacillus*. *BMC Genomics* **16**, 140, doi: 10.1186/s12864-015-1359-x (2015).
51. Kurata, A., Nishimura, M., Kishimoto, N. & Kobayashi, T. Draft genome sequence of a deep-sea bacterium, *Bacillus niacini* strain JAM F8, involved in the degradation of glycosaminoglycans. *Genome Announcements* **2**, e00983-14, doi: 10.1128/genomeA.00983-14 (2014).
52. Nguyen, L. T. & Vogel, H. J. Staphylokinase has distinct modes of interaction with antimicrobial peptides, modulating its plasminogen-activation properties. *Scientific Reports* **6**, 31817, doi: 10.1038/srep31817 (2016).
53. Coleman, D. C. *et al.* *Staphylococcus aureus* bacteriophages mediating the simultaneous lysogenic conversion of beta-lysin, staphylokinase and enterotoxin A: molecular mechanism of triple conversion. *Journal of General Microbiology* **135**, 1679–1697, doi: 10.1099/00221287-135-6-1679 (1989).

54. van Wamel, W. J., Rooijakkers, S. H., Ruyken, M., van Kessel, K. P. & van Strijp, J. A. The innate immune modulators staphylococcal complement inhibitor and chemotaxis inhibitory protein of *Staphylococcus aureus* are located on beta-hemolysin-converting bacteriophages. *Journal of Bacteriology* **188**, 1310–1315, doi: 10.1128/JB.188.4.1310-1315.2006 (2006).
55. Sitkiewicz, I., Stockbauer, K. E. & Musser, J. M. Secreted bacterial phospholipase A2 enzymes: better living through phospholipolysis. *Trends in Microbiology* **15**, 63–69, doi: 10.1016/j.tim.2006.12.003 (2007).
56. Beres, S. B. *et al.* Genome sequence of a serotype M3 strain of group A *Streptococcus*: phage-encoded toxins, the high-virulence phenotype, and clone emergence. *Proceedings of the National Academy of Sciences of the USA* **99**, 10078–10083, doi: 10.1073/pnas.152298499 (2002).
57. Mahony, J. & van Sinderen, D. Structural aspects of the interaction of dairy phages with their host bacteria. *Viruses* **4**, 1410–1424, doi: 10.3390/v4091410 (2012).
58. Sciarra, G. *et al.* Structure of lactococcal phage p2 baseplate and its mechanism of activation. *Proceedings of the National Academy of Sciences of the USA* **107**, 6852–6857, doi: 10.1073/pnas.1000232107 (2010).
59. Vinga, I. *et al.* Role of bacteriophage SPP1 tail spike protein gp21 on host cell receptor binding and trigger of phage DNA ejection. *Molecular Microbiology* **83**, 289–303, doi: 10.1111/j.1365-2958.2011.07931.x (2012).
60. Browning, C., Shneider, M. M., Bowman, V. D., Schwarzer, D. & Leiman, P. G. Phage pierces the host cell membrane with the iron-loaded spike. *Structure* **20**, 326–339, doi: 10.1016/j.str.2011.12.009 (2012).
61. Yamashita, E. *et al.* The host-binding domain of the P2 phage tail spike reveals a trimeric iron-binding structure. *Acta Crystallographica Sect. F Structural Biology and Crystallization Communications* **67**, 837–841, doi: 10.1107/S1744309111005999 (2011).
62. Doškař, J. *et al.* Genomic relatedness of *Staphylococcus aureus* phages of the International Typing Set and detection of serogroup A, B, and F prophages in lysogenic strains. *Canadian Journal of Microbiology* **46**, 1066–1076, doi: 10.1139/w00-097 (2000).
63. Chen, J. *et al.* Intra- and inter-generic transfer of pathogenicity island-encoded virulence genes by *cos* phages. *ISME Journal* **9**, 1260–1263, doi: 10.1038/ismej.2014.187 (2015).
64. Quiles-Puchalt, N. *et al.* Staphylococcal pathogenicity island DNA packaging system involving *cos*-site packaging and phage-encoded HNH endonucleases. *Proceedings of the National Academy of Sciences of the USA* **111**, 6016–6021, doi: 10.1073/pnas.1320538111 (2014).
65. Mir-Sanchis, I. *et al.* Staphylococcal SCCmec elements encode an active MCM-like helicase and thus may be replicative. *Nature Structural & Molecular Biology* **23**, 891–898, doi: 10.1038/nsmb.3286 (2016).
66. Novick, R. P., Edelman, I. & Lofdahl, S. Small *Staphylococcus aureus* plasmids are transduced as linear multimers that are formed and resolved by replicative processes. *Journal of Molecular Biology* **192**, 209–220, doi: 10.1016/0022-2836(86)90360-8 (1986).
67. Baptista, C., Santos, M. A. & Sao-Jose, C. Phage SPP1 reversible adsorption to *Bacillus subtilis* cell wall teichoic acids accelerates virus recognition of membrane receptor YueB. *Journal of Bacteriology* **190**, 4989–4996, doi: 10.1128/JB.00349-08 (2008).
68. Li, X. *et al.* An essential role for the baseplate protein Gp45 in phage adsorption to *Staphylococcus aureus*. *Scientific Reports* **6**, 26455, doi: 10.1038/srep26455 (2016).
69. McDonald, J. E., Smith, D. L., Fogg, P. C., McCarthy, A. J. & Allison, H. E. High-throughput method for rapid induction of prophages from lysogens and its application in the study of Shiga Toxin-encoding *Escherichia coli* strains. *Applied and Environmental Microbiology* **76**, 2360–2365, doi: 10.1128/AEM.02923-09 (2010).
70. Mašláňová, I. *et al.* Bacteriophages of *Staphylococcus aureus* efficiently package various bacterial genes and mobile genetic elements including SCCmec with different frequencies. *Environmental Microbiology Reports* **5**, 66–73, doi: 10.1111/j.1758-2229.2012.00378.x (2013).
71. Okonechnikov, K., Golosova, O., Fursov, M. & team, U. Unipro UGENE: a unified bioinformatics toolkit. *Bioinformatics* **28**, 1166–1167, doi: 10.1093/bioinformatics/bts091 (2012).
72. Besemer, J. & Borodovsky, M. GeneMark: web software for gene finding in prokaryotes, eukaryotes and viruses. *Nucleic Acids Research* **33**, W451–454, doi: 10.1093/nar/gki487 (2005).
73. Aziz, R. K. *et al.* The RAST Server: rapid annotations using subsystems technology. *BMC Genomics* **9**, 75, doi: 10.1186/1471-2164-9-75 (2008).
74. Altschul, S. F., Gish, W., Miller, W., Myers, E. W. & Lipman, D. J. Basic local alignment search tool. *Journal of Molecular Biology* **215**, 403–410, doi: 10.1016/S0022-2836(05)80360-2 (1990).
75. Marchler-Bauer, A. *et al.* CDD: NCBI's conserved domain database. *Nucleic Acids Research* **43**, D222–226, doi: 10.1093/nar/gku1221 (2015).
76. Mitchell, A. *et al.* The InterPro protein families database: the classification resource after 15 years. *Nucleic Acids Research* **43**, D213–221, doi: 10.1093/nar/gku1243 (2015).
77. Schattner, P., Brooks, A. N. & Lowe, T. M. The tRNAscan-SE, snoscan and snoGPS web servers for the detection of tRNAs and snoRNAs. *Nucleic Acids Research* **33**, W686–689, doi: 10.1093/nar/gki366 (2005).
78. Lagesen, K. *et al.* RNAmmer: consistent and rapid annotation of ribosomal RNA genes. *Nucleic Acids Research* **35**, 3100–3108, doi: 10.1093/nar/gkm160 (2007).
79. Finn, R. D., Clements, J. & Eddy, S. R. HMMER web server: interactive sequence similarity searching. *Nucleic Acids Research* **39**, W29–37, doi: 10.1093/nar/gkr367 (2011).
80. Drozdetskiy, A., Cole, C., Procter, J. & Barton, G. J. JPred4: a protein secondary structure prediction server. *Nucleic Acids Research* **43**, W389–394, doi: 10.1093/nar/gkv332 (2015).
81. Sullivan, M. J., Petty, N. K. & Beatson, S. A. Easyfig: a genome comparison visualizer. *Bioinformatics* **27**, 1009–1010, doi: 10.1093/bioinformatics/btr039 (2011).

Acknowledgements

This work was supported by a grant from the Czech Science Foundation (GP13-05069P). CIISB research infrastructure project LM2015043 funded by MEYS CR is gratefully acknowledged for financial support of the measurements at the Proteomics CF and the Cryo-electron Microscopy and Tomography CF. We wish to thank Hana Konečná for the SDS-PAGE separation of phage protein isolates.

Author Contributions

M.Z., I.M., A.I. and R.P. isolated the phages and designed the study. Horizontal gene transfer experiments were performed by I.M. and A.I.; M.Š. and P.P. performed the electron microscopy experiments. Whole-genome sequencing was performed by M.Z., K.B. and V.V.; A.I. and M.Z. analysed the data. K.M. and Z.Z. were responsible for proteomic analysis. M.Z., I.M., J.D., P.P. and R.P. wrote the manuscript. All the authors approved the final manuscript.

Additional Information

Supplementary information accompanies this paper at <http://www.nature.com/srep>

Competing Interests: The authors declare no competing financial interests.

How to cite this article: Zeman, M. *et al.* *Staphylococcus sciuri* bacteriophages double-convert for staphylokinase and phospholipase, mediate interspecies plasmid transduction, and package *mecA* gene. *Sci. Rep.* 7, 46319; doi: 10.1038/srep46319 (2017).

Publisher's note: Springer Nature remains neutral with regard to jurisdictional claims in published maps and institutional affiliations.



This work is licensed under a Creative Commons Attribution 4.0 International License. The images or other third party material in this article are included in the article's Creative Commons license, unless indicated otherwise in the credit line; if the material is not included under the Creative Commons license, users will need to obtain permission from the license holder to reproduce the material. To view a copy of this license, visit <http://creativecommons.org/licenses/by/4.0/>

© The Author(s) 2017

***Staphylococcus sciuri* bacteriophages double-convert for staphylokinase and phospholipase, mediate interspecies plasmid transduction, and package *mecA* gene**

M. Zeman¹, I. Mašlaňová¹, A. Indráková¹, M. Šiborová², K. Mikulášek², K. Bendíčková³, P. Plevka², V. Vrbovská^{1,3}, Z. Zdráhal², J. Doškař¹ and R. Pantůček*¹

¹Department of Experimental Biology, Faculty of Science, Masaryk University, Kotlářská 2, 611 37 Brno, Czech Republic. ²Central European Institute of Technology, Masaryk University, Kamenice 5, 625 00 Brno, Czech Republic. ³Czech Collection of Microorganisms, Department of Experimental Biology, Faculty of Science, Masaryk University, Kamenice 5, 625 00 Brno, Czech Republic.

Supplementary Table S1. Characteristics of strains used in this study.

Strain	Strain description	Reference
<i>S. sciuri</i> P575	φ575 host strain, human origin (urine)	Švec <i>et al.</i> , 2016
<i>S. sciuri</i> P879	φ879 host strain, human origin (wound swab)	Švec <i>et al.</i> , 2016
<i>S. sciuri</i> P581	φ581 host strain, human origin (blood culture)	Švec <i>et al.</i> , 2016
<i>S. sciuri</i> P612	propagation strain for φ575, human origin (urine)	Švec <i>et al.</i> , 2016
<i>S. sciuri</i> P723	propagation strain for φ879, animal origin (piglet), pSSC723 plasmid	Švec <i>et al.</i> , 2016
<i>S. lentus</i> P583	susceptible strain to φ581, human origin (blood culture)	this study
<i>S. sciuri</i> P574	plasmidless transduction recipient strain, human origin (urine)	Švec <i>et al.</i> , 2016
<i>S. sciuri</i> P600	plasmidless transduction recipient strain, human origin (urine)	Švec <i>et al.</i> , 2016
<i>S. cohnii</i> CCM 2736	type strain of <i>S. cohnii</i> , used in adsorption kinetics studies	CCM
<i>S. pseudintermedius</i> CCM 7315	type strain of <i>S. pseudintermedius</i> , used in adsorption kinetics studies	CCM
<i>S. haemolyticus</i> NRL/St 09/1069	clinical isolate used in adsorption kinetics studies, human origin (blood culture)	this study
<i>S. epidermidis</i> CCM 2123	type strain of <i>S. epidermidis</i> , used in adsorption kinetics studies	CCM
<i>S. aureus</i> RN1	strain NCTC 8325, used in adsorption kinetics studies	
<i>S. aureus</i> RN4220	prophageless derivative of 8325-4, <i>agr</i> + background, 11-bp deletion in <i>rsbU</i> , restriction-defective, used in adsorption kinetics studies and as transduction recipient	Kreiswirth <i>et al.</i> , 1983
<i>S. aureus</i> RN4220 Δ <i>tagO</i>	gene knockout mutant deficient in the peptidoglycan-anchored wall teichoic acid synthesis, used in adsorption kinetics studies	Xia <i>et al.</i> , 2011
<i>S. aureus</i> SA113 Δ <i>oat</i> ::Km	derivate of strain 8325, gene knockout mutant (Δ <i>oat</i> ::kan) deficient in the peptidoglycan O-acetylation, <i>agr</i> - background, 11-bp deletion in <i>rsbU</i>	Bera <i>et al.</i> , 2005
<i>S. aureus</i> PS187	propagation strain for phage 187, poly-glycerol-phosphate (GroP) WTA glycosylated with N-acetyl-D-galactosamine (GalNAc), used in adsorption kinetics studies	Winstel <i>et al.</i> , 2014

Legend: CCM, Czech Collection of Microorganisms (<http://www.sci.muni.cz/ccm/>) has provided type cultures.

Supplementary Table S2. Sensitivity of bacterial strains from the *S. sciuri* complex to bacteriophages ϕ 575 and ϕ 879. Phage suspensions containing to 10^4 PFU/ml were used for typing. Unless stated otherwise, the strains are of human origin.

Strain ¹	Year of isolation	Source	ϕ 575	ϕ 879
P548	1997	Pustule, dog	not sensitive	rare various plaques
P612	1999	Urine	various plaques	rare turbid plaques
P723	2003	Piglet	rare various plaques	clear plaques
P583	2000	Blood culture	not sensitive	rare turbid plaques
P537	1995	Urine	clear plaques	not sensitive
P536	1995	Burn	not sensitive	not sensitive
P539	1997	Furuncle		
P540	1997	Drain		
P543	1997	Eye		
P545	1998	Urine		
P549	1998	Urine		
P553	1998	Urine		
P554	1998	Urine		
P556	1998	Urine		
P563	1999	Mastitis, cow		
P568	1999	Urine		
P569	1999	Urine		
P572	1999	Nose, Norway rat		
P574	1999	Urine		
P575	2000	Urine		
P578	2000	Urine		
P581	2000	Blood culture		
P589	2001	Urine		
P597	2001	Catheter		
P600	2002	Urine		
P601	2002	Food		
P602	2002	Urine		
P605	2002	Wound		
P607	2002	Drain		
P609	2002	Decubitus		
P611	2003	Haemoculture		
P879	2003	Wound		
P880	2003	Vagina		
CCM 3473 ²	1973	Skin, squirrel		
CCM 4657	1992	Nose, Norway rat		
CCM 4835	1991	Food		

¹ Strains belong to *S. sciuri* species, except P583 and P597 that belong to *S. lentus* species

² Type strain of *S. sciuri* species

Supplementary Table S3. Dimensions of the phages on the basis of electron-microscopy analysis.
The results are an average from 10 independent measurements.

Microscopy technique	Bacteriophage	Head diameter [nm]	Tail length [nm]	Tail width [nm]
Transmission electron microscopy	φ575	60.4 ± 0.72	255.4 ± 2.39	9.6 ± 0.17
	φ879	65.7 ± 1.57	247.5 ± 1.69	9.7 ± 0.64
Cryo-electron microscopy	φ575	65.8 ± 1.54	261.4 ± 2.59	10.2 ± 0.56
	φ879	69.7 ± 1.41	261.4 ± 5.13	9.3 ± 0.47

Supplementary Table S4. Genome annotation of *Staphylococcus sciuri* phages ϕ 575 and ϕ 879.

Genome annotation of phage ϕ 575 (GenBank accession no. KY389063)							Genome annotation of phage ϕ 879 (GenBank accession no. KY389064)						
Gene no.	Start	End	Length [nt]	Strand	Predicted function	Gene identifier	Gene no.	Start	End	Length [nt]	Strand	Predicted function	Gene identifier
gp1	75	1256	1182	-	Phage integrase	<i>int</i>	gp1	143	1171	1029	-	Phage integrase	<i>int</i>
gp2	1396	2325	930	-	Abortive infection bacteriophage resistance protein	<i>abi</i>	gp2	1343	1531	189	+	Phage hypothetical protein	
gp3	2435	2839	405	-	Phage hypothetical protein		gp3	1505	2476	972	-	Phage hypothetical protein	
gp4	2900	3514	615	-	Phage <i>cl</i> -like repressor with peptidase and LexA domain	<i>cl</i>	gp4	2535	3155	621	-	Phage <i>cl</i> -like repressor with peptidase and LexA domain	<i>cl</i>
gp5	3686	3913	228	+	Phage HTH-type transcriptional regulator		gp5	3300	3539	240	+	Phage HTH-type transcriptional regulator	
gp6	3937	4713	777	+	Phage antirepressor protein	<i>ant</i>	gp6	3573	4355	783	+	Phage antirepressor protein	<i>ant</i>
gp7	4726	4920	195	+	Phage hypothetical protein		gp7	4369	4533	165	+	Phage hypothetical protein	
gp8	4907	5287	381	-	DUF2513 domain-containing phage protein		gp8	4545	4937	393	+	Phage antirepressor protein, BRO family	
gp9	5335	5640	306	+	Phage hypothetical protein		gp9	5038	5265	228	+	DUF771 domain-containing phage protein	
gp10	5647	5904	258	+	Phage hypothetical protein		gp10	5262	5441	180	+	Phage hypothetical protein, predicted transmembrane	
gp11	5879	6079	201	+	Phage hypothetical protein		gp11	5442	5747	306	+	DUF1108 domain-containing phage protein	
gp12	6127	6306	180	+	Phage hypothetical protein, predicted transmembrane		gp12	5835	7787	1953	+	ATPase involved in DNA repair, phage associated	<i>adr</i>
gp13	6307	6612	306	+	DUF1108 domain-containing phage protein		gp13	7784	8119	336	+	Phage hypothetical protein	
gp14	6699	8651	1953	+	ATPase involved in DNA repair, phage associated	<i>adr</i>	gp14	8282	8752	471	-	DUF2321 domain-containing phage protein	
gp15	8648	8983	336	+	Phage hypothetical protein		gp15	8816	9724	909	+	Recombinational DNA repair protein RecT (prophage associated)	<i>recT</i>
gp16	8980	9879	900	+	Recombinational DNA repair protein RecT (prophage associated)	<i>recT</i>	gp16	9820	10422	603	+	Phosphoribosyl phosphodiesterase - like protein in prophage	
gp17	9975	10577	603	+	Phosphoribosyl phosphodiesterase - like protein in prophage		gp17	10423	10905	483	+	Single-stranded DNA-binding protein	<i>ssb</i>
gp18	10578	11060	483	+	Single-stranded DNA-binding protein	<i>ssb</i>	gp18	10938	11867	930	+	Phage replication initiation protein, DnaD	<i>dnaD</i>
gp19	11093	12022	930	+	Phage replication initiation protein, DnaD	<i>dnaD</i>	gp19	11851	12558	708	+	Phage hypothetical protein	
gp20	12006	12713	708	+	DUF881 domain-containing phage protein		gp20	12555	12977	423	+	Phage Holliday junction resolvase, RusA-like	<i>rusA</i>
gp21	12707	13132	426	+	Phage Holliday junction resolvase, RusA-like	<i>rusA</i>	gp21	12977	13375	399	+	Phage hypothetical protein	
gp22	13132	13530	399	+	Phage hypothetical protein		gp22	13436	13651	216	+	YopX-like protein	<i>yopX</i>
gp23	13606	14013	408	-	Phage hypothetical protein		gp23	13645	13854	210	+	Phage hypothetical protein	
gp24	14023	14547	525	-	Phage hypothetical protein, predicted non-cytoplasmatic		gp24	13841	14299	459	+	Putative NTP pyrophosphohydrolase MazG family	<i>mazG</i>
gp25	14629	14799	171	+	Phage hypothetical protein, predicted non-cytoplasmatic		gp25	14333	14734	402	+	Putative phage RNA polymerase sigma 70 factor, region 3/4	<i>rpoD</i>
gp26	14871	15287	417	+	Phage hypothetical protein		gp26	14825	15223	399	+	Putative phage 5-methylcytosine-specific restriction endonuclease McrA-like protein	<i>mcrA</i>
gp27	15268	15477	210	+	Phage hypothetical protein		gp27	15393	15875	483	+	Phage terminase, small subunit	<i>terS</i>
gp28	15464	15922	459	+	Putative NTP pyrophosphohydrolase MazG family	<i>mazG</i>	gp28	15859	17586	1728	+	Phage terminase, large subunit	<i>terL</i>
gp29	15956	16357	402	+	Putative phage RNA polymerase sigma 70 factor, region 3/4	<i>rpoD</i>	gp29	17598	17798	201	+	Phage hypothetical protein, predicted transmembrane	
gp30	16448	16846	399	+	Putative phage 5-methylcytosine-specific restriction endonuclease McrA-like protein	<i>mcrA</i>	gp30	17804	19069	1266	+	Phage portal protein, HK97-like	<i>prt</i>
gp31	17018	17500	483	+	Phage terminase, small subunit	<i>terS</i>	gp31	19116	19658	543	+	Phage head maturation protease, HK97 family	<i>hmp</i>
gp32	17484	19211	1728	+	Phage terminase, large subunit	<i>terL</i>	gp32	19768	20994	1227	+	Phage major capsid protein, HK97-like	<i>mcp</i>

gp33	19223	19423	201	+	Phage hypothetical protein, predicted transmembrane	
gp34	19429	20694	1266	+	Phage portal protein, HK97-like	<i>prt</i>
gp35	20741	21283	543	+	Phage head maturation protease, HK97 family	<i>hmp</i>
gp36	21392	22618	1227	+	Phage major capsid protein, HK97-like	<i>mcp</i>
gp37	22661	22855	195	+	Phage hypothetical protein	
gp38	22867	23199	333	+	Phage DNA packaging, Head-Tail Connector Protein HK97 Gp6-like	<i>htc</i>
gp39	23183	23521	339	+	Putative phage head-tail adaptor	
gp40	23521	23898	378	+	Structural, putative tail-component HK97-Gp10-like	
gp41	23895	24275	381	+	Structural protein, putative tail component	
gp42	24288	25004	717	+	Phage major tail protein	<i>mtp</i>
gp43	25080	25529	450	+	Phage hypothetical protein	
gp44	25779	30749	4971	+	Structural, tail tape measure protein	<i>tmp</i>
gp45	30764	32284	1521	+	Structural, tail component protein	<i>tcp</i>
gp46	32300	36100	3801	+	Structural phage protein, putative tail spike with endopeptidase domain	<i>tsp</i>
gp47	36097	36252	156	+	Phage hypothetical protein	
gp48	36290	36631	342	+	Phage hypothetical protein	
gp49	36681	36980	300	+	DUF2951 domain-containing phage protein	
gp50	37069	37317	249	+	Phage holin	<i>hol</i>
gp51	37403	38272	870	+	Phage lysin, N-acetylmuramoyl-L-alanine amidase	<i>ami</i>
gp52	38629	38787	159	+	Antitoxin-like protein	
gp53	38812	39042	231	+	Phage hypothetical protein	
gp54	39551	40057	507	+	Phage-encoded staphylokinase	<i>sak</i>
gp55	40086	40586	501	-	ZipA protein N-terminal domain	<i>zipA</i>
gp56	40826	41098	273	+	Phage hypothetical protein, predicted transmembrane	
gp57	41117	41722	606	+	Phospholipase A2	<i>pla2</i>
gp58	41726	41932	207	+	Phage hypothetical protein, predicted membrane anchored	

gp33	21037	21231	195	+	Phage hypothetical protein	
gp34	21243	21575	333	+	Phage DNA packaging, Head-Tail Connector Protein HK97 Gp6-like	<i>htc</i>
gp35	21565	21897	333	+	Bacteriophage SPP1, head-tail adaptor-like protein	
gp36	21897	22274	378	+	Structural, putative tail-component HK97-Gp10-like protein	
gp37	22271	22651	381	+	Structural protein, putative tail component	
gp38	22664	23380	717	+	Phage major tail protein	<i>mtp</i>
gp39	23456	23905	450	+	Phage hypothetical protein	
gp40	24156	29153	4998	+	Structural, tail tape-measure protein	<i>tmp</i>
gp41	29168	30688	1521	+	Structural, tail component protein	<i>tcp</i>
gp42	30704	34507	3804	+	Structural phage protein, putative tail spike with endopeptidase domain	<i>tsp</i>
gp43	34507	34668	162	+	Phage hypothetical protein	
gp44	34709	34996	288	+	Phage hypothetical protein	
gp45	35037	35498	462	+	Phage hypothetical protein, predicted transmembrane	
gp46	35498	35884	387	+	Phage hypothetical protein, predicted membrane anchored	
gp47	35897	36157	261	+	Phage holin	<i>hol</i>
gp48	36233	37102	870	+	Phage lysin, N-acetylmuramoyl-L-alanine amidase	<i>ami</i>
gp49	37282	37458	177	+	Phage hypothetical protein	
gp50	37717	37917	201	-	Phage hypothetical protein	
gp51	38098	39099	1002	+	DUF4868 domain-containing phage protein	
gp52	39111	39668	558	+	Phage hypothetical protein, predicted transmembrane	
gp53	39727	40227	501	-	Cell division protein ZipA	<i>zipA</i>
gp54	40382	40882	501	-	Phage hypothetical protein, predicted membrane anchored	
gp55	40893	41303	411	-	YolD-like protein	<i>yolD</i>

Supplementary Table S5. Antimicrobial susceptibility profile of *S. sciuri* phage hosts and propagation strains. The testing was performed by disc diffusion method on Mueller Hinton agar. EUCAST clinical breakpoints V. 6.0 (http://www.eucast.org/clinical_breakpoints/) were used to interpret susceptibility testing.

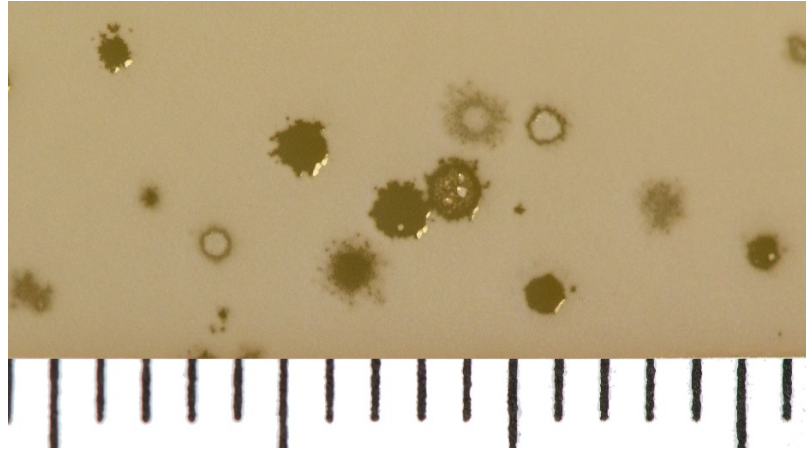
Antibiotic	Disc (Oxoid)	Prophage host strain		Phage propagation strain	
		P575	P879	P612	P723
Cefoxitin	FOX30	S	R	S	S
Oxacillin	OX1	S	R	S	S
Penicillin G	P1	R	R	R	R
Ciprofloxacin	CIP5	S	S	S	S
Clindamycin	DA2	R	R	R	R
Erythromycin	E15	S	S	S	S
Trimethoprim+Sulfamethoxazole	SXT25	S	S	S	S
Fusidic acid	FD10	R	R	R	R
Gentamicin	CN10	R	R	R	R
Rifampicin	RD5	S	S	S	S
Tigecycline	TGC15	S	S	S	S
Mupirocin	MUP200	R	R	S	R
Tetracycline	TE30	S	S	S	R
Chloramphenicol	C30	S	S	S	S
Linezolid	LZD10	S	S	S	S
Vancomycin	VA5	S	S	S	S
Kanamycin	K30	S	R	S	R
Novobiocin	NV5	R	R	R	R

S, susceptible; R, resistant

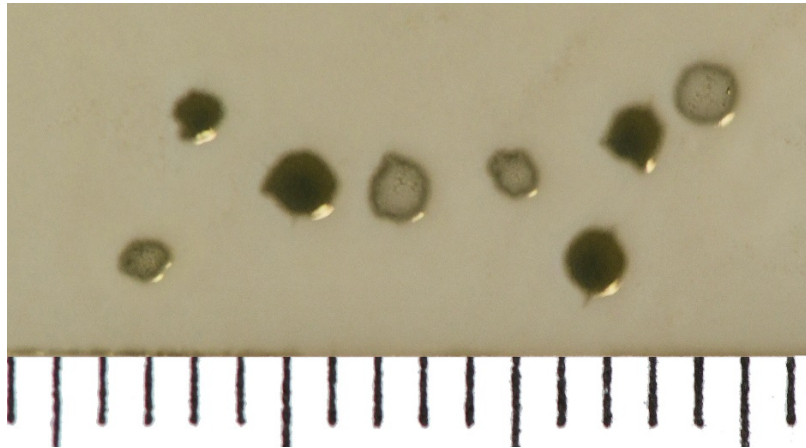
Supplementary Table S6. Primers and probes used for analyses of abilities of phages to package and transduce bacterial DNA.

Target gene	Sequence of primers and probes
Aminoglycoside adenylyltransferase (<i>aadD</i>)	FW: 5' CATCTGTGCCAGTTCGTA 3' RV: 5' AAATTCTCTAGCGATTCCAG 3' Probe: FAM- 5' CTCAGAGTCGGAAAGTTGACC 3'
Penicillin-binding protein (<i>mecA</i>)	FW: 5' AGYGTCAATYATTCCAGG 3' RV: 5' CYACATTRTTTCGGTCT 3' Probe: FAM- 5' CGTTCTGATTTCAATGGTTCAA 3'
Head-tail connector protein (<i>htc</i>)	FW: 5' TAAAAGCTTATTATGAGTGGG 3' RV: 5' TAATAGTACGCTGTTAGTGGA 3' Probe: Cy5- 5' ATTCATCAGTTACTGCACTCG 3'
Cassette chromosome recombinases A, B (<i>ccrAB</i>)	FW: 5' GAAATACCTCTATCCGCGTA 3' RV: 5' TAAACTTATTACCCGCAAGCC 3'
Cassette chromosome recombinase (<i>ccrC</i>)	FW: 5' TTATCAAATTGGTCCGCTA 3' RV: 5' GTAGTTCATCATTACGGGTT 3'

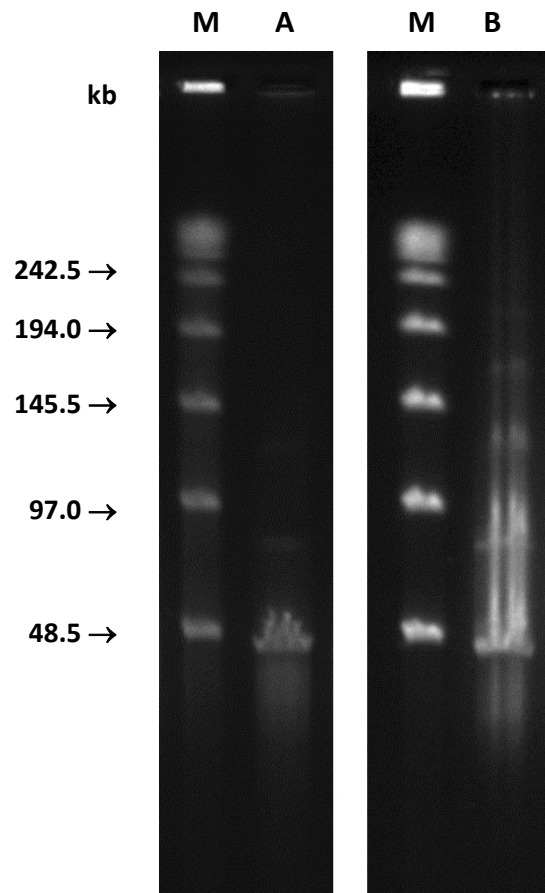
A ϕ 575



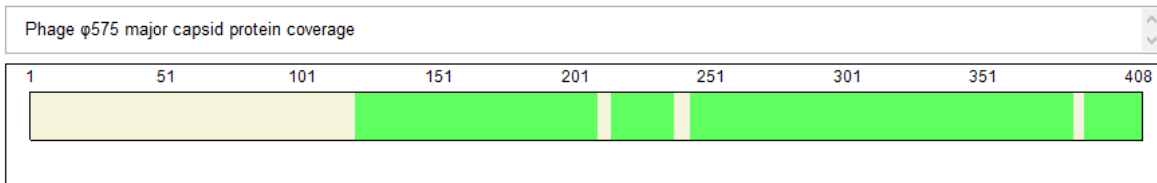
B ϕ 879



Supplementary Figure S1. Plaque morphology of *Staphylococcus sciuri* phages ϕ 575 (A) and ϕ 879 (B). The phage plaque assay was performed using the double-layer agar method on 2YT Agar. The ruler scale is in millimetres.



Supplementary Figure S2. Pulsed-field gel electrophoresis of bacteriophage DNA showing concatemer formation of phage genomic DNA as a result of interactions between cohesive ends. Lane M, Lambda DNA concatemers (Bio-Rad); Lane A, DNA of phage ϕ 575; Lane B, DNA of phage ϕ 879.

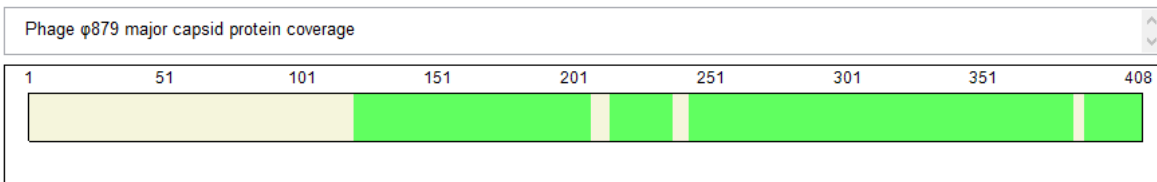


Sequence

```

1 MNKSKLKV INDLQRSIDL KIKVATRALN DDDLEKAEKL EQEISELRKQ IADKEEELSK LKDESSNDDD DPSNIEANRN NNPENRSKKT PNANLLGANH
101 ISNDVSQEVV DFTEYIEARA DIPGGSLLKTD SGYVVIPEEI VTEILKLKEV EFNLDKIVTV KRVKNGSGKY PVRRESQVAA LPEVEELAEN PELAVKPFQ
201 LSYDIKTRRG YFRISREAIE DSQIDVLKEL KLWLARTIAA TRNKAIIDVI QKGGPGELGD NTKLQTIAAE GIDGLKDAVN LNIRPNYEHN VALVSQTMFA
301 KLDKLDKNG NYLIQPDVKE ASQORLLGAK VEILPDETFG TAGNESLVFG NLKDALVLFV RSQVQAGWTD YMHFGECLMV ATRQDVRILD YKAAIVINYT
401 DAVTPEA

```



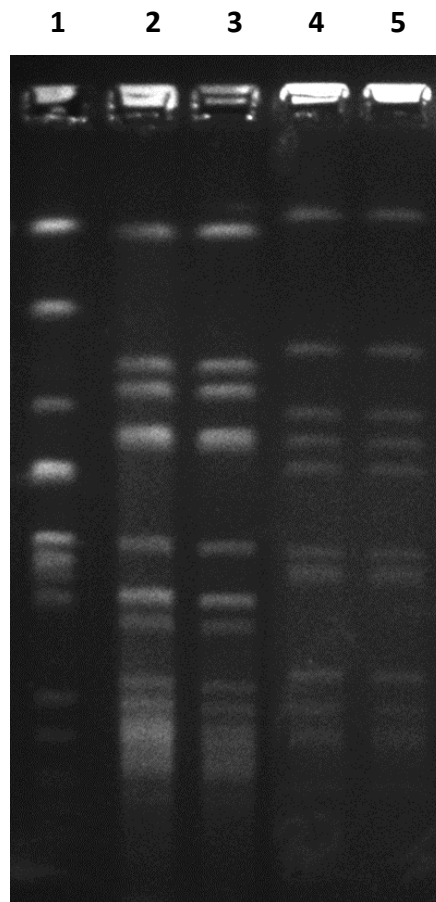
Sequence

```

1 MNKSKLKV IEDLQRSIDL KIKVATRALN DDDLEKAEKL EQEISELRKQ IADKEEELSK LKEESSNDED DPSNLEANRN NNPEKRSKKT PNANLLGANH
101 ISNDVSQEVV DFTEYIEARA DIPGGSLLKTD SGYVVIPEEI VTEILKLKEV EFNLDKIVTV KRVKNGSGKY PVRRESQVAA LPEVEELAEN PELAVKPFQ
201 LSYDIKTRRG YFRISREAIE DSQIDVLKEL KLWLARTIAA TRNKAIIDVI QKGGPGELGD NTKLQTIAAE GIDGLKDAVN LNIRPNYEHN VALVSQTMFA
301 KLDKLDKNG NYLIQPDVKE ASQORLLGAK VEILPDETFG TAGNESLVFG NLKDALVLFV RSQVQAGWTD YMHFGECLMV ATRQDVRILD YKAAIVINYT
401 DAVTPEA

```

Supplementary Figure S3. Sequence coverage of major capsid proteins of phages ϕ 575 and ϕ 879. Coverage of major capsid protein sequence is highlighted in green for both phages. Data evaluation was done using Proteome Discoverer v. 1.4 (Thermo Fisher Scientific). The sequence coverage is based purely on significant peptide hits ($p < 0.01$). Other filter criteria included: lowest peptide length (6 amino acid) and use only the best identified peptides for given peptide spectrum matches (rank 1).



Supplementary Figure S4. Pulsed-field gel electrophoresis analysis of transductants. The genetic background of interspecies and intraspecies transductants proved by *Sma*I macrorestriction analysis was in agreement with that of the recipient strains. Lane 1, donor strain *S. sciuri* P723 harbouring plasmid pSSC723; Lane 2, recipient strain *S. aureus* RN4220; Lane 3, transductant *S. aureus* RN4220::pSSC723; Lane 4, recipient strain *S. sciuri* P600; Lane 5, transductant *S. sciuri* P600::pSSC723.



Article

Characterization of *Staphylococcus intermedius* Group Isolates Associated with Animals from Antarctica and Emended Description of *Staphylococcus delphini*

Veronika Vrbovská ¹, Ivo Sedláček ², Michal Zeman ^{1,2}, Pavel Švec ², Vojtěch Kovařovic ¹, Ondřej Šedo ³, Monika Laichmanová ², Jiří Doškař ¹ and Roman Pantůček ^{1,*}

¹ Division of Genetics and Molecular Biology, Department of Experimental Biology, Faculty of Science, Masaryk University, Kotlářská 2, 611 37 Brno, Czech Republic; veronika.vrbovska@gmail.com (V.V.); michal.zeman91@gmail.com (M.Z.); 408266@mail.muni.cz (V.K.); doskar@sci.muni.cz (J.D.)

² Czech Collection of Microorganisms, Department of Experimental Biology, Faculty of Science, Masaryk University, Kamenice 5, 625 00 Brno, Czech Republic; ivo@sci.muni.cz (I.S.); mpavel@sci.muni.cz (P.Š.); monikadr@sci.muni.cz (M.L.)

³ Central European Institute of Technology, Masaryk University, Kamenice 5, 625 00 Brno, Czech Republic; sedo@sci.muni.cz

* Correspondence: pantucek@sci.muni.cz; Tel.: +420-549-49-6379

Received: 29 November 2019; Accepted: 30 January 2020; Published: 1 February 2020



Abstract: Members of the genus *Staphylococcus* are widespread in nature and occupy a variety of niches, however, staphylococcal colonization of animals in the Antarctic environment has not been adequately studied. Here, we describe the first isolation and characterization of two *Staphylococcus intermedius* group (SIG) members, *Staphylococcus delphini* and *Staphylococcus pseudintermedius*, in Antarctic wildlife. *Staphylococcus delphini* were found exclusively in Adélie penguins. The report of *S. pseudintermedius* from Weddell seals confirmed its occurrence in all families of the suborder Caniformia. Partial RNA polymerase beta-subunit (*rpoB*) gene sequencing, repetitive PCR fingerprinting with the (GTG)₅ primer, and matrix-assisted laser-desorption/ionization time-of-flight mass spectrometry gave consistent identification results and proved to be suitable for identifying SIG members. Comparative genomics of *S. delphini* isolates revealed variable genomic elements, including new prophages, a novel phage-inducible chromosomal island, and numerous putative virulence factors. Surface and extracellular protein distribution were compared between genomes and showed strain-specific profiles. The pathogenic potential of *S. delphini* was enhanced by a novel type of exfoliative toxin, trypsin-like serine protease cluster, and enterotoxin C. Detailed analysis of phenotypic characteristics performed on six Antarctic isolates of *S. delphini* and eight reference strains from different animal sources enabled us to emend the species description of *S. delphini*.

Keywords: *Staphylococcus delphini*; *Staphylococcus pseudintermedius*; Antarctica; mobile genetic elements; surface proteins; exfoliative toxin; Adélie penguin; Weddell seal

1. Introduction

Staphylococci are a major group of bacteria inhabiting the skin, skin glands, and mucous membranes of humans, other mammals, and birds, as well as the environment due to their ubiquity and adaptability [1]. However, there is very limited information available on staphylococcal isolates from Antarctica. Researchers have occasionally isolated staphylococcal strains from Antarctic environmental samples [2–6] and also from several animals obtained during their health evaluation, but they were mostly only classified to the genus level, such as isolates from whale wound lesions [7], a fish stomach [8], lesions on two dead Adélie penguins [9], or skin swabs of Weddell seals [10].

To the best of our knowledge, no member of the *Staphylococcus intermedius* group (SIG), which includes important veterinary pathogens, has been reported so far from animals in Antarctica. Originally, most isolates of SIG were classified as *S. intermedius*, before their subdivision into SIG members [11,12] comprised of the following four closely related but distinct coagulase-positive species: *S. intermedius* [13], *S. pseudintermedius* [14], *S. delphini* [15], and a human-originated *S. cornubiensis* [16]. The phenotypic and biochemical differentiation between the members of this group is complex and difficult and can result in unreliable species identification [17]. These species can be interchangeably misidentified as each other. Since SIG species are very similar to *Staphylococcus aureus* based on their clinical manifestations and biochemical characteristics such as coagulase positivity, SIG human clinical isolates have probably been misidentified as *S. aureus* in the past [18]. Protein profiling through matrix-assisted laser-desorption/ionization time-of-flight mass spectrometry (MALDI-TOF MS) seems to be the most reliable method to differentiate between SIG species [19,20]. Other effective methods for SIG diagnostics are sequencing of the housekeeping genes *nuc* [21], *sodA*, and *hsp60* [22], and for the discrimination of *S. pseudintermedius* by means of the *pta* housekeeping gene [23] or multilocus sequence typing (MLST) [24], as well as whole-genome sequencing [25,26].

SIG members are common colonizers of animal mucosal surfaces and are considered to be opportunistic pathogens in many infections of different animal hosts. Staphylococcal isolates from dogs previously identified as *S. intermedius* belong almost exclusively to the species *S. pseudintermedius*, while true *S. intermedius* are found predominantly in pigeons [11,12]. *S. pseudintermedius* is recognized as an important causative agent of pyoderma, dermatitis, and otitis externa in dogs, cats, horses, and other animals [27]. However, its host range is not restricted only to non-human animals, but colonization and zoonotic infections of humans are increasingly recognized [28–34]. The taxonomic description of *S. delphini*, in 1988 [15], was based on two strains isolated from purulent skin lesions of two dolphins. Recently, developments in diagnostics have led to the detection of *S. delphini* in a broad range of animals [11,12,35] and one reported human case, probably of zoonotic origin [36]. According to the multilocus sequence analysis of the *sodA*, *hsp60*, and *nuc* genes, *S. delphini* is divided into two phylogenetically distinct clades; group A closely related to the *S. delphini* type strain, and group B related to the *S. pseudintermedius* type strain [12]. The large number of different host associations suggests that multiple ecovars can exist among *S. delphini* isolates.

The aim of this study was to describe the SIG isolates from mammals and birds on James Ross and Seymour Islands in Antarctica, with a focus on *Staphylococcus delphini*. The SIG strains were characterized in detail by phenotypic and genotypic techniques and based on the results an emended description of *S. delphini* was provided.

2. Materials and Methods

2.1. Bacterial Strains and Their Biochemical Characterization

Bacterial strains were collected over the years from 2013 to 2019 on James Ross Island and Seymour Island, Antarctica (Figure 1). The sampling was a part of the Cultivable Fecal Bacteria Communities study, which was part of the CzechPolar project. Sampling intensity varied considerably with geographic location and weather conditions. The key element in the distribution of sampling intensity was the ice-free coast of James Ross and Seymour Islands. There are no seal colonies occupying littoral zone of both islands and samples were taken from occasionally found seals sunning on the coast. Penguin rookeries are in Seymour Island but only the droppings were collected in this territory for protection of the birds. Additional samples from penguins were taken by random sampling when penguins occurred on the coast. All samples originated from live animals only and the sampling procedure was fast to prevent any stress to the animals. The samples from the beak and cloaca of Adélie penguins (*Pygoscelis adeliae*) (82 specimens), the fresh droppings of South polar skua (*Stercorarius maccormicki*) (14 specimens), and kelp gull (*Larus dominicanus*) (11 specimens), and the anus and mouth of Weddell seals (*Leptonychotes weddellii*) (244 specimens), and Southern elephant

seals (*Mirounga leonina*) (12 individuals) were collected using the swab/transport tube system E-Swab (Dispolab, Brno, Czech Republic) and cultured on Mannitol Salt Agar (HiMedia Laboratories, Mumbai, India) at 35 °C for several days in the laboratory at J.G. Mendel Base, James Ross Island. Colonies with suspected staphylococcal morphology were picked daily, kept at 4 °C and transferred to the Czech Republic for further analyses.

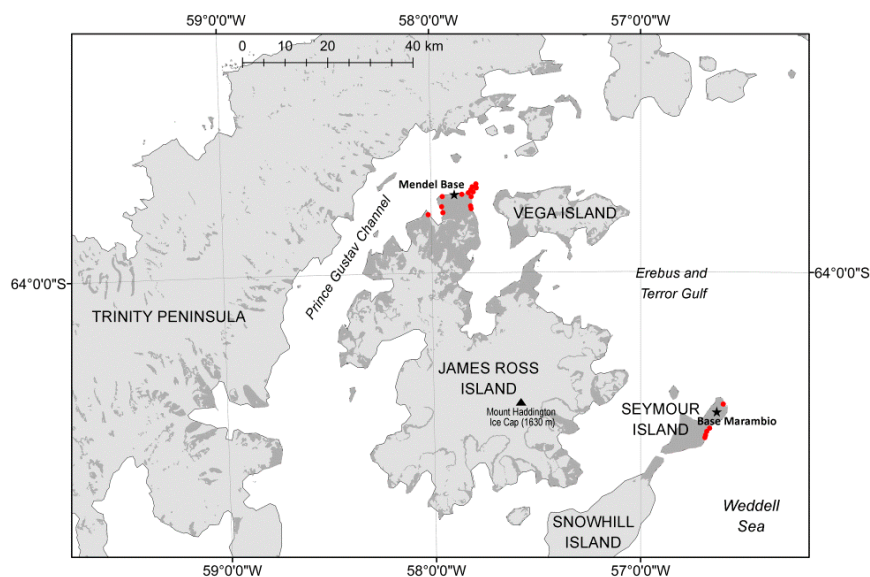


Figure 1. Sampling localities on James Ross Island and Seymour Island. Red mark, location of sampling site; asterisk, location of Antarctic base station; dark grey color, unglaciated area.

Type strains of *S. delphini* CCM 4115^T, *S. intermedius* CCM 5739^T, *S. pseudintermedius* CCM 7315^T, and *S. cornubiensis* CCM 8997^T were acquired from the Czech Collection of Microorganisms (Brno, Czech Republic). Reference strains of *S. delphini*: Nono (=CCM 4184) /dolphin/, CCM 2618 (=CCUG 51769) /mink/, P12548, P12549, and P12550 (=16-9169-2, 17-7762-1, and 18-3863-5, respectively) /all from minks/ [37], P12456 (=HT 2030677) /camel/, P12457 and P12458 (=8086 and 9106) /both from horses/ [11] and CCM 8998 (=MI 18-1587) /human/ [36] were described previously and kindly provided by the authors.

The phenotypic characterization of SIG strains was performed using the commercial kits API 50 CH and API ZYM (bioMérieux, Craponne, France) and by conventional physiological, biochemical, and growth tests discriminative for the genus *Staphylococcus* as described previously [2].

2.2. Partial 16S rRNA and RNA polymerase beta-subunit (*rpoB*) Gene Sequencing and Phylogenetic Analysis

Partial 16S rRNA gene amplification was performed as described previously [38]. PCR amplicons were sequenced with primer 553L in Eurofins Genomics sequencing facility (Ebersberg, Germany). Sequences were identified using the EzTaxon database [39].

Partial RNA polymerase β -subunit (*rpoB*) gene amplification was performed as described previously [40]. PCR amplicons obtained with the primers 1418F and 3554R were sequenced with primers 1418F and 1876R in Eurofins Genomics. Phylogenetic relationships were computed with the software MEGA version 10 [41]. Partial *rpoB* gene sequences were deposited into the GenBank/ENA/DDJB database under accession numbers MN729216–MN729246.

2.3. Rep-PCR

Repetitive PCR fingerprinting with the (GTG)₅ primer (rep-PCR) was performed as described previously [42]. Numerical analysis of the fingerprints and dendrogram construction was completed using the software BioNumerics version 7.6 (Applied Maths, Kortrijk, Belgium) and compared to

the in-house Czech Collection of Microorganisms rep-PCR database of type and reference strains representing hitherto described *Staphylococcus* spp.

2.4. MALDI-TOF MS

Protein fingerprints by MALDI-TOF MS were acquired with an ultrafleXtreme instrument (Bruker Daltonics, Bremen, Germany) by following the ethanol/formic acid extraction protocol [43]. As many as nine independent mass spectra were acquired for each sample, and only signals present in the minimum of seven of these mass spectra were used for the identification and cluster analysis. The mass spectral data were compared with entries in the latest version of the Biotyper database (version 9.0.0.0, 8468 references) and their mutual similarity was expressed by log(scores), where scores greater than 2.000 correlate to species identification with high confidence, log(score) values between 1.700 and 1.999 correspond to species identification with low confidence, and log(score) values lower than 1.699 result in no identification. A MALDI-TOF MS-based dendrogram was constructed with the software Biotyper (version 3.1, Bruker Daltonics) using the Pearson's product moment similarity coefficient and the unweighted pair group method with arithmetic average (UPGMA) as a grouping method.

2.5. Whole Genome Sequencing and Bioinformatic Analyses

Genomic DNA was isolated using a High Pure PCR Template Preparation Kit (Roche Diagnostics, Mannheim, Germany) according to the manufacturer's instructions with the modification of adding 20 μ L of lysostaphin (0.5 mg mL⁻¹) for cell lysis. An Illumina NextSeq sequencing platform was used for whole-genome shotgun sequencing of the strains P5747, P6456, and P8688. The purified genomic DNA was used for the preparation of a 500-bp sequencing library with a NEBNext@Ultra™ II DNA Library Prep Kit for Illumina (New England Biolabs, Ipswich, MA, USA). The samples were sequenced using a MID output cartridge in a 150-bp paired-end mode (Illumina, San Diego, CA, USA). The quality of sequencing reads was analyzed with FastQC version 0.11.8 [44]. Bases of lower quality and adapters were trimmed using the Spades version 3.13 implementation of BayesHammer. The de novo assembly of trimmed reads was performed with Spades version 3.13 [45], all k-mers 21 to 127 and follow-up mismatch correction. The package BMap version 38.73 was used to analyze various statistics of genomes [46]. Contigs of described *S. delphini* genomes were reordered according to the reference genome of *S. delphini* strain NCTC 12225^T (GenBank accession no. LR134263, NCTC 3000 Project) by Mauve Contig Mover as a part of Mauve version 2.4 [47]. The sequences of strains P5747, P6456, and P8688 were annotated by Prokka version 1.13.7 [48]. Subcellular localization of proteins of strains was predicted using PSORTb version 3.0 [49]. Proteins assigned to extracellular or cell wall categories were classified to gene ontology by cell2go [50]. Virulence factors were predicted using the VFAnalyzer tool available at the Virulence Factors Database [51]. OrthoVenn2 [52] was used to cluster predicted proteins to orthologous groups. Web-based tools PHASTER [53], CRISPR-Cas++ [54], and GView [55] were employed to find mobile genetic elements and dissimilar regions between analyzed genomes. Sequences were manipulated and examined in the cross-platform software Ugene version 1.31.1 [56]. The multiple sequence alignment was visualised using EasyFig version 2.3 [57].

Whole genome-based phylogenetic analysis was also carried out in order to check the species status of SIG isolates. Average nucleotide identity values (ANI) were calculated with OrthoANIu version 1.2 [58] and digital DNA–DNA hybridization (dDDH) values with the Genome-to-Genome Distance Calculator (GGDC) version 2.1 using the formula 2 recommended for draft genomes [57]. Up-to-date Bacterial Core Gene set (UBCG) software version 3.0 [59] was used to compare 92 core genes between *S. delphini* strains.

Assembly accession numbers of genomes retrieved from NCBI genome database are as follows: 8086 (GCF_000308115.1) [25], NCTC 12225^T (GCF_900636325.1), LMG 22219^T (GCF_001792775.2), NCTC 11048^T (GCF_900458545.1) [60], NW1^T (GCF_900183575.1) [16], 14S03309-1 (GCF_002374115.1), 14S03313-1 (GCF_002374125.1), 14S03318-1 (GCF_002369645.1), and 215100905101-2 (GCF_002369695.1) [26].

The Whole-Genome Shotgun projects of the *S. delphini* strains P5747 and P6456, and *S. pseudintermedius* P8688 have been deposited in DDBJ/ENA/GenBank under the accession numbers WNLD000000000, WNLE000000000, and JAACIP000000000, respectively.

3. Results

3.1. Bacterial Strain Collection and Identification of Staphylococci

During the austral summers from 2013 to 2019 on James Ross Island and Seymour Island, Antarctica, a total of 363 animal-related samples were collected in order to isolate staphylococcal species. The swabbed seals and penguins exhibited no disease symptoms at the time of sampling. Pure cultures of Gram-positive, catalase-positive cocci, able to grow in the presence of 12% NaCl, resistant to bacitracin and susceptible to furazolidone were chosen for partial 16S rRNA gene sequencing. In total, 150 *Staphylococcus* spp. strains were identified and most of them classified to the species level (Table S1). The most prevalent staphylococcal isolates were *Staphylococcus haemolyticus* ($n = 28$, predominantly in seals and droppings of skua), *Staphylococcus epidermidis* ($n = 22$, seals only), *Staphylococcus intermedius* group ($n = 22$, seals and penguins), *Staphylococcus sciuri* ($n = 18$, predominantly in penguins and droppings of skua), *Staphylococcus aureus*/*Staphylococcus argenteus*/*Staphylococcus schweitzeri* complex ($n = 14$, in all sources), *Staphylococcus capitis*/*Staphylococcus caprae* complex ($n = 12$, seals only), *Staphylococcus saprophyticus*/*Staphylococcus edaphicus* complex ($n = 9$, predominantly in seals), and *Staphylococcus schleiferi* subsp. *coagulans* ($n = 6$, in all sources).

Twenty-two of the 150 strains were originally identified as members of the *Staphylococcus intermedius* group based on partial 16S rRNA gene sequencing. The strains of SIG were further characterized in detail by genotypic and phenotypic methods and compared with the type strains *S. delphini* CCM 4115^T, *S. intermedius* CCM 5739^T, *S. pseudintermedius* CCM 7315^T, and *S. cornubiensis* CCM 8997^T, as well as with *S. delphini* reference strains CCM 4184, CCM 2618, P12456, P12457, P12458, P12548, P12549, P12550, and CCM 8998 isolated previously from various sources.

3.2. *rpoB* Gene Sequencing

Since 16S rRNA analysis has limited discriminatory power for identifying some staphylococcal species, the phylogenetic position of SIG strains assigned by the 16S rRNA gene sequencing was assessed using the sequence data of the partial *rpoB* gene that was previously shown to be effective for the species differentiation of staphylococci [40,61]. The computed neighbor-joining phylogenetic tree based on the partial *rpoB* gene sequence showed that SIG isolates clustered into two major groups corresponding to *S. delphini* and *S. pseudintermedius* (Figure 2). Strains recovered from Adélie penguins clustered together with the *S. delphini* type strain CCM 4115^T, whereas strains isolated from Weddell seals created a cluster with *S. pseudintermedius* type strain CCM 7315^T.

3.3. Repetitive Sequence-Based PCR (Rep-PCR) Fingerprinting

The repetitive sequence-based PCR (rep-PCR) fingerprinting technique using the (GTG)₅ primer placed the SIG isolates into two clusters corresponding to *S. delphini* and *S. pseudintermedius* at the similarity level of 54% and clearly separated them from *S. intermedius* and *S. cornubiensis* type strains (Figure 3). These results confirmed the *rpoB*-based identification of these strains. *S. delphini* strains exhibited more variable profiles (74% to 100% similarity between strains) than *S. pseudintermedius* (80% to 98%). Five *S. delphini* strains P5747, P5749, P5833, P5835, and P6070 were closely related, while strain P6456 separated from them and clustered together with the *S. delphini* P12458 strain recovered from horse nasal swab.

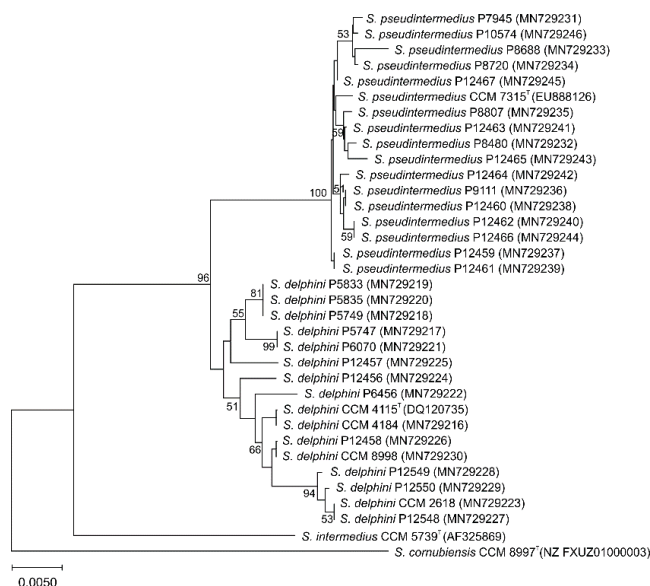


Figure 2. Unrooted neighbor-joining tree based on partial RNA polymerase beta-subunit (*rpoB*) gene sequence comparison, showing the clustering of Antarctic *Staphylococcus intermedius* group isolates and type and reference strains. The percentage of 500 tree replications above 50% in which the associated strains clustered together is shown next to the branches. The tree is drawn to scale, with branch lengths in the same units as those of the evolutionary distances used to infer the phylogenetic tree. The evolutionary distances were computed using the Tajima–Nei method and are in the units of the number of base substitutions per site. All ambiguous positions were removed for each sequence pair (pairwise deletion option). There was a total of 845 positions in the final dataset.

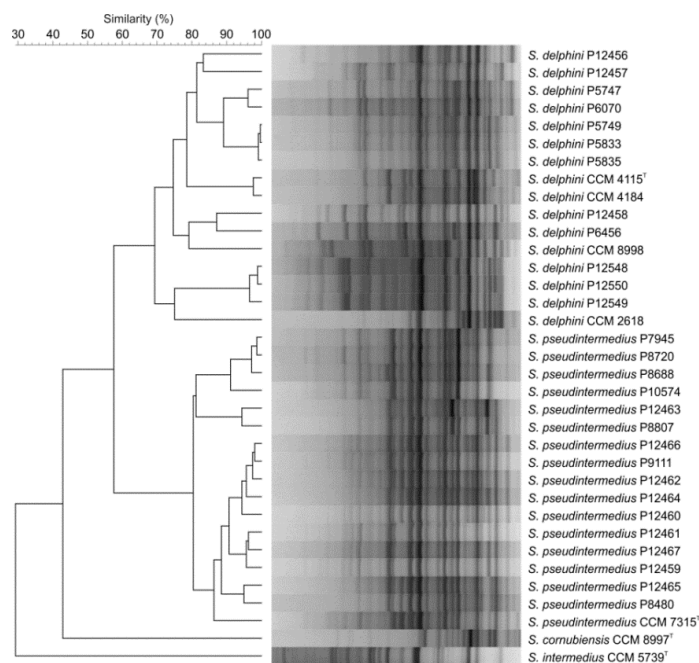


Figure 3. Dendrogram based on cluster analysis of repetitive sequence-based PCR (rep-PCR) fingerprints obtained with (GTG)₅ primer from analyzed isolates and type and reference strains of *Staphylococcus intermedius* group. The dendrogram was calculated with Pearson's correlation coefficients with unweighted pair group method with arithmetic average (UPGMA) clustering method (*r*, expressed as percentage similarity values).

3.4. MALDI-TOF MS

All SIG isolates and reference strains were analyzed by MALDI-TOF MS fingerprinting. Out of the *S. delphini* strains involved in the study, 14 were assigned to *S. delphini* entries of the Biotyper database (six with high confidence and eight with low confidence), while two strains, P5747 and P6070, did not exhibit significant similarity to any of the database entries. All sixteen *S. delphini* strains shared several signals (3787, 4111, 4278, 5302, 6241, 6341, 7438, 8032, 8147, 9028, 9649, and 10506 Da; detected doubly protonated forms of these proteins are not listed), while no peaks characteristic of the strain origin (isolation source/region) were found.

As for *S. pseudintermedius* strains, 13 strains were identified accordingly by using the Biotyper Database (two with high confidence and 11 with low confidence), while the four remaining strains (P7945, P8807, P9111, and P12464) did not exhibit significant similarity to any of the database entries. All 17 *S. pseudintermedius* strains shared several peaks (4278, 5303, 5843, 6241, 6875, 7438, 8032, 8147, 8622, 8649, 9028, 10081, and 10506 Da; detected doubly protonated forms of these proteins are not listed). Seven signals shared by all strains of *S. delphini* and *S. pseudintermedius* (4278, 6241, 7438, 8032, 8147, 9028, and 10506 Da) indicate the close relatedness of these two species. MALDI-TOF MS-based identification outputs correlated with the dendrogram derived from the protein signals (Figure 4). In addition, two *S. delphini* strains, P5747 and P6070, and four *S. pseudintermedius* strains, P7945, P8807, P9111, and P12464 unassigned to *S. delphini* or *S. pseudintermedius* by the MALDI MS-based scoring identification workflow and grouped using cluster analysis (Figure 4) in agreement with the *rpoB*-based and rep-PCR identification (Figure 3).

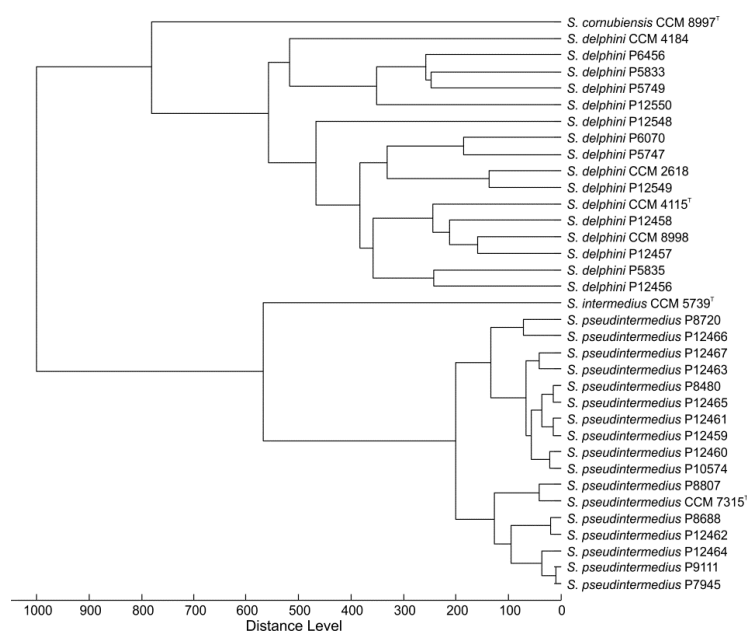


Figure 4. Matrix-assisted laser-desorption/ionization time-of-flight (MALDI-TOF) mass spectra-based dendrogram of analyzed isolates and type and reference strains of *Staphylococcus intermedius* group. The dendrogram was constructed using Pearson's product moment coefficient as a measure of similarity and the unweighted pair group average linked method (UPGMA) as a grouping method.

3.5. Biochemical Identification

The physiological and biochemical properties of SIG Antarctic isolates and 13 strains isolated from other sources were examined (Table 1). Antarctic isolates of both *S. delphini* and *S. pseudintermedius* phenotypically do not correspond to previously described profiles of the species and did not allow their correct classification. Contrary to the original description, all the studied *S. delphini* strains were gelatinase positive, but lecithinase negative and produced acid from trehalose. Coagulase, arginine

dihydrolase, urease, hydrolysis of Tween 80, acid production from glycerol, mannitol, β -gentiobiose, or turanose were strain-dependent for *S. delphini* (Table 1). Similarly, *S. pseudintermedius* from seals differs from the valid description by negative acetoin production and gave variable results for coagulase, arginine dihydrolase, and growth at 45 °C and acid production from mannitol, α -methyl-D-glucoside, and turanose (Table 1). Species from SIG are closely related and phenotypic classification to the species level remains insufficient due to the already reported lack of distinguishable biochemical tests for correct and reliable identification [11,12]. Phenotypic tests applicable for the presumptive species identification of SIG members based on our study, especially for *S. delphini* and *S. pseudintermedius*, are summarized in Table 2.

All strains were positive for the following conventional tests: production of catalase, growth in 12% NaCl, bacitracin resistance, furazolidone and novobiocin susceptibility, production of DNase, pyrrolidonyl arylamidase, nitrate reduction, and growth at 37 °C. Negative for production of oxidase, starch hydrolysis, and growth at 20 °C and 48 °C, production of ornithine decarboxylases, and Voges-Proskauer (acetoin). With the API ZYM kit, positive reactions were obtained for the enzymatic activity of alkaline phosphatase, acid phosphatase, esterase (C4), esterase-lipase (C8), leucine arylamidase and β -galactosidase; and negative reactions for the enzymes lipase (C14), valine arylamidase, cystine arylamidase, trypsin, α -chymotrypsin, naphthol-AS-BI-phosphohydrolase, α -galactosidase, β -glucuronidase, α -glucosidase, β -glucosidase, N-acetyl- β -glucosaminidase, α -mannosidase, and α -fucosidase. In the API 50 CH tests, all strains gave positive reactions for acid production from glycerol, ribose, galactose, glucose, fructose, mannose, N-acetyl-glucosamine, maltose, lactose, and sucrose. Negative acid production from erythritol, D-arabinose, L-arabinose, D-xylose, L-xylose adonitol, β -methyl-D-xyloside, sorbose, rhamnose, dulcitol, inositol, sorbitol, α -methyl-D-mannoside, amygdalin, arbutin, salicin, cellobiose, melibiose, inulin, melezitose, raffinose, starch, glycogen, xylitol, D-lyxose, D-tagatose, D-fucose, L-fucose, D-arabitol, L-arabitol, D-gluconate, 2-keto-gluconate, and 5-keto-gluconate; and negative esculin hydrolysis.

3.6. Comparative Genomic Analysis of *Staphylococcus delphini* Isolates

Two genomes of *S. delphini* Antarctic strains that differed from each other in several characteristics were shotgun sequenced and annotated. Strain P5747 was not successfully identified by the MALDI-TOF MS scoring algorithm, was urease negative, and did not produce acid from lactose; strain P6456 formed a distant cluster in the rep-PCR based dendrogram and *rpoB* gene phylogenetic tree and did not produce acid from mannitol. The size of the draft genomes of strains P5747 and P6456 was 2.54 and 2.65 Mb, comprised of 47 and 104 contigs, with an average G+C content of 38.2 and 38.1 mol%, respectively (Table S2). The genome assemblies were compared to whole-genome sequences of *S. delphini* type strain NCTC 12225^T and horse isolates *S. delphini* 8086 [25] and *S. delphini* 215100905101-2 [26] (Figure 5). Comparative genomic analysis of predicted genes in the above five genomes identified 2460 gene clusters and 596 singletons. The majority of the orthologous clusters (up to 1899) were shared by all the analyzed strains. Fifty-six clusters were unique for Antarctic strains and responsible for plasmid maintenance, phage DNA replication, and a response to phosphate starvation. All non-Antarctic *S. delphini* strains have additional genes for biofilm formation, the regulation of L-carnitine utilization, and a phosphoenolpyruvate-dependent sugar phosphotransferase system. Antarctic *S. delphini* lack the presence of the genes that confer resistance to fosfomycin as compared with the strains of equine origin.

Table 1. Variable phenotypic reactions of *Staphylococcus intermedius* group strains under study.

Species	Strain	Source	Locality	Conventional Test Results							API 50 CH							API ZYM				
				COA	ARG	URE	TWE	GEL	Cas	E-Y	C45	GLY	MAN	SOR	ARB	MDG	LAC	TRE	GEN	TUR	N-PH	α-FU
<i>S. delphini</i>	CCM 4115 ^T	dolphin	Italy	+	+	+	-	-	-	+	+	w	+	-	-	-	+	-	-	w	-	-
<i>S. delphini</i>	CCM 4184	dolphin	Italy	+	w	+	-	-	-	+	+	w	+	-	-	-	+	-	-	w	-	-
<i>S. delphini</i>	P5747	penguin	Antarctica	w	-	-	w	+	+	-	+	-	w	-	-	-	-	+	-	w	-	-
<i>S. delphini</i>	P5749	penguin	Antarctica	w	w	+	+	+	+	-	+	w	w	-	-	-	+	+	-	w	-	-
<i>S. delphini</i>	P5833	penguin	Antarctica	w	-	+	+	+	+	-	+	w	+	-	-	-	+	+	-	w	-	-
<i>S. delphini</i>	P5835	penguin	Antarctica	-	-	+	+	+	+	-	+	w	+	-	-	-	+	+	-	w	-	-
<i>S. delphini</i>	P6070	penguin	Antarctica	-	-	-	+	+	+	-	+	-	+	-	-	-	+	+	-	w	-	-
<i>S. delphini</i>	P6456	penguin	Antarctica	w	-	+	-	+	+	-	w	w	-	-	-	-	w	+	-	-	-	-
<i>S. delphini</i>	P12456	camel	France	w	w	+	-	+	+	-	-	+	+	-	w	-	+	+	+	w	+	-
<i>S. delphini</i>	P12457	horse	UK	+	w	+	-	+	+	-	-	w	+	+	-	-	w	+	+	w	w	w
<i>S. delphini</i>	P12458	horse	UK	w	w	+	+	+	+	-	+	w	w	-	-	-	+	+	-	w	-	-
<i>S. delphini</i>	CCM 2618	mink	Czechia	+	-	+	+	+	+	-	+	+	+	-	-	-	+	+	-	w	-	w
<i>S. delphini</i>	P12548	mink	Denmark	w	-	+	-	+	+	-	+	w	-	-	-	-	+	+	-	w	-	w
<i>S. delphini</i>	P12549	mink	Denmark	w	-	+	+	+	+	-	+	w	+	-	-	-	+	+	-	w	-	-
<i>S. delphini</i>	P12550	mink	Denmark	w	w	+	+	+	+	-	+	w	+	-	-	-	+	+	-	w	-	w
<i>S. delphini</i>	CCM 8998	human	USA	+	+	+	+	+	-	-	+	w	+	-	-	-	+	+	-	+	-	-
<i>S. pseudintermedius</i>	CCM 7315 ^T	cat	Belgium	+	+	+	-	+	-	-	+	+	+	-	-	w	+	+	-	+	-	-
<i>S. pseudintermedius</i>	P7945	seal	Antarctica	w	w	+	-	+	+	-	-	w	-	-	-	-	+	+	-	-	-	-
<i>S. pseudintermedius</i>	P8480	seal	Antarctica	+	-	+	-	+	+	-	+	+	-	-	-	w	+	+	-	w	-	-
<i>S. pseudintermedius</i>	P8688	seal	Antarctica	+	-	+	-	+	+	-	-	w	-	-	-	-	+	+	-	-	w	-
<i>S. pseudintermedius</i>	P8720	seal	Antarctica	w	+	+	-	+	+	-	-	w	-	-	-	-	+	+	-	-	-	-
<i>S. pseudintermedius</i>	P8807	seal	Antarctica	+	+	+	-	+	+	-	w	+	-	-	-	w	+	+	-	w	-	-
<i>S. pseudintermedius</i>	P9111	seal	Antarctica	+	w	+	-	+	+	-	w	+	+	-	-	w	+	+	-	w	-	-
<i>S. pseudintermedius</i>	P12459	seal	Antarctica	w	-	+	-	+	+	-	+	w	-	-	-	w	+	+	-	-	-	-
<i>S. pseudintermedius</i>	P12460	seal	Antarctica	-	w	+	-	+	+	-	+	w	+	-	-	w	+	+	-	+	-	-
<i>S. pseudintermedius</i>	P12461	seal	Antarctica	w	w	+	-	+	+	-	+	+	-	-	-	w	+	+	-	+	-	-
<i>S. pseudintermedius</i>	P12462	seal	Antarctica	-	-	+	-	+	+	-	+	+	+	-	-	w	+	+	-	+	-	-
<i>S. pseudintermedius</i>	P12463	seal	Antarctica	-	w	+	-	+	+	-	+	+	-	-	-	w	+	+	-	+	-	-
<i>S. pseudintermedius</i>	P12464	seal	Antarctica	-	w	+	-	+	+	-	+	+	+	-	-	w	+	+	-	+	-	-
<i>S. pseudintermedius</i>	P12465	seal	Antarctica	w	w	+	-	+	+	-	+	+	-	-	-	-	+	+	-	+	-	-
<i>S. pseudintermedius</i>	P12466	seal	Antarctica	w	w	+	-	+	+	-	w	+	+	-	-	w	+	+	-	+	-	-
<i>S. pseudintermedius</i>	P12467	seal	Antarctica	+	w	+	-	+	+	-	+	+	-	-	-	w	+	+	-	-	-	-
<i>S. pseudintermedius</i>	P10574	seal	Antarctica	-	+	+	-	+	+	-	-	w	-	-	-	-	+	+	-	-	-	-
<i>S. intermedius</i>	CCM 5739 ^T	pigeon	Czechia	w	-	+	-	+	+	-	+	w	+	-	-	w	+	+	+	w	-	-
<i>S. cornubiensis</i>	CCM 8997 ^T	human	UK	+	+	+	+	+	+	+	+	+	+	-	-	-	+	+	-	+	-	-

Legend: COA, coagulase; ARG, arginine dihydrolase; URE, urease; TWE, hydrolysis of Tween 80; GEL, hydrolysis of gelatin; Cas, hydrolysis of casein; E-Y, egg-yolk reaction (lecithinase); C45, growth at 45 °C; GLY, acid from glycerol; MAN, acid from mannitol; SOR, acid from sorbitol; ARB, acid from arbutin; MDG, acid from α-methyl-D-glucoside; LAC, acid from lactose; TRE, acid from trehalose; GEN, acid from β-gentiobiose; TUR, acid from turanose; N-PH, naphthol-AS-BI-phosphohydrolase; α-FU, α-fucosidase; +, positive; -, negative; w, weak.

Table 2. Proposal of phenotypic traits suitable for differentiation of *Staphylococcus intermedius* group species.

Species	Strains	TWE	E-Y	MAN	MDG
<i>S. delphini</i>	16 strains	d (63%)	- (6%)	+ (88%)	- (0%)
<i>S. pseudintermedius</i>	17 strains	- (0%)	- (0%)	(-) (29%)	(+) (71%)
<i>S. intermedius</i>	CCM 5739 ^T	-	-	+	w
<i>S. cornubiensis</i>	CCM 8997 ^T	+	+	+	-

Legend: TWE, hydrolysis of Tween 80; E-Y, egg-yolk reaction (lecithinase); MAN, acid from mannitol; MDG, acid from α -methyl-D-glucoside; +, 85% to 100%; (+), 70% to 84%; d, 31% to 69%; (-), 15% to 29%; -, 0% to 14%; w, weak.

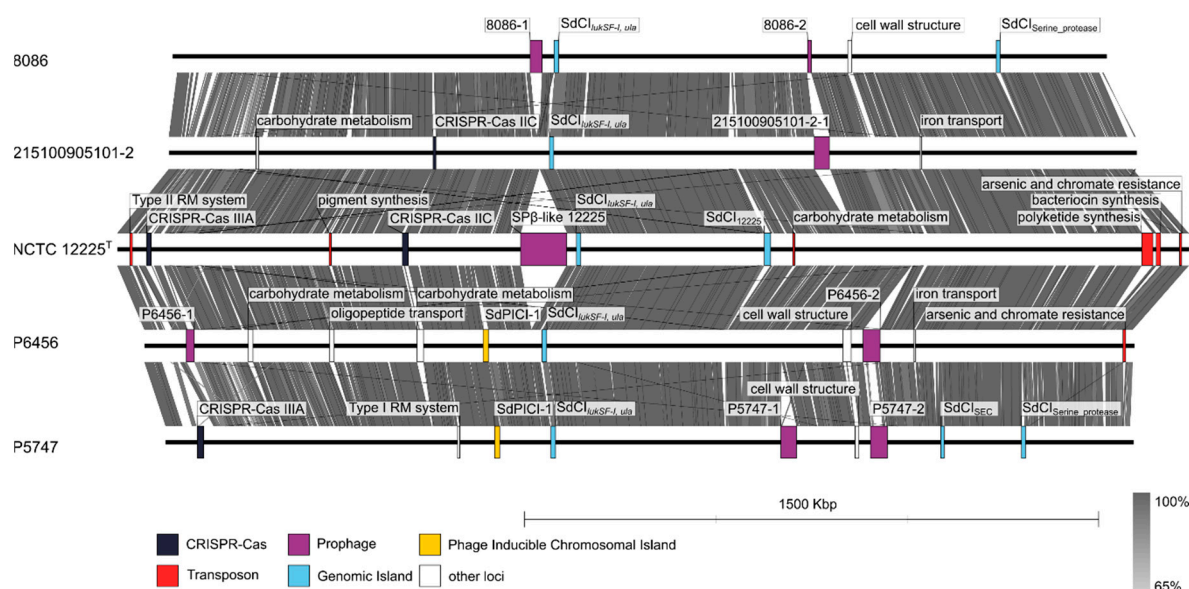


Figure 5. Whole-genome comparison of *Staphylococcus delphini* penguin isolates P5747 (GenBank accession no. WNLD000000000) and P6456 (WNLE000000000) with horse strains 8086 (CAIA000000000), 215100905101-2 (MWUT000000000), and type strain NCTC 12225^T from a dolphin (LR134263). Genomic regions with major differences between neighboring genomes and significant mobile genetic elements are highlighted in rectangles and are color-coded according to the legend. Prophage genomes 8086-1, 8086-2, and P6456-1 were located on different contigs, and therefore are not complete in the whole-genome comparison. Conserved regions with more than 65% homology are indicated with different shades of grey as determined by blastn.

Variability in *S. delphini* genome structure is mostly associated with mobile genetic elements and numerous genomic islets (Table S2 and Figure 5). The genomes of *S. delphini* strains P5747 and P6456 contain predicted plasmid contigs, prophages, a novel *S. delphini* phage-inducible chromosomal island (PICI) designated SdPICI-1 inserted between the chaperone GroEL and glucosamine-6-phosphate N-acetyltransferase genes, and genomic island designated SdCI_{SEC} encoding staphylococcal enterotoxin C (SEC) and putative proteins involved in its transfer. *Staphylococcus delphini* strain P5747 harbours CRISPR type IIIA, a distinctive gene cluster for purine metabolism, genes encoding sphingomyelinase C, sialidase B, putative genes for capsular polysaccharide synthesis located near the *oriC* region, and trypsin-like serine protease gene cluster. A genomic island containing bi-component leukocidin locus *lukSF-I* and the L-ascorbate transport and utilization (*ula*) operon was observed in all the analyzed genomes. The genome of *S. delphini* strain P6456 contains a gene for a novel exfoliative toxin (locus tag: FMF08_11915) in the *oriC* environ, gene clusters for the intake and metabolism of saccharides and oligopeptides, and a composite transposon for arsenic and chromate resistance.

The genes for virulence factors, surface and extracellular proteins are dispersed throughout *S. delphini* genomes. Majority of these proteins have similar distribution to other SIG members (Table S3).

The comparative analysis showed three major differences in those proteins from *S. delphini* strains and representative SIG members originating from different hosts as follows: (i) variability of serine proteases including exfoliative toxin-like proteins, (ii) different polysaccharide capsule synthesis proteins, and (iii) extensive variability of putative proteins with unknown function containing a LPXTG motif anchoring to cell wall peptidoglycan (Table S3).

To evaluate the intergenomic distances between the *S. delphini* genomes, ANI and dDDH values were determined (Table 3). The calculated ANI values among analyzed *S. delphini* genomes ranged from 96.28% to 98.66%, and unambiguously confirmed the position of both strains P5747 and P6456 as *S. delphini* species and at the same time showed that *S. pseudintermedius* and *S. intermedius* type strains are well below the thresholds of 95% to 96% for species delineation [62]. The calculated dDDH values among *S. delphini* were relatively low and indicated an extensive variability that could represent specialization to specific hosts. As a further extension to genome-based phylogeny the Up-to-date Bacterial Core Gene (UBCG) tool was used to compare 92 core genes among analyzed *S. delphini* genomes (Figure 6). This analysis confirmed that the strains do not divide to distinctive lineages according to their animal host.

Table 3. Intergenomic distances between the genomes of *Staphylococcus intermedius* group strains in percent, represented by average nucleotide identity (ANI) and digitally derived genome-to-genome distances (GGD) emulating DNA–DNA hybridization values.

Strain	P5747		P6456		NCTC 12225 ^T		215100905101-2 8086				NCTC 11048 ^T		LMG 22219 ^T		NW1 ^T	
	GGD	ANI	GGD	ANI	GGD	ANI	GGD	ANI	GGD	ANI	GGD	ANI	GGD	ANI	GGD	ANI
<i>S. delphini</i> P5747	-	-	70.2	96.3	70.5	96.5	77.4	97.6	85.6	98.4	35.8	88.6	55.1	93.9	33.5	87.4
<i>S. delphini</i> P6456	70.2	96.3	-	-	87.5	98.7	69.5	96.3	69.0	96.3	35.5	88.4	51.3	93.1	33.2	87.2
<i>S. delphini</i> NCTC 12225 ^T	70.5	96.5	87.5	98.7	-	-	70.4	96.6	70.1	96.4	35.9	88.6	51.2	93.1	33.5	87.4
<i>S. delphini</i> 215100905101-2	77.4	97.6	69.5	96.3	70.4	96.6	-	-	78.4	97.6	35.7	88.6	54.7	93.7	33.6	87.8
<i>S. delphini</i> 8086	85.6	98.4	69.0	96.3	70.1	96.4	78.4	97.6	-	-	35.6	88.6	54.9	93.9	33.6	87.5
<i>S. intermedius</i> NCTC 11048 ^T	35.8	88.6	35.5	88.4	35.9	88.6	35.7	88.6	35.6	88.7	-	-	34.9	88.0	36.2	88.6
<i>S. pseudintermedius</i> LMG 22219 ^T	55.1	93.9	51.3	93.1	51.2	93.1	54.7	93.7	54.9	93.9	34.9	88.0	-	-	32.9	87.2
<i>S. cornubiensis</i> NW1 ^T	33.5	87.4	33.2	87.2	33.5	87.4	33.6	87.8	33.6	87.6	36.2	88.6	32.9	87.2	-	-

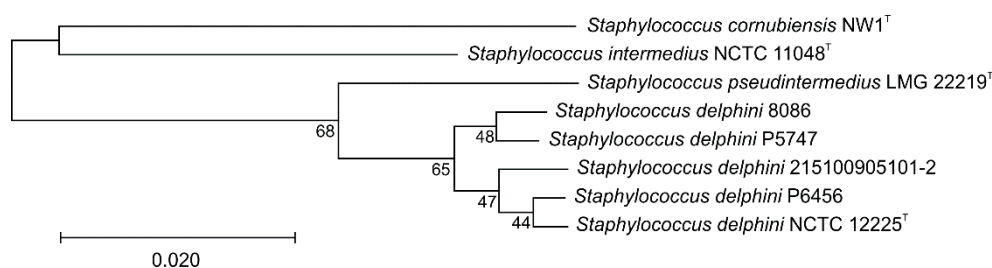


Figure 6. Core gene set phylogenetic tree of *Staphylococcus delphini* strains from different animals (penguin isolates P5747 and P6456, horse strains 8086 and 215100905101-2, and a dolphin strain NCTC 12225^T). The phylogenetic tree was constructed using Up-to-date bacterial core gene set (UBCG) concatenated alignment of 92 core genes. A total of 86,031 nucleotide positions were used. Maximum likelihood phylogenetic tree was inferred using Fasttree version 2.1.10 using GTR + CAT model. Gene support indices are given at branching points (maximal possible value is 92). Bar, 0.1 substitution per position.

4. Discussion

The analyzed SIG strains were collected in several consecutive years at three different locations. Species identification based on previously evaluated 16S ribosomal DNA-based identification [63] showed the presence of 16 staphylococcal taxa. Some of the recently described staphylococcal species shared high similarity in their 16S rRNA sequence and were distinguished on the basis of whole-genome sequencing, therefore they are identified as species complexes. Among the most prevalent staphylococcal species isolated from Antarctic wildlife were *S. haemolyticus*, *S. epidermidis*, and *S. sciuri*, which have been previously collected in Antarctic environmental samples [4–6,64].

In this study, several strains of *S. aureus* were also collected, which corresponds with the findings of Van Elk et al. [65], who recovered an *S. aureus* isolate from Antarctic southern elephant seal and suggested that it could be a host species-specific and coevolved variant which is not closely related to *S. aureus* strains from terrestrial species, based on MLST analysis.

To the best of our knowledge, this is the first report of the isolation and characterization of *S. delphini* and *S. pseudintermedius* from Antarctic animals, penguins and seals. SIG species, thus, seem to be ubiquitous and the most common coagulase-positive staphylococci recovered from non-human animals, in which they can act as opportunistic pathogens and cause a variety of infections. *Staphylococcus delphini* has been previously isolated from a broad range of phylogenetically unrelated mammals (dolphins, cows, horses, camels, and mustelids). The isolation of *S. delphini* from the Antarctic Adélie penguin is the only report from birds except for rare isolates from pigeons [12]. *S. pseudintermedius* is a predominant opportunistic pathogen of canine hosts, and the clonal diversity and broad geographic distribution of *S. pseudintermedius* suggests that it has coevolved with the suborder Caniformia ("dog-like" carnivorans) for a long time in evolutionary terms [11,66,67]. Aarestrup [67] isolated SIG strains from the skin of healthy members of six phylogenetic groups within Caniformia, but not successfully from the seal family (*Phocidae*). The report of the occurrence of *S. pseudintermedius* in Weddell seals supports the theory of *S. pseudintermedius* coevolution with Caniformia, and it is evident that the bacteria can coexist with their hosts in the extreme polar environment. It is likely that SIG species shared a common ancestor and evolved with their specific host adaptation, analogously to the relationship between *S. aureus* and its sister primate-associated species *Staphylococcus simiae* [68,69] or *Staphylococcus schweitzeri* [70]. In addition, this study concluded that members of SIG are distributed worldwide and inhabit an even wider range of hosts than was previously thought.

Differentiating between species belonging to SIG is problematic. In addition, some strains previously described as *S. intermedius* have been reassigned to other species within SIG [12,71]. Identification based on conventional biochemical, physiological, and growth tests in a routine microbiology laboratory is difficult, since SIG members share many phenotypic characteristics, the expression of many biochemical properties is variable, and taxonomic descriptions were done with various identification sets utilizing different reaction substrates. We evaluated the performance of molecular-based and phenotype-based techniques for the ability to differentiate and identify members of SIG, including Antarctic isolates. The study demonstrated that *rpoB* gene sequencing and rep-PCR gave consistent results and differentiated the isolates into distinctive clusters corresponding to individual species within SIG. Cluster analysis based on MALDI-TOF MS protein data was able to separate the *S. pseudintermedius* and *S. delphini* Antarctic isolates, place them together with corresponding type strains, and create separate clusters from *S. intermedius* and *S. cornubiensis* type strains. Unlike a recent report [72], mass spectrometry was unable to identify two Antarctic isolates of *S. delphini* using a MALDI-TOF MS-based scoring identification workflow.

The Antarctic *S. delphini* and *S. pseudintermedius* isolates phenotypically differ from both the type and used reference strains. The type strain of *S. delphini* is described as negative for trehalose and thermonuclease. Because the species description of *S. delphini* was based on only two strains, in our study we tested a set of Antarctic isolates supplemented with *S. delphini* reference strains from different animals, including a human isolate. All Antarctic *S. delphini* strains were positive for acid production from trehalose, similarly to Sasaki et al. [12] who also reported some *S. delphini* strains to be positive for trehalose and thermonuclease. Moreover, in our study we found positive gelatinase activity among *S. delphini* isolates and reference strains, which contradicted their species description, as well as lecithinase production, which was positive for the type strain but negative for the tested strains. It is possible that strains from diverse animals represent distinctive ecotypes with specific ecological adaptations. Variation in phenotype, borderline dDDH values between strains (Table 3), and previously reported polymorphisms in housekeeping genes [12] suggest that more subspecies exists within *S. delphini* species.

Similar to *S. aureus* [73,74], the major differences in the *S. delphini* genomes are due to variable genetic elements. Various prophages with low similarity to known phage sequences in available databases were found in all strains. Two different types of wall teichoic acids synthesis loci were found in the analyzed genomes. Since wall teichoic acids serve as receptors for bacteriophage adsorption [74] and the phage adsorption is sufficient for efficient transduction [75] we hypothesize that differences in phage receptors can drive the diversification of *S. delphini* genomes. The staphylococcal cassette chromosome *mec*, which was described in methicillin-resistant *S. pseudintermedius* [76], was not detected in any of the analyzed *S. delphini* genomes. The presence of CRISPR/Cas and the type of *cas* genes was not related to the animal source of the isolation, thus the loci could have been acquired independently. *Staphylococcus aureus* pathogenicity islands (SaPI) are well described representatives of PICI and contribute to horizontal gene transfer [77]. In contrast to SaPI, *S. delphini* PICI SdPICI-1 was only observed in strains isolated from penguins and contained genes for phage-related head structural proteins and both terminase subunits, which has been observed in some PICIs of Gram-negative bacteria [78]. The finding of genomic island harboring leukocidin encoding genes *lukFS-I* among all analyzed strains confirms its ancient origin [25] and also its preservation among *S. delphini* strains in the polar environment. Virulence potential of all analyzed *S. delphini* strains is enhanced by the presence of SEC encoding genes, which have been previously detected in *S. pseudintermedius* isolates and associated with canine pyoderma [79,80]. Distribution of other toxin genes is variable among the strains (Table S3). Putative exfoliative toxin from P6456 strain has 53% amino acid identity with *S. pseudintermedius* exfoliative toxins EXI and ExpB [81,82]. Furthermore, an island with multiple paralog genes encoding trypsin-like serine proteases related to exfoliative toxins [83] was found in strain P5747 (Figure 5 and Table S3), being a possible virulence factor.

Staphylococcus delphini genomes of the type strain, the strains representing two different phylogenetic branches of equine origin and the selected genomes of SIG isolates from other animals, were used for the comparative genomic analysis with focus on virulence, cell wall anchored proteins, and extracellular proteins (Table S3). These proteins most likely play a role in adaptation to the host and in a defence against host immunity. Homologs of *S. delphini* surface proteins were found in other SIG species, but many proteins were strain-specific, suggesting specific adaptation and virulence. However, there was no distinctive pattern of surface proteins corresponding to individual animal hosts. The location of these genes for surface proteins was predominantly on the chromosomes and not on the mobile genetic elements indicating both common ancestry and differential gene loss among strains as well as gene gain via horizontal transfer events. Despite numerous putative virulence factors found in analyzed genomes of *S. delphini*, further studies are needed to consider their role in animal pathogenesis or the possible risk of zoonotic infection to humans.

5. Emended Description of *Staphylococcus delphini* (Varaldo et al., 1988)

The description is based on the original description and observations of six isolates from penguins and eight reference strains from animals and human (Table 1). The morphological, biochemical, and physiological characteristics are generally those of the *S. delphini* description [15] with the exception of gelatin and lecithin hydrolysis and trehalose acidification, which were strain dependent. In contrast to type strain CCM 4115^T and reference strain CCM 4184, both from dolphins [15], all the studied *S. delphini* strains were gelatinase positive, but lecithinase negative and produced acid from trehalose. Below are the mentioned emended positive and negative test results not included in the original description.

Acid is produced from glycerol, ribose, galactose, and N-acetyl-glucosamine (API 50 CH). Esterase (C4), esterase-lipase (C8), acid phosphatase, pyrrolidonyl arylamidase, leucine arylamidase, and β -galactosidase positive (API ZYM). Resistant to bacitracin (0.04 U) and susceptible to furazolidone (100 μ g). Negative oxidase, ornithine decarboxylase, esculin and starch hydrolysis, and growth at 20 °C. Acid production is negative from erythritol, D-arabinose, D-xylose, adonitol, β -methyl-D-xyloside, sorbose, rhamnose, dulcitol, inositol, sorbitol, α -methyl-D-mannoside, α -methyl-D-glucoside, amygdalin, arbutin, salicine, cellobiose, melibiose, inulin, melezitose, raffinose, starch, glycogen,

D-lyxose, D-tagatose, D-fucose, L-fucose, D-arabitol, L-arabitol, gluconate, 2-keto-gluconate, and 5-keto-gluconate (API 50 CH). No enzymatic activity found for lipase (C14), valine arylamidase, cystine arylamidase, trypsin, α -chymotrypsin, α -galactosidase, β -glucuronidase, α -glucosidase, β -glucosidase, N-acetyl- β -glucosaminidase, and α -mannosidase (API ZYM). Variable reactions are shown in Table 1. Isolated from mucous membranes of different animals, occasionally humans. G + C content of 38 mol% calculated from whole genomic sequence.

Supplementary Materials: The following are available online at <http://www.mdpi.com/2076-2607/8/2/204/s1>: Table S1: *Staphylococcus* spp. strains identified in animal-related samples from James Ross Island and Seymour Island, Antarctica, Table S2: Comparison of selected genomic features of *Staphylococcus delphini* strains P5747 and P6456 from penguins, and *S. delphini* strains from other hosts, Table S3: Distribution of virulence factors, surface and extracellular proteins among the *Staphylococcus delphini* strains from different hosts and from the reference and type strains of other SIG species.

Author Contributions: Design of the study and conceptualization, R.P., I.S., and V.V.; sampling, isolation and preliminary identification of the strains, I.S. and M.L.; performance of experiments and investigations, V.V., I.S., P.Š., and O.Š.; analysis of data, V.V., I.S., M.Z., P.Š., V.K., and R.P.; writing—original draft preparation, V.V., M.Z., and I.S.; writing—review and editing, V.V., R.P., I.S., P.Š., and J.D.; visualization, M.Z., P.Š., V.K., and R.P.; supervision, R.P.; funding acquisition, R.P., I.S., and J.D. All authors have read and agreed to the published version of the manuscript.

Funding: This work was supported by the Ministry of Education, Youth and Sports of the Czech Republic (MEYS CR) (grant number LM2015078) and by the Ministry of Health of the Czech Republic (grant number 16-29916A to R.P.). The CIISB research infrastructure project (LM2018127), the NCMG research infrastructure project (LM2015091) and the project CEITEC 2020 (LQ1601) funded by MEYS CR, are gratefully acknowledged for the financial support of the MALDI-TOF MS measurements at the Proteomics Core Facility and whole-genome sequencing at the Genomics Core Facility of CEITEC. Students participating in this work were supported by the Grant Agency of Masaryk University (MUNI/A/1127/2019 to J.D.).

Acknowledgments: We are grateful for the scientific infrastructure of the J.G. Mendel Czech Antarctic Station as part of the Czech Polar Research Infrastructure (CzechPolar2) and to its crew for their assistance, as well as to the Czech Antarctic Foundation for their support. We wish to thank Eva Staňková and Jana Bajerová (Czech Collection of Microorganisms, Masaryk University) and Tereza Gelbíčová (Veterinary Research Institute, Brno) for technical assistance. Prof. J. Ross Fitzgerald (University of Edinburgh, UK), Dr. Nanett K. Nikolaisen (Technical University of Denmark, Denmark), and Dr. Stephen A. Kania (University of Tennessee, USA) are gratefully acknowledged for providing us with bacterial strains.

Conflicts of Interest: The authors declare no conflicts of interest.

References

1. Götz, F.; Bannerman, T.; Schleifer, K.-H. The Genera *Staphylococcus* and *Micrococcus*. In *The Prokaryotes. Volume 4: Bacteria: Firmicutes, Cyanobacteria*; Dworkin, M., Falkow, S., Rosenberg, E., Schleifer, K.-H., Stackebrandt, E., Eds.; Springer Science: New York, NY, USA, 2006; Volume 4, pp. 5–75.
2. Pantůček, R.; Sedláček, I.; Indráková, A.; Vrbovská, V.; Mašlaňová, I.; Kovařovic, V.; Švec, P.; Králová, S.; Křištofová, L.; Kečliková, J.; et al. *Staphylococcus edaphicus* sp. nov., isolated in Antarctica, harbors the *mecC* gene and genomic islands with a suspected role in adaptation to extreme environments. *Appl. Env. Microbiol.* **2018**, *84*. [[CrossRef](#)]
3. Shivaji, S.; Begum, Z.; Shiva Nageswara Rao, S.S.; Vishnu Vardhan Reddy, P.V.; Manasa, P.; Sailaja, B.; Prathiba, M.S.; Thamban, M.; Krishnan, K.P.; Singh, S.M.; et al. Antarctic ice core samples: Culturable bacterial diversity. *Res. Microbiol.* **2013**, *164*, 70–82. [[CrossRef](#)] [[PubMed](#)]
4. Peeters, K.; Hodgson, D.A.; Convey, P.; Willems, A. Culturable diversity of heterotrophic bacteria in Forlidas Pond (Pensacola Mountains) and Lundstrom Lake (Shackleton Range), Antarctica. *Microbiol. Ecol.* **2011**, *62*, 399–413. [[CrossRef](#)] [[PubMed](#)]
5. Arenas, F.A.; Pugin, B.; Henriquez, N.A.; Arenas-Salinas, M.A.; Diaz-Vasquez, W.A.; Pozo, M.F.; Munoz, C.M.; Chasteen, T.G.; Perez-Donoso, J.M.; Vasquez, C.C. Isolation, identification and characterization of highly tellurite-resistant, tellurite-reducing bacteria from Antarctica. *Polar Sci.* **2014**, *8*, 40–52. [[CrossRef](#)]
6. Leiva, S.; Alvarado, P.; Huang, Y.; Wang, J.; Garrido, I. Diversity of pigmented Gram-positive bacteria associated with marine macroalgae from Antarctica. *FEMS Microbiol. Lett.* **2015**, *362*, fnv206. [[CrossRef](#)] [[PubMed](#)]

7. Sieburth, J.M. Gastrointestinal microflora of Antarctic birds. *J. Bacteriol.* **1959**, *77*, 521–531. [[CrossRef](#)] [[PubMed](#)]
8. Vazquez, S.C.; Merino, L.N.R.; Maccormack, W.P.; Fraile, E.R. Protease-producing psychrotrophic bacteria isolated from Antarctica. *Polar Biol.* **1995**, *15*, 131–135. [[CrossRef](#)]
9. Nievas, V.F.; Leotta, G.A.; Vigo, G.B. Subcutaneous clostridial infection in Adelie penguins in Hope Bay, Antarctica. *Polar Biol.* **2007**, *30*, 249–252. [[CrossRef](#)]
10. Mellish, J.; Tuomi, P.; Hindle, A.; Jang, S.; Horning, M. Skin microbial flora and effectiveness of aseptic technique for deep muscle biopsies in Weddell seals (*Leptonychotes weddellii*) in McMurdo Sound, Antarctica. *J. Wildlife Dis.* **2010**, *46*, 655–658. [[CrossRef](#)]
11. Bannoehr, J.; Ben Zakour, N.L.; Waller, A.S.; Guardabassi, L.; Thoday, K.L.; van den Broek, A.H.M.; Fitzgerald, J.R. Population genetic structure of the *Staphylococcus intermedius* group: Insights into *agr* diversification and the emergence of methicillin-resistant strains. *J. Bacteriol.* **2007**, *189*, 8685–8692. [[CrossRef](#)]
12. Sasaki, T.; Kikuchi, K.; Tanaka, Y.; Takahashi, N.; Kamata, S.; Hiramatsu, K. Reclassification of phenotypically identified *Staphylococcus intermedius* strains. *J. Clin. Microbiol.* **2007**, *45*, 2770–2778. [[CrossRef](#)] [[PubMed](#)]
13. Hájek, V. *Staphylococcus intermedius*, a new species isolated from animals. *Int. J. Syst. Bacteriol.* **1976**, *26*, 401–408. [[CrossRef](#)]
14. Devriese, L.A.; Vancanneyt, M.; Baele, M.; Vanechoutte, M.; De Graef, E.; Snauwaert, C.; Cleenwerck, I.; Dawyndt, P.; Swings, J.; Decostere, A.; et al. *Staphylococcus pseudintermedius* sp. nov., a coagulase-positive species from animals. *Int. J. Syst. Evol. Microbiol.* **2005**, *55*, 1569–1573. [[CrossRef](#)] [[PubMed](#)]
15. Varaldo, P.E.; Kilpperbalz, R.; Biavasco, F.; Satta, G.; Schleifer, K.H. *Staphylococcus delphini* sp. nov., a coagulase-positive species isolated from dolphins. *Int. J. Syst. Bacteriol.* **1988**, *38*, 436–439. [[CrossRef](#)]
16. Murray, A.K.; Lee, J.; Bendall, R.; Zhang, L.; Sunde, M.; Schau Slette-meas, J.; Gaze, W.; Page, A.J.; Vos, M. *Staphylococcus cornubiensis* sp. nov., a member of the *Staphylococcus intermedius* group (SIG). *Int. J. Syst. Evol. Microbiol.* **2018**, *68*, 3404–3408. [[CrossRef](#)]
17. Bond, R.; Loeffler, A. What’s happened to *Staphylococcus intermedius*? Taxonomic revision and emergence of multi-drug resistance. *J. Small Anim. Pr.* **2012**, *53*, 147–154. [[CrossRef](#)]
18. Viau, R.; Hujer, A.M.; Hujer, K.M.; Bonomo, R.A.; Jump, R.L.P. Are *Staphylococcus intermedius* infections in humans cases of mistaken identity? A case series and literature review. *Open Forum Infect. Dis.* **2015**, *2*, ofv110. [[CrossRef](#)]
19. Decristophoris, P.; Fasola, A.; Benagli, C.; Tonolla, M.; Petrini, O. Identification of *Staphylococcus intermedius* group by MALDI-TOF MS. *Syst. Appl. Microbiol.* **2011**, *34*, 45–51. [[CrossRef](#)]
20. Murugaiyan, J.; Walther, B.; Stamm, I.; Abou-Elnaga, Y.; Brueggemann-Schwarze, S.; Vincze, S.; Wieler, L.H.; Lubke-Becker, A.; Semmler, T.; Roesler, U. Species differentiation within the *Staphylococcus intermedius* group using a refined MALDI-TOF MS database. *Clin. Microbiol. Infect.* **2014**, *20*, 1007–1014. [[CrossRef](#)]
21. Sasaki, T.; Tsubakishita, S.; Tanaka, Y.; Sakusabe, A.; Ohtsuka, M.; Hirotaki, S.; Kawakami, T.; Fukata, T.; Hiramatsu, K. Multiplex-PCR method for species identification of coagulase-positive staphylococci. *J. Clin. Microbiol.* **2010**, *48*, 765–769. [[CrossRef](#)]
22. Lee, J.; Murray, A.; Bendall, R.; Gaze, W.; Zhang, L.H.; Vos, M. Improved detection of *Staphylococcus intermedius* group in a routine diagnostic laboratory. *J. Clin. Microbiol.* **2015**, *53*, 961–963. [[CrossRef](#)] [[PubMed](#)]
23. Slette-meas, J.S.; Mikalsen, J.; Sunde, M. Further diversity of the *Staphylococcus intermedius* group and heterogeneity in the *MboI* restriction site used for *Staphylococcus pseudintermedius* species identification. *J. Vet. Diagn. Invest.* **2010**, *22*, 756–759. [[CrossRef](#)] [[PubMed](#)]
24. Solyman, S.M.; Black, C.C.; Duim, B.; Perreten, V.; van Duijkeren, E.; Wagenaar, J.A.; Eberlein, L.C.; Sadeghi, L.N.; Videla, R.; Bemis, D.A.; et al. Multilocus sequence typing for characterization of *Staphylococcus pseudintermedius*. *J. Clin. Microbiol.* **2013**, *51*, 306–310. [[CrossRef](#)] [[PubMed](#)]
25. Ben Zakour, N.L.; Beatson, S.A.; van den Broek, A.H.M.; Thoday, K.L.; Fitzgerald, J.R. Comparative genomics of the *Staphylococcus intermedius* group of animal pathogens. *Front. Cell. Infect. Microbiol.* **2012**, *2*, 44. [[CrossRef](#)] [[PubMed](#)]
26. Verstappen, K.M.; Huijbregts, L.; Spaninks, M.; Wagenaar, J.A.; Fluit, A.C.; Duim, B. Development of a real-time PCR for detection of *Staphylococcus pseudintermedius* using a novel automated comparison of whole-genome sequences. *PLoS ONE* **2017**, *12*, e0189520. [[CrossRef](#)]

27. Bannoehr, J.; Franco, A.; Iurescia, M.; Battisti, A.; Fitzgerald, J.R. Molecular diagnostic identification of *Staphylococcus pseudintermedius*. *J. Clin. Microbiol.* **2009**, *47*, 469–471. [[CrossRef](#)] [[PubMed](#)]
28. Borjesson, S.; Gomez-Sanz, E.; Ekstrom, K.; Torres, C.; Gronlund, U. *Staphylococcus pseudintermedius* can be misdiagnosed as *Staphylococcus aureus* in humans with dog bite wounds. *Eur. J. Clin. Microbiol.* **2015**, *34*, 839–844. [[CrossRef](#)]
29. Lainhart, W.; Yarbrough, M.L.; Burnham, C.A. The brief case: *Staphylococcus intermedius* group—look what the dog dragged in. *J. Clin. Microbiol.* **2018**, *56*, e00839-17. [[CrossRef](#)]
30. Hanselman, B.A.; Kruth, S.A.; Rousseau, J.; Weese, J.S. Coagulase positive staphylococcal colonization of humans and their household pets. *Can. Vet. J.* **2009**, *50*, 954–958.
31. Ishihara, K.; Shimokubo, N.; Sakagami, A.; Ueno, H.; Muramatsu, Y.; Kadosawa, T.; Yanagisawa, C.; Hanaki, H.; Nakajima, C.; Suzuki, Y.; et al. Occurrence and molecular characteristics of methicillin-resistant *Staphylococcus aureus* and methicillin-resistant *Staphylococcus pseudintermedius* in an academic veterinary hospital. *Appl. Env. Microbiol.* **2010**, *76*, 5165–5174. [[CrossRef](#)]
32. Sasaki, T.; Kikuchi, K.; Tanaka, Y.; Takahashi, N.; Kamata, S.; Hiramatsu, K. Methicillin-resistant *Staphylococcus pseudintermedius* in a veterinary teaching hospital. *J. Clin. Microbiol.* **2007**, *45*, 1118–1125. [[CrossRef](#)]
33. Soedarmanto, I.; Kanbar, T.; Ulbegi-Mohyla, H.; Hijazin, M.; Alber, J.; Lammler, C.; Akineden, O.; Weiss, R.; Moritz, A.; Zschock, M. Genetic relatedness of methicillin-resistant *Staphylococcus pseudintermedius* (MRSP) isolated from a dog and the dog owner. *Res. Vet. Sci.* **2011**, *91*, E25–E27. [[CrossRef](#)] [[PubMed](#)]
34. Van Hoovels, L.; Vankeerberghen, A.; Boel, A.; Van Vaerenbergh, K.; De Beenhouwer, H. First case of *Staphylococcus pseudintermedius* infection in a human. *J. Clin. Microbiol.* **2006**, *44*, 4609–4612. [[CrossRef](#)] [[PubMed](#)]
35. Guardabassi, L.; Schmidt, K.R.; Petersen, T.S.; Espinosa-Gongora, C.; Moodley, A.; Agerso, Y.; Olsen, J.E. *Mustelidae* are natural hosts of *Staphylococcus delphini* group A. *Vet. Microbiol.* **2012**, *159*, 351–353. [[CrossRef](#)] [[PubMed](#)]
36. Magleby, R.; Bemis, D.A.; Kim, D.; Carroll, K.C.; Castanheira, M.; Kania, S.A.; Jenkins, S.G.; Westblade, L.F. First reported human isolation of *Staphylococcus delphini*. *Diagn. Microbiol. Infect. Dis.* **2019**, *94*, 274–276. [[CrossRef](#)]
37. Nikolaisen, N.K.; Lassen, D.C.K.; Chriel, M.; Larsen, G.; Jensen, V.F.; Pedersen, K. Antimicrobial resistance among pathogenic bacteria from mink (*Neovison vison*) in Denmark. *Acta. Vet. Scand.* **2017**, *59*, 60. [[CrossRef](#)]
38. Novakova, D.; Sedlacek, I.; Pantucek, R.; Stetina, V.; Svec, P.; Petras, P. *Staphylococcus equorum* and *Staphylococcus succinus* isolated from human clinical specimens. *J. Med. Microbiol.* **2006**, *55*, 523–528. [[CrossRef](#)]
39. Yoon, S.H.; Ha, S.M.; Kwon, S.; Lim, J.; Kim, Y.; Seo, H.; Chun, J. Introducing EzBioCloud: a taxonomically united database of 16S rRNA gene sequences and whole-genome assemblies. *Int. J. Syst. Evol. Microbiol.* **2017**, *67*, 1613–1617. [[CrossRef](#)]
40. Mellmann, A.; Becker, K.; von Eiff, C.; Keckevoet, U.; Schumann, P.; Harmsen, D. Sequencing and staphylococci identification. *Emerg. Infect. Dis.* **2006**, *12*, 333–336. [[CrossRef](#)]
41. Kumar, S.; Stecher, G.; Li, M.; Nnyaz, C.; Tamura, K. MEGA X: Molecular Evolutionary Genetics Analysis across computing platforms. *Mol. Biol. Evol.* **2018**, *35*, 1547–1549. [[CrossRef](#)]
42. Švec, P.; Pantůček, R.; Petráš, P.; Sedláček, I.; Nováková, D. Identification of *Staphylococcus* spp. using (GTG)₅-PCR fingerprinting. *Syst. Appl. Microbiol.* **2010**, *33*, 451–456. [[CrossRef](#)]
43. Freiwald, A.; Sauer, S. Phylogenetic classification and identification of bacteria by mass spectrometry. *Nat. Protoc.* **2009**, *4*, 732–742. [[CrossRef](#)] [[PubMed](#)]
44. Wingett, S.W.; Andrews, S. FastQ Screen: A tool for multi-genome mapping and quality control. *F1000 Research* **2018**, *7*, 1338. [[CrossRef](#)] [[PubMed](#)]
45. Nurk, S.; Bankevich, A.; Antipov, D.; Gurevich, A.A.; Korobeynikov, A.; Lapidus, A.; Prjibelski, A.D.; Pyskhin, A.; Sirotkin, A.; Sirotkin, Y.; et al. Assembling single-cell genomes and mini-metagenomes from chimeric MDA products. *J. Comput. Biol.* **2013**, *20*, 714–737. [[CrossRef](#)] [[PubMed](#)]
46. Bushnell, B. *BBMap Short-Read Aligner, and Other Bioinformatics Tools*; Lawrence Berkeley National Lab.: Berkeley, CA, USA; Available online: <http://sourceforge.net/projects/bbmap/> (accessed on 1 March 2019).
47. Darling, A.E.; Mau, B.; Perna, N.T. progressiveMauve: multiple genome alignment with gene gain, loss and rearrangement. *PLoS ONE* **2010**, *5*, e11147. [[CrossRef](#)]
48. Seemann, T. Prokka: rapid prokaryotic genome annotation. *Bioinformatics* **2014**, *30*, 2068–2069. [[CrossRef](#)]

49. Yu, N.Y.; Wagner, J.R.; Laird, M.R.; Melli, G.; Rey, S.; Lo, R.; Dao, P.; Sahinalp, S.C.; Ester, M.; Foster, L.J.; et al. PSORTb 3.0: Improved protein subcellular localization prediction with refined localization subcategories and predictive capabilities for all prokaryotes. *Bioinformatics* **2010**, *26*, 1608–1615. [[CrossRef](#)]
50. Yu, C.S.; Cheng, C.W.; Su, W.C.; Chang, K.C.; Huang, S.W.; Hwang, J.K.; Lu, C.H. CELLO2GO: A web server for protein subCELLular Localization prediction with functional gene ontology annotation. *PLoS ONE* **2014**, *9*, e99368. [[CrossRef](#)]
51. Liu, B.; Zheng, D.; Jin, Q.; Chen, L.; Yang, J. VFDB 2019: A comparative pathogenomic platform with an interactive web interface. *Nucleic Acids Res.* **2019**, *47*, D687–D692. [[CrossRef](#)]
52. Xu, L.; Dong, Z.; Fang, L.; Luo, Y.; Wei, Z.; Guo, H.; Zhang, G.; Gu, Y.Q.; Coleman-Derr, D.; Xia, Q.; et al. OrthoVenn2: A web server for whole-genome comparison and annotation of orthologous clusters across multiple species. *Nucleic Acids Res.* **2019**, *47*, W52–W58. [[CrossRef](#)]
53. Arndt, D.; Grant, J.R.; Marcu, A.; Sajed, T.; Pon, A.; Liang, Y.; Wishart, D.S. PHASTER: A better, faster version of the PHAST phage search tool. *Nucleic Acids Res.* **2016**, *44*, W16–W21. [[CrossRef](#)]
54. Couvin, D.; Bernheim, A.; Toffano-Nioche, C.; Touchon, M.; Michalik, J.; Néron, B.; Rocha, E.P.C.; Vergnaud, G.; Gautheret, D.; Pourcel, C. CRISPRCasFinder, an update of CRISPRFinder, includes a portable version, enhanced performance and integrates search for Cas proteins. *Nucleic Acids Res.* **2018**, *46*, W246–W251. [[CrossRef](#)] [[PubMed](#)]
55. Petkau, A.; Stuart-Edwards, M.; Stothard, P.; Van Domselaar, G. Interactive microbial genome visualization with GView. *Bioinformatics* **2010**, *26*, 3125–3126. [[CrossRef](#)] [[PubMed](#)]
56. Okonechnikov, K.; Golosova, O.; Fursov, M. Unipro UGENE: A unified bioinformatics toolkit. *Bioinformatics* **2012**, *28*, 1166–1167. [[CrossRef](#)] [[PubMed](#)]
57. Sullivan, M.J.; Petty, N.K.; Beatson, S.A. Easyfig: A genome comparison visualizer. *Bioinformatics* **2011**, *27*, 1009–1010. [[CrossRef](#)]
58. Yoon, S.H.; Ha, S.M.; Lim, J.; Kwon, S.; Chun, J. A large-scale evaluation of algorithms to calculate average nucleotide identity. *Antonie van Leeuwenhoek* **2017**, *110*, 1281–1286. [[CrossRef](#)]
59. Na, S.I.; Kim, Y.O.; Yoon, S.H.; Ha, S.M.; Baek, I.; Chun, J. UBCG: Up-to-date bacterial core gene set and pipeline for phylogenomic tree reconstruction. *J. Microbiol.* **2018**, *56*, 280–285. [[CrossRef](#)]
60. Cole, K.; Foster, D.; Russell, J.E.; Golubchik, T.; Llewelyn, M.; Wilson, D.J.; Crook, D.; Paul, J.; Modernising Medical Microbiology Consortium. Draft genome sequences of 64 type strains of 50 species and 25 subspecies of the genus *Staphylococcus* Rosenbach 1884. *Microbiol. Resour. Announc.* **2019**, *8*, e00062-19. [[CrossRef](#)]
61. Stepan, J.; Pantucek, R.; Doskar, J. Molecular diagnostics of clinically important staphylococci. *Folia Microbiol.* **2004**, *49*, 353–386. [[CrossRef](#)]
62. Richter, M.; Rossello-Mora, R. Shifting the genomic gold standard for the prokaryotic species definition. *Proc. Natl. Acad. Sci. USA* **2009**, *106*, 19126–19131. [[CrossRef](#)]
63. Becker, K.; Harmsen, D.; Mellmann, A.; Meier, C.; Schumann, P.; Peters, G.; von Eiff, C. Development and evaluation of a quality-controlled ribosomal sequence database for 16S ribosomal DNA-based identification of *Staphylococcus* species. *J. Clin. Microbiol.* **2004**, *42*, 4988–4995. [[CrossRef](#)]
64. Ah Tow, L.; Cowan, D.A. Dissemination and survival of non-indigenous bacterial genomes in pristine Antarctic environments. *Extremophiles* **2005**, *9*, 385–389. [[CrossRef](#)] [[PubMed](#)]
65. van Elk, C.E.; Boelens, H.A.M.; van Belkum, A.; Foster, G.; Kuiken, T. Indications for both host-specific and introduced genotypes of *Staphylococcus aureus* in marine mammals. *Vet. Microbiol.* **2012**, *156*, 343–346. [[CrossRef](#)] [[PubMed](#)]
66. Wayne, R.K. Molecular evolution of the dog family. *Trends Genet.* **1993**, *9*, 218–224. [[CrossRef](#)]
67. Aarestrup, F.M. Comparative ribotyping of *Staphylococcus intermedius* isolated from members of the *Canoidea* gives possible evidence for host-specificity and co-evolution of bacteria and hosts. *Int. J. Syst. Evol. Microbiol.* **2001**, *51*, 1343–1347. [[CrossRef](#)] [[PubMed](#)]
68. Pantůček, R.; Sedláček, I.; Petráš, P.; Koukalová, D.; Švec, P.; Štětina, V.; Vancanneyt, M.; Chrastinová, L.; Vokurková, J.; Růžičková, V.; et al. *Staphylococcus simiae* sp. nov., isolated from South American squirrel monkeys. *Int. J. Syst. Evol. Microbiol.* **2005**, *55*, 1953–1958. [[CrossRef](#)] [[PubMed](#)]
69. Suzuki, H.; Lefebure, T.; Bitar, P.P.; Stanhope, M.J. Comparative genomic analysis of the genus *Staphylococcus* including *Staphylococcus aureus* and its newly described sister species *Staphylococcus simiae*. *BMC Genom.* **2012**, *13*, 3. [[CrossRef](#)]

70. Tong, S.Y.; Schaumburg, F.; Ellington, M.J.; Corander, J.; Pichon, B.; Leendertz, F.; Bentley, S.D.; Parkhill, J.; Holt, D.C.; Peters, G.; et al. Novel staphylococcal species that form part of a *Staphylococcus aureus*-related complex: the non-pigmented *Staphylococcus argenteus* sp. nov. and the non-human primate-associated *Staphylococcus schweitzeri* sp. nov. *Int. J. Syst. Evol. Microbiol.* **2015**, *65*, 15–22. [[CrossRef](#)]
71. Fitzgerald, J.R. The *Staphylococcus intermedius* group of bacterial pathogens: species re-classification, pathogenesis and the emergence of methicillin resistance. *Vet. Derm.* **2009**, *20*, 490–495. [[CrossRef](#)]
72. Canver, M.C.; Tekle, T.; Compton, S.T.; Callan, K.; Burd, E.M.; Zimmer, B.L.; Bemis, D.A.; Carroll, K.C.; Westblade, L.F. Performance of five commercial identification platforms for identification of *Staphylococcus delphini*. *J. Clin. Microbiol.* **2019**, *57*, e00721-19. [[CrossRef](#)]
73. Chua, K.Y.; Stinear, T.P.; Howden, B.P. Functional genomics of *Staphylococcus aureus*. *Brief Funct. Genom.* **2013**, *12*, 305–315. [[CrossRef](#)]
74. Ingmer, H.; Gerlach, D.; Wolz, C. Temperate phages of *Staphylococcus aureus*. *Microbiol. Spectr.* **2019**, *7*. [[CrossRef](#)]
75. Maslanova, I.; Stribna, S.; Doskar, J.; Pantucek, R. Efficient plasmid transduction to *Staphylococcus aureus* strains insensitive to the lytic action of transducing phage. *FEMS Microbiol. Lett.* **2016**, *363*, fnw211. [[CrossRef](#)] [[PubMed](#)]
76. Pires Dos Santos, T.; Damborg, P.; Moodley, A.; Guardabassi, L. Systematic review on global epidemiology of methicillin-resistant *Staphylococcus pseudintermedius*: Inference of population structure from multilocus sequence typing data. *Front. Microbiol.* **2016**, *7*, 1599. [[CrossRef](#)] [[PubMed](#)]
77. Novick, R.P.; Christie, G.E.; Penades, J.R. The phage-related chromosomal islands of Gram-positive bacteria. *Nat. Rev. Microbiol.* **2010**, *8*, 541–551. [[CrossRef](#)] [[PubMed](#)]
78. Fillol-Salom, A.; Martinez-Rubio, R.; Abdulrahman, R.F.; Chen, J.; Davies, R.; Penades, J.R. Phage-inducible chromosomal islands are ubiquitous within the bacterial universe. *ISME J.* **2018**, *12*, 2114–2128. [[CrossRef](#)]
79. Becker, K.; Keller, B.; von Eiff, C.; Bruck, M.; Lubritz, G.; Etienne, J.; Peters, G. Enterotoxigenic potential of *Staphylococcus intermedius*. *Appl. Env. Microbiol.* **2001**, *67*, 5551–5557. [[CrossRef](#)]
80. Hendricks, A.; Schuberth, H.-J.; Schueler, K.; Lloyd, D.H. Frequency of superantigen-producing *Staphylococcus intermedius* isolates from canine pyoderma and proliferation-inducing potential of superantigens in dogs. *Res. Vet. Sci.* **2002**, *73*, 273–277. [[CrossRef](#)]
81. Iyori, K.; Hisatsune, J.; Kawakami, T.; Shibata, S.; Murayama, N.; Ide, K.; Nagata, M.; Fukata, T.; Iwasaki, T.; Oshima, K.; et al. Identification of a novel *Staphylococcus pseudintermedius* exfoliative toxin gene and its prevalence in isolates from canines with pyoderma and healthy dogs. *FEMS Microbiol. Lett.* **2010**, *312*, 169–175. [[CrossRef](#)]
82. Futagawa-Saito, K.; Makino, S.; Sunaga, F.; Kato, Y.; Sakurai-Komada, N.; Ba-Thein, W.; Fukuyasu, T. Identification of first exfoliative toxin in *Staphylococcus pseudintermedius*. *FEMS Microbiol. Lett.* **2009**, *301*, 176–180. [[CrossRef](#)]
83. Nishifuji, K.; Sugai, M.; Amagai, M. Staphylococcal exfoliative toxins: “Molecular scissors” of bacteria that attack the cutaneous defense barrier in mammals. *J. Derm. Sci.* **2008**, *49*, 21–31. [[CrossRef](#)]





Supplementary materials

Characterization of *Staphylococcus intermedius* Group Isolates Associated with Animals from Antarctica and Emended Description of *Staphylococcus delphini*

Veronika Vrbovská¹, Ivo Sedláček², Michal Zeman^{1,2}, Pavel Švec², Vojtěch Kovařovic¹, Ondřej Šedo³, Monika Laichmanová², Jiří Doškař¹ and Roman Pantůček^{1,*}

¹ Division of Genetics and Molecular Biology, Department of Experimental Biology, Faculty of Science, Masaryk University, Kotlářská 2, 611 37 Brno, Czech Republic;

² Czech Collection of Microorganisms, Department of Experimental Biology, Faculty of Science, Masaryk University, Kamenice 5, 625 00 Brno, Czech Republic;

³ Central European Institute of Technology, Masaryk University, Kamenice 5, 625 00 Brno, Czech Republic;

* Correspondence: pantucek[at]sci.muni.cz; Tel.: +420-549-49-6379 (R.P.)

This document contains supplementary materials:

Table S1. *Staphylococcus* spp. strains identified in animal-related samples from James Ross Island and Seymour Island, Antarctica.

Table S2. Comparison of selected genomic features of *Staphylococcus delphini* strains P5747 and P6456 from penguins, and *S. delphini* strains from other hosts.

Table S3. Distribution of virulence factors, surface and extracellular proteins among the *Staphylococcus delphini* strains from different hosts and from the reference and type strains of other SIG species.

Table S1. *Staphylococcus* spp. strains identified in animal-related samples from James Ross Island and Seymour Island, Antarctica.

Strain No.	Source	Year of isolation	Closest match	Partial 16S rRNA gene - identification score
<i>Staphylococcus aureus</i> - <i>Staphylococcus epidermidis</i> phylogenetic clade				
P5738	penguin, beak	2014	<i>Staphylococcus aureus</i> / <i>S. argenteus</i> / <i>S. schweitzeri</i>	100%
P5744	penguin, cloaca	2014	<i>Staphylococcus aureus</i> / <i>S. argenteus</i> / <i>S. schweitzeri</i>	100%
P5772	skua bird droppings	2014	<i>Staphylococcus aureus</i> / <i>S. argenteus</i> / <i>S. schweitzeri</i>	100%
P7183	penguin, beak	2016	<i>Staphylococcus aureus</i> / <i>S. argenteus</i> / <i>S. schweitzeri</i>	100%
P7781	penguin, beak	2017	<i>Staphylococcus aureus</i> / <i>S. argenteus</i> / <i>S. schweitzeri</i>	100%
P7797	seal, mouth	2017	<i>Staphylococcus aureus</i> / <i>S. argenteus</i> / <i>S. schweitzeri</i>	100%
P8154	seal, mouth	2017	<i>Staphylococcus aureus</i> / <i>S. argenteus</i> / <i>S. schweitzeri</i>	100%
P8452	lake water	2017	<i>Staphylococcus aureus</i> / <i>S. argenteus</i> / <i>S. schweitzeri</i>	100%
P8750	seal, anus	2017	<i>Staphylococcus aureus</i> / <i>S. argenteus</i> / <i>S. schweitzeri</i>	100%
P8753	seal, anus	2017	<i>Staphylococcus aureus</i> / <i>S. argenteus</i> / <i>S. schweitzeri</i>	100%
P8992	seal, anus	2017	<i>Staphylococcus aureus</i> / <i>S. argenteus</i> / <i>S. schweitzeri</i>	100%
P9166	seal, mouth	2017	<i>Staphylococcus aureus</i> / <i>S. argenteus</i> / <i>S. schweitzeri</i>	100%
P9115	seal, mouth	2017	<i>Staphylococcus aureus</i> / <i>S. argenteus</i> / <i>S. schweitzeri</i>	99.61%
R 6/2	elephant seal, anus	2019	<i>Staphylococcus aureus</i> / <i>S. argenteus</i> / <i>S. schweitzeri</i>	100%
P4768	unknown, droppings	2013	<i>Staphylococcus epidermidis</i>	100%
P4961	unknown, feather	2013	<i>Staphylococcus epidermidis</i>	100%
P8092	seal, anus	2017	<i>Staphylococcus epidermidis</i>	100%
P8579	seal, mouth	2017	<i>Staphylococcus epidermidis</i>	100%
P8586	seal, anus	2017	<i>Staphylococcus epidermidis</i>	100%
P8725	seal, anus	2017	<i>Staphylococcus epidermidis</i>	100%
P8816	skua, droppings	2017	<i>Staphylococcus epidermidis</i>	100%
P9120	elephant seal, mouth	2017	<i>Staphylococcus epidermidis</i>	99%
P9131	seal, droppings	2017	<i>Staphylococcus epidermidis</i>	99.61%
P9151	seal, anus	2017	<i>Staphylococcus epidermidis</i>	100%
P10571	seal, anus	2018	<i>Staphylococcus epidermidis</i>	99.42%
R 5/2	elephant seal, anus	2019	<i>Staphylococcus epidermidis</i>	100%
T 8/2	seal, anus	2019	<i>Staphylococcus epidermidis</i>	100%
T 10/7	seal, mouth	2019	<i>Staphylococcus epidermidis</i>	100%
T 11/2	seal, mouth	2019	<i>Staphylococcus epidermidis</i>	100%
T 18/4	seal, mouth	2019	<i>Staphylococcus epidermidis</i>	100%
T 19/5	seal, mouth	2019	<i>Staphylococcus epidermidis</i>	100%
T 19/6	seal, mouth	2019	<i>Staphylococcus epidermidis</i>	100%
T 49/3	seal, anus	2019	<i>Staphylococcus epidermidis</i>	99.43%
T 57/4	seal, mouth	2019	<i>Staphylococcus epidermidis</i>	99.43%
T 62/2	seal, anus	2019	<i>Staphylococcus epidermidis</i>	99.81%
T 66/2	seal, anus	2019	<i>Staphylococcus epidermidis</i>	99.81%
P8539	seal, mouth	2017	<i>Staphylococcus caprae</i> / <i>S. capitis</i>	100%
P8707	seal, anus	2017	<i>Staphylococcus caprae</i> / <i>S. capitis</i>	100%
P8806	seal, anus	2017	<i>Staphylococcus caprae</i> / <i>S. capitis</i>	100%
P8859	seal, mouth	2017	<i>Staphylococcus caprae</i> / <i>S. capitis</i>	100%
P8863	seal, anus	2017	<i>Staphylococcus caprae</i> / <i>S. capitis</i>	100%
P9104	seal, mouth	2017	<i>Staphylococcus caprae</i> / <i>S. capitis</i>	99.61%
P9107	seal, mouth	2017	<i>Staphylococcus caprae</i> / <i>S. capitis</i>	100%
P9145	seal, mouth	2017	<i>Staphylococcus caprae</i> / <i>S. capitis</i>	100%
P9190	seal, anus	2017	<i>Staphylococcus caprae</i> / <i>S. capitis</i>	100%
T 28/1	seal, mouth	2019	<i>Staphylococcus caprae</i> / <i>S. capitis</i>	100%
T 36/2	seal, anus	2019	<i>Staphylococcus caprae</i> / <i>S. capitis</i>	99.62%
T 38/2	seal, anus	2019	<i>Staphylococcus caprae</i> / <i>S. capitis</i>	99.23%
P7134	penguin, droppings	2016	<i>Staphylococcus warneri</i>	100%
P7141	unknown, droppings	2016	<i>Staphylococcus warneri</i>	99.81%
P8643	penguin, beak	2017	<i>Staphylococcus warneri</i>	100%
P10576	seal, anus	2018	<i>Staphylococcus warneri</i>	99.81%
T 17/4	seal, anus	2019	<i>Staphylococcus pasteurii</i>	100%
T 10/8	seal, mouth	2019	<i>Staphylococcus pasteurii</i>	100%

Table S1. Continued.

Strain No.	Source	Year of isolation	Closest match	Partial 16S rRNA gene - identification score
<i>Staphylococcus haemolyticus</i> phylogenetic clade				
P5756	fresh skua bird droppings	2014	<i>Staphylococcus haemolyticus</i>	100%
P5757	fresh skua bird droppings	2014	<i>Staphylococcus haemolyticus</i>	99.61%
P6353	penguin, cloaca	2015	<i>Staphylococcus haemolyticus</i>	100%
P7139	unknown, droppings	2016	<i>Staphylococcus haemolyticus</i>	99.61%
P7142	skua, droppings	2016	<i>Staphylococcus haemolyticus</i>	100%
P7167	skua, droppings	2016	<i>Staphylococcus haemolyticus</i>	100%
P8018	seal, anus	2017	<i>Staphylococcus haemolyticus</i>	100%
P8019	seal, anus	2017	<i>Staphylococcus haemolyticus</i>	100%
P8184	seal, mouth	2017	<i>Staphylococcus haemolyticus</i>	100%
P8567	seal, anus	2017	<i>Staphylococcus haemolyticus</i>	99.81%
P8656	seal, droppings	2017	<i>Staphylococcus haemolyticus</i>	100%
P8696	seal, anus	2017	<i>Staphylococcus haemolyticus</i>	99.61%
P8721	seal, mouth	2017	<i>Staphylococcus haemolyticus</i>	100%
P8782	seal, anus	2017	<i>Staphylococcus haemolyticus</i>	100%
P9002	seal, mouth	2017	<i>Staphylococcus haemolyticus</i>	99.61%
P9097	seal, anus	2017	<i>Staphylococcus haemolyticus</i>	99.61%
P9130	skua, droppings	2017	<i>Staphylococcus haemolyticus</i>	99.61%
P9139	seal, mouth	2017	<i>Staphylococcus haemolyticus</i>	100%
P9140	seal, mouth	2017	<i>Staphylococcus haemolyticus</i>	99.61%
P9175	penguin, cloaca	2017	<i>Staphylococcus haemolyticus</i>	99.61%
P9191	seal, mouth	2017	<i>Staphylococcus haemolyticus</i>	100%
P10074	seal, anus	2018	<i>Staphylococcus haemolyticus</i>	99.62%
F 1/5	skua, droppings	2019	<i>Staphylococcus haemolyticus</i>	100%
T 14/1	seal, mouth	2019	<i>Staphylococcus haemolyticus</i>	100%
T 14/3	seal, mouth	2019	<i>Staphylococcus haemolyticus</i>	99.62%
T 43/1	seal, mouth	2019	<i>Staphylococcus haemolyticus</i>	99.04%
T 47/4	seal, anus	2019	<i>Staphylococcus haemolyticus</i>	99.04%
T 51/1	seal, anus	2019	<i>Staphylococcus haemolyticus</i>	99.62%
P9148	seal, mouth	2017	<i>Staphylococcus hominis</i>	99.22%
<i>Staphylococcus simulans</i> phylogenetic clade				
P9179	penguin, droppings	2017	<i>Staphylococcus auricularis</i>	100%
<i>Staphylococcus saprophyticus</i> phylogenetic clade				
P7145	skua, droppings	2016	<i>Staphylococcus saprophyticus</i> / <i>S. eadaphicus</i>	99.8%
P7160	penguin, cloaca	2016	<i>Staphylococcus saprophyticus</i> / <i>S. eadaphicus</i>	100%
T 54/8A	seal, mouth	2019	<i>Staphylococcus saprophyticus</i> / <i>S. eadaphicus</i>	100%
T 60/3	seal, anus	2019	<i>Staphylococcus saprophyticus</i> / <i>S. eadaphicus</i>	99.81%
P8769	seal, mouth	2017	<i>Staphylococcus saprophyticus</i> / <i>S. eadaphicus</i>	100%
P8490	seal, anus	2017	<i>Staphylococcus saprophyticus</i> / <i>S. eadaphicus</i>	100%
T 52/5	seal, mouth	2019	<i>Staphylococcus saprophyticus</i> / <i>S. eadaphicus</i>	99.42%
T 54/3	seal, anus	2019	<i>Staphylococcus saprophyticus</i> / <i>S. eadaphicus</i>	99.42%
T 69/4	seal, mouth	2019	<i>Staphylococcus saprophyticus</i> / <i>S. eadaphicus</i>	99.61%
T 40/4	seal, anus	2019	<i>Staphylococcus cohnii</i>	99.62%
T 54/5	seal, mouth	2019	<i>Staphylococcus cohnii</i>	99.62%
T 56/2	seal, anus	2019	<i>Staphylococcus cohnii</i>	99.81%
T 56/3A	seal, anus	2019	<i>Staphylococcus cohnii</i>	99.81%
P10515	seal, mouth	2018	<i>Staphylococcus cohnii</i>	98.08%
P7715	penguin, droppings	2017	<i>Staphylococcus equorum</i>	99.81%
T 51/3	seal, anus	2019	<i>Staphylococcus equorum</i>	99.62%
T 54/7	seal, mouth	2019	<i>Staphylococcus succinus</i>	99.42%
T 61/2	seal, anus	2019	<i>Staphylococcus succinus</i>	99.62%

Table S1. Continued.

Strain No.	Source	Year of isolation	Closest match	Partial 16S rRNA gene - identification score
<i>Staphylococcus hyicus</i> - <i>Staphylococcus intermedius</i> phylogenetic clade				
P5747	penguin, beak	2014	<i>Staphylococcus intermedius</i> group	100%
P5749	penguin, cloaca	2014	<i>Staphylococcus intermedius</i> group	100%
P5833	penguin, beak	2014	<i>Staphylococcus intermedius</i> group	100%
P5835	penguin, cloaca	2014	<i>Staphylococcus intermedius</i> group	100%
P6070	penguin, beak	2014	<i>Staphylococcus intermedius</i> group	100%
P6456	penguin, beak	2015	<i>Staphylococcus intermedius</i> group	100%
P7945	seal, anus	2017	<i>Staphylococcus intermedius</i> group	100%
P8480	seal, anus	2017	<i>Staphylococcus intermedius</i> group	100%
P8688	seal, anus	2017	<i>Staphylococcus intermedius</i> group	100%
P8720	seal, mouth	2017	<i>Staphylococcus intermedius</i> group	100%
P8807	seal, anus	2017	<i>Staphylococcus intermedius</i> group	100%
P9111	seal, mouth	2017	<i>Staphylococcus intermedius</i> group	100%
P10574	seal, anus	2018	<i>Staphylococcus intermedius</i> group	100%
P12459	seal, anus	2019	<i>Staphylococcus intermedius</i> group	100%
P12460	seal, anus	2019	<i>Staphylococcus intermedius</i> group	100%
P12461	seal, mouth	2019	<i>Staphylococcus intermedius</i> group	100%
P12462	seal, anus	2019	<i>Staphylococcus intermedius</i> group	100%
P12463	seal, anus	2019	<i>Staphylococcus intermedius</i> group	100%
P12464	seal, mouth	2019	<i>Staphylococcus intermedius</i> group	100%
P12465	seal, anus	2019	<i>Staphylococcus intermedius</i> group	100%
P12466	seal, anus	2019	<i>Staphylococcus intermedius</i> group	100%
P12467	seal, anus	2019	<i>Staphylococcus intermedius</i> group	100%
P5746	penguin, cloaca	2014	<i>Staphylococcus schleiferi</i>	100%
P5841	penguin, beak	2014	<i>Staphylococcus schleiferi</i>	100%
P6543	seal, anus	2015	<i>Staphylococcus schleiferi</i>	100%
P8578	seal, anus	2017	<i>Staphylococcus schleiferi</i>	100%
R 9/1	elephant seal, anus	2019	<i>Staphylococcus schleiferi</i>	99.81%
F 2/1	skua, droppings	2019	<i>Staphylococcus schleiferi</i>	100%
<i>Staphylococcus sciuri</i> phylogenetic clade				
P4774	unknown, droppings	2013	<i>Staphylococcus sciuri</i>	100%
P5740	penguin, beak	2014	<i>Staphylococcus sciuri</i>	100%
P5742	penguin, cloaca	2014	<i>Staphylococcus sciuri</i>	100%
P5748	penguin, beak	2014	<i>Staphylococcus sciuri</i>	100%
P5761	fresh kelp gull droppings	2014	<i>Staphylococcus sciuri</i>	100%
P5762	fresh kelp gull droppings	2014	<i>Staphylococcus sciuri</i>	100%
P5768	fresh skua bird droppings	2014	<i>Staphylococcus sciuri</i>	100%
P5844	penguin, beak	2014	<i>Staphylococcus sciuri</i>	100%
P5846	penguin, cloaca	2014	<i>Staphylococcus sciuri</i>	100%
P6153	penguin, beak	2014	<i>Staphylococcus sciuri</i>	100%
P6183	fresh skua bird droppings	2014	<i>Staphylococcus sciuri</i>	100%
P6454	penguin, beak	2015	<i>Staphylococcus sciuri</i>	100%
P6464	penguin, beak	2015	<i>Staphylococcus sciuri</i>	100%
P7149	kelp gull, droppings	2016	<i>Staphylococcus sciuri</i>	99.81%
P9174	penguin, beak	2017	<i>Staphylococcus sciuri</i>	99.81%
R 3/5	elephant seal, anus	2019	<i>Staphylococcus sciuri</i>	99.43%
R 4/3	elephant seal, mouth	2019	<i>Staphylococcus sciuri</i>	99.43%
R 4/7	elephant seal, mouth	2019	<i>Staphylococcus sciuri</i>	99.43%
P5770	penguin, droppings	2014	<i>Staphylococcus sciuri</i> / <i>S. fleuretti</i> / <i>S. vitulinus</i>	99.02%
F 5/4	unknown, droppings	2019	<i>Staphylococcus sciuri</i> / <i>S. fleuretti</i> / <i>S. vitulinus</i>	99.02%

Table S2. Comparison of selected genomic features of *Staphylococcus delphini* strains P5747 and P6456 from penguins, and *S. delphini* strains from other hosts.

Genome	<i>S. delphini</i> P5747 (penguin)	<i>S. delphini</i> P6456 (penguin)	<i>S. delphini</i> NCTC 12225 ^T (dolphin)	<i>S. delphini</i> 8086 (horse)	<i>S. delphini</i> 215100905101-2 (horse)	
WGS Project no.	WNLD00000000.1	WNLE00000000.1	LR134263.1	CAIA00000000.1	MWUT00000000.1	
Size (Mb)	2.54	2.65	2.80	2.51	2.53	
Contigs	47	104	1	211	30	
GC content (mol%)	38.2	38.1	37.8	38.3	38.3	
Total genes	2488	2572	2633	2399	2394	
Protein coding sequences	2292	2386	2452	2315	2281	
Genes with clusters of orthologous groups ^a	2179	2260	2201	2214	2220	
Prophages	P5747-1 (41.2 kb); P5747-2 (44.4 kb)	P6456-1*, P6456-2*	SPβ-like 12225 (120.3 kb)	8086-1*, 8086-2*	215100905101-2-1 (39.5 kb)	
Plasmids ^b	pSD1 (3.2 kb); pSD2 (3.1 kb); pSD3 (2.5 kb)	pSD2 (3.1 kb); pSD3 (2.5 kb); pSD4 (3.1 kb) ^c	-	-	-	
Phage-inducible chromosomal islands	SdPIC1-1 (13.7 kb)	SdPIC1-1 (13.7 kb)	-	-	-	
Other chromosomal island	SdCI _{lukSF-I, ula} (11.5 kb), SdCI _{SEC} (9.5 kb), SdCI _{Serine_protease} (7.3 kb)	SdCI _{lukSF-I, ula} (11.5 kb)	SdCI _{lukSF-I, ula} (11.5 kb), SdCI ₁₂₂₂₅ (14.8 kb)	SdCI _{lukSF-I, ula} (11.5 kb), SdCI _{Serine_protease} (12.1 kb) ^d	SdCI _{lukSF-I, ula} (11.5 kb)	
Subcellular localization of encoded proteins ^e						
	Cytoplasmic	1350	1384	1418	1332	1303
	Cytoplasmic Membrane	650	671	670	634	630
	Cellwall	34	34	31	39	33
	Extracellular	54	46	47	42	38
	Unknown	204	251	286	268	277
RM systems	type I (<i>hsdMSR</i>), type II (HindIII)	type I (incomplete - <i>hsdMS</i>), type II (HindIII)	type I (<i>hsdMSR</i>), type II (FokI)	type I (<i>hsdMSR</i>)	type I (<i>hsdMSR</i>)	
CRISPR-Cas	type III-A	-	type II-C; type III-A	-	type II-C	

* phages are incomplete and dispersed on multiple contigs

^a core genome consist of 1899 structural genes in given set

^b all detected plasmids are cryptic, encoding Rep protein and hypothetical proteins

^c plasmid sequences on multiple contigs, unable to distinguish between one or more separated plasmids

^d SdCI_{Serine_protease} is on two separate contigs for strain 8086, the length is approximate

^e predicted by PSORTb 3.0

Table S3. Continued.

Class	Predicted function	Gene	Genome / Protein accession numbers												
			<i>S. delphini</i> NCTC 12225 ^T (dolphin)	<i>S. delphini</i> P5747 (penguin)	<i>S. delphini</i> P6456 (penguin)	<i>S. delphini</i> 215100905101-2 (horse)	<i>S. delphini</i> 8086 (horse)	<i>S. delphini</i> 14S03313-1 (horse)	<i>S. delphini</i> 14S03318-1 (marten)	<i>S. delphini</i> 14S03309-1 (pigeon)	<i>S. pseudintermedius</i> LMG 22219 ^T (cat)	<i>S. pseudintermedius</i> P8688 (seal)	<i>S. intermedius</i> NCTC 11048 ^T (pigeon)	<i>S. cornubiensis</i> NWT ^T (human)	
			GCF_00636325.1	GCF_009720305.1	GCF_009720295.1	GCF_002369695.1	GCF_000308115.1	GCF_002374125.1	GCF_002369645.1	GCF_002374115.1	GCF_001792775.2	GCA_009939245.1	GCF_900458545.1	GCF_900183575.1	
Immune evasion	Adenosine synthase	<i>adsA</i>	WP_096596233.1	WP_155260988.1	WP_155259296.1	WP_096589112.1	WP_019165402.1	WP_096606818.1	WP_096544639.1	-	WP_037542320.1	NCJ14595.1	SUM45865.1	WP_086428047.1	
	Polysaccharide capsule	-	WP_096597982.1 WP_096597232.1 WP_096596211.1	WP_155260716.1 WP_155261758.1 WP_155261047.1 WP_155261153.1 WP_155260717.1	WP_155259479.1 WP_155260057.1 WP_096542578.1	WP_096543029.1 WP_096543007.1 WP_096542578.1	WP_019165802.1 WP_019167167.1 WP_026066994.1 WP_039838313.1	WP_096606426.1 WP_096605264.1 WP_096542578.1	WP_096546510.1 WP_096544497.1 WP_096544283.1	WP_019165802.1 WP_096592328.1 WP_096661961.1 WP_096591365.1	WP_014613151.1 WP_103263702.1 WP_014614306.1	NCJ13750.1 NCJ14507.1 NCJ13577.1	SUM45956.1 SUM45471.1 SUM46132.1 SUM47211.1 SUM45472.1	WP_086428572.1 WP_086428569.1 WP_086428134.1 WP_086429146.1 WP_086428571.1 WP_086428581.1 WP_086429480.1 WP_086428570.1 WP_086428165.1	
		<i>galE</i>	WP_096597290.1	WP_019166591.1	WP_155259394.1	WP_019166591.1	WP_019166591.1	WP_019166591.1	WP_019166591.1	WP_096544436.1	WP_096590871.1	WP_015729527.1	NCJ14411.1	SUM45989.1	WP_086428165.1
	Immunodominant antigen	<i>isaA</i>	WP_096596443.1	WP_155260946.1	WP_155259231.1	WP_096542905.1	WP_019164949.1	WP_096606599.1	WP_096544786.1	WP_019164949.1	WP_014612972.1	NCJ15198.1	SUM45794.1	WP_086427976.1	
		<i>isaB</i>	WP_096598090.1	WP_155262118.1	WP_155260417.1	WP_096539601.1	WP_019166374.1	WP_096604729.1	WP_096546318.1	WP_096662084.1	WP_014614839.1	NCJ15585.1	SUM45288.1	WP_086428728.1	
	Secretory antigen precursor	<i>ssaA</i>	WP_096597266.1 WP_096597260.1	WP_155261055.1 WP_155261054.1	WP_155259384.1 WP_096597260.1	WP_096542552.1 WP_096542560.1	WP_019165367.1 WP_019165363.1	WP_096605640.1 WP_096542560.1	WP_096544468.1 WP_096544476.1	WP_096590891.1 WP_019165363.1	WP_015729537.1 WP_014613162.1	NCJ14491.1 NCJ14495.1	SUM45972.1 SUM45968.1	WP_086428149.1 WP_086428146.1	
<i>ssaB</i>		WP_096597266.1	WP_155261055.1	WP_155259384.1	WP_096542552.1	WP_019165367.1	WP_096605640.1	WP_096544468.1	WP_096590891.1	WP_015729537.1	NCJ14491.1	SUM45972.1	WP_086428149.1		
Adherence	Clumping factor A	<i>clfA</i>	-	WP_155260821.1 WP_155260820.1	WP_155259885.1 WP_155259118.1	WP_096543116.1	WP_014614797.1	-	WP_096546353.1 WP_096546065.1	WP_096662080.1	-	NCJ15232.1	SUM45308.1 SUM45629.1	-	
	Clumping factor B	<i>clfB</i>	-	-	-	-	WP_019167000.1	-	-	-	-	-	-	-	
	Collagen adhesion	<i>cna</i>	-	-	-	-	-	-	WP_096606518.1	WP_096545686.1	-	-	-	-	
	Elastin binding protein	<i>ebpS</i>	WP_096596248.1	WP_019165998.1	WP_096542773.1	WP_096541026.1	WP_019165282.1	WP_096605307.1	WP_096545540.1	WP_096661794.1	WP_099987111.1	NCJ14989.1	SUM46715.1	WP_086427749.1	
	Fibronectin binding proteins	<i>fnbB</i>	WP_096596309.1	WP_155261510.1	WP_155259848.1	WP_096541241.1	WP_019165356.1	WP_096606482.1	WP_096545417.1	WP_096661811.1	WP_112424790.1	-	SUM46794.1	WP_086427824.1	
	Intercellular adhesion	<i>icaA</i>	WP_096596031.1	WP_155260651.1	WP_155259087.1	WP_096540014.1	WP_019166834.1	-	-	WP_019166834.1	WP_101431304.1	GWDS5_09330*	SUM45578.1	WP_086428671.1	
		<i>icaB</i>	WP_096596029.1	-	WP_155259341.1	WP_096540010.1	WP_019166832.1	WP_096604431.1	WP_096546001.1	WP_096662060.1	WP_103263494.1	NCJ15261.1	SUM45576.1	WP_086428669.1	
		<i>icaC</i>	WP_096596028.1	WP_155260791.1	WP_155259085.1	WP_096540008.1	WP_019166831.1	WP_096604433.1	WP_096545999.1	WP_096593797.1	WP_014612782.1	NCJ15262.1	SUM45575.1	WP_086428668.1	
	Ser-Asp rich fibrinogen-binding proteins	<i>sdrC</i>	WP_096596063.1	-	-	-	-	-	-	-	-	-	SUM43760.1 SUM43658.1	-	
		<i>sdrD</i>	WP_096598315.1	WP_155262069.1	WP_155260135.1	WP_096595588.1	WP_026067054.1	WP_096606702.1	WP_096543518.1	WP_096661881.1	-	NCJ13608.1	SUM47308.1	WP_086429410.1	
		<i>sdrE</i>	WP_096596064.1	WP_155260816.1	WP_155259116.1	WP_096595684.1 WP_158224546.1	WP_019165862.1	WP_096604377.1	WP_096546059.1	WP_096662054.1	-	-	SUM45624.1	WP_086428706.1 WP_119184415.1	
	MSCRAMM family adhesin	-	-	-	-	-	-	-	WP_142302650.1	-	-	-	-	-	
	IgG-binding protein	<i>sbi</i>	-	-	-	-	-	-	-	WP_096662037.1	-	-	-	-	
	Staphylococcal protein A	<i>spa2</i>	-	-	-	-	-	-	-	WP_096591397.1	-	-	SUM45452.1	WP_086428550.1	
	N-acetylmuramoyl-L-alanine amidase	<i>atl</i>	WP_096596071.1 WP_096595957.1	WP_155261763.1	WP_155260061.1 WP_155260554.1	WP_096595580.1 WP_096539908.1	WP_026066996.1 WP_019165733.1	WP_096604517.1	WP_096543477.1 WP_096546602.1	WP_096592220.1 WP_096662014.1	WP_014614312.1 WP_014612723.1	NCJ13582.1 NCJ13896.1	SUM47217.1 SUM45489.1	WP_086429636.1 WP_086428606.1	
	Lipoprotein diacylglycerol transferase	<i>lgt</i>	WP_096596548.1	WP_155261892.1	WP_155260237.1	WP_096542309.1	WP_019166113.1	WP_096605044.1	WP_014613931.1	WP_096593999.1	WP_014614497.1	NCJ15041.1	SUM47458.1	WP_086428514.1	
Lipoprotein-specific signal peptidase II	<i>lspA</i>	WP_096596174.1	WP_019165555.1	WP_155259968.1	WP_096540618.1	WP_019165555.1	WP_096540618.1	WP_096543842.1	WP_019165555.1	WP_014614161.1	NCJ14715.1	-	WP_086429113.1		
Cell wall anchor protein	<i>sasF</i>	WP_096596397.1	WP_155260907.1	WP_155259194.1	WP_096595748.1	WP_019166502.1	WP_096605801.1	WP_096544873.1	WP_096591196.1	WP_103263651.1	NCJ15154.1	SUM45746.1	WP_086429024.1		
Surface 5'-nucleotidase	<i>sasH</i>	-	-	-	-	WP_019165558.1	-	-	-	-	-	-	-		
YSIRK-type signal peptide-containing proteins with LPXTG domain	-	WP_126489868.1	WP_155260739.1 WP_155260895.1	WP_155259183.1	WP_096595750.1	WP_019165736.1 WP_019165898.1	WP_096605823.1	WP_096546834.1 WP_096546600.1	WP_096662013.1	WP_112424773.1 WP_142671672.1	NCJ13920.1 NCJ15309.1	SUM45730.1	WP_119184408.1 WP_119184405.1		
	-	WP_096596001.1	WP_155260957.1	WP_155259643.1	WP_096539956.1	WP_019166800.1	WP_096604471.1	WP_096545946.1	WP_096662010.1	WP_103263484.1	GWDS5_09480* GWDS5_09480*	-	WP_086428636.1		
	-	WP_096598635.1	WP_155260642.1	WP_155260443.1	WP_096539671.1	WP_019166934.1	WP_096604680.1	WP_096546622.1	WP_096662072.1	WP_063279061.1	NCJ15627.1	SUM45341.1	WP_086428768.1		
	-	WP_096596063.1	WP_155259115.1	WP_155259115.1	-	-	-	-	-	-	-	-	-		
Surface protein anchoring	Unknown LPXTG domain containing proteins	-	-	WP_155261832.1	-	WP_096542755.1	WP_019165986.1	-	-	WP_096592157.1	WP_014614371.1	NCJ13643.1	SUM45443.1	WP_086428952.1	
		-	-	-	WP_155260512.1	-	WP_019166773.1	-	WP_096546656.1	WP_096662018.1	-	-	SUM45461.1	WP_086428561.1	
		-	-	WP_155261511.1	-	-	WP_019166538.1	-	-	-	-	NCJ14904.1	-	-	
		-	-	WP_155260826.1	-	-	WP_083849007.1	-	-	-	WP_142671673.1	NCJ15230.1	-	WP_086429411.1	
		-	-	-	-	-	-	-	-	-	-	-	SUM45492.1	-	
		-	-	-	-	-	-	-	-	-	-	-	SUM45729.1	-	
		-	-	-	-	WP_096595626.1	-	-	-	-	-	-	-	-	-
		-	-	-	-	-	-	WP_039838176.1	-	-	-	-	-	-	-
		-	-	-	-	-	-	WP_039838492.1	-	-	-	-	-	-	-
		-	-	-	WP_155259884.1	-	-	-	-	-	-	-	-	-	-
-	-	-	-	-	-	WP_039838492.1	-	-	-	-	-	-	-		

Table S3. Continued.

Class	Predicted function	Gene	Genome / Protein accession numbers												
			<i>S. delphini</i> NCTC 12225 ^T (dolphin)	<i>S. delphini</i> P5747 (penguin)	<i>S. delphini</i> P6456 (penguin)	<i>S. delphini</i> 215100905101-2 (horse)	<i>S. delphini</i> 8086 (horse)	<i>S. delphini</i> 14503313-1 (horse)	<i>S. delphini</i> 14503318-1 (marten)	<i>S. delphini</i> 14503309-1 (pigeon)	<i>S. pseudintermedius</i> LMG 22219 ^T (cat)	<i>S. pseudintermedius</i> P8688 (seal)	<i>S. intermedium</i> NCTC 11048 ^T (pigeon)	<i>S. cornubiensis</i> NW1 ^T (human)	
			GCF_900636325.1	GCF_009720305.1	GCF_009720295.1	GCF_002369695.1	GCF_000308115.1	GCF_002374125.1	GCF_002369645.1	GCF_002374115.1	GCF_001792775.2	GCA_009939245.1	GCF_900458545.1	GCF_900183575.1	
Cell division	Cell division protein	<i>divB</i>	WP_096596160.1	WP_155261695.1	WP_096596160.1	WP_096540591.1	WP_019165664.1	WP_096605182.1	WP_096545724.1	WP_096593096.1	WP_014614179.1	NCJ14699.1	SUM47016.1	WP_086429098.1	
	Cell division initiation protein	<i>divC</i>	WP_019165010.1 WP_096596156.1	WP_019165010.1	WP_019165010.1	WP_096543154.1	WP_019165010.1	WP_019165010.1	WP_019165010.1	WP_019165010.1	WP_014614798.1	NCJ13822.1	-	WP_086429490.1	
	Autolysin	<i>lytA</i>	-	WP_155261051.1	WP_155259371.1	-	WP_019165358.1	-	-	WP_096661962.1	WP_015729543.1	NCJ14500.1	-	-	
	N-acetylmuramoyl-L-alanine amidase	<i>lytD</i>	WP_096596697.1	WP_019165956.1	WP_155259622.1	WP_096542040.1	WP_019165956.1	WP_096542040.1	WP_019165956.1	WP_019165956.1	WP_014613595.1	NCJ14010.1	SUM46414.1	WP_086427488.1	
Transporters	ABC transporter substrate-binding protein	-	WP_096598170.1	-	WP_155259279.1	WP_096542812.1	-	WP_096542812.1	WP_096544677.1	WP_096591046.1	WP_014613020.1	-	-	WP_086428022.1	
		-	WP_096598178.1	-	WP_155259275.1	WP_096542822.1	-	WP_096606860.1	WP_096544687.1	-	WP_037542303.1	-	-	WP_086428017.1	
		-	WP_096596403.1	WP_155260914.1	WP_155259199.1	WP_096541885.1	WP_019166312.1	-	WP_096544863.1	WP_096591186.1	WP_015729662.1	NCJ15159.1	SUM45751.1	WP_086429030.1	
		-	-	WP_155260849.1	-	-	WP_019167021.1	-	WP_096546126.1	WP_096593542.1	-	-	-	SUM45660.1	WP_086428861.1
		<i>troA</i>	WP_096596571.1	-	WP_155260313.1	WP_096540292.1	WP_019166244.1	WP_096605036.1	WP_096544091.1	WP_096638128.1	WP_014614644.1	NCJ14123.1	-	-	WP_086428519.1
	Nickel ABC transporter	<i>opp-1A</i>	WP_096598140.1	WP_155260637.1	WP_155260437.1	WP_096539659.1	WP_019166928.1	WP_096604692.1	WP_096546233.1	WP_096591551.1	WP_014614880.1	NCJ15619.1	SUM45334.1	WP_086428762.1	
	ABC transporter permease	-	WP_096597250.1	-	-	-	-	-	-	-	-	-	-	-	
	Copper-translocating P-type ATPase	<i>zntA</i>	-	-	-	-	WP_019165821.1	-	-	-	-	-	-	-	
	DMT family transporter	<i>ycdZ</i>	-	-	-	-	WP_019166257.1	-	-	-	-	-	-	-	
	Phenylalanine-tRNA ligase subunit beta	-	-	-	WP_155260000.1	-	-	-	-	-	-	-	-	-	
Heavy metal translocating P-type ATPase	-	-	WP_155261165.1	-	-	-	-	-	-	-	-	-	-		
Divalent metal cation transporter	-	-	WP_155261384.1	-	-	-	-	-	-	-	-	-	-		
Peptidases	Peptidase	-	WP_096597960.1	WP_155261166.1	WP_155259488.1	WP_096543009.1	WP_019165822.1	WP_096606408.1	WP_096547115.1	WP_096662133.1	WP_037542547.1	NCJ13872.1	SUM46158.1	WP_086429186.1	
	Signal peptidase I	-	WP_096542133.1	WP_155262071.1	WP_155260188.1	WP_096542133.1	WP_019166008.1	WP_096542133.1	WP_096542133.1	WP_096661894.1	WP_014614397.1	NCJ13666.1	SUM47362.1	WP_086428973.1	
	M23 family metallopeptidase	-	WP_096596442.1	WP_155260945.1	WP_155259230.1	WP_096542907.1	WP_026066938.1	-	WP_096544788.1	WP_026066938.1	-	-	NCJ15197.1	SUM45793.1	WP_086427975.1
		-	WP_096595998.1	-	-	WP_096539950.1	-	-	-	-	-	-	-	-	-
	Peptidase P60	-	-	-	-	-	-	-	-	-	WP_000768373.1	-	-	-	
	Peptidase	-	WP_096597599.1	WP_155261198.1	-	-	-	WP_096606349.1	WP_096547250.1	-	WP_015729408.1	NCJ13837.1	-	-	
Peptidase T	<i>pepT</i>	-	-	WP_155260239.1	-	-	-	-	-	-	-	-	-		
Other cell wall proteins	Peptidoglycan-binding protein	<i>lysM</i>	WP_096598096.1	WP_155262119.1	WP_155260419.1	WP_096539603.1	WP_019166377.1	WP_096604727.1	WP_096546301.1	WP_096557038.1	WP_014614841.1	NCJ15587.1	SUM45291.1	WP_086428731.1	
	Competence protein	<i>comGC</i>	WP_096541451.1	WP_155261425.1	WP_096541451.1	WP_096541451.1	WP_019165232.1	WP_096541451.1	WP_096547032.1	WP_096541451.1	WP_015729165.1	NCJ15346.1	SUM46663.1	WP_086427699.1	
	Dipeptide-binding protein	<i>oppA</i>	WP_096596536.1	WP_155261834.1	WP_155260158.1	WP_096542759.1	WP_019165989.1	WP_096604776.1	WP_096543577.1	WP_096592152.1	WP_020220047.1	NCJ13647.1	SUM47343.1	WP_086428955.1	
	Kinase-associated lipoprotein B	<i>kapB</i>	WP_096596513.1	WP_155261853.1	WP_019166974.1	WP_019166974.1	WP_019166974.1	WP_096604822.1	WP_096543628.1	WP_019166974.1	WP_014614413.1	NCJ13686.1	SUM47376.1	WP_086428989.1	
	Malate dehydrogenase (quinone)	<i>mqa2</i>	WP_096543297.1	WP_155260819.1	WP_096543297.1	WP_096595678.1	WP_019165095.1	WP_096543297.1	WP_096546063.1	WP_019165095.1	WP_014612817.1	NCJ15233.1	SUM45628.1	WP_086429552.1	
	Malate-quinone-oxidoreductase 1	<i>mqa1</i>	WP_096597125.1	WP_155261011.1	WP_155259325.1	WP_096543189.1	WP_019165505.1	WP_096605528.1	WP_096544589.1	WP_096590975.1	WP_014613089.1	NCJ14563.1	SUM45897.1	WP_086428078.1	
	Phosphodiesterase	-	WP_096596503.1	WP_019166993.1	WP_155260195.1	WP_096542188.1	WP_019166993.1	WP_096604838.1	WP_096543651.1	WP_096594020.1	WP_103263530.1	NCJ13709.1	SUM47400.1	WP_086429366.1	
	Protein-disulfide isomerase	-	WP_096595914.1	WP_155260686.1	WP_155260490.1	WP_096539787.1	WP_019166051.1	WP_096604591.1	WP_096546722.1	WP_096591434.1	WP_096548384.1	NCJ15698.1	SUM45414.1	WP_086428837.1	
	Ribonuclease H	-	WP_096596278.1	WP_155261483.1	WP_096554780.1	WP_096541138.1	WP_019165318.1	WP_096554780.1	WP_096545479.1	WP_096591828.1	WP_020219606.1	NCJ14945.1	SUM46753.1	WP_086427785.1	
	Small heat shock protein	<i>hsp20</i>	WP_096596042.1	WP_155260800.1	WP_096596042.1	WP_019166846.1	WP_019166846.1	WP_096604418.1	-	WP_019166846.1	WP_015729757.1	NCJ15253.1	SUM45605.1	WP_086428680.1	
Thioredoxin-dependent thiol peroxidase	<i>bcp</i>	WP_096597706.1	WP_155261241.1	WP_155259578.1	WP_096543363.1	WP_019166484.1	WP_096606878.1	WP_096546362.1	WP_096592832.1	WP_014613508.1	NCJ15520.1	SUM46284.1	WP_086429233.1		

Table S3. Continued.

Class	Predicted function	Gene	Genome / Protein accession numbers											
			<i>S. delphini</i> NCTC 12225 ^T (dolphin)	<i>S. delphini</i> P5747 (penguin)	<i>S. delphini</i> P6456 (penguin)	<i>S. delphini</i> 215100905101-2 (horse)	<i>S. delphini</i> 8086 (horse)	<i>S. delphini</i> 14S03313-1 (horse)	<i>S. delphini</i> 14S03318-1 (marten)	<i>S. delphini</i> 14S03309-1 (pigeon)	<i>S. pseudintermedius</i> LMG 22219 ^T (cat)	<i>S. pseudintermedius</i> P8688 (seal)	<i>S. intermedium</i> NCTC 11048 ^T (pigeon)	<i>S. cornubiensis</i> NW1 ^T (human)
			GCF_900636325.1	GCF_009720305.1	GCF_009720295.1	GCF_002369695.1	GCF_000308115.1	GCF_002374125.1	GCF_002369645.1	GCF_002374115.1	GCF_001792775.2	GCA_009939245.1	GCF_900458545.1	GCF_900183575.1
Other extracellular proteins	Chitinase	<i>csn</i>	-	-	-	-	WP_019165731.1	-	-	-	-	-	-	
	CsbD-like protein	-	WP_096541591.1	WP_155261373.1	WP_096541591.1	WP_096541591.1	-	WP_096541591.1	WP_096545141.1	WP_096545141.1	WP_014613736.1	NCJ15430.1	SUM43551.1	
	DUF1307 domain-containing protein	-	-	WP_142294444.1	-	-	-	-	-	-	-	-	SUM46567.1	
	Formate dehydrogenase subunit alpha	-	-	WP_155261050.1	-	-	-	-	-	-	-	-	-	
	DUF669 domain-containing protein	-	-	-	-	-	-	-	-	-	-	-	SUM46349.1	
	Subtilisin A	<i>sboA</i>	WP_096598771.1	-	-	-	-	-	-	-	-	-	-	
	YolD-like family protein	-	-	-	-	-	-	-	-	-	WP_001798151.1	-	-	
	Alpha/beta hydrolase	-	WP_096596067.1	WP_155260649.1	WP_155260447.1	WP_096540054.1	WP_083849004.1	WP_096604757.1	WP_096546349.1	WP_096662087.1	WP_063279062.1	NCJ15628.1	-	WP_086428865.1
	Amidase domain-containing protein	-	WP_096596398.1	WP_155260908.1	WP_155259195.1	WP_096541872.1	WP_019166305.1	WP_096605799.1	WP_096544871.1	WP_096661996.1	WP_103263650.1	NCJ15155.1	SUM45747.1	WP_086429025.1
	Carboxylesterase family protein	-	-	-	-	-	-	-	WP_142302633.1	-	-	-	-	
	Deferrochelate/ peroxidase	-	WP_096596559.1	WP_155261994.1	WP_019165102.1	WP_096595605.1	WP_019166265.1	WP_096595605.1	WP_096544122.1	WP_096661927.1	-	NCJ14102.1	SUM47619.1	WP_086428405.1
	DUF1722 domain-containing protein	-	-	WP_155261877.1	-	-	-	WP_096604866.1	-	-	-	-	-	-
	Adenosylmethionine-8-amino-7-oxononanoate transaminase	<i>bioA</i>	WP_096596024.1	-	-	-	-	-	-	-	-	-	-	
	Cell fate regulator	<i>yaaT</i>	WP_096598399.1	-	WP_155260402.1	WP_096543167.1	-	-	-	-	-	-	-	
	Hypothetical proteins	-	-	-	-	-	-	-	-	-	-	WP_103263459.1	-	WP_086428075.1
		-	-	-	-	-	-	-	-	-	-	NCJ13602.1	-	-
		-	-	-	-	-	-	-	-	-	-	NCJ14457.1	-	-
		-	-	-	-	-	-	-	-	-	-	NCJ14406.1	-	-
		-	-	-	-	-	-	WP_026067011.1	-	-	-	-	-	-
		-	-	-	WP_155260499.1	-	-	-	-	-	-	-	-	-
		-	-	WP_155261267.1	-	-	-	-	-	-	-	-	-	-
		-	WP_096596966.1	-	WP_096541503.1	-	-	-	-	-	-	-	-	-
		-	WP_096598679.1	-	-	-	-	-	-	-	-	-	-	-
		-	WP_126489886.1	-	-	-	-	-	-	-	-	-	-	-
		-	-	WP_155262125.1	WP_155260084.1	WP_096595558.1	-	-	-	-	-	-	-	-
		-	-	-	-	-	-	-	-	WP_096543794.1	-	-	-	-
		-	-	-	-	-	-	-	-	WP_096545244.1	-	-	-	-
		-	-	-	-	-	-	-	WP_096606315.1	-	-	-	-	-
-		-	-	-	-	-	-	-	-	WP_096662163.1	-	-	-	
-		-	-	-	-	-	-	-	-	WP_096662188.1	-	-	-	
-		-	-	-	-	-	-	-	-	-	-	-	WP_015728984.1	
-		-	-	-	-	-	-	WP_096606888.1	-	-	-	-	-	
-		-	-	-	-	-	-	-	-	WP_112424797.1	-	-	-	
-		-	-	-	-	-	-	-	-	-	-	SUM43753.1	-	
-	-	-	-	-	-	-	-	-	-	-	SUM43646.1	-		
-	-	-	-	-	-	-	-	-	-	-	SUM43753.1	-		
-	-	-	-	-	-	-	-	-	-	-	SUM43646.1	-		
-	-	-	-	-	-	-	-	-	-	-	SUM43779.1	-		
-	-	-	-	-	-	-	-	-	-	-	SUM43893.1	-		
-	-	-	-	-	-	-	-	-	-	-	SUM46387.1	-		
-	WP_096596082.1	WP_155261984.1	WP_155260049.1	WP_096542975.1	WP_019165887.1	-	-	-	-	-	WP_096596568.1	-		
-	-	-	-	-	-	-	-	-	-	-	-	SUM46893.1	-	
-	-	-	-	-	-	-	-	-	-	-	-	SUM47179.1	-	

Pseudomonas leptonychotis sp. nov., isolated from Weddell seals in Antarctica

Dana Nováková¹, Pavel Švec^{1,*}, Michal Zeman², Hans-Jürgen Busse³, Ivana Mašlaňová², Roman Pantůček², Stanislava Králová¹, Lucie Křištofová¹ and Ivo Sedláček¹

Abstract

A taxonomic study was carried out on four Gram-stain-negative strains P5773^T, P6169, P4708 and P6245, isolated from anus or mouth samples of Weddell seals at James Ross Island, Antarctica. The results of initial 16S rRNA gene sequence analysis showed that all four strains formed a group placed in the genus *Pseudomonas* and found *Pseudomonas guineae* and *Pseudomonas peli* to be their closest neighbours with 99.9 and 99.2% sequence similarity, respectively. Sequence analysis of *rpoD*, *rpoB* and *gyrB* housekeeping genes confirmed the highest similarity of isolates to *P. peli* (*rpoD*) and to *P. guineae* (*rpoB* and *gyrB*). The average nucleotide identity value below 86%, as calculated from the whole-genome sequence data, showed the low genomic relatedness of P5773^T to its phylogenetic neighbours. The complete genome of strain P5773^T was 4.4 Mb long and contained genes encoding proteins with biotechnological potential. The major fatty acids of the seal isolates were summed feature 8 (C_{18:1}ω7c), summed feature 3 (C_{16:1}ω7c/C_{16:1}ω6c) and C_{16:0}. The major respiratory quinone was Q9. The major polar lipids were phosphatidylethanolamine, phosphatidylglycerol and diphosphatidylglycerol. Putrescine and spermidine are predominant in the polyamine pattern. Further characterization performed using repetitive sequence-based PCR fingerprinting and MALDI-TOF MS analysis showed that the studied isolates formed a coherent cluster separated from the remaining *Pseudomonas* species and confirmed that they represent a novel species within the genus *Pseudomonas*, for which the name *Pseudomonas leptonychotis* sp. nov. is suggested. The type strain is P5773^T (=CCM 8849^T=LMG 30618^T).

The genus *Pseudomonas* includes more than 200 species [1] that inhabit diverse environments in different geographical areas. Many of them were isolated from soil, rocks or water in Antarctica during the last few years. The cold-adapted bacteria *Pseudomonas guineae* [2], *Pseudomonas prosekii* [3], *Pseudomonas gregormendelii* [4] and *Pseudomonas versuta* [5] were obtained from soil or rocks. The species *Pseudomonas deceptionensis* was isolated on Deception Island from Antarctic marine sediment [6]. Reddy *et al.* [7] described *Pseudomonas antarctica*, *Pseudomonas meridiana* and *Pseudomonas proteolytica* from cyanobacterial mats. However, no *Pseudomonas* species have been originally isolated and described from seals so far. It is known that harbour seals can suffer from

different eye infections caused by *Pseudomonas aeruginosa* [8] or other *Pseudomonas* species. [9]. Fleming and Bexton [10] indicated *P. aeruginosa* to be one of the most frequent aerobic bacteria found in these animals. Here we describe a novel *Pseudomonas* species based on four strains isolated from Weddell seals (*Leptonychotes weddellii*) in Antarctica.

The specimens of rectal or mouth swabs obtained from randomly sampled *L. weddellii*, which are predominant throughout the Antarctic coasts as well as on coastal fast ice and neighbouring islands up to 30 km from the continent. They were collected on James Ross Island, Antarctica, during the Austral summers in 2013 and 2014 using the E-Swabs

Author affiliations: ¹Czech Collection of Microorganisms, Department of Experimental Biology, Faculty of Science, Masaryk University, Kamenice 5, 625 00 Brno, Czech Republic; ²Section of Genetics and Molecular Biology, Department of Experimental Biology, Faculty of Science, Masaryk University, Kottlářská 2, 611 37 Brno, Czech Republic; ³Institute of Microbiology, University of Veterinary Medicine Vienna, A-1210 Vienna, Austria.

*Correspondence: Pavel Švec, mpavel@sci.muni.cz

Keywords: *Pseudomonas leptonychotis*; Antarctica; Weddell seal; polyphasic taxonomy.

Abbreviations: ANI, average nucleotide identity; dDDH, digital DNA-DNA hybridization; FAME, fatty acid methyl ester; MALDI TOF-MS, matrix-assisted laser desorption/ionization time-of-flight mass spectrometry; WGS, whole-genome sequencing.

The GenBank/EMBL/DDBJ accession numbers for the 16S rRNA, *rpoB*, *rpoD* and *gyrB* gene sequences of *Pseudomonas leptonychotis* P5773^T (=CCM 8849^T), P6169, P4708 and P6245 (=CCM 8987) are MK104124–MK104127 for the 16S rRNA gene, MK105606–MK105609 for the *rpoB* gene, MK125496, MK125498, MK125497 and MK125499 for the *rpoD* gene, and MN103342–MN103345 for the *gyrB* gene. The Whole Genome Shotgun project of the *Pseudomonas leptonychotis* strain P5773^T (=CCM 8849^T) has been deposited at DDBJ/ENA/GenBank under the accession number RFLV00000000. The version described in this paper is RFLV01000000.

Two supplementary tables and six figures are available with the online version of this article.

swab/transport tube system (Dispolab). The samples were cultivated on MacConkey agar (Oxoid) at 30 °C for 24 h and various colonies were picked up from smears of the samples. Four Gram-stain-negative bacteria exhibiting the basic phenotypical features typical for the genus *Pseudomonas* were sampled from different seals. Strains P5773^T (=CCM 8849^T=LMG 30618^T; locality, beach under Bibby Point; year of isolation, 2014), P4708 (Cape Lachman, 2013) and P6169 (coast close to the Johan George Mendel Czech Antarctic Station, 2014) were isolated from anal mucous membranes and strain P6245 (=CCM 8987) was collected from oral membranes (coast near Halozetes Valley, 2014). The samples were cultivated on MacConkey agar at 30 °C for 24 h and various colonies were picked up from smears of the samples. Pure cultures were sub-cultivated on Columbia blood agar supplemented with 5% sheep blood and tentatively classified by conventional tube and plate tests [11].

The reference type strains *P. guineae* CCM 7752^T and *P. peli* CCM 7693^T were obtained from the Czech Collection of Microorganisms (Masaryk University, Brno; www.sci.muni.cz/ccm/).

DNA for sequencing 16S rRNA, *rpoD*, *rpoB* and *gyrB* genes was extracted by alkaline lysis as described previously [12]. The partial 16S rRNA gene corresponding to coordinates 8–1542 used for *Escherichia coli* were amplified by PCR with FastStart PCR Master Mix (Roche Diagnostics) and the universal primers pA (AGAGTTTGATCCTGGCTCAG) and pH (AAGGAGGTGATCCAGCCGCA) [13]. The 16S rRNA amplicons were purified using a High Pure PCR Product Purification Kit (Roche Diagnostics). The sequencing was performed using the PCR primers and with internal forward F1 (GTGGGGAKCRAACAGGATTAG) and reverse R2 (CACATSMTCMCCRCTTGT) [14] primers at the Eurofins MWG Operon sequencing facility (Ebersberg, Germany). All four seal strains exhibited identical partial 16S rRNA gene sequences. The global alignment tool for 16S rRNA gene sequences implemented at the EzBioCloud [15] assigned the analysed strains into the genus *Pseudomonas* and found *P. guineae* and *P. peli* to be the phylogenetically closest relatives, with 16S rRNA gene sequence similarities of 99.9 and 99.2%, respectively. The phylogenetic analysis based on 16S rRNA gene sequences was performed using the software MEGA version 6 [16]. Genetic distances were corrected using Kimura's two-parameter model. The evolutionary history was inferred using the neighbour-joining method using a bootstrap test based on 1000 replications and confirmed by the maximum-likelihood method (Fig. S1, available in the online version of this article).

Due to a high number of phylogenetically closely related *Pseudomonas* species (Table S1) and low discriminatory power of the 16S rRNA gene for their separation, a further comparison of *rpoD*, *rpoB* and *gyrB* housekeeping gene sequences was carried out. The gene fragment amplification was performed with PsEG30F (ATYGAAATCGCCAARCG) and PsEG90R (CGGTTGATKTCCTTGA) primers for the *rpoD* gene [17] and with LAPS (TGGCCGAGAACCAGTTCGCGT) and

LAPS27 (CGGCTTCGTCCAGCTTGTTTCAG) primers for the *rpoB* gene [18] and *gyrB*_PseuLep_Fw2 (ACAA-GGAAGAAGGCGTATC) and *gyrB*_PseuLep_Rv2 (TGTA-GAGTTCGGAAAGGGCA) primers designed for *gyrB* gene. The *gyrB* gene fragments were amplified using OneTaq Quick-Load 2X Master Mix with Standard Buffer. The following thermal programme was applied for the amplification: 94 °C for 30 s, 30 cycles of 94 °C for 30 s + 49 °C for 30 s + 68 °C for 70 s, and final 5 min at 68 °C. The sequencing was performed at the Eurofins MWG Operon sequencing facility. Sequence identity ranges among the novel *Pseudomonas* strains were 99.7–100%, 98.9–100% and 98.8–100% for partial *rpoD*, *rpoB* and *gyrB* genes, respectively. The *rpoD* gene of strain P5773^T had 89% sequence identity to *P. peli* LMG 23201^T and 95% identity to *P. guineae* CCM 7752^T. The partial *rpoB* sequence of the strain showed 95% sequence identity to *P. guineae* CCM 7752^T when compared to the reference/deposited genes in the GenBank/EMBL/DDJB database. The *gyrB* gene of strain P5773^T had 87.5% identity to *P. peli* LMG 23201^T and *P. anguilliseptica* LMG 21629^T and had 88.2% sequence identity to *P. guineae* CCM 7752^T. These data corresponded with the interspecies sequence identity of the above-mentioned genes obtained in several previously described *Pseudomonas* species [19]. The result of a multilocus sequence analysis of the concatenated partial *rpoD*, *rpoB* and *gyrB* gene sequences is shown in Fig. 1a. The neighbour-joining tree reconstructed using concatenated partial sequences of proteins RpoB, RpoD and GyrB is shown in Fig. 1b.

Whole-genome sequencing (WGS) of strain P5773^T was performed in the frame of the identification service provided by the BCCM/LMG Bacteria Collection (Laboratory of Microbiology, Department of Biochemistry and Microbiology, Faculty of Sciences, Ghent University, Belgium). Genomic DNA was isolated with a Maxwell 16 Tissue DNA Purification Kit and a Maxwell 16 Instrument. The integrity and purity of the DNA solution was evaluated on a 1.0% (w/v) agarose gel and by spectrophotometric measurements at 234, 260 and 280 nm. A Quantus fluorometer was used to estimate the DNA concentration of the solution. The library was prepared using an in-house adapted protocol of the NEB preparation kit. WGS was performed by the Oxford Genomics Centre, University of Oxford, UK by using an Illumina Nextseq sequencing platform. Paired-end sequence reads were generated using the Illumina HiSeq 4000 platform (PE150 reads). Assembly and error correction of raw reads was performed with SPAdes 3.12 [20] with all k-mers 21–127 and follow-up mismatch correction. Genome assembly evaluation was performed with QUAST 5.0.1 [21]. The complete sequence of the 16S rRNA gene was extracted from WGS data using RNAmmer 1.2 [22] and matched that obtained by Sanger sequencing.

The size of the complete genome was 4394381 bp and consisted of 29 contigs longer than 200 bp (N50=2322232 bp; N75=496239 bp; L50=1, L75=3, mean coverage 260×), with an average G+C content of 58.8 mol%. A total of 3995 coding sequences and 66 RNA genes were annotated in the genome of strain P5773^T. One prophage and no plasmids were detected.

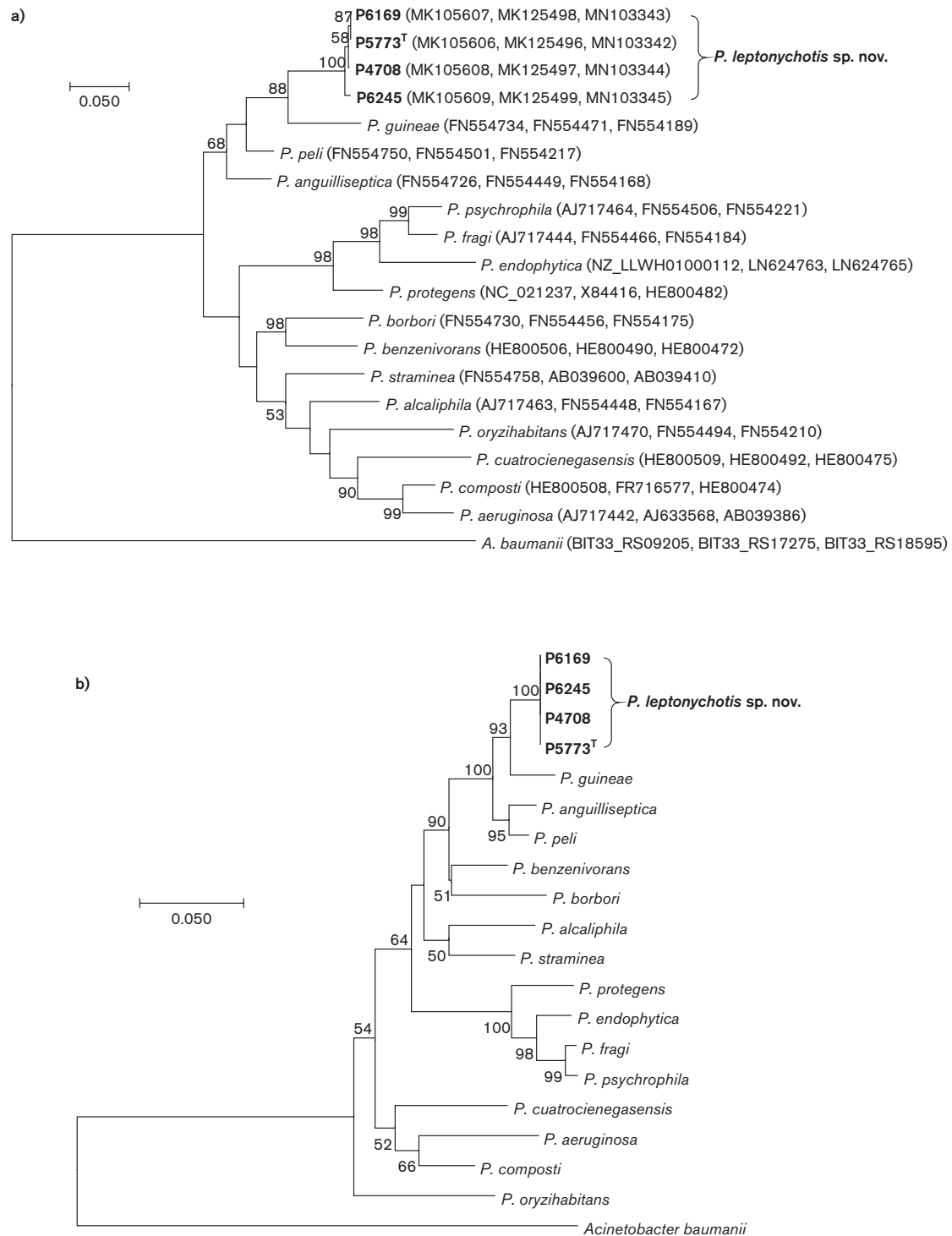


Fig. 1. (a) Maximum-likelihood tree reconstructed using concatenated partial gene sequences of three housekeeping genes (*rpoB*, *rpoD* and *gyrB*), showing the relationships of isolates of strains P5773^T, P6169, P4708, P6245 and selected *Pseudomonas* species representing phylogenetic neighbours and different intragenus phylogenetic lineages. The tree with the highest log-likelihood is shown and bootstrap probability values (percentages of 1000 tree replications) greater than 50% are shown at the branch points. The tree is drawn to scale, with branch lengths measured in the number of substitutions per site. There were 2374 positions in the final dataset. GenBank accession numbers of the *rpoB*, *rpoD* and *gyrB* sequences, respectively, are given in parentheses. (b) Neighbour-joining tree reconstructed using concatenated partial sequences of proteins RpoB, RpoD and GyrB, showing the relationships of strains P5773^T, P6169, P4708, P6245 and selected *Pseudomonas* species representing phylogenetic neighbours and different intragenus phylogenetic lineages. Bootstrap probability values (percentages of 1000 tree replications) greater than 50% are shown at the branch points. The evolutionary distances are in the units of the number of amino acid substitutions per site. There were 791 amino acid positions in the final dataset.

Three clusters *ureDABC*, *ureEFG* and *urtABCDE* of a total of 12 genes responsible for urea degradation were identified, however no activity of urease was detected. The annotation predicted a number of genes encoding potential virulence factors such as the alginate production pathway, the production of hydrogen cyanide, antibiotic efflux and modification systems, and various proteins such as the inhibitor of vertebrate lysozyme. There is a further biotechnological potential of the haloalkane dehalogenase (locus_tag: D8779_17660; protein accession: TIH07172) encoded by strain P5773^T, as it could be used in biocatalysis, remediation and biosensing [23].

Average nucleotide identity (ANI) values were calculated by OrthoANu [24] and digital DNA–DNA hybridization (dDDH) values with the Genome-to-Genome Distance Calculator (GGDC 1.2) [25], taking the recommended Formula 2 into account. To evaluate the intergenomic distances between the genome sequence of strain P5773^T and the ten reference type strains, ANI and dDDH values were determined (Table S1). The resulting ANI values ranged in the selected genomes between 73.9–85.4%, and dDDH values were between 20.5–29.8%, which is clearly below the threshold of 95–96% and 70%, respectively, recommended for species delineation [26, 27]. As a further extension to genome-based phylogeny the Up-to-date Bacterial Core Gene set (UBCG) software version 3.0 [28] was used to compare 92 core genes between strain P5773^T and other closely related *Pseudomonas* species (Fig. S2). This analysis confirmed that *Pseudomonas leptonychotis* stands as separate species in the genus *Pseudomonas*.

The four studied strains and those of the type strains of two phylogenetically closest species, *P. guineae* CCM 7752^T and *P. peli* CCM 7693^T, revealed by gene sequence analyses, were tested for the following biochemical and physiological properties using conventional tube and plate tests: oxidase (OXItest, Erba-Lachema); catalase (ID colour Catalase; bioMérieux); urea hydrolysis [29]; oxidation-fermentation (OF test) [30]; arginine dihydrolase, ornithine and lysine decarboxylases [31]; acid production from fructose, maltose, mannitol and xylose [32]; hydrolysis of Tween 80, gelatin [33], casein and tyrosine [34]; DNA, lecithine (egg-yolk reaction) [35]; *O*-nitrophenyl- β -D-galactopyranoside (ONPG) [36]; hydrolysis of aesculin and starch; growth on Simmons citrate; nitrate and nitrite reduction [37]; and utilization of acetamide and sodium malonate [38, 39]. Bacterial growth was tested on tryptone soya agar (TSA; Oxoid), nutrient agar CM3 (Oxoid), plate count agar (PCA; Oxoid), brain heart infusion agar (BHI; Oxoid), MacConkey agar (Hi-Media), Reasoner's 2A (R2A) agar (Oxoid) and Columbia blood agar base (Oxoid) with 5% sheep blood. The temperature range for growth (0, 1, 2, 3, 5, 10, 20, 30, 35 and 37°C) and NaCl concentration tolerance (0.5, 1, 2, 3, 4, 5 and 6%, w/v) were tested on TSA adjusted accordingly. The pH range tolerance was tested in tryptone soya broth (Oxoid) adjusted to pH 5.0–8.0 (in increments of 1.0 pH unit) using the buffer system 0.1 M KH₂PO₄/0.1 M NaOH. The two commercial kits, API ZYM (bioMérieux) and the GEN III MicroPlate (Biolog), were used according to the manufacturers' instructions.

Susceptibility to a wide spectrum of antibiotics was tested by the disc diffusion method on Mueller–Hinton medium (Oxoid). The following antibiotics relevant for Gram-negative rods were tested: ampicillin (10 µg), carbenicillin (100 µg), cefixime (5 µg), ceftazidim (10 µg), cephalothin (30 µg), ciprofloxacin (5 µg), gentamicin (10 µg), chloramphenicol (30 µg), imipenem (10 µg), kanamycin (30 µg), cotrimoxazol (25 µg), piperacillin (30 µg), polymyxin B (300 U) streptomycin (10 µg) and tetracycline (30 µg). EUCAST/CLSI standards were followed for cultivation and inhibition zone diameter readings [40, 41].

The cellular morphology of strain P5773^T was observed by transmission electron microscopy (Morgagni 268D Philips, FEI) using a sample stained with 2% ammonium molybdate (Fig. S3).

The results of phenotypic characterization are given in the species description below. The key physiological and biochemical tests allowing phenotypic differentiation of the studied strains from closely related species are listed in Table 1.

Repetitive sequence-based PCR fingerprinting with the REP primers (REP-PCR) was applied for strain typing and additional characterization of the isolates. The REP-PCR and cluster analyses were performed as previously described by Gevers *et al.* [42] with a minor modification described by Švec *et al.* [12]. The REP-PCR fingerprints of the tested strains were analysed along with patterns of 50 different *Pseudomonas* type and reference cultures obtained from an in-house CCM database (Fig. S4). All seal strains formed a cluster differentiated from other *Pseudomonas* type and reference strains. Individual seal strains revealed visually similar fingerprints sharing certain basic band-patterns but they differed, which confirmed that the analysed isolates represent different strains.

For the fatty acid methyl esters analysis (FAME), bacterial cultures were grown on TSA at 28±2°C for 24 h to reach the late exponential stage of growth according to the four quadrants streak method [43]. The extraction and analysis of fatty acid methyl esters using an Agilent 7890B gas chromatograph was performed according to the standard protocol of the Sherlock MIDI Identification System (MIDI Sherlock version 6.2; MIDI database, RTSBA 6.21). The fatty acid profile of the seal strains was similar to those of another *Pseudomonas* species. The most abundant fatty acids of the analysed isolates were summed feature 8 (C_{18:1}ω7c; 33.6 %, on average), summed feature 3 (C_{16:1}ω7c/C_{16:1}ω6c; 29%) and C_{16:0} (17.5%). A comparison to the closest relatives (Table S2) showed similar fatty acid profiles, confirming that the novel species belongs to the genus *Pseudomonas*.

The cultures for MALDI-TOF MS were grown on TSA at 30°C for 24 h. The preparation of protein extracts, their analysis using an Ultraflex III system (Bruker Daltonics) and data processing by Flex Analysis software (version 3.4, Bruker Daltonics) and BioTyper (version 3.0, Bruker Daltonics) was done as described previously [44]. For the reconstruction

Table 1. Phenotypical tests differentiating P5773^T from type strains of phylogenetically closely related *Pseudomonas* species

Strains: 1, P5773^T; 2 *Pseudomonas guineae* CCM 7752^T; 3, *Pseudomonas peli* CCM 7693^T; +, Positive; –, negative.

Characteristic	1*	2	3
Growth:			
at 35 °C	+	–	+
in 4% NaCl	–	+	+
Utilization of:			
Malonate	+	–	–
Hydrolysis of:			
Tween 80	+	–	+
Gelatin	+	–	–
Casein	+	–	–
DNA	–	–	+
Biolog system tests:			
D-Fructose-6-PO ₄	+	–	+
D-Serine	+	–	–
L-Aspartic acid	+	–	–
L-Histidine	+	–	–
L-Serine	–	+	+
γ-Amino-butyric acid	+	–	+
Acetoacetic Acid	+	–	+

*The remaining three seal strains exhibited reactions in the given tests that were identical to those for P5773^T.

of a dendrogram, signals present in at least 70% of all the analyses for one sample were transformed into MSPs (main spectra projections) and the dendrogram was generated using the UPGMA method (unweighted pair group method with arithmetic mean) based on the MSPs' similarity. The resulting dendrogram showed that the novel strains form a single cluster clearly distinguished from the phylogenetically closest relatives *P. guineae* CCM 7752^T and *P. peli* CCM 7693^T (Fig. S5).

Quinones, polar lipids and polyamines were extracted from freeze-dried biomass grown on TSA medium. Quinones and polar lipids were analysed as described previously [45–48]. The quinone system was composed of 93.8% Q9, 2.7% Q10 and 1.8% Q8. The polar lipid profile was composed of the major lipids phosphatidylethanolamine, phosphatidylglycerol and diphosphatidylglycerol, a moderate amount of phosphatidylserine, and a minor amount of an unidentified phospholipid (Fig. S6). Polyamines were extracted and analysed as described recently [46, 49, 50]. The polyamine pattern consisted of the major components putrescine [27.0 μmol g (dry weight)⁻¹] and spermidine [15.2 μmol g (dry weight)⁻¹]

and minor amounts of cadaverine [3.6 μmol g (dry weight)⁻¹], 1,3-diaminopropane [0.6 μmol g (dry weight)⁻¹] and spermine [0.1 μmol g (dry weight)⁻¹]. This polyamine pattern is well in line with that reported for other *Pseudomonas* species [46, 49, 51].

All the obtained results, including those from phylogenetic analysis using 16S rRNA genes, multilocus sequence analysis, whole-genome sequence analysis, FAME, MALDI-TOF MS, REP-PCR fingerprints analysis and extensive phenotyping, demonstrated that the strains from Weddell seals analysed in this study represent a novel species within the genus *Pseudomonas*.

DESCRIPTION OF *PSEUDOMONAS LEPTONYCHOTIS* SP. NOV.

Pseudomonas leptonychotis sp. nov. (lep.to.ny.cho'tis. N.L. gen. n. *leptonychotis*, of *Leptonychotes*, the genus of seals from which the isolates were recovered).

Cells are Gram-stain-negative, motile, slim rods (2–4 μm long and 0.5–0.7 μm wide) occurring mainly in groups or singly. Longer cells may be curved. One or more polar flagella can be observed. Colonies are yellowish, circular with slightly irregular margins, smooth and shiny, reaching about 2 mm in diameter when cultivated on TSA at 30 °C for 24 h. Older cultures get sticky. They grow well on PCA, TSA, nutrient agar CM3, BHI agar, MacConkey agar, as well as on Columbia agar supplemented with 5% sheep blood without haemolysis; no or weak growth is observed on R2A agar. The species grows well in the temperature range 2–35 °C, in the presence of 0.5–3% NaCl and at a pH ranging from 6 to 8. Optimal growth is revealed in 25 °C, 1% NaCl and pH 7. No fluorescein pigment is observed on King B medium. Oxidase and catalase reactions are positive. Oxidative, but no fermentative metabolism is observed with the OF test. Nitrate reduction variable and nitrite reduction negative. Positive for Simmons citrate and sodium malonate utilization and hydrolysis of Tween 80, casein, lecithine and tyrosine. Negative for acetamide utilization, production of levane from sucrose and hydrolysis of aesculin, ONPG, DNA, urea and starch. Acid is not produced from mannose or maltose. Arginine dihydrolase, as well as lysine and ornithine decarboxylase, is negative. Variable acid production from fructose and xylose and hydrolysis of gelatin. Production of alkaline phosphatase, esterase (C4), esterase lipase (C8), lipase (C14), leucine arylamidase, valine arylamidase (weak) and acid phosphatase is positive with the API ZYM kit. Negative reaction for cystine arylamidase, trypsin, α-chymotrypsin, naphthol-AS-BI-phosphohydrolase, α-galactosidase, β-galactosidase, β-glucuronidase, α-glucosidase, β-glucosidase, N-acetyl-β-glucosaminidase, α-mannosidase and α-fucosidase.

Carbon source utilization ability via respiration, determined in Biolog GEN III MicroPlate test panels, is positive for D-fructose-6-PO₄, D-serine, L-alanine, L-arginine, L-aspartic acid, L-glutamic acid, L-histidine, methyl pyruvate, L-lactic acid, citric acid, α-keto-glutaric acid (weak), D-malic acid,

L-malic acid, bromo-succinic acid, Tween 40, γ -amino-butyric acid, β -hydroxy-D,L-butyric acid, acetoacetic acid, propionic acid and acetic acid. Utilization test results are negative for maltose, trehalose, cellobiose, sucrose, turanose, stachyose, raffinose, lactose, methyl β -D-glucoside, D-salicin, N-acetyl-D-glucosamine, N-acetyl- β -D-mannosamine, N-acetyl-D-galactosamine, N-acetyl neuraminic acid, α -D-glucose, D-mannose, D-galactose, 3-methyl glucose, inosine, D-sorbitol, D-mannitol, D-arabitol, myo-inositol, glycerol, D-glucose-6-PO₄, D-aspartic acid, gelatine, glycyl-L-proline, L-pyroglytamic acid, L-serine, D-gluconic acid, quinic acid, D-saccharic acid, p-hydroxy phenylacetic acid, D-lactic acid methyl ester and formic acid. Variable utilization of dextrin, D-fucose, L-fucose, D-glucuronic and mucic acid. Utilization of gentiobiose, melibiose, D-fructose, L-rhamnose, pectin, D-galacturonic acid, D-galactonic acid lactone, glucuronamide, α -hydroxy-butyric acid and α -keto butyric acid is borderline or negative.

Summed feature 8 (C_{18:1} ω 7c), summed feature 3 (C_{16:1} ω 7c/C_{16:1} ω 6c) and C_{16:0} are the major cellular fatty acids. The quinone system contains predominantly ubiquinone Q-9. In the polar lipid profile, phosphatidylethanolamine, diphosphatidylglycerol and phosphatidylglycerol are predominant. Phosphatidylserine is present in moderate amounts and an unidentified phospholipid (PL1) is found in a trace amount. The polyamine pattern is characterized by the major compound putrescine and spermine and small amounts of 1,3-diaminopropane; cadaverine and spermine are also present.

The strains are sensitive to carbenicillin, ceftazidim, ciprofloxacin, gentamicin, imipenem, kanamycin, cotrimoxazole, piperacillin, polymyxin B, streptomycin and tetracycline. The strains are resistant to ampicillin, cefixime, cephalothin and chloramphenicol.

The type strain, P5773^T (=CCM 8849^T=LMG 30618^T), was isolated from anal mucous membrane of a seal (*Leptonychotes weddellii*) at a beach under Bibby Point, James Ross Island, Antarctica in 2014. Almost all characteristics of the type strain P5773^T are in agreement with the species description. The strain-dependent test results of P5773^T are as follows: positive for xylose acidification, hydrolysis of gelatin and dextrin utilization, while negative for acid production from fructose and utilization of gentiobiose, melibiose, D-fructose, D-fucose, L-fucose, L-rhamnose, pectin, D-galacturonic acid, D-galactonic acid lactone, D-glucuronic acid, glucuronamide, mucic acid, α -hydroxy-butyric acid and α -keto butyric acid. The genomic DNA G+C content of the type strain is 58.8 mol%, the genome size is approximately 4.4 Mb.

The GenBank/EMBL/DDBJ accession numbers for the 16S rRNA, *rpoB*, *rpoD* and *gyrB* gene sequences of *Pseudomonas leptonychotis* P5773^T (=CCM 8849^T), P6169, P4708 and P6245 (=CCM 8987) are MK104124–MK104127 for the 16S rRNA gene, MK105606–MK105609 for the *rpoB* gene, MK125496, MK125498, MK125497 and MK125499 for the *rpoD* gene, and MN103342–MN103345 for *gyrB* gene. The Whole Genome Shotgun project of the *Pseudomonas leptonychotis*

strain P5773^T (=CCM 8849^T) has been deposited at DDBJ/ENA/GenBank under the accession number RFLV00000000. The version described in this paper is RFLV01000000.

Funding information

The study was partly supported by the Ministry of Education, Youth and Sports of the Czech Republic projects CzechPolar2 (LM2015078), ECOPOLARIS (CZ.02.1.01/0.0/0.0/16_013/0001708) and the Proteomics Core Facility (LM2015043). M. Z., I. M. and R. P. were supported by the Ministry of Health of the Czech Republic (16-29916A) and the Grant Agency of Masaryk University (MUNI/A/0958/2018).

Acknowledgements

We would like to thank the scientific infrastructure of the Johan George Mendel Czech Antarctic Station and its crew for their assistance and the Czech Antarctic Foundation for their support. S. K. is a beneficiary of Brno PhD talent financial aid. We wish to thank Dr Daniel Krsek (NRL for Diagnostic Electron Microscopy of Infectious Agents, National Institute of Public Health, Prague, Czech Republic) for transmission electron microscopy, Bernhard Schink (University of Konstanz, Germany) for name correction and Eva Staňková and Jana Bajzerová (CCM, Brno, Czech Republic) for excellent technical assistance.

Conflicts of interest

The authors declare that there are no conflicts of interest.

References

1. Parte AC. LPSN-list of prokaryotic names with standing in nomenclature. *Nucleic Acids Res* 2014;42:D613–D616.
2. Bozal N, Montes MJ, Mercadé E. *Pseudomonas guineae* sp. nov., a novel psychrotolerant bacterium from an Antarctic environment. *Int J Syst Evol Microbiol* 2007;57:2609–2612.
3. Kosina M, Barták M, Mašlaňová I, Pascutti AV, Šedo O et al. *Pseudomonas prosekii* sp. nov., a novel psychrotrophic bacterium from Antarctica. *Curr Microbiol* 2013;67:637–646.
4. Kosina M, Švec P, Černoštlávková J, Barták M, Snopková K et al. Description of *Pseudomonas gregormendelii* sp. nov., a novel psychrotrophic bacterium from James Ross Island, Antarctica. *Curr Microbiol* 2016;73:84–90.
5. See-Too WS, Salazar S, Ee R, Convey P, Chan KG et al. *Pseudomonas versuta* sp. nov., isolated from Antarctic soil. *Syst Appl Microbiol* 2017;40:191–198.
6. Carrión O, Miñana-Galbis D, Montes MJ, Mercadé E. *Pseudomonas deceptionensis* sp. nov., a psychrotolerant bacterium from the Antarctic. *Int J Syst Evol Microbiol* 2011;61:2401–2405.
7. Reddy GSN, Matsumoto GI, Schumann P, Stackebrandt E, Shivaji S. Psychrophilic pseudomonads from Antarctica: *Pseudomonas antarctica* sp. nov., *Pseudomonas meridiana* sp. nov. and *Pseudomonas proteolytica* sp. nov. *Int J Syst Evol Microbiol* 2004;54:713–719.
8. Lockwood SK, Chovan JL, Gaydos JK. Aerobic bacterial isolations from harbor seals (*Phoca vitulina*) stranded in Washington: 1992–2003. *J Zoo Wildl Med* 2006;37:281–291.
9. Thornton SM, Nolan S, Gulland FM. Bacterial isolates from California sea lions (*Zalophus californianus*), harbor seals (*Phoca vitulina*), and northern elephant seals (*Mirounga angustirostris*) admitted to a rehabilitation center along the central California coast, 1994–1995. *J Zoo Wildl Med* 1998;29:171–176.
10. Fleming M, Bexton S. Conjunctival flora of healthy and diseased eyes of grey seals (*Halichoerus grypus*): implications for treatment. *Vet Rec* 2016;179:99.
11. Sedláček I, Králová S, Kýrová K, Mašlaňová I, Busse HJ et al. Red-pink pigmented *Hymenobacter coccineus* sp. nov., *Hymenobacter lapidarius* sp. nov. and *Hymenobacter glacialis* sp. nov., isolated from rocks in Antarctica. *Int J Syst Evol Microbiol* 2017;67:1975–1983.
12. Švec P, Nováková D, Žáčková L, Kukletová M, Sedláček I. Evaluation of (GTG)_n-PCR for rapid identification of *Streptococcus mutans*. *Antonie van Leeuwenhoek* 2008;94:573–579.

13. Edwards U, Rogall T, Blöcker H, Emde M, Böttger EC. Isolation and direct complete nucleotide determination of entire genes. Characterization of a gene coding for 16S ribosomal RNA. *Nucleic Acids Res* 1989;17:7843–7853.
14. Kýrová K, Sedláček I, Pantůček R, Králová S, Holochová P et al. *Rufibacter ruber* sp. nov., isolated from fragmentary rock. *Int J Syst Evol Microbiol* 2016;66:4401–4405.
15. Yoon S-H, Ha SM, Kwon S, Lim J, Kim Y et al. Introducing EzBioCloud: a taxonomically united database of 16S rRNA gene sequences and whole-genome assemblies. *Int J Syst Evol Microbiol* 2017;67:1613–1617.
16. Tamura K, Stecher G, Peterson D, Filipski A, Kumar S. MEGA6: molecular evolutionary genetics analysis version 6.0. *Mol Biol Evol* 2013;30:2725–2729.
17. Mulet M, Bennasar A, Lalucat J, García-Valdés E. An *rpoD*-based PCR procedure for the identification of *Pseudomonas* species and for their detection in environmental samples. *Mol Cell Probes* 2009;23:140–147.
18. Ait Tayeb L, Ageron E, Grimont F, Grimont PAD. Molecular phylogeny of the genus *Pseudomonas* based on *rpoB* sequences and application for the identification of isolates. *Res Microbiol* 2005;156:763–773.
19. Ramírez-Bahena M-H, Cuesta MJ, Tejedor C, Igual JM, Fernández-Pascual M et al. *Pseudomonas endophytica* sp. nov., isolated from stem tissue of *Solanum tuberosum* L. in Spain. *Int J Syst Evol Microbiol* 2015;65:2110–2117.
20. Nurk S, Bankevich A, Antipov D, Gurevich A, Korobeynikov A. Assembling genomes and mini-metagenomes from highly chimeric reads. In: Deng M, Jiang R, Sun F, Zhang X (editors). *Research in Computational Molecular Biology. RECOMB 2013. Lecture Notes in Computer Science*, 7821. Berlin, Heidelberg: Springer; 2013. pp. 7158–7170.
21. Gurevich A, Saveliev V, Vyahhi N, Tesler G. QUAST: quality assessment tool for genome assemblies. *Bioinformatics* 2013;29:1072–1075.
22. Lagesen K, Hallin P, Rødland EA, Staerfeldt HH, Rognes T et al. RNAmmer: consistent and rapid annotation of ribosomal RNA genes. *Nucleic Acids Res* 2007;35:3100–3108.
23. Koudelakova T, Bidmanova S, Dvorak P, Pavelka A, Chaloupkova R et al. *Haloalkane dehalogenases*: biotechnological applications. *Biotechnol J* 2013;8:32–45.
24. Yoon SH, Ha SM, Lim J, Kwon S, Chun J. A large-scale evaluation of algorithms to calculate average nucleotide identity. *Antonie van Leeuwenhoek* 2017;110:1281–1286.
25. Meier-Kolthoff JP, Auch AF, Klenk HP, Göker M. Genome sequence-based species delimitation with confidence intervals and improved distance functions. *BMC Bioinformatics* 2013;14:60.
26. Richter M, Rosselló-Móra R. Shifting the genomic gold standard for the prokaryotic species definition. *Proc Natl Acad Sci USA* 2009;106:19126–19131.
27. Meier-Kolthoff JP, Klenk HP, Göker M. Taxonomic use of DNA G+C content and DNA-DNA hybridization in the genomic age. *Int J Syst Evol Microbiol* 2014;64:352–356.
28. Na SI, Kim YO, Yoon SH, Ha SM, Baek I et al. UBCG: up-to-date bacterial core gene set and pipeline for phylogenomic tree reconstruction. *J Microbiol* 2018;56:280–285.
29. Christensen WB. Urea decomposition as a means of differentiating *Proteus* and paracolon cultures from each other and from *Salmonella* and *Shigella* types. *J Bacteriol* 1946;52:461–466.
30. Hugh R, Leifson E. The taxonomic significance of fermentative versus oxidative metabolism of carbohydrates by various gram negative bacteria. *J Bacteriol* 1953;66:24–26.
31. Brooks K, Sodeman T. A rapid method for determining decarboxylase and dihydrolase activity. *J Clin Pathol* 1974;27:148–152.
32. Weyant RS, Moss CW, Weaver RE, Hollis DG, Jordan JG et al. *Identification of Unusual Pathogenic Gram-Negative Aerobic and Facultatively Anaerobic Bacteria*, 2nd ed. Baltimore, MD: Williams & Wilkins; 1996. pp. 15–16.
33. Páčová Z, Kocur M. New medium for detection of esterase and gelatinase activity. *Zb Bakt Hyg* 1984;258:69–73.
34. Kurup VP, Babcock JB. Use of casein, tyrosine, and hypoxanthine in the identification of nonfermentative gram-negative bacilli. *Med Microbiol Immunol* 1979;167:71–75.
35. Owens JJ. The egg yolk reaction produced by several species of bacteria. *J Appl Bacteriol* 1974;37:137–148.
36. Lowe GH. The rapid detection of lactose fermentation in paracolon organisms by the demonstration of beta-D-galactosidase. *J Med Lab Technol* 1962;19:21–25.
37. Barrow GI, Feltham RKA. *Cowan and Steel's Manual for the Identification of Medical Bacteria*, 3rd ed. Great Britain: Cambridge University Press; 1993.
38. Oberhofer TR, Rowen JW. Acetamide agar for differentiation of nonfermentative bacteria. *Appl Microbiol* 1974;28:720–721.
39. Ewing WH. *Enterobacteriaceae. Biochemical Methods for Group Differentiation*. Atlanta: Public Health Service Publication no 734 CDC; 1960.
40. CLSI. Performance standards for antimicrobial susceptibility testing. *Twenty-Fifth Informational Supplement* 2015;35:No. 3. ISBN 1-56238-989-0.
41. EUCAST. Breakpoint tables for interpretation of MICs and zone diameters, version 7.1. *The European Committee on Antimicrobial Susceptibility Testing*.
42. Gevers D, Huys G, Swings J. Applicability of rep-PCR fingerprinting for identification of *Lactobacillus* species. *FEMS Microbiol Lett* 2001;205:31–36.
43. Sasser M. *Identification of Bacteria by Gas Chromatography of Cellular Fatty Acids*, MIDI Technical Note 101. Newark, DE: MIDI Inc; 1990.
44. Mašlačová I, Wertheimer Z, Sedláček I, Švec P, Indráková A et al. Description and comparative genomics of *Macrococcus caseolyticus* subsp. *hominis* subsp. nov., *Macrococcus goetzii* sp. nov., *Macrococcus epidermidis* sp. nov., and *Macrococcus bohemicus* sp. nov., novel macrococci from human clinical material with virulence potential and suspected uptake of foreign DNA by natural transformation. *Front Microbiol* 2018;9:1178.
45. Altenburger P, Kämpfer P, Makrithathis A, Lubitz W, Busse HJ. Classification of bacteria isolated from a medieval wall painting. *J Biotechnol* 1996;47:39–52.
46. Stolz A, Busse HJ, Kämpfer P. *Pseudomonas knackmussii* sp. nov. *Int J Syst Evol Microbiol* 2007;57:572–576.
47. Tindall BJ. Lipid composition of *Halobacterium lacusprofundi*. *FEMS Microbiol Lett* 1990a;66:199–202.
48. Tindall BJ. A comparative study of the lipid composition of *Halobacterium saccharovorum* from various sources. *Syst Appl Microbiol* 1990b;13:128–130.
49. Busse J, Auling G. Polyamine pattern as a chemotaxonomic marker within the *Proteobacteria*. *Syst Appl Microbiol* 1988;11:1–8.
50. Busse HJ, Bunka S, Hensel A, Lubitz W. Discrimination of members of the family *Pasteurellaceae* based on polyamine patterns. *Int J Syst Bacteriol* 1997;47:698–708.
51. Hauser E, Kämpfer P, Busse HJ. *Pseudomonas psychrotolerans* sp. nov. *Int J Syst Evol Microbiol* 2004;54:1633–1637.

International Journal of Systematic and Evolutionary Microbiology

Supplementary materials

Pseudomonas leptonychotis sp. nov., isolated from Weddell seals in Antarctica

Dana Nováková¹, Pavel Švec^{1*}, Michal Zeman², Hans-Jürgen Busse³, Ivana Mašlaňová²,
Roman Pantůček², Stanislava Králová¹, Lucie Křištofová¹ and Ivo Sedláček¹

¹Czech Collection of Microorganisms, Department of Experimental Biology, Faculty of Science, Masaryk University, Kamenice 5, 625 00 Brno, Czech Republic

²Section of Genetics and Molecular Biology, Department of Experimental Biology, Faculty of Science, Masaryk University, Kotlářská 2, 611 37 Brno, Czech Republic

³Institute of Microbiology, University of Veterinary Medicine Vienna, A-1210 Vienna, Austria

*Corresponding author:

Pavel Švec, e-mail: mpavel@sci.muni.cz

Table S1. Comparison of P5773^T genome with those of the phylogenetic close *Pseudomonas* spp. by Genome-to-Genome Distance Calculator (GGDC) and Average Nucleotide Identity (ANI) analysis, and overall genomes characteristics.

Data from: *direct submission, Joint Genome Institute; †von Neubeck *et al.*, *Int J Syst Evol Microbiol* 2016;66:1163-1173; ‡Ramírez-Bahena *et al.*, *Int J Syst Evol Microbiol* 2015;65:2110-2117.

dDDH, digital DNA-DNA hybridization; CI, confidence interval of method from GGDC.

Reference genome	dDDH [%]	CI dDDH [%]	ANI [%]	16S rRNA identity [%]	Genome size [Mb]	G+C [mol%]	GenBank WGS accession nos.
<i>Pseudomonas anguilliseptica</i> DSM 12111 ^{T*}	29.8	27.4 - 32.3	85.4	97.44	5.23	60.2	NZ_FNESC00000000
<i>Pseudomonas guineae</i> LMG 24016 ^{T*}	29.2	26.8 - 31.7	85.1	99.86	4.15	58.5	NZ_FOQL00000000
<i>Pseudomonas peli</i> DSM 17833 ^{T*}	28.7	26.4 - 31.2	84.9	99.17	4.49	59.7	NZ_FMTL00000000
<i>Pseudomonas borbori</i> DSM 17834 ^{T*}	23.8	21.5 - 26.3	80.4	97.09	5.27	63.0	NZ_FOWX00000000
<i>Pseudomonas cuatrocieneegasensis</i> CIP 109853 ^{T*}	23.3	21.1 - 25.8	79.4	98.02	5.36	61.8	NZ_FOFP00000000
<i>Pseudomonas composti</i> CCUG 59231 ^{T*}	21.5	19.2 - 23.9	77.6	97.79	5.39	62.4	NZ_FOWP00000000
<i>Pseudomonas fragi</i> NRRL B-727 ^{T*}	21.5	19.3 - 23.9	75.7	97.23	5.07	59.3	NZ_LT629783
<i>Pseudomonas helleri</i> DSM 29165 ^{T†}	20.8	18.6 - 23.2	75.2	97.46	5.68	58.1	NZ_JYLD00000000
<i>Pseudomonas psychrophila</i> DSM 17535 ^{T†}	20.8	18.6 - 23.2	74.8	97.23	5.33	57.5	NZ_JYKZ00000000
<i>Pseudomonas endophytica</i> BSTT44 ^{T‡}	20.5	18.3 - 22.9	73.9	97.52	4.97	55.2	NZ_LLWH00000000

Table S2. Comparison of cellular fatty acid composition profiles of the strains P5773^T, P6169, P4708 and P6245 with phylogenetically closely related *Pseudomonas* species.

TR, trace amounts (< 1 %); ND, not detected.

Fatty acid	P5773 ^T	P6169	P4708	P6245	<i>P. guineae</i> CCM 7752 ^T	<i>P. peli</i> CCM 7693 ^T
C _{10:0} 3OH	2.9	1.8	2.7	3.1	3.6	3.5
C _{12:0}	4.2	4.4	4.4	4.4	4.6	4.6
C _{12:0} 3OH	3.3	2.1	3.7	3.4	3.4	3.8
C _{15:1} ω6c	TR	TR	ND	TR	TR	1.4
C _{16:0}	16.9	17.9	17.5	17.7	18.6	15.5
C _{17:0} iso	1.0	TR	2.6	1.0	TR	1.1
C _{17:1} ω8c	2.1	3.2	1.6	1.0	1.2	4.2
C _{17:1} ω6c	1.0	1.7	1.0	TR	TR	1.6
C _{17:0}	1.6	3.6	1.3	TR	1.1	3.1
C _{18:0}	TR	1.0	TR	TR	1.5	TR
Summed Feature 3*	28.4	27.3	29.8	30.5	32.4	27.3
Summed Feature 8†	34.9	32.9	33.4	33.2	30.1	30.4

*C_{16:1} ω7c/C_{16:1} ω6c; †C_{18:1} ω7c

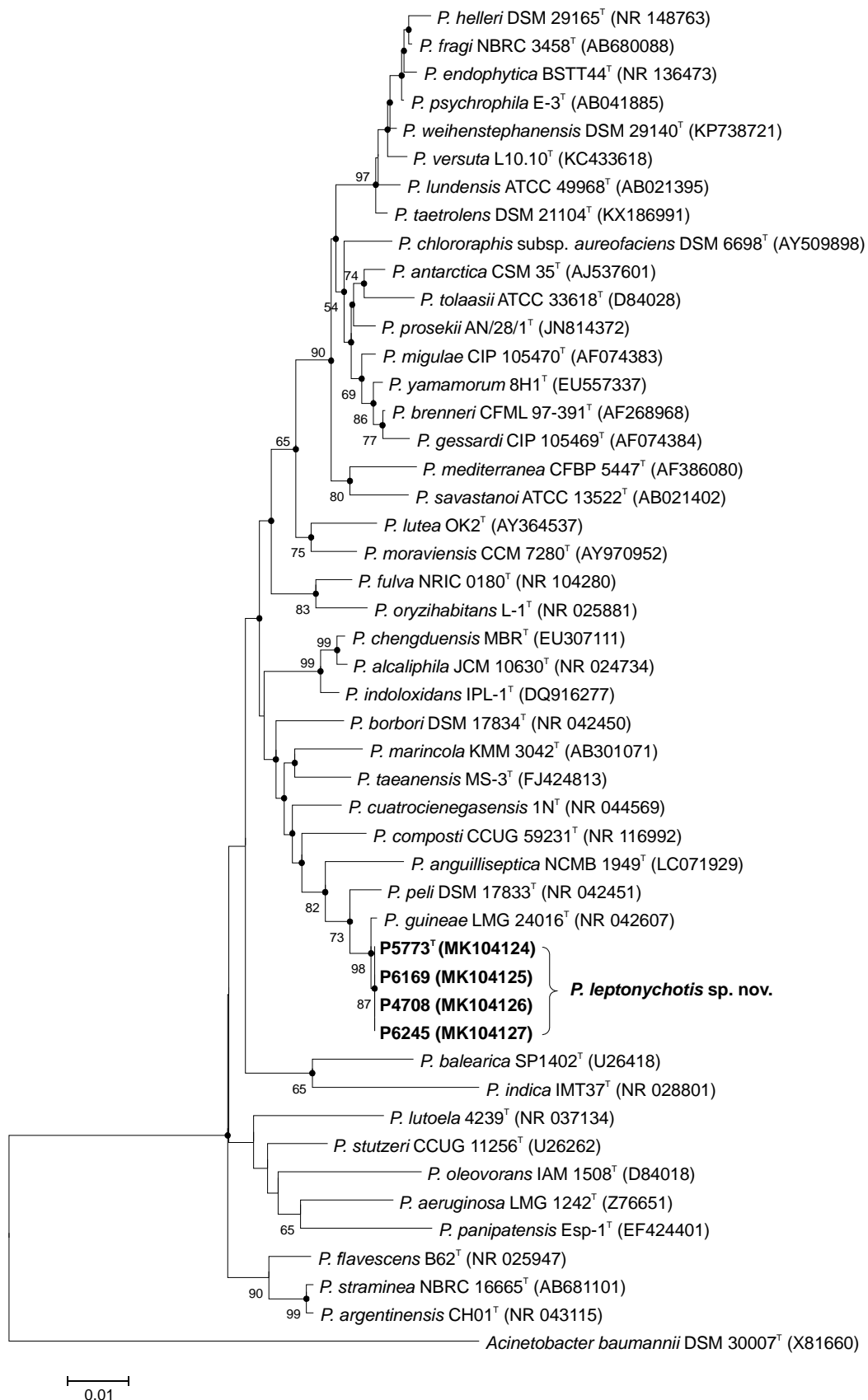


Fig. S1. Neighbour-joining tree based on the 16S rRNA gene sequences comparison showing the phylogenetic position of strains P5773^T, P6169, P4708 and P6245 and reference *Pseudomonas* spp. strains. Bootstrap probability values (percentages of 1000 tree replications) greater than 50% are shown at the branch points. *Acinetobacter baumannii* DSM 30007^T was used as an outgroup. Bar, 0.01 substitutions per nucleotide position. Filled circles indicate that the corresponding nodes are also obtained in the maximum-likelihood tree.

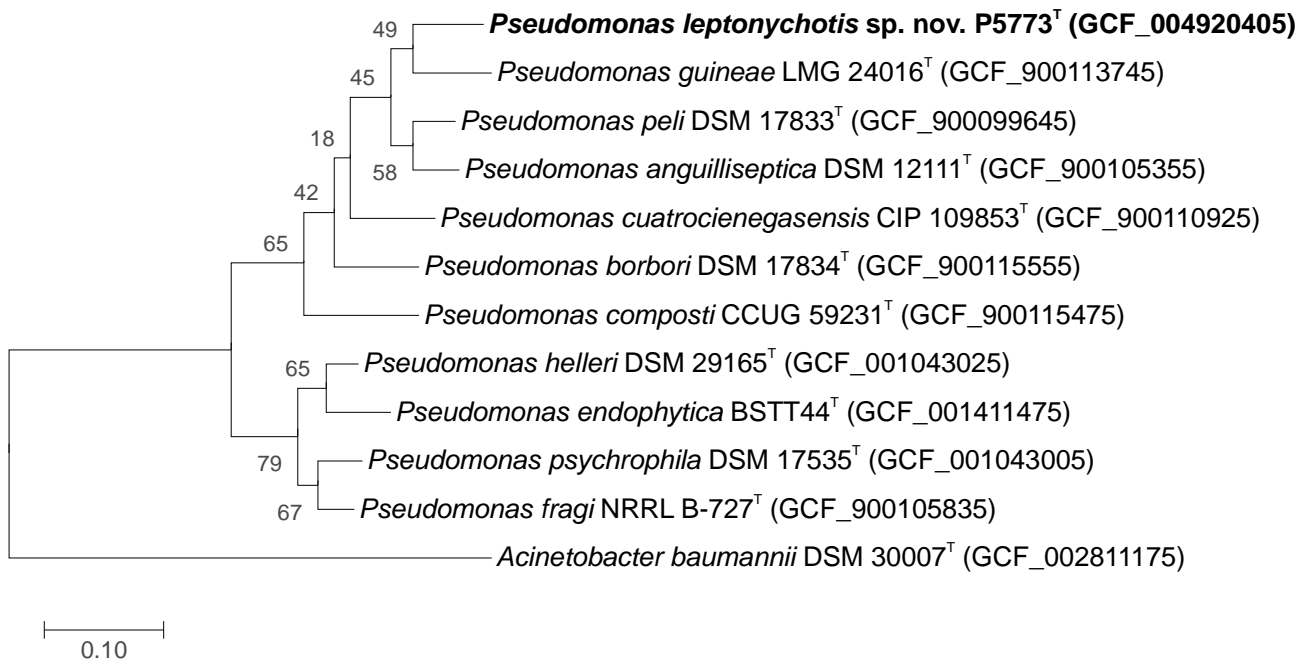


Fig. S2. Core gene set phylogenetic tree of *Pseudomonas leptonychotis* sp. nov. P5773^T and closely related species. Phylogenetic tree was constructed using Up-to-date bacterial core gene set (UBCG; concatenated alignment of 92 core genes). A total of 89,745 nucleotide positions were used. Maximum likelihood phylogenetic tree was inferred using Fasttree ver. 2.1.10 using GTR + CAT model. Gene support indices are given at branching points (maximal possible value is 92). *Acinetobacter baumannii* DSM 30007^T has been used as an outgroup. Assembly accession numbers are given in parentheses. Bar, 0.1 substitution per position.

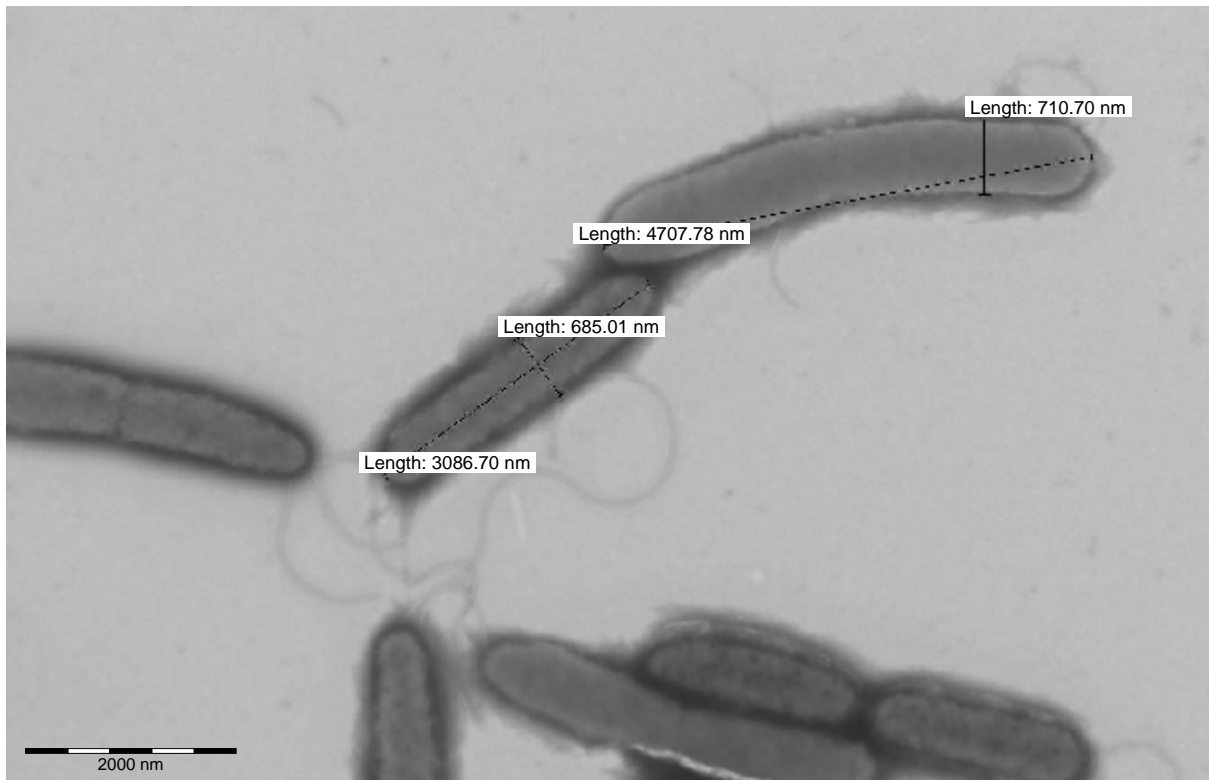


Fig. S3. Cell morphology of strain *Pseudomonas leptonychotis* sp. nov. P5773^T observed using transmission electron microscopy performed with a Morgagni 268D Philips (FEI Company, USA) electron microscope. Negative staining with 2% ammonium molybdate. Bar represents 2000 nm (original magnification $\times 10\,000$).

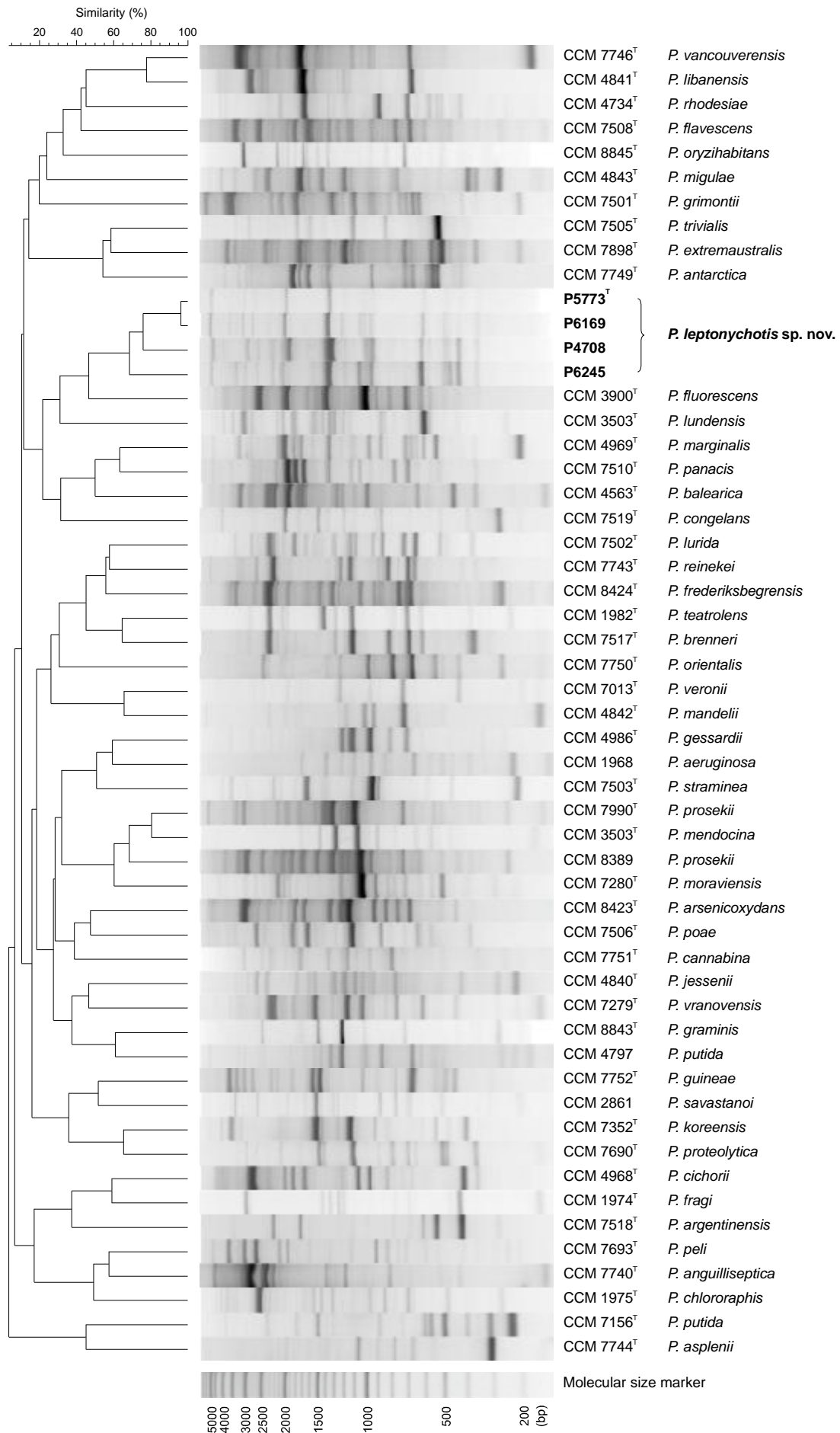


Fig. S4. Cluster analysis of REP-PCR fingerprints of the tested strains and selected representative type and reference *Pseudomonas* spp. strains.

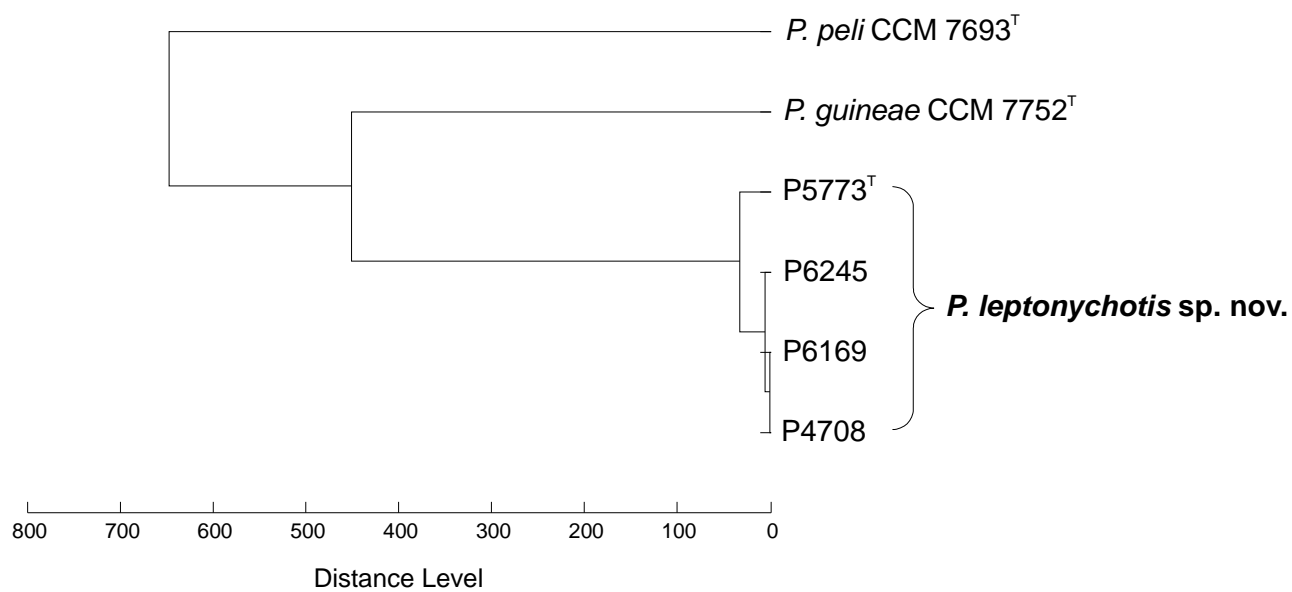


Fig. S5. Dendrogram obtained by cluster analysis of MALDI-TOF MS spectra of analysed seal isolates and closely related *Pseudomonas* species. Distance is displayed in relative units.

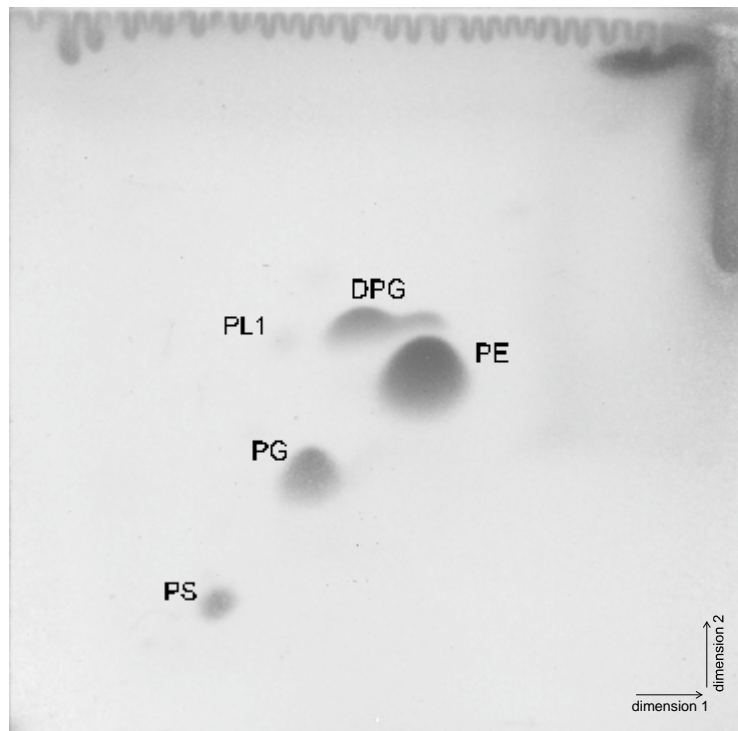


Fig. S6. Total polar lipids of the strain P5773^T after two-dimensional TLC. 1st dimension: chloroform/methanol/water (65:25:4, by vol); 2nd dimension: chloroform/acetic acid/methanol/water (80:15:12:4, by vol) and detection with 5 % ethanolic molybdatophosphoric acid and heating at 120 °C. PG, phosphatidylglycerol; DPG, diphosphatidylglycerol; PE, phosphatidylethanolamine; PS, phosphatidylserine; PL1, unidentified phospholipid.

Pseudomonas karstica sp. nov. and *Pseudomonas spelaei* sp. nov., isolated from calcite moonmilk deposits from caves

Pavel Švec^{1,*}, Marcel Kosina¹, Michal Zeman², Pavla Holočová¹, Stanislava Králová¹, Eva Němcová³, Lenka Micenková⁴, Urvashi⁵, Vipin Gupta⁶, Utkarsh Sood⁷, Rup Lal⁷, Suresh Korpole⁵ and Ivo Sedláček¹

Abstract

A taxonomic study of two fluorescent *Pseudomonas* strains (HJ/4^T and SJ/9/1^T) isolated from calcite moonmilk samples obtained from two caves in the Moravian Karst in the Czech Republic was carried out. Results of initial 16S rRNA gene sequence analysis assigned both strains into the genus *Pseudomonas* and showed *Pseudomonas yamanorum* 8H1^T as their closest neighbour with 99.8 and 99.7% 16S rRNA gene similarities to strains HJ/4^T and SJ/9/1^T, respectively. Subsequent sequence analysis of *rpoD*, *rpoB* and *gyrB* housekeeping genes confirmed the highest similarity of both isolates to *P. yamanorum* 8H1^T, but phylogeny and sequences similarities implied that they are representatives of two novel species within the genus *Pseudomonas*. Further study comprising whole-genome sequencing followed by average nucleotide identity and digital DNA–DNA hybridization calculations, repetitive sequence-based PCR fingerprinting with the REP and ERIC primers, automated ribotyping with the *EcoRI* restriction endonuclease, cellular fatty acid analysis, quinone and polar lipid characterization, and extensive biotyping confirmed clear separation of both analysed strains from the remaining *Pseudomonas* species and showed that they represent two novel species within the genus *Pseudomonas* for which the names *Pseudomonas karstica* sp. nov. (type strain HJ/4^T=CCM 7891^T=LMG 27930^T) and *Pseudomonas spelaei* sp. nov. (type strain SJ/9/1^T=CCM 7893^T=LMG 27931^T) are suggested.

Members of the genus *Pseudomonas* are ubiquitous organisms inhabiting a wide variety of environments comprising waters, soils, plants, animals and humans. They are saprophytes involved in the decomposition of organic materials and remediation of xenobiotic compounds. *Pseudomonas* organisms play an important role in the food industry and the genus also contains recognised human, animal and plant pathogens [1–3]. Phylogenetically, the genus *Pseudomonas* is assigned in the phylum *Proteobacteria* within the class *Gammaproteobacteria* [4].

The present study describes a taxonomic investigation of two fluorescent *Pseudomonas* strains, HJ/4^T (=CCM 7891^T=LMG

27930^T) and SJ/9/1^T (=CCM 7893^T=LMG 27931^T), isolated from calcite moonmilk samples obtained from two caves in the Moravian Karst in the Czech Republic. Moonmilk is a generic term for a soft, wet, plastic, fine-grained speleothem with variable mineralogy present on ceilings, floors and walls of caves [5]. It consists of crystal aggregates of carbonate minerals, such as calcite and hydromagnesite, other minerals, such as aragonite and gypsum, and non-carbonate minerals, such as silicate, phosphate and sulfate [6]. Some types of moonmilk are assumed to be of microbial origin, created either by direct precipitation of calcite by micro-organisms or by forming a nucleation surface on which minerals precipitate

Author affiliations: ¹Department of Experimental Biology, Czech Collection of Microorganisms, Faculty of Science, Masaryk University, Kamenice 5, 625 00 Brno, Czech Republic; ²Department of Experimental Biology, Section of Genetics and Molecular Biology, Faculty of Science, Masaryk University, Kotlářská 2, 611 37 Brno, Czech Republic; ³Centre for Cardiovascular Surgery and Transplantation, Pekařská 53, 656 91 Brno, Czech Republic; ⁴Research Centre for Toxic Compounds in the Environment, Faculty of Science, Masaryk University, Kamenice 5, 625 00 Brno, Czech Republic; ⁵Microbial Type Culture Collection and Gene Bank (MTCC), CSIR-Institute of Microbial Technology, Sector 39A, Chandigarh 160 036, India; ⁶PhiXGen Pvt. Ltd.101, GH-11, Atlantis CGHS Ltd.Sector-47, Gurugram, Haryana-122001, India; ⁷The Energy and Resources Institute, Lodhi Road New Delhi-110003, India.

*Correspondence: Pavel Švec, mpavel@sci.muni.cz

Keywords: *Pseudomonas karstica*; *Pseudomonas spelaei*; sp. nov.; moonmilk; caves.

Abbreviations: ANI, average nucleotide identity; dDDH, digital DNA–DNA hybridization; FAME, fatty acid methyl ester; WGS, whole-genome sequencing.

The GenBank/ENA/DBJ accession numbers for the 16S rRNA, *rpoB* and *rpoD* gene sequences of *Pseudomonas karstica* HJ/4^T (=CCM 7891^T) are HQ844524, HQ844521 and HQ844517, respectively and those of *Pseudomonas spelaei* SJ/9/1^T (=CCM 7893^T) are HQ844525, HQ844523 and HQ844518, respectively. The whole-genome shotgun projects of *P. karstica* HJ/4^T and *P. spelaei* SJ/9/1^T have been deposited in GenBank/ENA/DBJ under the accession numbers WLYI000000000 and WNNK000000000, respectively. The versions described in this paper are WLYI01000000 and WNNK01000000, respectively.

One supplementary table and six supplementary figures are available with the online version of this article.

[7–10]. Moonmilk is considered to be biologically active due to a significant presence of abundant populations of taxonomically diverse groups of metabolically active auto- and heterotrophic micro-organisms (archaea, bacteria and fungi) confirmed by both, culture-dependent and culture-independent techniques [5, 11–15].

Strain HJ/4^T was isolated from a moonmilk sample from the ‘Horní v chobotu’ cave (49° 21′ 50″ N, 16° 42′ 50″ E) and strain SJ/9/1^T was obtained from moonmilk sampled from the wall in the ‘Suchožlebská zazděná’ cave (49° 21′ 42″ N, 16° 43′ 2″ E). An illustrative image of a moonmilk layer on the ‘Suchožlebská zazděná’ cave wall is given in Fig. S1 (available in the online version of this article). The moonmilk samples were aseptically retrieved into sterile bottles and transported to the laboratory in a cooling bag within 24 h. One gram of each sample was resuspended in 35 ml sterile saline solution (0.9% NaCl). Plates with NWRI agar (peptone, 3.0 g; casein, 0.5 g; K₂HPO₄, 0.2 g; MgSO₄·7H₂O, 0.05 g; FeCl₃·6H₂O, 0.001 g; agar, 15.0 g; distilled water, 1000 ml; pH 7.2; sterilized at 0.1 MPa for 15 min) were inoculated with 100 μl suspension and incubated in aerobic conditions at 10 °C. Randomly chosen single colonies representing different morphotypes were picked up after 5 days of cultivation, purified and maintained on glass beads at –70 °C [16].

Reference strains *Pseudomonas brenneri* CCM 7517^T, *Pseudomonas migulae* CCM 4843^T and *Pseudomonas proteolytica* CCM 7690^T were obtained from the Czech Collection of Microorganisms (Masaryk University, Brno; www.sci.muni.cz/ccm) and *Pseudomonas yamanorum* DSM 26522^T from the DSMZ-German Collection of Microorganisms and Cell Cultures (Leibniz Institute, Braunschweig, www.dsmz.de).

DNA for the initial sequence analysis of the 16S rRNA gene was extracted using a method described by Mariani *et al.* [17]. PCR using HotStart *Taq* polymerase (Qiagen) and targeting the 16S rRNA gene was performed with universal eubacterial primers UNBC1 (5′-TGAAGAGTTTGGATCATGGCTCAG-3′) and UNB2 (5′-AGGAGGTGATCCAGCCGCA-3′) based on those described by Wiedmann *et al.* [18]. The amplification program started with the initial cycle at 95 °C for 15 min, followed by 35 cycles of 95 °C for 10 s, 62 °C for 30 s and 72 °C for 90 s and finished with a final step of 72 °C for 10 min. DNA bands of the expected size of approximately 1500 bp were purified from the gel with a QIAquick Gel Extraction Kit (Qiagen) and subjected to cycle sequencing using the BigDye Terminator version 3.1 Cycle Sequencing Kit (Applied Biosystems). The primer pair used for sequencing was the same as for PCR completed with other pairs targeting different regions of the 16S rRNA gene to gain overlaps. One pair of primers was described by Nadkarni *et al.* [19] and, additionally, primers 16SV5F (5′-GCCGCAAGGTTAAAACCTCAA-3′) and 16SV5R (5′-AGGCCAGGTAAGGTTCTTCG-3′) were designed in this study. The cycle sequencing products were purified using the BigDye XTerminator Purification Kit (Applied Biosystems). A direct-sequencing procedure was done on ABI Prism 3100 Avant apparatus (Applied Biosystems) according to the manufacturer’s instructions.

Fragments of the 16S rRNA gene were assembled into one consensus sequence using the CLUSTAL W program [20]. Initial comparison of obtained 16S rRNA gene sequences within the EzBioCloud online database (www.ezbiocloud.net; [21]) assigned analysed strains into the genus *Pseudomonas* and showed *P. yamanorum* 8H1^T as the closest neighbour with 99.8 and 99.7% 16S rRNA gene similarities to strains HJ/4^T and SJ/9/1^T, respectively. Further close phylogenetic neighbours of strains HJ/4^T and SJ/9/1^T were *P. brenneri* CFML 97-391^T with 99.7 and 99.5%, *P. proteolytica* CMS 64^T with 99.5 and 99.2%, and *P. migulae* CIP 105470^T with 99.4 and 99.5% similarities, respectively. For comparison of 16S rRNA gene sequences between the two analysed strains, HJ/4^T and SJ/9/1^T, the pairwise nucleotide sequence alignment tool available within the EzBioCloud database was used and the results showed 99.6% similarity. Phylogenetic analysis and reconstruction of a phylogenetic tree was performed using MEGA 7 software [22]. The phylogenetic position of strains HJ/4^T and SJ/9/1^T within the genus *Pseudomonas* revealed by the maximum likelihood [23] clustering method (Fig. S2) corresponded with those obtained using the neighbour-joining [24] and maximum-parsimony [25] methods (data not shown) and confirmed *P. yamanorum* as their closest phylogenetic neighbour.

Because of the low discriminatory power of the 16S rRNA gene sequence analysis for differentiation of *Pseudomonas* species, further comparison of *rpoD*, *rpoB* and *gyrB* house-keeping gene sequences enabling reliable differentiation of individual species [26] was carried out. The *rpoD* gene fragment amplification and determination was performed with primers PsEG30F (5′-ATYGAAATCGCCAARCG-3′) and PsEG90R (5′-CGGTTGATKTCCTTGA-3′) [27] and the *rpoB* gene was amplified using primers LAPS (5′-TGGC CGAGAACCAGTTCCGCGT-3′) and LAPS27 (5′-CGGC TTCGTCAGCTTGTTTCAG-3′) [28]. The PCR amplifications were accomplished with some modifications: the *rpoD* gene thermal program started at 94 °C for 3 min, followed by 25 cycles of 94 °C for 30 s, 60 °C for 30 s and 72 °C for 75 s and by a final step of 72 °C for 7 min; the *rpoB* gene thermal program started at 95 °C for 5 min, followed by 30 cycles of 95 °C for 35 s, 48 °C for 75 s and 72 °C for 75 s and by a final step of 72 °C for 7 min. The amplified sequences were purified using the High Pure PCR product purification Kit (Roche Diagnostics). The sequencing procedures were performed at the Eurofins MWG Operon sequencing facility (Ebersberg, Germany). The *gyrB* gene sequences of strains SJ/9/1^T and HJ/4^T were retrieved from their whole-genome sequences as described below. The *rpoD*, *rpoB* and *gyrB* sequences of the type strains of other *Pseudomonas* species were obtained from the GenBank database. Comparison of individual sequences was carried out using the BioNumerics software (version 7.6, Applied Maths). Strain HJ/4^T revealed highest similarities to *P. yamanorum* 8H1^T with 97.4% (*rpoB*) and 93.2% (*gyrB*) and *P. brenneri* DSM 15294^T with 91.8% (*rpoD*) and strain SJ/9/1^T was the closest relative of *P. yamanorum* 8H1^T with 97.9% (*rpoB*) and 93.2% (*gyrB*) and *P. proteolytica* CIP 108464^T with 93.2% (*rpoD*) similarities. Similarity values between strains

HJ/4^T and SJ/9/1^T were 97.4% (*rpoB*), 93.0% (*gyrB*) and 92.7% (*rpoD*). All these values are well below the maximal threshold similarities between *Pseudomonas* species for *rpoD* (99.86%), *gyrB* (99.62%) and *rpoB* (99.78%) genes described by Mulet et al. [26]. Further phylogenetic analysis and reconstruction of a phylogenetic tree was performed using MEGA7 software [22]. Maximum-likelihood trees showing a multilocus sequence analysis of the concatenated partial *rpoD*, *rpoB* and *gyrB* genes sequences and concatenated partial sequences of proteins RpoB, RpoD and GyrB from strains HJ/4^T and SJ/9/1^T and their close phylogenetic relatives are shown in Fig. 1. Both phylogenetic trees confirmed the separation of strains HJ/4^T and SJ/9/1^T from their phylogenetically close *Pseudomonas* species and showed *P. yamanorum* as their closest phylogenetic relative.

DNA for the whole-genome sequencing (WGS) of strains HJ/4^T and SJ/9/1^T was isolated using High Pure PCR Template Preparation Kit (Roche Diagnostics) and libraries were prepared using Nextera XT DNA Library Prep Kit (Illumina) according to the protocols provided by the manufacturers. Sequencing was performed using MiSeq Reagent Kits version 2 (500-cycles) on a MiSeq 2000 sequencer according to the manufacturer's instructions (Illumina). Quality of sequencing reads was analysed using FastQC version 0.11.8 [29] and bases of lower quality and adapters were trimmed by Trimgalore version 0.6.1 [30] based on Cutadapt [31]. *De novo* assembly of trimmed reads was performed by Unicycler version 0.4.8-beta [32] with all k-mers 21–127 and follow up mismatch correction. The BBtools package [33] was used to analyse various statistics of the genomes. The complete sequence of the 16S rRNA gene was extracted from WGS data using RNAmmer version 1.2 [34] and matched that obtained by Sanger sequencing. The sequences were compared using BioNumerics software (version 7.6, Applied Maths). Average nucleotide identity (ANI) values were calculated using OrthoANIu [35] and digital DNA–DNA hybridization (dDDH) values using the Genome-to-Genome Distance Calculator (GGDC version 2.1) [36] taking the recommended Formula 2 into account (Table 1). ANI values for the tested *Pseudomonas* species were in the range of 81.1–87.8%, and those for dDDH were between 25.3–35.0%, which is below the threshold of 95–96 and 70%, respectively, recommended for species delineation [37, 38]. Up-to-date Bacterial Core Gene set (UBCG) software version 3.0 [39] was used as a further extension to the genome-based phylogeny to compare 91 core genes between strains HJ/4^T and SJ/9/1^T and other closely related *Pseudomonas* species. The obtained results (Fig. S3) confirmed the separation of the analysed strains from each other and from their phylogenetically closest *Pseudomonas* species.

Repetitive sequence-based PCR (rep-PCR) fingerprinting with the REP and ERIC primers and automated ribotyping with *EcoRI* restriction endonuclease were applied for additional genotypic characterization of the isolates. Both, REP-PCR primer pair REP1R-I (5'-IIICGICGICATCIGGC-3') and REP2-I (5'-IIICGNCNCATCNGGC-3') and ERIC-PCR primer pair ERIC1R (5'-ATG TAA GCT CCT GGG GAT

TCA C-3') and ERIC2 (5'-AAG TAA GTG ACT GGG GTG AGC G-3') along with their PCR protocols were described by Versalovic et al. [40]. The Rep-PCR fingerprinting procedure and cluster analysis of obtained fingerprints were performed as previously described by Gevers et al. [41] with a minor modification described by Švec et al. [42]. The automatic ribotyping was performed using the RiboPrinter Microbial Characterization System (DuPont Qualicon) in accordance with the manufacturer's instructions. Numerical analyses and dendrogram reconstruction were done using BioNumerics software (version 7.6, Applied Maths). The ribotype patterns were imported into the BioNumerics software using the load samples import script provided by the manufacturer. Fingerprint profiles acquired by all three techniques differentiated strains HJ/4^T and SJ/9/1^T from each other and separated them from the type strains of the phylogenetically closest species (Fig. S4) in full agreement with the results obtained with the aforementioned molecular methods.

For cellular fatty acid analysis, both strains (HJ/4^T and SJ/9/1^T) were grown on tryptic soy broth agar (BD) at 30±2 °C for 24 h until bacterial communities reached the late-exponential stage of growth according to the four-quadrant streak method [43]. Reference strains of closely related *Pseudomonas* species, namely *P. brenneri* CCM 7517^T, *P. migulae* CCM 4843^T, *P. proteolytica* CCM 7690^T and *P. yamanorum* DSM 26522^T, were cultured in parallel under the same conditions for comparative purposes. Extraction and subsequent analysis of fatty acid methyl esters was performed using an Agilent 7890B gas chromatograph according to the standard protocol of the Sherlock MIDI Identification System (version 6.2; RTSBA 6.21 database). The predominant fatty acids (≥10 %) of HJ/4^T and SJ/9/1^T were C_{16:0}, summed feature 3 (C_{16:1} ω7c/C_{16:1} ω6c) and summed feature 8 (C_{18:1} ω7c/C_{18:1} iso ω6c), and corresponded to the fatty acids found in closely related *Pseudomonas* species analysed along with the investigated strains (Table S1). Both strains, HJ/4^T and SJ/9/1^T, contained C_{10:0} 3OH, C_{12:0} and C_{12:0} corresponding to the description of the genus *Pseudomonas* [1]. Additionally, both analysed strains shared a common characteristic feature, higher amounts of C_{17:0} cyclo, allowing their differentiation from other closely related species.

The extraction of quinones and polar lipids was done according to an integrated method described by Minnikin et al. [44]. The purified menaquinone mixtures were separated by reversed-phase column in an HPLC (1260 Infinity, Agilent Technology). Methanol-isopropyl ether (4:1, v/v) was used as a mobile phase with a flow rate of 1 ml min⁻¹. The column temperature was set to 45 °C. The sample volume injected was 10 μl and monitored at 270 nm. The HPLC method used was as described by Tamaoka [45]. Both analysed strains revealed menaquinone 7 as the predominant respiratory quinone. The abovementioned extract was also used for polar lipids analysis by two-dimensional TLC. The solvent system used for the first dimension of TLC was chloroform:methanol:water (65:25:4, v/v/v) and for the second dimension it was chloroform:acetic acid:methanol:water (80:15:12:4, v/v/v/v) [46]. Total lipids were detected by spraying the TLC plate with molybdatophosphoric acid reagent, phospholipids were detected by spraying

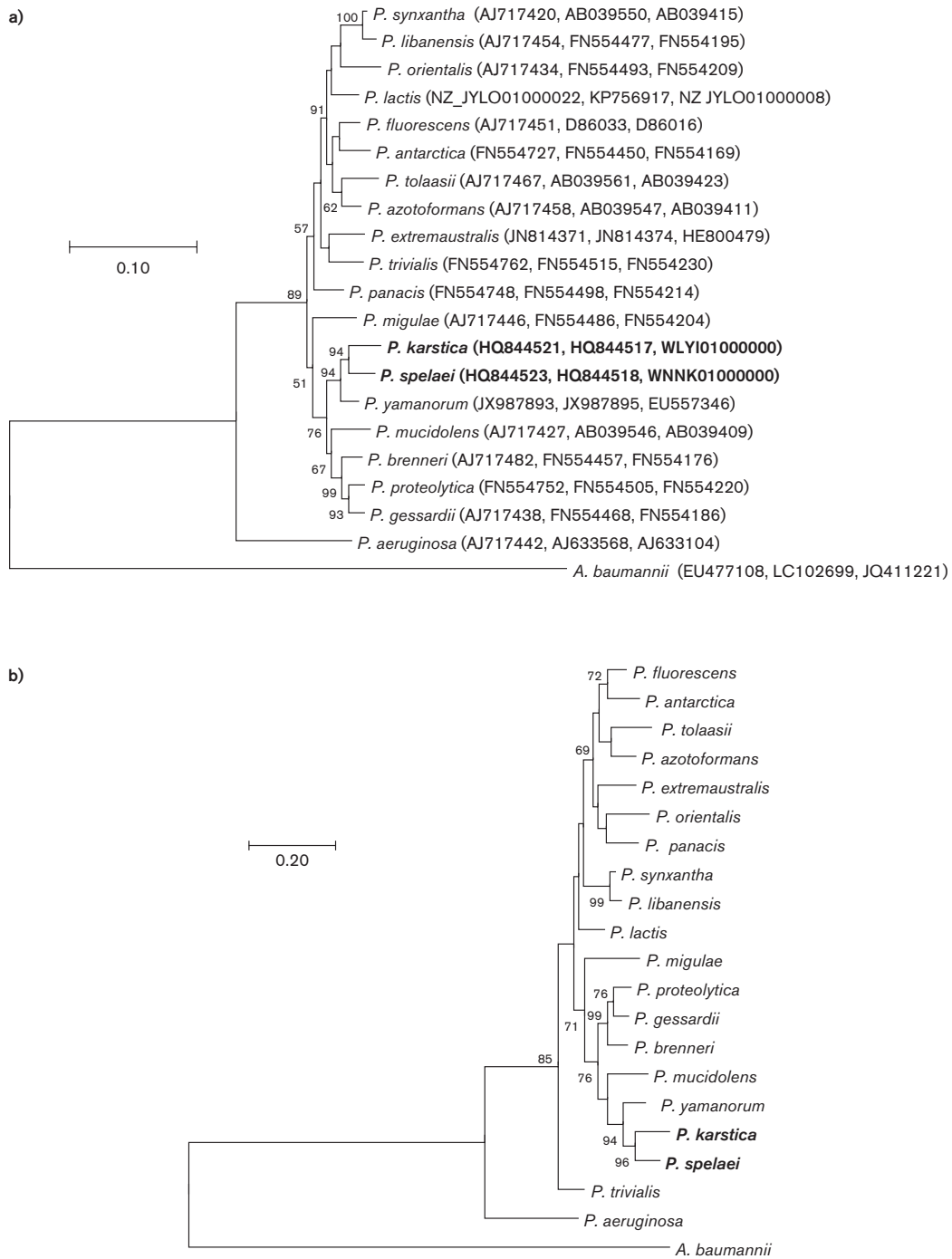


Fig. 1. (a) Maximum-likelihood tree reconstructed using concatenated partial gene sequences of the *rpoB*, *rpoD* and *gyrB* housekeeping genes showing the relationships of strains HJ/4^T and SJ/9/1^T and phylogenetically closest *Pseudomonas* species. The evolutionary distances were computed using Kimura's two-parameter method [63] and are in the units of the number of base substitutions per site. The tree with the highest log-likelihood is shown and bootstrap probability values (percentages of 1000 tree replications) greater than 50% are shown at the branch points. The tree is drawn to scale, with branch lengths measured in the number of substitutions per site. There were 2305 positions in the final dataset. GenBank accession numbers of the *rpoB*, *rpoD* and *gyrB* sequences, respectively, are given in parentheses. (b) Maximum-likelihood tree reconstructed using concatenated partial amino acid sequences of proteins RpoB, RpoD and GyrB, showing the relationships of strains HJ/4^T and SJ/9/1^T and phylogenetically closest *Pseudomonas* species. Bootstrap probability values (percentages of 1000 tree replications) greater than 50% are shown at the branch points. The evolutionary distances are in the units of the number of amino acid substitutions per site. There were 642 amino acid positions in the final dataset. *Acinetobacter baumannii* was used as an outgroup in both analyses. Bar, 0.1 substitutions per position.

Table 1. Comparison of HJ/4^T (=CCM 7891^T) and SJ/9/1^T (=CCM 7893^T) genomes with those of the phylogenetic close *Pseudomonas* species by the Genome-to-Genome Distance Calculator (GGDC) and average nucleotide identity (ANI) analysis, and overall characteristics of genomes

dDDH, digital DNA–DNA hybridization; CI, confidence interval of the method from GGDC.

<i>Pseudomonas karstica</i> HJ/4 ^T							
Reference genome	16S rRNA gene identity (%)	dDDH (%)	CI dDDH (%)	ANI (%)	Genome size (Mb)	DNA G+C content (mol%)	RefSeq assembly accession no.
<i>P. yamanorum</i> LMG 27247 ^T	99.8	31.00	[28.6–33.5]	85.6	7.09	60.3	GCF_900105735
<i>P. brenneri</i> DSM 15294 ^T	99.7	29.70	[27.3–32.2]	85.0	5.99	60.2	GCF_007858285
<i>P. spelaei</i> SJ/9/1 ^T	99.6	35.00	[32.5–37.5]	87.8	5.76	58.9	GCF_009707515
<i>P. proteolytica</i> DSM 15321 ^T	99.5	29.60	[27.2–32.1]	84.9	6.35	60.4	GCF_007858275
<i>P. migulae</i> NBRC 103157 ^T	99.4	25.30	[23–27.8]	81.1	6.67	59.1	GCF_002091715
<i>P. gessardii</i> DSM 17152 ^T	99.2	29.80	[27.4–32.3]	85.0	6.51	60.4	GCF_001983165
<i>P. panacis</i> DSM 18529 ^T	99.2	29.00	[26.7–31.5]	84.6	6.80	61.1	GCF_007858175
<i>P. synxantha</i> NCTC 10696 ^T	99.2	28.20	[25.9–30.7]	84.0	6.84	59.6	GCF_901482615
<i>P. libanensis</i> DSM 17149 ^T	99.2	28.30	[26–30.8]	84.0	6.21	60.2	GCF_001439685
<i>P. mucidolens</i> NCTC 8068 ^T	99.1	29.30	[27–31.8]	84.7	5.85	59.1	GCF_900475945
<i>P. azotoformans</i> LMG 21611 ^T	99.0	28.80	[26.4–31.3]	84.2	6.73	61.0	GCF_900103345
<i>P. lactis</i> DSM 29167 ^T	99.0	28.30	[26–30.8]	84.0	6.73	60.0	GCF_001439845
<i>Pseudomonas spelaei</i> SJ/9/1 ^T							
Reference genome	16S rRNA gene identity (%)	dDDH (%)	CI dDDH (%)	ANI (%)	Genome size (Mb)	DNA G+C (mol%)	RefSeq assembly accession no.
<i>P. yamanorum</i> LMG 27247 ^T	99.7	32.40	[30–34.9]	86.7	7.09	60.3	GCF_900105735
<i>P. karstica</i> strain HJ/4 ^T	99.6	35.00	[32.5–37.5]	87.8	6.57	59.3	GCF_009724245
<i>P. brenneri</i> DSM 15294 ^T	99.5	29.90	[27.6–32.4]	85.4	5.99	60.2	GCF_007858285
<i>P. migulae</i> NBRC 103157 ^T	99.5	25.60	[23.3–28.1]	81.5	6.67	59.1	GCF_002091715
<i>P. proteolytica</i> DSM 15321 ^T	99.2	29.90	[27.5–32.4]	85.0	6.35	60.4	GCF_007858275
<i>P. libanensis</i> DSM 17149 ^T	99.1	28.80	[26.4–31.3]	84.5	6.21	60.2	GCF_001439685
<i>P. gessardii</i> DSM 17152 ^T	99.0	30.00	[27.6–32.5]	85.5	6.51	60.4	GCF_001983165
<i>P. panacis</i> DSM 18529 ^T	99.0	29.80	[27.5–32.3]	85.0	6.80	61.1	GCF_007858175

Continued

Table 1. Continued

<i>P. mucidolens</i> NCTC 8068 ^T	99.0	29.20	[26.8–31.7]	84.7	5.85	59.1	GCF_900475945
<i>P. synxantha</i> NCTC 10696 ^T	99.0	28.70	[26.3–31.2]	84.3	6.84	59.6	GCF_901482615
<i>P. azotoformans</i> LMG 21611 ^T	98.9	29.20	[26.9–31.7]	84.7	6.73	61.0	GCF_900103345
<i>P. lactis</i> DSM 29167 ^T	98.9	28.70	[26.4–31.2]	84.3	6.73	60.0	GCF_001439845

with molybdenum blue reagent (Sigma), aminolipids and glycolipids were detected by spraying with ninhydrin (0.3% in ethanol) and α -naphthol reagents, respectively. The polar lipid profiles of strains HJ/4^T and SJ/9/1^T showed the presence of phosphatidylethanolamine, phosphatidylglycerol and an unidentified aminoglycolipid as major lipids. Minor lipids of strain HJ/4^T were an unidentified glycolipid, an unidentified glycopospholipid, an unidentified phospholipid and an unidentified lipid and those of the strain SJ/9/1^T were two unidentified glycolipids, an unidentified glycopospholipid, two unidentified phospholipids and an unidentified lipid (Fig. S5). These results are in agreement with the polar lipid composition of other pseudomonads. Phosphatidylethanolamine and phosphatidylglycerol were typically found in other members of the genus *Pseudomonas* [2]. The polar lipid profile of the phylogenetically closest species, *P. yamanorum* [47], revealed the presence of phosphatidylethanolamine, phosphatidylglycerol and an unidentified phospholipid. It can be differentiated from HJ/4^T and SJ/9/1^T by the presence of diphosphatidylglycerol and the absence of minor portions of an aminoglycolipid, glycolipids, a glycopospholipid and an unidentified lipid and a phospholipid.

The cultures used for the phenotypic characterization were grown for 24 h at 30 °C on trypton soya agar (TSA; Merck). Cells were stained according to the Gram-stain procedure using the Poly Stainer System (IUL Instruments) and cell morphology was noted under light microscopy using a BX53 microscope (Olympus). The KOH lysis test method [48] was used to confirm the Gram-staining results. The number and position of flagella was evaluated using negative staining electron microscopy. Samples of bacterial cultures for negative staining were suspended in a drop of distilled water. The resulting suspension was covered with a grid coated formvar film (Sigma-Aldrich) and carbon (Agar Scientific). The grid was removed from the suspension after 5 min, and the residual water was dried off with a strip of filtration paper. A drop of 2% aqueous phosphotungstic acid was placed onto the grid for a few seconds, then the excess stain was dried off with filtration paper. Sections prepared in this way were observed under an electron microscope Philips 208s Morgagni (FEI) at $\times 7500$ magnification and an accelerating voltage of 80 kV (Fig. S6).

The basic phenotyping was performed using the following conventional tube and plate tests relevant for Gram-negative

rods: glucose oxidation and fermentation (OF test) [49], fluorescein production on King B medium [50]; oxidase (OXItest; Erba-Lachema) and catalase (ID Color Catalase; bioMérieux) production, O-nitrophenyl- β -D-galactopyranoside (ONPG) test [51], Simmons citrate [52], arginine dihydrolase, lysine and ornithine decarboxylase [53], reduction of nitrates and nitrites [52]; hydrolysis of DNA (CM321; Oxoid), aesculin [52], Tween 80, gelatin [54], tyrosine, casein [55] and starch [52]; production of urease [56], lecithinase (egg yolk reaction) [57] and H₂S on triple sugar iron medium [52], utilization of acetamide [58] and sodium malonate [59], acid production from D-fructose, D-xylose, D-glucose, D-mannitol and maltose [60]. Bacterial growth was tested on TSA (Oxoid), nutrient agar CM3 (Oxoid), plate count agar (Oxoid), Reasoner's 2A agar (Oxoid), brain heart infusion agar (Oxoid), MacConkey agar (Hi-Media) and Columbia blood agar base (Oxoid) with 5% sheep blood. The temperature range for growth (0, 1, 3, 4, 22, 30, 35, 37 and 42 °C) and NaCl concentration tolerance (0.5, 1, 2, 3, 4, 5 and 6%, w/v) were tested on TSA adjusted accordingly. The pH range tolerance was tested in tryptone soya broth (Oxoid) adjusted to pH 3.0–10.0 (at intervals of 1.0 pH unit) using the buffer system 0.1 M KH₂PO₄/0.1 M NaOH. Motility was observed in glucose oxidation tubes. Additional phenotypic features were characterized using the Biolog GEN III MicroPlate (Biolog) and API ZYM kits (bioMérieux) according to the manufacturers' instructions. Biolog results were read with a Biolog MicroStation system (MicroLog3 4.20.05) after 24 h incubation at 25 °C.

The results of phenotypic characterization are given in the species descriptions. The key physiological and biochemical tests allowing phenotypic differentiation of the studied strains from closely related species are listed in Table 2.

Antibiotic susceptibility testing was carried out using the MIKROLATEST MIC NEFERM kit according to the manufacturer's instructions (Erba Lachema). The kit was designed for antibiotic susceptibility testing of non-fermentative Gram-negative bacteria and included ampicillin/sulbactam, piperacillin, piperacillin/tazobactam, ceftazidime, aztreonam, meropenem, gentamicin, amikacin, colistin, ciprofloxacin, tigecycline and trimethoprim/sulfamethoxazole in eight different concentrations relevant for individual antibiotics. The clinical minimum inhibitory concentration breakpoints of antibiotics were determined according to EUCAST [61] and CLSI [62] standards. The strain HJ/4^T was susceptible to

Table 2. Phenotypic traits differentiating strains HJ/4^T and SJ/9/1^T from type strains of phylogenetically closely related *Pseudomonas* species

Strains: 1, HJ/4^T; 2, SJ/9/1^T; 3, *Pseudomonas migulae* CCM 4843^T; 4, *Pseudomonas brenneri* CCM 7517^T; 5, *Pseudomonas proteolytica* CCM 7690^T; 6, *Pseudomonas yamanorum* DSM 26522^T; +, positive; -, negative; all data were obtained in this study.

	1	2	3	4	5	6
OF oxidation test	+	+	+	-	+	+
Nitrite reduction	-	-	-	+	+	-
Hydrolysis of:						
Gelatin	+	+	-	+	+	+
Tween 80	+	+	-	+	+	-
Lecithin	+	+	-	+	+	+
Casein	+	+	-	+	+	+
DNA	-	-	-	-	-	+
Assimilation of (GEN III, Biolog):						
N-Acetyl-D-glucosamine	-	+	-	-	-	+
D-Aspartic acid	+	-	-	-	-	-
L-Rhamnose	+	-	-	+	+	+
Quinic acid	-	+	+	+	+	+
p-Hydroxy-phenylacetic acid	-	-	-	+	+	+

ceftazidime (8 mg ml⁻¹), meropenem (2 mg ml⁻¹), gentamicin (1 mg ml⁻¹), amikacin (1 mg ml⁻¹), colistin (2 mg ml⁻¹) and ciprofloxacin (0.06 mg ml⁻¹) according to both EUCAST and CLSI. The strain was resistant to aztreonam (growth in all dilutions) according to both EUCAST and CLSI, and resistant to piperacillin (32 mg ml⁻¹) and piperacillin/tazobactam (64/4 mg ml⁻¹) according to EUCAST but intermediate according to CLSI. The MICs not defined in EUCAST and CLSI were 8 mg ml⁻¹ for tigecycline and 2/38 mg ml⁻¹ for trimethoprim/sulfamethoxazole and the growth was spotted in all ampicillin/sulbactam dilutions, i.e. at the concentration of 128/64 mg ml⁻¹. Strain SJ/9/1^T was susceptible to piperacillin (4 mg ml⁻¹), piperacillin/tazobactam (4/4 mg ml⁻¹), ceftazidime (8 mg ml⁻¹), meropenem (0.5 mg ml⁻¹), gentamicin (0.25 mg ml⁻¹), amikacin (0.5 mg/ml) and ciprofloxacin (0.06 mg ml⁻¹) according to EUCAST and CLSI as well. The resistance was observed for aztreonam (growth in all dilutions) and colistin (16 mg ml⁻¹) according to both EUCAST and CLSI. The MICs not defined in EUCAST and CLSI were 1 mg ml⁻¹ for tigecycline and 0.25/4.75 mg ml⁻¹ for trimethoprim/sulfamethoxazole and the growth was spotted in all ampicillin/sulbactam dilutions, i.e. at the concentration of 128/64 mg ml⁻¹.

The phylogenetic, genomic, chemotaxonomic, physiological and biochemical data obtained in this study showed that the analysed strains originating from moonmilk samples represent two novel species within the genus *Pseudomonas*

for which the names *Pseudomonas karstica* sp. nov. and *Pseudomonas spelaei* sp. nov. are proposed.

DESCRIPTION OF *PSEUDOMONAS KARSTICA* SP. NOV.

Pseudomonas karstica (kar.sti'ca. N.L. n. *karstum*, karst, geological formation shaped by the dissolution of a layer or layers of soluble bedrock; L. fem. suff. *-ica*, suffix used with the sense of pertaining to; N.L. fem. adj. *karstica*, pertaining to karst, isolated from the calcite moonmilk in The Moravian Karst).

Cells are Gram-stain-negative short rods and motile by a single polar flagellum. Colonies grown on TSA medium are smooth with regular margins and 1–2 mm in diameter when cultivated at 20 °C for 48 h. Grows well on plate count agar, Reasoner's 2A agar, nutrient agar CM3, brain heart infusion agar, MacConkey agar and on Columbia agar supplemented with 5% sheep blood with haemolysis and produces fluorescent pigment on King B medium. Growth occurs in the temperature range of 0–30 °C, in the presence of 0.5–3% NaCl and at a pH ranging from pH 4 to 9. Oxidase- and catalase-positive with oxidative but not fermentative metabolism observed with the OF test. Positive results are found for utilization of Simmons citrate and sodium malonate, production of arginine dihydrolase, hydrolysis of tyrosine, casein and lecithin (weak), and acid production from fructose, glucose, mannitol and xylose, while negative for reduction of nitrate and nitrite, utilization of acetamide, production of H₂S, lysine and ornithine decarboxylase, hydrolysis of aesculin, starch, gelatin, Tween 80, urea, DNA and ONPG, and acid production from maltose.

Enzymatic characterization by the API ZYM kit reveals positive tests for the production of esterase lipase (C 8), leucine arylamidase, and acid phosphatase, weak production of alkaline phosphatase, esterase (C 4), valine arylamidase and naphthol-AS-BI-phosphohydrolase, and negative test results for the production of lipase (C 14), cystine arylamidase, trypsin, α -chymotrypsin, α -galactosidase, β -galactosidase, β -glucuronidase, α -glucosidase, β -glucosidase, *N*-acetyl- β -glucosaminidase, α -mannosidase and α -fucosidase.

Phenotype characterization using Biolog GEN III Micro-Plate test panels shows positive reactions for α -D-glucose, D-galactose, D-fucose, L-rhamnose, D-aspartic acid, L-aspartic acid, L-glutamic acid, L-serine, D-galacturonic acid, L-galactonic acid lactone, D-gluconic acid, D-glucuronic acid, glucuronamide, mucic acid, citric acid, L-malic acid, Tween 40, acetic acid, pH 6, 1% sodium lactate, fusidic acid, D-serine, troleandomycin, rifamycin SV, lincomycin, vancomycin, tetrazolium violet, tetrazolium blue and aztreonam; negative reactions for dextrin, maltose, cellobiose, gentiobiose, sucrose, turanose, stachyose, raffinose, lactose, melibiose, methyl β -D-glucoside, D-salicin, *N*-acetyl-D-glucosamine, *N*-acetyl- β -D-mannosamine, *N*-acetyl-D-galactosamine, *N*-acetyl neuraminic acid, 3-methyl glucose, L-fucose, D-sorbitol, D-glucose-6-PO₄, gelatin, glycyl-L-proline,

L-arginine, L-pyroglytamic acid, pectin, quinic acid, *p*-hydroxy-phenylacetic acid, methyl pyruvate, D-lactic acid methyl ester, α -keto-glutaric acid, D-malic acid, bromo-succinic acid, α -hydroxy-butyrac acid, β -hydroxy-D,L-butyrac acid, α -keto-butyrac acid, acetoacetic acid, propionic acid, formic acid, pH 5, 4% and 8% NaCl, minocycline, nalidixic acid, lithium chloride, potassium tellurite, sodium butyrate, and sodium bromate and borderline reactions for trehalose, D-mannose, D-fructose, inosine, D-mannitol, D-arabitol, myo-inositol, glycerol, D-fructose-6-PO₄, D-serine, L-alanine, L-histidine, D-saccharic acid, L-lactic acid, γ -amino-butyrac acid, 1% NaCl, guanidine HCl and niaproof 4.

The major fatty acids are C_{16:0}, summed feature 3 (C_{16:1} ω 7c/C_{16:1} ω 6c) and summed feature 8 (C_{18:1} ω 7c/C_{18:1} iso ω 6c). The quinone system contains predominantly menaquinone 7 and the predominant polar lipids are phosphatidylethanolamine, phosphatidylglycerol and an unidentified aminoglycolipid.

The type strain, HJ/4^T (=CCM 7891^T=LMG 27930^T), was isolated from a moonmilk sample obtained from the wall of the ‘Horní v chobotu’ cave (The Moravian Karst, Czech Republic, 49° 21′ 50″ N, 16° 42′ 50″ E). The genomic DNA G+C content of the type strain is 58.9 mol%, and the genome size is approximately 5.76 Mb. The GenBank/ENA/DDBJ accession numbers for the 16S rRNA, *rpoB* and *rpoD* gene sequences of *Pseudomonas karstica* HJ/4^T are HQ844524, HQ844521 and HQ844517. The whole-genome shotgun projects have been deposited in GenBank/ENA/DDBJ under the accession number WLYI00000000; the version described in this paper is WLYI01000000.

DESCRIPTION OF *PSEUDOMONAS SPELAEI* SP. NOV.

Pseudomonas spelaei (spe.lae'i. L. gen. n. *spelaei* of a cavern).

Cells are Gram-stain-negative short rods and motile by a single polar flagellum. Colonies grown on TSA medium are smooth with regular margins and 1–2 mm in diameter when cultivated at 20 °C for 48 h. Grows well on plate count agar, Reasoner's 2A agar, nutrient agar CM3, brain heart infusion agar, MacConkey agar and on Columbia agar supplemented with 5% sheep blood with haemolysis and produces fluorescent pigment on King B medium. Growth occurs in the temperature range of 0–30 °C, in the presence of 0.5–3% NaCl and at a pH ranging from pH 4 to 9. Oxidase- and catalase-positive with oxidative but not fermentative metabolism observed with the OF test. Positive results are found for utilization of Simmons citrate and sodium malonate, production of arginine dihydrolase, hydrolysis of tyrosine, casein, gelatine, Tween 80 and lecithin, and acid production from fructose (weak), glucose, mannitol (weak) and xylose while negative for reduction of nitrate and nitrite, utilization of acetamide, production of H₂S, lysine and ornithine decarboxylase, hydrolysis of aesculin, starch, urea, DNA and ONPG, and acid production from maltose.

The enzymatic characterization by API ZYM kit reveals positive tests for the production of alkaline phosphatase,

esterase (C 4), esterase lipase (C 8), leucine arylamidase, valine arylamidase, acid phosphatase and naphthol-AS-BI-phosphohydrolase, weak production of trypsin, but negative test results for the production of lipase (C 14), cystine arylamidase, α -chymotrypsin, α -galactosidase, β -galactosidase, β -glucuronidase, α -glucosidase, β -glucosidase, *N*-acetyl- β -glucosaminidase, α -mannosidase and α -fucosidase.

Phenotype characterization using Biolog GEN III MicroPlate test panels showed positive reactions for trehalose, *N*-acetyl-D-glucosamine, α -D-glucose, D-mannose, D-fructose, D-galactose, D-fucose, L-fucose, inosine, D-mannitol, D-arabitol, myo-inositol, glycerol, D-fructose-6-PO₄, D-serine, L-alanine, L-arginine, L-aspartic acid, L-glutamic acid, L-histidine, L-serine, D-gluconic acid, glucuronamide, mucic acid, quinic acid, D-saccharic acid, L-lactic acid, citric acid, α -keto-glutaric acid, L-malic acid, bromo-succinic acid, Tween 40, γ -amino-butyrac acid, acetic acid, pH 6, 1% NaCl, 1% sodium lactate, D-serine, troleandomycin, rifamycin SV, lincomycin, niaproof 4, vancomycin, tetrazolium violet, tetrazolium blue and aztreonam; negative reactions for dextrin, maltose, cellobiose, gentiobiose, sucrose, turanose, stachyose, raffinose, lactose, melibiose, methyl β -D-glucoside, D-salicin, *N*-acetyl- β -D-mannosamine, *N*-acetyl-D-galactosamine, *N*-acetyl neuraminic acid, 3-methyl glucose, L-rhamnose, D-glucose-6-PO₄, D-aspartic acid, gelatine, glycyl-L-proline, pectin, D-glucuronic acid, *p*-hydroxy-phenylacetic acid, D-lactic acid methyl ester, α -hydroxy-butyrac acid, α -keto-butyrac acid, acetoacetic acid, propionic acid, 4% and 8% NaCl, fusidic acid, minocycline, guanidine HCl, nalidixic acid, lithium chloride, sodium butyrate, and sodium bromate, and borderline reactions for D-sorbitol, L-pyroglytamic acid, D-galacturonic acid, L-galactonic acid lactone, methyl pyruvate, D-malic acid, β -hydroxy-D,L-butyrac acid, formic acid, pH 5 and potassium tellurite.

The major fatty acids are C_{16:0}, summed feature 3 (C_{16:1} ω 7c/C_{16:1} ω 6c) and summed feature 8 (C_{18:1} ω 7c/C_{18:1} iso ω 6c). The quinone system contains predominantly menaquinone 7 and the predominant polar lipids are phosphatidylethanolamine, phosphatidylglycerol and an unidentified aminoglycolipid.

The type strain, SJ/9/1^T (=CCM 7893^T=LMG 27931^T), was isolated from a moonmilk sample obtained from the walls of the ‘Suchožlebská zazděná’ cave (The Moravian Karst, Czech Republic, 49° 21′ 42″ N, 16° 43′ 2″ E). The genomic DNA G+C content of the type strain is 59.3 mol%, and the genome size is approximately 6.57 Mb. The GenBank/ENA/DDBJ accession numbers for the 16S rRNA, *rpoB* and *rpoD* gene sequences of *Pseudomonas spelaei* SJ/9/1^T are HQ844525, HQ844523 and HQ844518, respectively. The whole-genome shotgun projects have been deposited in GenBank/ENA/DDBJ under the accession number WNNK00000000; the version described in this paper is WNNK01000000.

Funding information

This work was funded by the Czech Collection of Microorganisms (Masaryk University, Brno) and partially supported by the Ministry of Education, Youth and Sports of the Czech Republic projects LM2018121,

CZ.02.1.01/0.0/0.0/18_046/0015975 and CZ.02.1.01/0.0/0.0/16_013/001761.

Acknowledgements

We acknowledge Denisa Poullová (Department of Geological Sciences, Masaryk University) for help with the moonmilk sampling, Eva Staňková and Jana Bajarová (Czech Collection of Microorganisms, Masaryk University) for excellent technical assistance, and Dr. Pavel Kulich (Veterinary Research Institute, Department of Chemistry and Toxicology, Laboratory of Electron Microscopy) for transmission electron microscopy. Dr. Jean Euzéby is gratefully acknowledged for nomenclature revisions. S. K. is a beneficiary of Brno PhD talent financial aid.

Conflicts of interest

The authors declare that there are no conflicts of interest.

References

- Palleroni NJ, Genus I. *Pseudomonas* Migula 1894, 237AL (Nom. Cons., Opin. 5 of the Jud. Comm. 1952, 121). In: Garrity GM, Brenner DJ, Krieg NR, Staley JT (editors). *Bergey's Manual of Systematic Bacteriology, Volume 2, The Proteobacteria, Part B The Gammaproteobacteria*, 2015. New York: Springer. pp. 323–379.
- Moore ERB, Tindall BJ, Martins Dos Santos VAP, Pieper DH, Ramos J-L et al. Nonmedical: *Pseudomonas*. In: Dworkin M, Falkow S, Rosenberg E, Schleifer KH, Stackebrandt E et al. (editors). *The Prokaryotes: A Handbook on the Biology of Bacteria, Third Edition, Volume 6, Proteobacteria: Gamma Subclass*. New York, USA: Springer; 2006. pp. 646–703.
- Høiby N, Ciofu O, Bjarnsholt T. *Pseudomonas*. In: Jorgensen JH, Pfaller MA, Carroll KC, Landry ML, Funke G et al. (editors). *Manual of Clinical Microbiology*. Washington, USA: ASM Press; 2015. pp. 773–790.
- Parte AC. LPSN--list of prokaryotic names with standing in nomenclature. *Nucleic Acids Res* 2014;42:D613–D616.
- Cañaveras JC, Cuezva S, Sanchez-Moral S, Lario J, Laiz L et al. On the origin of fiber calcite crystals in moonmilk deposits. *Naturwissenschaften* 2006;93:27–32.
- Baskar S, Baskar R, Routh J. Biogenic evidences of Moonmilk deposition in the Mawmluh cave, Meghalaya, India. *Geomicrobiol J* 2011;28:252–265.
- Castanier S, Le Métayer-Levrel G, Perthuisot J-P. Ca-carbonates precipitation and limestone genesis — the microbiogeologist point of view. *Sediment Geol* 1999;126:9–23.
- Jones B, Kahle CF. Morphology, relationship, and origin of fiber and dendrite calcite crystals. *J Sediment Petrol* 1993;63:1018–1031.
- Richter DK, Immenhauser A, Neuser RD. Electron Backscatter diffraction documents randomly orientated c-axes in moonmilk calcite fibres: evidence for biologically induced precipitation. *Sedimentology* 2008;55:487–497.
- Maciejewska M, Adam D, Naômé A, Martinet L, Tenconi E et al. Assessment of the Potential Role of *Streptomyces* in Cave Moonmilk Formation. *Front Microbiol* 2017;8:1181.
- Curry M, Boston P, Spilde M, Baichtal J, Campbell A. Cottonballs, a unique subaqueous moonmilk, and abundant subaerial moonmilk in cataract cave, Tongass national forest, Alaska. *Int J Speleol* 2009;38:111–128.
- Reitschuler C, Spötl C, Hofmann K, Wagner AO, Illmer P. Archaeal distribution in moonmilk deposits from alpine caves and their ecophysiological potential. *Microb Ecol* 2016;71:686–699.
- Summers Engel A, Paoletti M, Beggio M, Dorigo L, Pamio A et al. Comparative microbial community composition from secondary carbonate (moonmilk) deposits: implications for the *Cansiliella servadeii* cave hygropetric food web. *Int J Speleol* 2013;42:181–192.
- Reitschuler C, Lins P, Schwarzenauer T, Spötl C, Wagner AO et al. New undescribed lineages of non-extremophilic archaea form a homogeneous and dominant element within alpine moonmilk microbiomes. *Geomicrobiol J* 2015;32:890–902.
- Rooney DC, Hutchens E, Clipson N, Baldini J, McDermott F. Microbial community diversity of moonmilk deposits at Ballynamindra cave, Co. Waterford, Ireland. *Microb Ecol* 2010;60:753–761.
- Jones D, Pell PA, Sneath PHA. Maintenance of bacteria on glass beads at -60 °C to -76 °C. In: Kirsop BE, Doyle A (editors). *Maintenance of Microorganism and Cultured Cells. A Manual of Laboratory Methods*. London: Academic Press; 1991. pp. 45–50.
- Mariani BD, Levine MJ, Booth RE, Tuan RS. Development of a novel, rapid processing protocol for polymerase chain reaction-based detection of bacterial infections in synovial fluids. *Mol Biotechnol* 1995;4:227–237.
- Wiedmann M, Weilmeier D, Dineen SS, Ralyea R, Boor KJ. Molecular and phenotypic characterization of *Pseudomonas* spp. isolated from milk. *Appl Environ Microbiol* 2000;66:2085–2095.
- Nadkarni MA, Martin FE, Jacques NA, Hunter N. Determination of bacterial load by real-time PCR using a broad-range (universal) probe and primers set. *Microbiology* 2002;148:257–266.
- Thompson JD, Higgins DG, Gibson TJ. CLUSTAL W: improving the sensitivity of progressive multiple sequence alignment through sequence weighting, position-specific gap penalties and weight matrix choice. *Nucleic Acids Res* 1994;22:4673–4680.
- Yoon S-H, Ha S-M, Kwon S, Lim J, Kim Y et al. Introducing EzBioCloud: a taxonomically united database of 16S rRNA gene sequences and whole-genome assemblies. *Int J Syst Evol Microbiol* 2017;67:1613–1617.
- Kumar S, Stecher G, Tamura K. MEGA7: molecular evolutionary genetics analysis version 7.0 for bigger datasets. *Mol Biol Evol* 2016;33:1870–1874.
- Felsenstein J. Evolutionary trees from DNA sequences: a maximum likelihood approach. *J Mol Evol* 1981;17:368–376.
- Saitou N, Nei M. The neighbor-joining method: a new method for reconstructing phylogenetic trees. *Mol Biol Evol* 1987;4:406–425.
- Fitch WM. Toward defining the course of evolution: minimum change for a specific tree topology. *Syst Zool* 1971;20:406–416.
- Mulet M, Lalucat J, García-Valdés E. DNA sequence-based analysis of the *Pseudomonas* species. *Environ Microbiol* 2010;12:1513–1530.
- Mulet M, Bennisar A, Lalucat J, García-Valdés E. An *rpoD*-based PCR procedure for the identification of *Pseudomonas* species and for their detection in environmental samples. *Mol Cell Probes* 2009;23:140–147.
- Ait Tayeb L, Ageron E, Grimont F, Grimont PAD. Molecular phylogeny of the genus *Pseudomonas* based on *rpoB* sequences and application for the identification of isolates. *Res Microbiol* 2005;156:763–773.
- Andrews S. FastQC: a quality control tool for high throughput sequence data. 2019. Available online at: <https://www.bioinformatics.babraham.ac.uk/projects/fastqc>.
- Krueger F. Trim Galore: wrapper script for quality and adapter trimming. 2019. Available online at: https://www.bioinformatics.babraham.ac.uk/projects/trim_galore.
- Martin M. Cutadapt removes adapter sequences from high-throughput sequencing reads. *EMBnet J* 2011;17:10–12.
- Wick RR, Judd LM, Gorrie CL, Holt KE. Unicycler: resolving bacterial genome assemblies from short and long sequencing reads. *PLoS Comput Biol* 2017;13:e1005595.
- Bushnell B. BBMap: BBTools is a suite of bioinformatics tools for analysis of DNA and RNA sequence data. 2019. Available online at: <https://sourceforge.net/projects/bbmap>
- Lagesen K, Hallin P, Rødland EA, Staerfeldt H-H, Rognes T et al. RNAmmer: consistent and rapid annotation of ribosomal RNA genes. *Nucleic Acids Res* 2007;35:3100–3108.
- Yoon S-H, Ha S-min, Lim J, Kwon S, Chun J. A large-scale evaluation of algorithms to calculate average nucleotide identity. *Antonie van Leeuwenhoek* 2017;110:1281–1286.
- Meier-Kolthoff JP, Auch AF, Klenk H-P, Göker M. Genome sequence-based species delimitation with confidence intervals and improved distance functions. *BMC Bioinformatics* 2013;14:60.

37. Richter M, Rosselló-Móra R. Shifting the genomic gold standard for the prokaryotic species definition. *Proc Natl Acad Sci USA* 2009;106:19126–19131.
38. Meier-Kolthoff JP, Klenk H-P, Göker M. Taxonomic use of DNA G+C content and DNA-DNA hybridization in the genomic age. *Int J Syst Evol Microbiol* 2014;64:352–356.
39. Na S-I, Kim YO, Yoon S-H, Ha S-M, Baek I et al. UBCG: up-to-date bacterial core gene set and pipeline for phylogenomic tree reconstruction. *J Microbiol* 2018;56:280–285.
40. Versalovic J, Schneider M, de Bruijn FJ, Lupski JR. Genomic fingerprinting of bacteria using repetitive sequence-based polymerase chain reaction. *Methods Mol Cell Biol* 1994;5:25–40.
41. Gevers D, Huys G, Swings J. Applicability of rep-PCR fingerprinting for identification of *Lactobacillus* species. *FEMS Microbiol Lett* 2001;205:31–36.
42. Švec P, Nováková D, Žáčková L, Kukletová M, Sedláček I. Evaluation of (GTG)₅-PCR for rapid identification of *Streptococcus mutans*. *Antonie van Leeuwenhoek* 2008;94:573–579.
43. Sasser M. *Identification of Bacteria by Gas Chromatography of Cellular Fatty Acids*, MIDI Technical Note 101. Newark, DE, USA: Microbial ID, Inc; 1990.
44. Minnikin DE, O'Donnell AG, Goodfellow M, Alderson G, Athalye M et al. An integrated procedure for the extraction of bacterial isoprenoid quinones and polar lipids. *J Microbiol Methods* 1984;2:233–241.
45. Tamaoka J. Analysis of bacterial menaquinone mixtures by reverse-phase high-performance liquid chromatography. *Methods Enzymol* 1986;123:251–256.
46. Komagata K, Suzuki K-I. Lipid and Cell-Wall Analysis in Bacterial Systematics. In: Colwell RR, Grigorova R (editors). *Methods in Microbiology*, 19. Academic Press; 1988. pp. 161–207.
47. Arnau VG, Sánchez LA, Delgado OD. *Pseudomonas yamanorum* sp. nov., a psychrotolerant bacterium isolated from a subantarctic environment. *Int J Syst Evol Microbiol* 2015;65:424–431.
48. Carlone GM, Valadez MJ, Pickett MJ. Methods for distinguishing Gram-positive from Gram-negative bacteria. *J Clin Microbiol* 1982;16:1157–1159.
49. Hugh R, Leifson E. The taxonomic significance of fermentative versus oxidative metabolism of carbohydrates by various Gram negative bacteria. *J Bacteriol* 1953;66:24–26.
50. King EO, Ward MK, Raney DE. Two simple media for the demonstration of pyocyanin and fluorescein. *J Lab Clin Med* 1954;44:301–307.
51. Lowe GH. The rapid detection of lactose fermentation in paracolon organisms by the demonstration of beta-D-galactosidase. *J Med Lab Technol* 1962;19:21–25.
52. Barrow GI, Feltham RKA. *Cowan and Steel's Manual for the Identification of Medical Bacteria*, 3rd ed. Great Britain: Cambridge University Press; 1993.
53. Brooks K, Sodeman T. A rapid method for determining decarboxylase and dihydrolase activity. *J Clin Pathol* 1974;27:148–152.
54. Páčová Z, Kocur M. New medium for detection of esterase and gelatinase activity. *Zentralbl Bakteriol Mikrobiol Hyg A* 1984;258:69–73.
55. Kurup VP, Babcock JB. Use of casein, tyrosine, and hypoxanthine in the identification of nonfermentative Gram-negative bacilli. *Med Microbiol Immunol* 1979;167:71–75.
56. Christensen WB. Urea decomposition as a means of differentiating *Proteus* and paracolon cultures from each other and from *Salmonella* and *Shigella* types. *J Bacteriol* 1946;52:461–466.
57. Owens JJ. The egg yolk reaction produced by several species of bacteria. *J Appl Bacteriol* 1974;37:137–148.
58. Oberhofer TR, Rowen JW. Acetamide agar for differentiation of nonfermentative bacteria. *Appl Microbiol* 1974;28:720–721.
59. Ewing WH. *Enterobacteriaceae. Biochemical methods for group differentiation. Public Health Service Publication No 734 CDC*. Atlanta; 1960.
60. Weyant RS, Moss CW, Weaver RE, Hollis DG, Jordan JJ et al. *Identification of Unusual Pathogenic Gram-Negative Aerobic and Facultatively Anaerobic Bacteria*, 2nd edn. Baltimore, MD: Williams & Wilkins; 1996. pp. 15–16.
61. EUCAST. Breakpoint tables for interpretation of MICs and zone diameters, version 7.1. The European Committee on antimicrobial susceptibility testing. www.eucast.org 2017.
62. CLSI. Performance standards for antimicrobial susceptibility testing. Twenty-Fifth informational supplement 2015;35.
63. Kimura M. A simple method for estimating evolutionary rates of base substitutions through comparative studies of nucleotide sequences. *J Mol Evol* 1980;16:111–120.

Five reasons to publish your next article with a Microbiology Society journal

1. The Microbiology Society is a not-for-profit organization.
2. We offer fast and rigorous peer review – average time to first decision is 4–6 weeks.
3. Our journals have a global readership with subscriptions held in research institutions around the world.
4. 80% of our authors rate our submission process as 'excellent' or 'very good'.
5. Your article will be published on an interactive journal platform with advanced metrics.

Find out more and submit your article at microbiologyresearch.org.

International Journal of Systematic and Evolutionary Microbiology

Supplementary materials

***Pseudomonas karstica* sp. nov. and *Pseudomonas spelaei* sp. nov., isolated from calcite moonmilk deposits from caves**

Pavel Švec^{1,*}, Marcel Kosina¹, Michal Zeman², Pavla Holochová¹, Stanislava Králová¹, Eva Němcová³, Lenka Micenková⁴, Urvashi⁵, Vipin Gupta⁶, Utkarsh Sood⁷, Rup Lal⁷, Suresh Korpole⁵, Ivo Sedláček¹

¹Department of Experimental Biology, Czech Collection of Microorganisms, Faculty of Science, Masaryk University, Kamenice 5, 625 00 Brno, Czech Republic

²Department of Experimental Biology, Section of Genetics and Molecular Biology, Faculty of Science, Masaryk University, Kotlářská 2, 611 37 Brno, Czech Republic

³Centre for Cardiovascular Surgery and Transplantation, Pekařská 53, 656 91 Brno, Czech Republic

⁴Research Centre for Toxic Compounds in the Environment, Faculty of Science, Masaryk University, Kamenice 5, 625 00 Brno, Czech Republic

⁵Microbial Type Culture Collection and Gene Bank (MTCC), CSIR-Institute of Microbial Technology, Sector 39A, Chandigarh 160 036, India

⁶PhiXGen Pvt. Ltd.101, GH-11, Atlantis CGHS Ltd.Sector-47, Gurugram, Haryana-122001, India

⁷The Energy and Resources Institute, Lodhi Road New Delhi-110003, India

*Corresponding author:

Pavel Švec, e-mail: mpavel@sci.muni.cz

Table S1. Cellular fatty acid composition (as a percentage of the total) of strains HJ/4^T and SJ/9/1^T and the type strains of phylogenetically closely related *Pseudomonas* species.

All data were obtained in this study. Cultivation conditions used: 24h / 30±2 °C; TSBA agar (DB).

Fatty acids revealing less than 1 % are not shown. TR, trace amount (< 1 %).

Fatty acid	<i>P. karstica</i> HJ/4 ^T	<i>P. spelaei</i> SJ/9/1 ^T	<i>P. breneri</i> CCM 7517 ^T	<i>P. migulae</i> CCM 4843 ^T	<i>P. proteolytica</i> CCM 7690 ^T	<i>P. yamanorum</i> DSM 26522 ^T
C _{10:0} 3OH	3.1	3.6	3.1	3.4	2.6	2.9
C _{12:0}	1.7	3.0	2.2	3.8	2.4	2.2
C _{12:0} 2OH	4.7	4.0	4.3	3.4	4.4	4.5
C _{12:0} 3OH	3.6	3.9	3.6	3.7	3.4	3.3
C _{16:0}	34.9	41.0	34.0	33.0	32.3	36.4
C _{17:0} cyclo	4.8	6.0	TR	2.5	TR	1.5
C _{18:0}	1.4	1.2	1.0	TR	1.1	1.0
Summed Feature 3*	30.9	29.4	37.2	35.5	37.4	37.2
Summed Feature 8†	13.2	6.5	12.9	12.8	14.6	10.1

Summed Features contain two fatty acids that cannot be perfectly resolved. *Summed Feature 3 includes C_{16:1} ω7c / C_{16:1} ω6c; †Summed Feature 8 includes C_{18:1} ω7c / C_{18:1} iso ω6c.



Fig. S1. Moonmilk deposits on the "Suchožlebská zazzděná" cave wall (49°21'42"N, 16°43'2"E).

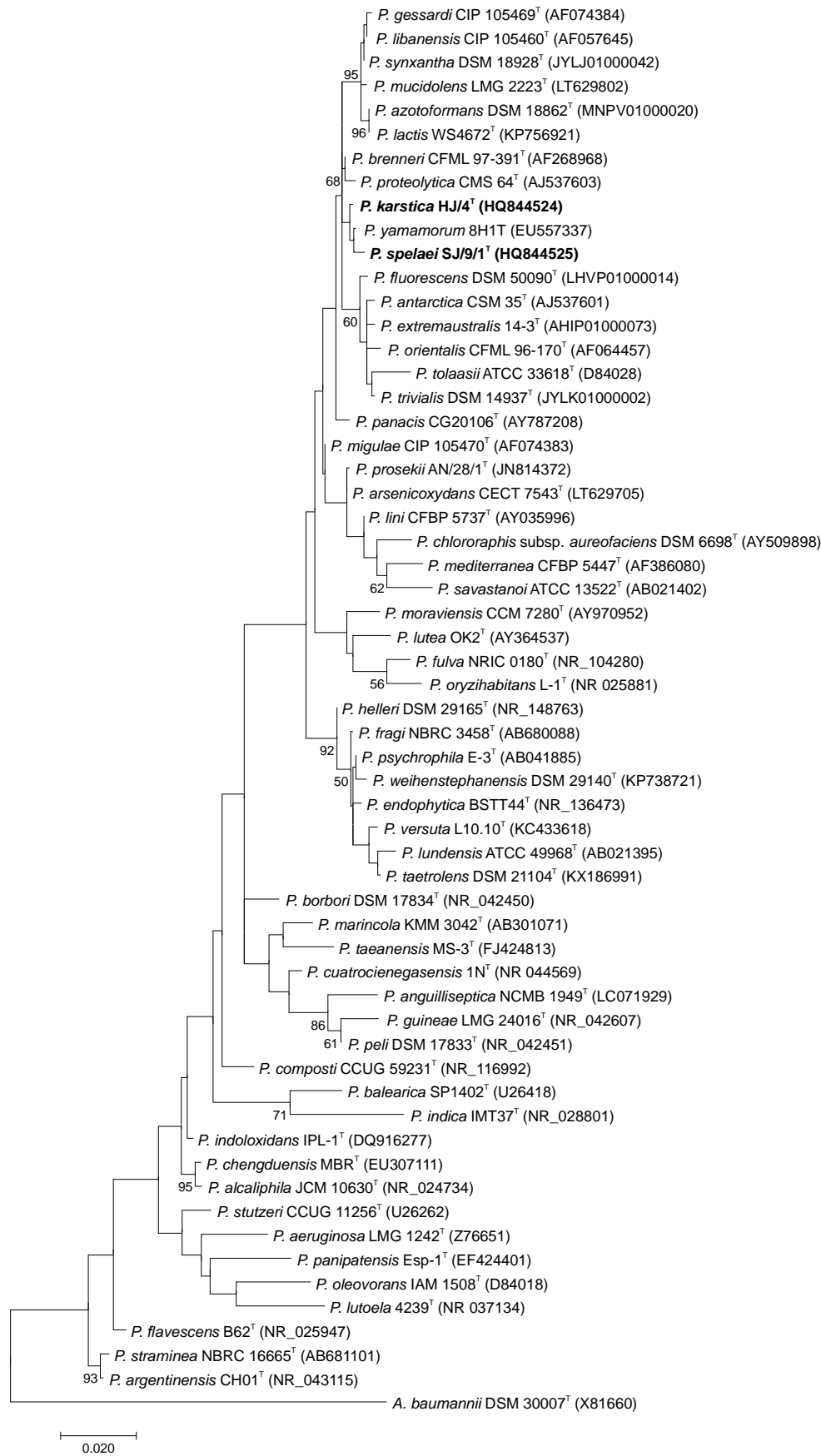


Fig. S2. Maximum likelihood tree based on the 16S rRNA gene sequences comparison showing the phylogenetic position of strains HJ/4^T, SJ/9/1^T and reference *Pseudomonas* spp. strains. The evolutionary distances were computed using the Kimura 2-parameter method and are in the units of the number of base substitutions per site. Bootstrap probability values (percentages of 1000 tree replications) greater than 50 % are shown at the branch points. All positions with less than 95 % site coverage were eliminated. *Acinetobacter baumannii* DSM 30007^T was used as an outgroup. Bar, 0.02 substitutions per nucleotide position.

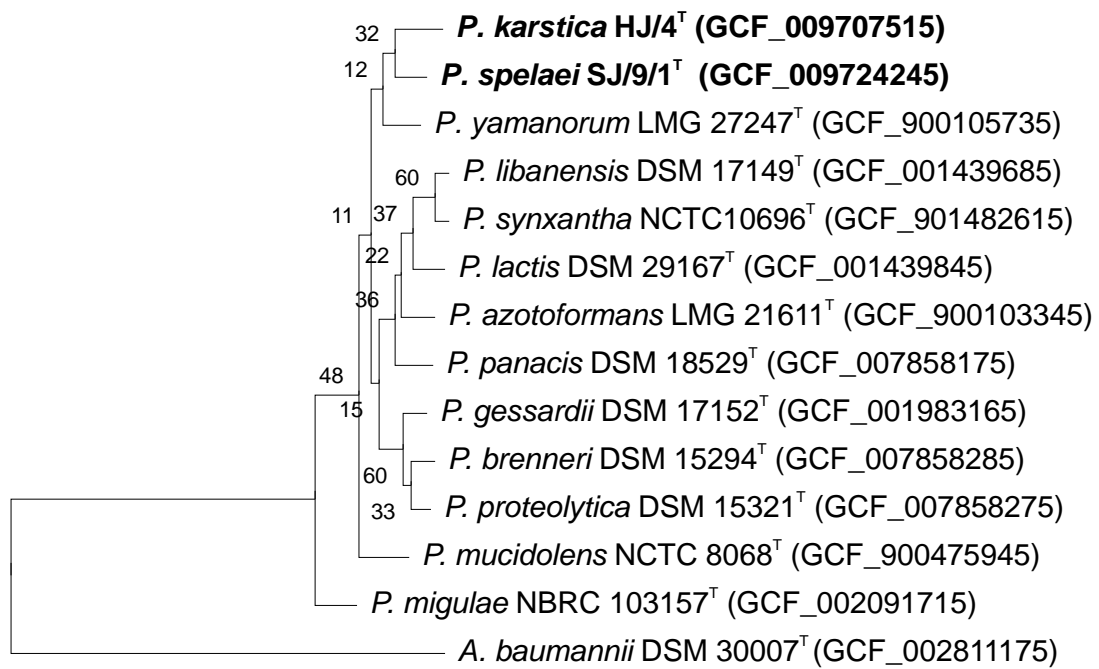
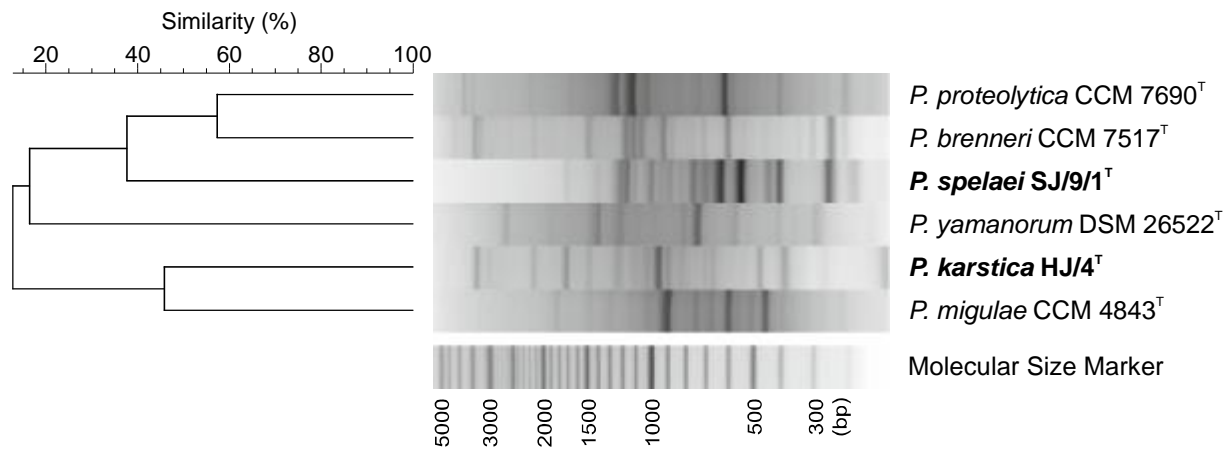
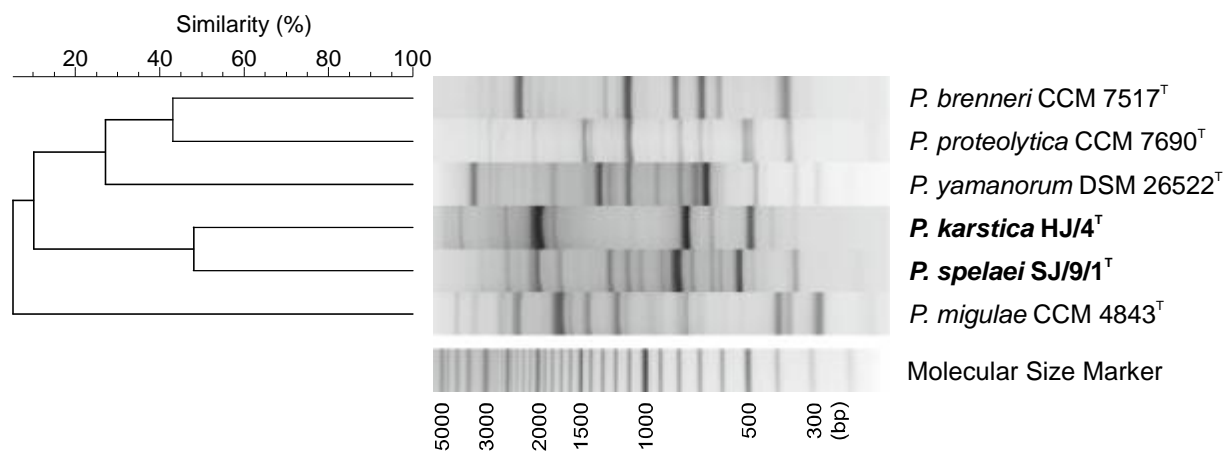


Fig. S3. Core gene set phylogenetic tree of strains HJ/4^T, SJ/9/1^T and closely related species. Phylogenetic tree was constructed using Up-to-date bacterial core gene set (UBCG; concatenated alignment of 91 core genes). A total of 89,388 nucleotide positions were used. Maximum likelihood phylogenetic tree was inferred using Fasttree v2.1.10 using GTR + CAT model. Gene support indices are given at branching points (maximal possible value is 91). *Acinetobacter baumannii* DSM 30007^T has been used as an outgroup. Assembly accession numbers are given in parentheses. Bar, 0.1 substitution per position.

a) ERIC-PCR



b) REP-PCR



c) *Eco*RI ribotyping

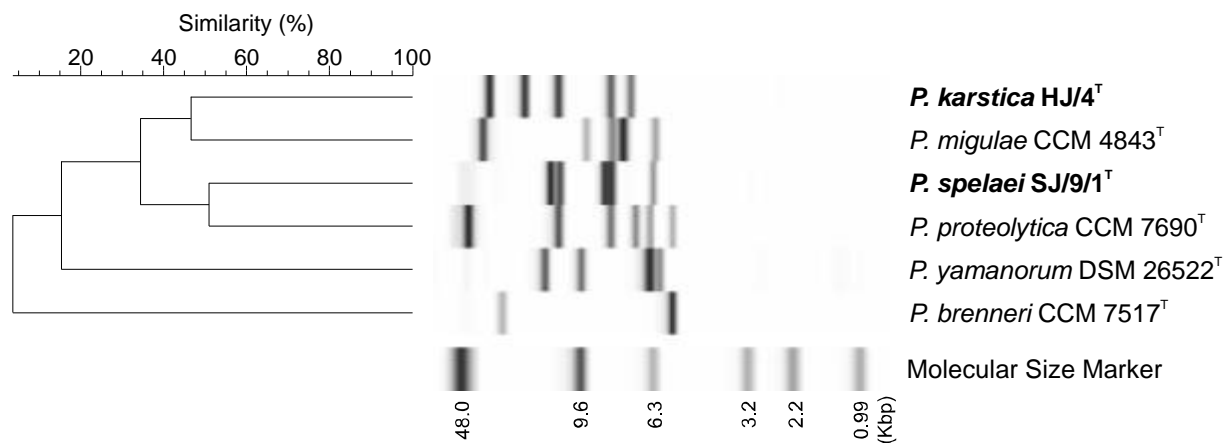


Fig. S4. Dendrograms based on cluster analysis of rep-PCR fingerprints obtained with (a) ERIC and (b) REP primers and (c) *Eco*RI ribotype patterns from strains HJ/4^T and SJ/9/1^T and the type strains of the phylogenetically closely related species. The dendrograms were calculated with Pearson's correlation coefficients with UPGMA clustering method (r , expressed as percentage similarity values).

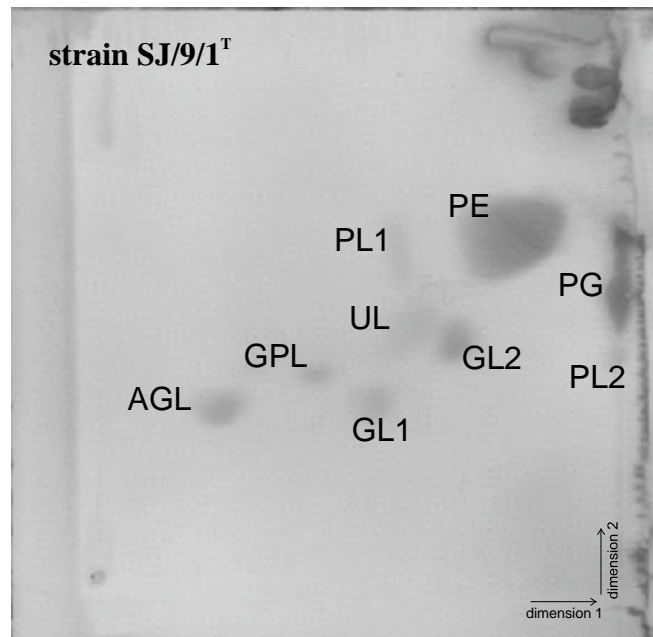
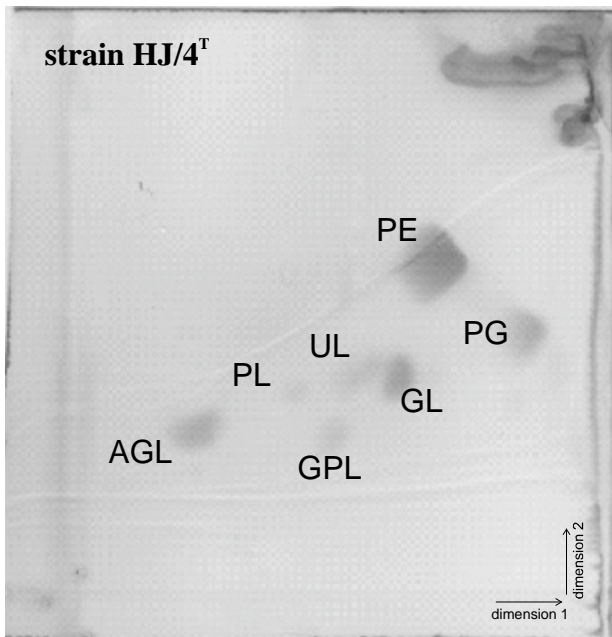
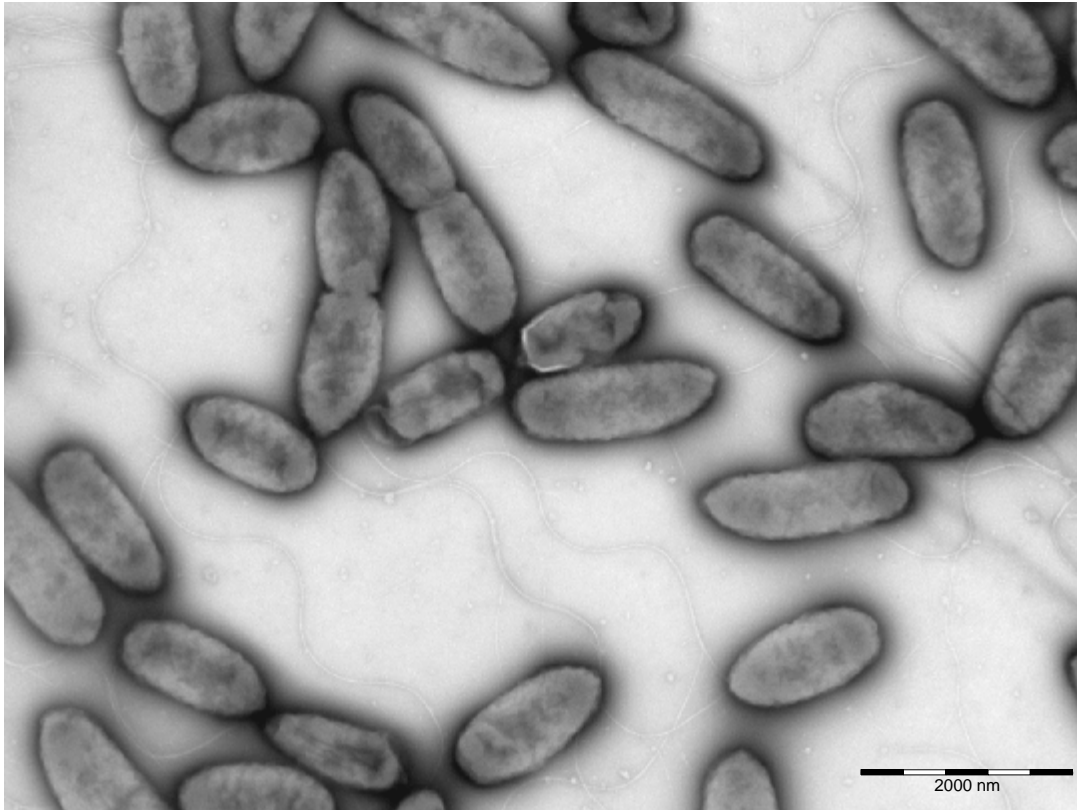


Fig. S5. Total polar lipids of the strains HJ/4^T and SJ/9/1^T after two-dimensional TLC. PE, phosphatidylethanolamine; PG, phosphatidylglycerol; AGL, unidentified aminoglycolipid; GL, unidentified glycolipid; GPL, unidentified glycophospholipid; PL, unidentified phospholipid; UL, unidentified lipid.

Pseudomonas karstica HJ/4^T



Pseudomonas spelaei SJ/9/1^T

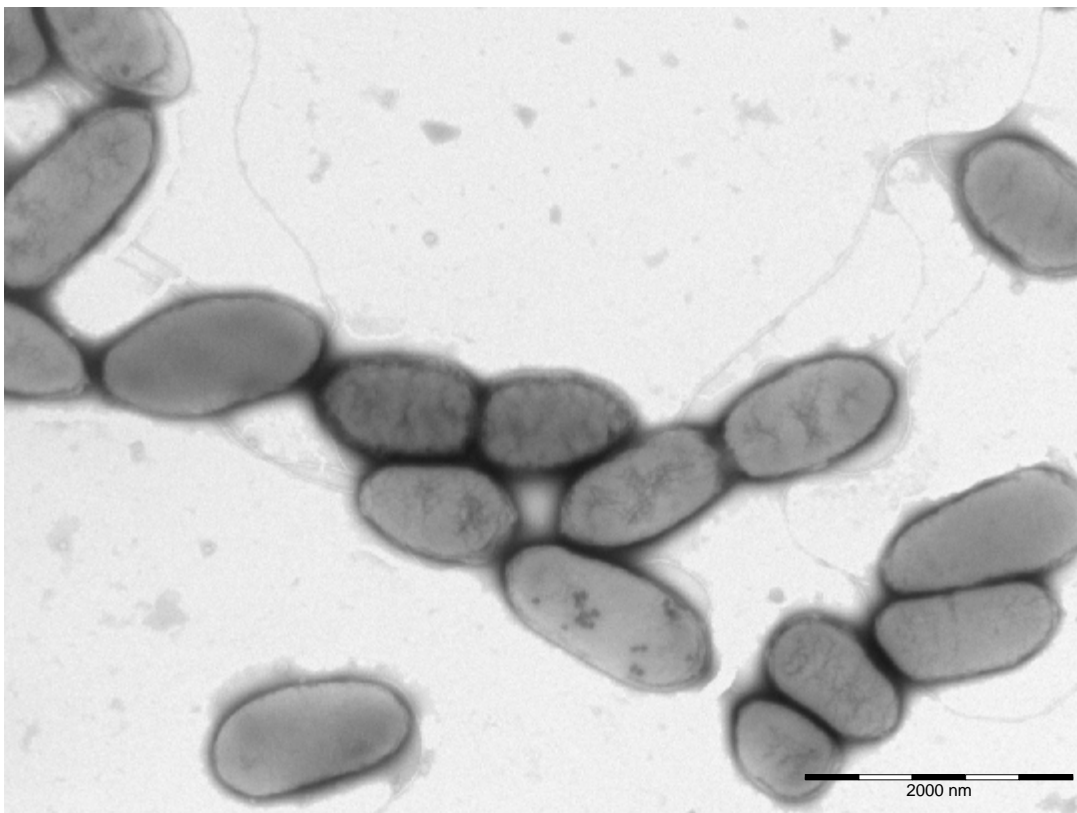


Fig. S6. Cell morphology of strains HJ/4^T and SJ/9/1^T observed using transmission electron microscopy performed with a Philips 208S Morgagni electron microscope (FEI, Czech Republic). Negative staining with 2% phosphotungstic acid. Bar represents 2000 nm (original magnification $\times 7\,500$).

Hymenobacter terrestris sp. nov. and *Hymenobacter lapidiphilus* sp. nov., isolated from regoliths in Antarctica

Ivo Sedláček^{1,*}, Roman Pantůček², Michal Zeman², Pavla Holochová¹, Ondřej Šedo³, Eva Staňková¹, Pavel Švec¹, Stanislava Králová¹, Petra Vídeňská⁴, Lenka Micenková⁴, Urvashi⁵, Suresh Korpole⁵ and Rup Lal⁶

Abstract

A group of four psychrotrophic bacterial strains was isolated on James Ross Island (Antarctica) in 2013. All isolates, originating from different soil samples, were collected from the ice-free northern part of the island. They were rod-shaped, Gram-stain-negative, and produced moderately slimy red-pink pigmented colonies on R2A agar. A polyphasic taxonomic approach based on 16S rRNA gene sequencing, whole-genome sequencing, MALDI-TOF MS, rep-PCR analyses, chemotaxonomic methods and extensive biotyping was used to clarify the taxonomic position of these isolates. Phylogenetic analysis based on 16S rRNA gene sequences showed that the isolates belonged to the genus *Hymenobacter*. The closest relative was *Hymenobacter humicola* CCM 8763^T, exhibiting 98.3 and 98.9% 16S rRNA pairwise similarity with the reference isolates P5342^T and P5252^T, respectively. Average nucleotide identity, digital DNA–DNA hybridization and core gene distances calculated from the whole-genome sequencing data confirmed that P5252^T and P5342^T represent two distinct *Hymenobacter* species. The menaquinone systems of both strains contained MK-7 as the major respiratory quinone. The predominant polar lipids for both strains were phosphatidylethanolamine and one unidentified glycolipid. The major components in the cellular fatty acid composition were summed feature 3 (C_{16:1}ω7c/C_{16:1}ω6c), C_{16:1}ω5c, summed feature 4 (anteiso-C_{17:1}B/iso-C_{17:1}I), anteiso-C_{15:0} and iso-C_{15:0} for all isolates. Based on the obtained results, two novel species are proposed, for which the names *Hymenobacter terrestris* sp. nov. (type strain P5252^T=CCM 8765^T=LMG 31495^T) and *Hymenobacter lapidiphilus* sp. nov. (type strain P5342^T=CCM 8764^T=LMG 30613^T) are suggested.

The genus *Hymenobacter* was proposed by Hirsch *et al.* [1] in 1998, who described this new genus on the basis of the psychrophilic, slowly growing bacterium *Hymenobacter roseosalivarius* isolated from continental Antarctic soils and sandstone. Later, Peeters *et al.* [2] recovered hymenobacters in high numbers in terrestrial microbial mat samples from Utsteinen nunatak, Antarctica. Over the last few years many novel hymenobacters have been discovered from different sources including cold environments, such as a glacial till

[3], glacier ice core [4, 5], karst cave soils [6, 7], permafrost in mountains [8, 9], marine sediment in the Arctic [10] and deep-sea water [11]. A few novel hymenobacters have recently been found in Antarctica as well, such as *Hymenobacter nivis* discovered from red snow [12], *Hymenobacter coccineus*, *Hymenobacter lapidarius* and *Hymenobacter glacialis* from rocks [13], *Hymenobacter rubripertinctus* from Antarctic tundra soil [14], *Hymenobacter amundsenii* from regoliths [15], and *Hymenobacter humicola* from Antarctic soils [16].

Author affiliations: ¹Department of Experimental Biology, Czech Collection of Microorganisms, Faculty of Science, Masaryk University, Kamenice 5, 625 00 Brno, Czech Republic; ²Department of Experimental Biology, Section of Genetics and Molecular Biology, Faculty of Science, Masaryk University, Kamenice 5, 625 00 Brno, Czech Republic; ³Central European Institute of Technology, Masaryk University, Kamenice 5, 625 00 Brno, Czech Republic; ⁴Research Centre for Toxic Compounds in the Environment, Faculty of Science, Masaryk University, Kamenice 5, 625 00 Brno, Czech Republic; ⁵Microbial Type Culture Collection and Gene Bank (MTCC), CSIR – Institute of Microbial Technology, Sector 39A, Chandigarh 160 036, India; ⁶The Energy and Resources Institute, Lodhi Road, New Delhi – 110003, India.

***Correspondence:** Ivo Sedláček, ivo@sci.muni.cz

Keywords: *Hymenobacter*; regoliths; taxonomy; Antarctica.

Abbreviations: ANI, average nucleotide identity; dDDH, digital DNA–DNA hybridization; FAME, fatty acid methyl esters; MK, menaquinone; WGS, whole-genome sequencing.

The GenBank/EMBL/DBJ accession number for the complete 16S rRNA gene sequences of *Hymenobacter terrestris* P5252^T is MH760415 and for *Hymenobacter lapidiphilus* P5342^T is MN414324. The GenBank/EMBL/DBJ accession numbers for the partial 16S rRNA gene sequences of other *H. terrestris* and *H. lapidiphilus* isolates are MH760416 (P5353) and MN414325 (P5314), respectively. The Whole Genome Shotgun projects for *Hymenobacter lapidiphilus* sp. nov. P5342^T and *Hymenobacter terrestris* sp. nov. P5252^T have been deposited at DDBJ/ENA/GenBank under accessions JABKAU000000000 and JABKAV000000000. The versions described in this paper are versions JABKAU010000000 and JABKAV010000000. Four supplementary figures and four supplementary tables are available with the online version of this article.

Table 1. Source of *Hymenobacter terrestris* sp. nov. and *Hymenobacter lapidiphilus* sp. nov. strains

Species	Strain	Source; locality	GPS coordinates
<i>Hymenobacter terrestris</i>	P5252 ^T (=CCM 8765 ^T)	Streamside soil; Crame Col	57° 53' 20" W 63° 49' 35" S
	P5353 (=CCM 8963)	Dark soil; the base of Bibby Point	57° 56' 00" W 63° 48' 20" S
<i>Hymenobacter lapidiphilus</i>	P5314 (=CCM 8962)	Stone fragment; the base of Bibby Point	57° 56' 00" W 63° 48' 20" S
	P5342 ^T (=CCM 8764 ^T)	Hyaloclastite breccia; Lachman Crags	57° 51' 30" W 63° 51' 00" S

The genus *Hymenobacter* is a member of the family *Hymenobacteraceae* in the phylum *Bacteroidetes*. At the time of writing, a total of 82 species in the genus *Hymenobacter* with validly published names have been described (<https://lpsn.dsmz.de/>; accessed May 2020) [17]. Members of the genus are characterized as aerobic, Gram-negative, non-spore-forming rods, predominantly containing the fatty acids anteiso- $C_{15:0}$, iso- $C_{15:0}$, $C_{16:1}$ ω7c/iso- $C_{15:0}$ 2-OH, and iso- $C_{17:1}$ I/anteiso $C_{17:1}$ B as characteristic fatty acids and menaquinone MK-7 as the major respiratory quinone [18]. *Hymenobacter*s usually form mucous colonies with red to pink pigments and many colour variations [19], and this feature facilitates their isolation from primocultures. Pigmentation is a common attribute of chromogenic bacteria, and bacterial pigments are multifunctional in nature, such as for UV radiation resistance [15], light-harvesting, photoprotection or antioxidant function in cell membranes, where they constitute an integral part of the complex membrane structure [20]. Pigments from soil-derived bacteria have additional biological activities, such as anti-tumour, anti-fungal, anti-bacterial or anti-viral activity [21]. In this study, we describe two novel species of the genus *Hymenobacter*, based on the taxonomic investigation of four isolates obtained from regolith samples from James Ross Island, Antarctica, in 2013.

A group of four strains analysed in this study was isolated from different soil samples in the ice-free northern part of James Ross Island, Antarctica (Table 1). Sampling and strain isolation were performed as described previously [15]. Reference strains of the phylogenetically related *Hymenobacter humicola* CCM 8763^T, *H. aerophilus* CCM 8584^T, *H. psychrophilus* CCM 8561^T, *H. actinosclerus* CCM 8740^T, *H. amundsenii* CCM 8682^T and *H. rubripertinctus* CCM 8852^T were obtained from the Czech Collection of Microorganisms (<http://www.sci.muni.cz/ccm/>).

Genomic DNA for phylogenetic analysis was extracted according to Kýrová et al. [22]. The amplification of partial 16S rRNA gene sequences corresponding to coordinates 8–1542 (*Escherichia coli* nomenclature) was done by PCR with Fast-Start PCR Master (Roche Diagnostics) and conserved forward primer pA (5'-AGAGTTTGATCCTGGCTCAG-3') and reverse primer pH (5'-AAGGAGGTGATCCAGCCGCA-3')

[23]. Comparison of the obtained 16S rRNA gene sequences within the EzBioCloud database (<https://www.ezbiocloud.net/>) placed all four strains within the genus *Hymenobacter* and indicated *H. humicola* CCM 8763^T, *H. aerophilus* DSM 13606^T, *H. psychrophilus* CGMCC 1.8975^T and *H. actinosclerus* CCUG 39621^T to be the closest relatives. The 16S rRNA gene sequence similarities with representative isolate P5252^T were 98.8, 98.7, 98.8 and 97.9%, and with P5342^T they were 98.3, 98.4, 97.9 and 97.1%, respectively (Table S1). The 16S rRNA gene sequence similarity between P5252^T and P5342^T was 98.6%. These values were around or below the 98.7% 16S rRNA gene sequence similarity recently used as the threshold for differentiating among bacterial species [24]. The remaining *Hymenobacter* species exhibited sequence similarities lower than 97%. The unrooted phylogenetic tree based on 16S rRNA gene sequence comparison (Fig. 1) demonstrated the phylogenetic position of the four newly analysed *Hymenobacter* strains within the *Hymenobacter roseosalivarius* phylogenetic clade.

Whole-genome sequencing (WGS) was performed to characterize the taxonomic position of strains P5252^T and P5342^T in more detail. Genomic DNA of P5252^T was isolated using FastPrep Lysing Matrix type B and FastPrep homogenizer (MP Biomedicals), and purified with a High Pure PCR Template Preparation Kit (Roche Diagnostics). A DNA library was prepared using the Nextera XT DNA Library Prep Kit (Illumina), according to the manufacturer's protocol. Sequencing was performed using MiSeq Reagent Kits v2 (500-cycles) in a MiSeq 2000 sequencer according to the manufacturer's instructions (Illumina). DNA isolation and WGS of P5342^T was performed as a service by LMG/BCCM and by the Oxford Genomics Centre (University of Oxford). Genomic DNA was isolated using a Maxwell 16 Tissue DNA Purification Kit (Promega) and a Maxwell 16 Instrument (Promega). Library preparation was performed using an in-house adapted protocol of the NEB prep kit. Paired-end sequence reads were generated using the Illumina HiSeq 4000 platform (PE150 reads). Quality checking, trimming and the assembly of sequencing reads were performed as described previously [25]. The size of the draft genome for P5252^T was 4.180 Mb and consisted of 180 contigs longer than 200 bp (N50=20; L50=60.502 kB; mean coverage 154×). The draft genome for P5342^T was 4.612 Mb and consisted of 121 contigs longer than 200 bp (N50=15; L50=111.359 kB; mean coverage 229×). The assembled contigs larger than 200 bp were used for subsequent analysis and annotated with the NCBI Prokaryotic Genome Annotation Pipeline [26].

Phylogenetic analysis based on the core gene set was done using UBCG v3.0 [27], and showed that the analysed strains P5252^T and P5342^T formed a common branch with the type strains of *H. humicola*, *H. psychrophilus*, *H. actinosclerus* and *H. aerophilus* (Fig. S1, available in the online version of this article).

To calculate average nucleotide identity (ANI) values, OrthoANIu v1.2 was used [28]. Whole-genome sequences of the related *H. humicola* CCM 8763^T (GenBank accession

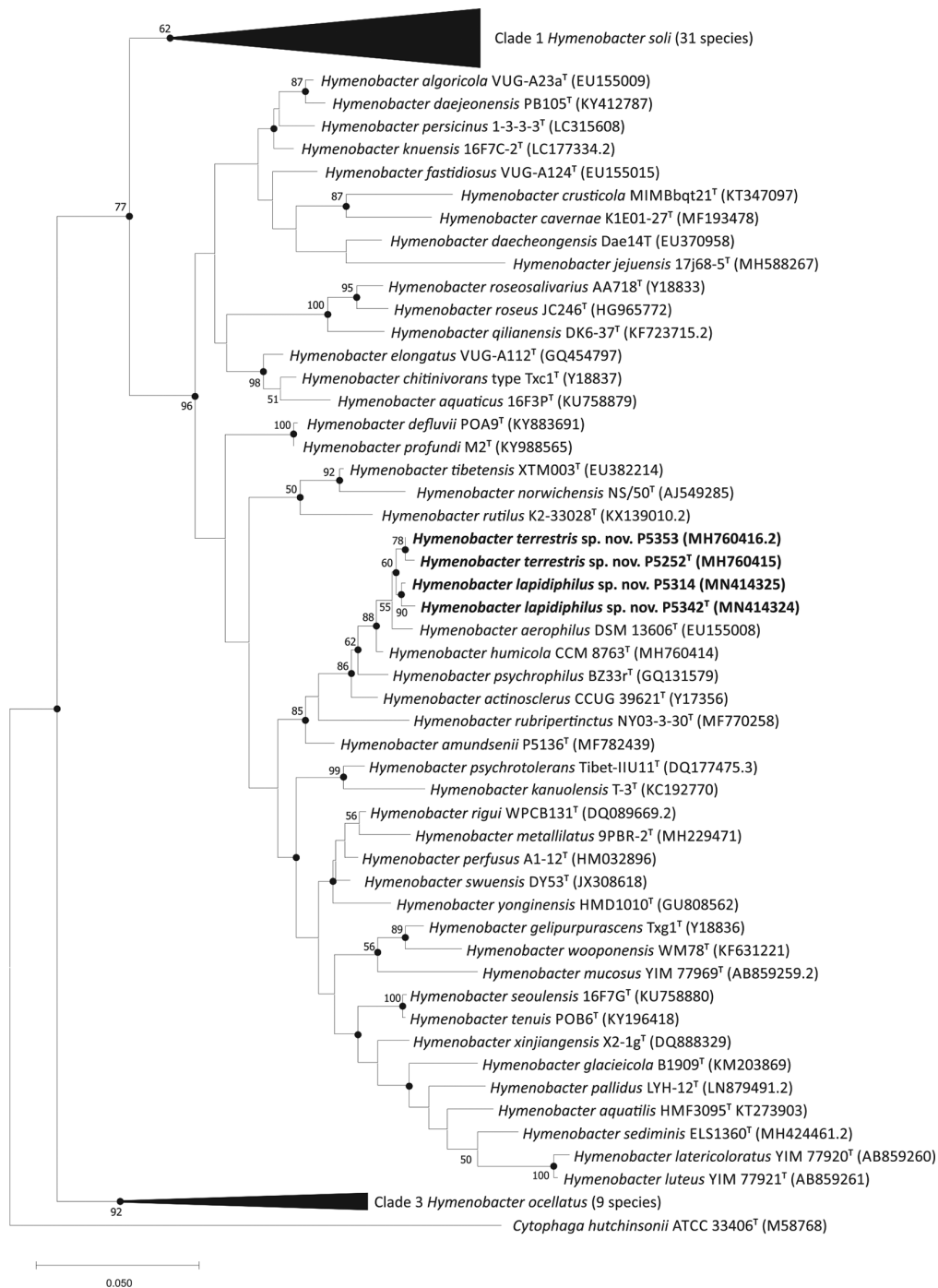


Fig. 1. Unrooted phylogenetic tree based on 16S rRNA gene sequence comparison, showing the phylogenetic position of two novel *Hymenobacter* species within the *Hymenobacter roseosalivarius* phylogenetic clade. Two other phylogenetic clades of *Hymenobacter soli* and *Hymenobacter ocellatus* are shown as collapsed branches. The evolutionary history was inferred by using the maximum-likelihood method and General Time Reversible model [44]. The percentage of 500 tree replications above 50% in which the associated taxa clustered together [45] is shown next to the branches. Initial tree(s) for the heuristic search were obtained automatically by applying the Neighbor-Join and BioNJ algorithms to a matrix of pairwise distances estimated using the Maximum Composite Likelihood approach, and then selecting the topology with superior log likelihood value. The tree is drawn to scale, with branch lengths measured in the number of substitutions per site. The analysis involved 90 nucleotide sequences. There were a total of 1583 positions in the final alignment. Filled circles indicate that the corresponding nodes were also obtained in the tree reconstructed by the neighbour-joining method [46] with evolutionary distances computed using the Maximum Composite Likelihood method [47]. Evolutionary analyses were conducted in MEGA software version 10 [48].

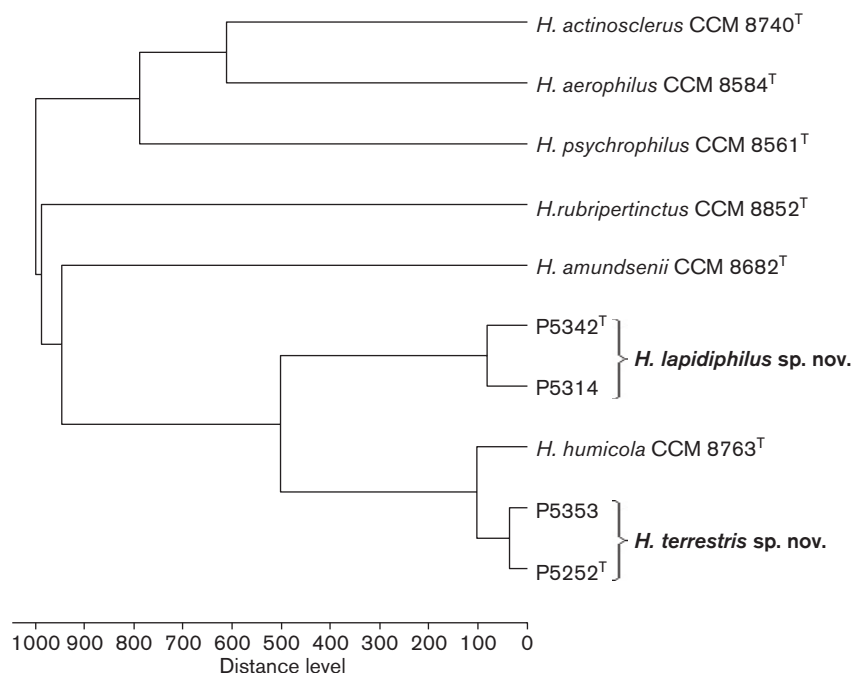


Fig. 2. Dendrogram obtained by cluster analysis of MALDI-TOF mass spectra of analysed *H. terrestris* sp. nov. and *H. lapidiphilus* sp. nov. strains and the type strains of closely related *Hymenobacter* species constructed by Biotyper 3.0 (Bruker Daltonics) software using the Pearson's product moment coefficient as a measure of similarity and UPGMA as a grouping method. Distance is displayed in relative units.

NZ_QVLT00000000) [15], *H. aerophilus* DSM 13606^T (NZ_ARNJ00000000) [29], *H. psychrophilus* CGMCC 1.8975^T (NZ_FNOV00000000) [30], *H. actinosclerus* CCUG 39621^T (NZ_FOHS01000001) [31], *H. amundsenii* CCM 8682^T (NZ_NIRR00000000) [16] and *H. rubripertinctus* NY03-3-30^T (NZ_QYCN00000000) [14] were obtained from the NCBI database. The ANI values calculated between P5252^T, P5342^T and the phylogenetically closest species *H. humicola*, *H. aerophilus*, *H. psychrophilus*, *H. actinosclerus*, *H. amundsenii* and *H. rubripertinctus* are listed in Table S1 and were well below the proposed cut-off values (95–96%) recommended for species delineation [24]. The digital DNA–DNA hybridization (dDDH) similarity values of P5252^T and the aforementioned reference species ranged from 25.6 to 35.1%, and the dDDH values of P5342^T and the reference species ranged from 26.1 to 36.1%, respectively. The dDDH similarity value between P5252^T and P5342^T was 39.2% (Table S1). Both ANI and dDDH data clearly confirmed the genomic separation of isolates P5252^T and P5342^T from each other as well as from related *Hymenobacter* species, and showed that P5252^T and P5342^T are members of two novel species, as implied by 16S rRNA gene sequencing results.

To estimate the DNA G+C content, draft genome sequences were used. The G+C content of P5252^T was 59.9 mol%, and that of P5342^T was 60.5 mol%, which corresponded with the range of 55–70 mol% observed in other *Hymenobacter* species [9, 18].

Protein fingerprinting was carried out by means of MALDI-TOF MS (matrix-assisted laser-desorption/ionization time-of-flight MS) using an UltrafleXtreme instrument (Bruker Daltonic), conducted after samples were treated with the ethanol/formic acid/extraction protocol [32]. The obtained MALDI-TOF profiles separated the analysed isolates into two clusters [33] that were clearly distinguished from the majority of the phylogenetically related *Hymenobacter* species (Fig. 2). These data were in agreement with DNA-based analyses and clearly supported the finding that the aforementioned isolates represent two distinct novel species within the genus *Hymenobacter*.

The genomic relatedness among isolated strains was studied by rep-PCR analyses with the BOX, ERIC, (GTG)₅ and REP primers according to Sedláček *et al.* [34]. The resulting DNA fragments obtained in individual rep-PCRs were separated within a single electrophoretic gel, and numerical analysis of the obtained fingerprints and dendrogram reconstruction were done using the software BioNumerics 7.6 (Applied Maths). Each strain gave a unique PCR pattern (Fig. S2), confirming their non-clonal origin.

Fatty acid methyl ester (FAME) analysis was performed with cells grown on R2A agar (Difco) incubated at 20±2 °C for 72 h, as described by Švec *et al.* [35]. The predominant fatty acids of all isolates were summed feature 3 (C_{16:1} ω7c/C_{16:1} ω6c), C_{16:1} ω5c, summed feature 4 (anteiso-C_{17:1} B/iso-C_{17:1} I), anteiso-C_{15:0} and iso-C_{15:0}. The complete cellular fatty acid

Table 2. Phenotypic characteristics that differentiate *Hymenobacter terrestris* sp. nov. and other *Hymenobacter* species

Taxa: 1. *Hymenobacter terrestris* sp. nov.; 2. *Hymenobacter lapidiphilus* sp. nov.; 3. *H. humicola* CCM 8763^T; 4. *H. psychrophilus* CCM 8561^T; 5. *H. actinosclerus* CCM 8740^T; 6. *H. aerophilus* CCM 8584^T; 7. *H. amundsenii* CCM 8682^T; 8. *H. rubripertinctus* CCM 8852^T. +, Positive; w, weakly positive; –, negative; all data were taken from this study.

Characteristic	1*	2*	3	4	5	6	7	8
Growth at 5°C	+	+	+	+	–	–	+	–
Growth at 30°C	–	–	–	–	+	+	–	–
Growth in 1% (w/v) NaCl	w	w	–	+	+	+	+	+
Growth on TSA	–	–	–	–	–	+	–	–
Growth at pH 6	–	–	–	–	+	+	–	+
Growth at pH 9	–	–	–	+	–	–	–	+
Acid from maltose	+	+	–	–	w	+	+	+
Hydrolysis of:								
DNA	+	+	+	–	–	+	w	+
Starch	+	+	+	+	–	w	+	+
Tween 80	–	–	–	+	+	+	–	–
Casein	+	+	+	+	+	–	+	+
API ZYM:								
Cystein arylamidase	–	w	w	–	–	–	w	–
Naphthol-AS-BI phosphohydrolase	–	w	w	w	w	w	w	+
α-Glucosidase	w	w	–	–	–	w	+	w
Biolog GEN III:								
L-Histidine	–	–	+	–	–	–	–	+
L-Serine	–	w	+	–	–	–	+	–
Methyl β-D-glucoside	+	–	–	–	–	–	–	–
D-Aspartic acid	–	+	–	–	–	–	+	–
D-Gluconic acid	+	–	–	–	–	–	–	–
Acetic acid	–	+	+	+	–	+	w	+

*Data are uniform for all isolates of *H. terrestris* sp. nov. and *H. lapidiphilus* sp. nov.

profiles of the four new strains and five reference strains (Table S2) corresponded to those typically found in other *Hymenobacter* species, differing only quantitatively [18]. These results showed that differentiation of the proposed novel species from their phylogenetically closest neighbours solely by using FAME is not possible.

Quinones and polar lipids were extracted from freeze-dried biomass of strains P5252^T and P5342^T grown on R2A medium and analysed as described previously [36, 37]. MK-7 was the only respiratory quinone of P5252^T and P5342^T. The predominant polar lipids for both type strains were phosphatidylethanolamine and one unidentified glycolipid. In addition to major polar lipids, the type strains of both proposed species exhibited qualitatively and quantitatively different profiles. A more complex profile of P5342^T consists of one additional

unidentified glycolipid, four unidentified aminoglycolipids and five unidentified lipids. The profile of P5252^T revealed the presence of the same unidentified lipids (4 and 5) and aminoglycolipids (1 and 2), and additionally one unidentified lipid L6 and one phospholipid were found in this strain. Two-dimensional TLC showing the total polar lipids of strains P5342^T and P5252^T is presented in Fig. S3.

All four new isolates were aerobic, Gram-stain-negative short rods that produced moderately slimy colonies with a pink-red colour on R2A agar. They were differentiated from related *Hymenobacter* species by the test results given in Table 2. The KOH lysis test method [38] was used to confirm the Gram-staining results of the analysed strains. Samples for electron microscopical evaluation (Fig. S4) were obtained as a rinse of bacterial cultures grown on R2A agar [16] and 30 randomly

selected cells from 10 transmission electron micrographs were measured to specify the variability of sizes. The presence of flexirubin-type pigments was investigated using a 20% (w/v) KOH solution [39]. Growth on several media such as plate count agar (PCA; Oxoid), tryptone soya agar (TSA; Oxoid), nutrient agar CM03 (Oxoid), MacConkey agar (Becton Dickinson) and brain heart infusion agar (BHI; Oxoid) was evaluated at 15 °C. Anaerobic growth on R2A agar was tested in an anaerobic jar at 15 °C for 72 h using Anaerocult A (Merck) and compared to those cultivated in the ambient atmosphere. Growth at different temperatures (1, 5, 10, 15, 20, 25 and 30 °C) and tolerance to various NaCl concentrations (0.5, 1, 2 and 3%, w/v) were determined based on cultivation on R2A agar plates for up to 4 days [13]. The pH range for growth was tested on R2A agar plates adjusted to pH 6.0–9.0 using different buffer systems (pH 6.0–8.0, 0.1 M KH₂PO₄/0.1 M NaOH; pH 9.0, 0.1 M NaHCO₃/0.1 M Na₂CO₃; at intervals of 1 pH unit) for 1 week at 15 °C [40]. Liquid cultures were not used, because of the poor growth of *Hymenobacter* isolates in broth media [19]. Basic phenotyping was performed using conventional tube and plate tests relevant for Gram-negative rods as described previously [35]. The hydrolytic activities (e.g. amylase, lipase and protease) were tested by using R2A agar plates supplemented with appropriate substrates [41]. These key tests were inoculated with cells grown at 20 °C for 48 h on R2A agar. Additional biotyping with the GEN III MicroPlate identification test kit, using protocol C1 (Biolog), and API ZYM kit (bioMérieux) according to the manufacturer's instructions, enabled a comprehensive characterization of isolates. Inoculated kits were incubated at 20 °C, and the results were read after 18 h (API ZYM) or 3 days (GEN III MicroPlate). Antibiotic resistance patterns were tested by the disc diffusion method on R2A agar for 2 days at 20 °C. Sixteen antibiotic discs (Oxoid) generally used for Gram-negative rods were chosen [35] and EUCAST/CLSI standards were strictly followed for cultivation and inhibition zone diameter readings [42, 43]. The complete phenotypic characterization of the four analysed strains is summarized in the species descriptions below.

The polyphasic classification of four isolates (P5252^T, P5353, P5342^T and P5314) using 16S rRNA gene sequencing, WGS, MALDI-TOF MS, rep-PCR typing, chemotaxonomic analyses (menaquinone, polar lipids and FAMES), and extended phenotyping demonstrated that the aforementioned group of strains isolated from different inorganic environmental samples in Antarctica forms two coherent clusters that represent two novel *Hymenobacter* species, for which the names *Hymenobacter terrestris* sp. nov. and *Hymenobacter lapidiphilus* sp. nov. are proposed.

DESCRIPTION OF *HYMENOBACTER TERRESTRIS* SP. NOV.

Hymenobacter terrestris sp. nov. (ter.res'tris. L. masc. adj. *terrestris* belonging to soil). The description of the species is based on two isolates.

Cells are Gram-stain-negative non-spore-forming pleomorphic short rods, 755–1120 nm wide and 1400–2610 nm long, occurring predominantly in irregular clusters or singly. Colonies on R2A agar are circular with irregular margins, flat to slightly convex, smooth, glistening, moderately slimy, reddish pigmented and 1–2 mm in diameter after 4 days of cultivation at 15 °C. Non-flexirubin-type pigment is present. Good growth occurs on R2A agar and PCA agar. No growth is observed on nutrient agar, TSA, BHI or MacConkey agar at 15 °C. Aerobic; no growth on R2A agar under anaerobic conditions. Good growth is observed between 1 and 20 °C, but not at 30 °C. Cells only grow in the pH range 7.0–8.0. Good growth occurs on R2A medium in the presence of 0.5% (w/v) NaCl and weak growth in the presence of 1% NaCl; the presence of 2% NaCl inhibits growth. Glucose is not fermented to acid in OF test medium. Positive for catalase, alkaline phosphatase, acid phosphatase, esterase lipase (C8) (weak), α -glucosidase (weak), leucine arylamidase and valine arylamidase by API ZYM. Positive for hydrolysis of gelatin, casein, DNA and starch. Acid is produced from maltose. Negative for esterase (C4), trypsin, α -chymotrypsin, naphthol-AS-BI-phosphohydrolase, α -galactosidase, β -galactosidase, β -glucuronidase, β -glucosidase, α -mannosidase and α -fucosidase by API ZYM. Negative for nitrate and nitrite reduction, fluorescein (King B medium), acid from fructose, xylose and mannitol, urease, oxidase, lysine and ornithine decarboxylase, arginine dihydrolase, Simmons citrate, acetamide and malonate utilization. Negative for hydrolysis of Tween 80, ONPG, tyrosine and lecithin. Variable phenotypic reactions of *H. terrestris* strains are listed in Table S3. Resistant to aztreonam and ceftazidime, but sensitive to ampicillin, carbenicillin, cephalothin, ciprofloxacin, chloramphenicol, imipenem, cotrimoxazole, piperacillin, polymyxin B, streptomycin and tetracycline. Susceptibility to cefixime, gentamicin and kanamycin is strain-dependent (Table S3). On GEN III MicroPlates (Biolog), exhibits positive utilization of dextrin, melibiose, methyl β -D-glucoside, α -D-glucose, D-glucose 6-phosphate, gelatin, glycyl-L-proline, L-arginine, L-aspartic acid, L-glutamic acid, D-gluconic acid and β -hydroxy-DL-butyric acid as a carbon source. Negative utilization results for trehalose, cellobiose, gentiobiose, sucrose, turanose, stachyose, raffinose, lactose, D-salicin, N-acetyl-D-glucosamine, N-acetyl- β -D-mannosamine, N-acetylneuraminic acid, D-fructose, 3-methyl glucose, D-fucose, L-fucose, L-rhamnose, inosine, D-mannitol, D-arabitol, *myo*-inositol, glycerol, D-fructose 6-phosphate, D-aspartic acid, D-serine, L-alanine, L-histidine, L-pyroglutamic acid, L-serine, D-galacturonic acid, D-galactonic acid lactone, mucic acid, quinic acid, *p*-hydroxy phenylacetic acid, methyl pyruvate, D-lactic acid methyl ester, L-lactic acid, citric acid, α -ketoglutaric acid, D-malic acid, L-malic acid, bromosuccinic acid, α -hydroxy-butyric acid, α -ketobutyric acid and formic acid. The strain-dependent results obtained with the Biolog GEN III MicroPlate are shown in Table S4. Summed feature 3 (C_{16:1} ω 7c/C_{16:1} ω 6c), C_{16:1} ω 5c, summed feature 4 (anteiso-C_{17:1}B/iso-C_{17:1}I), anteiso-C_{15:0} and iso-C_{15:0} are major cellular fatty acids. The polar lipid profile of strain P5252^T contains phosphatidylethanolamine and an unidentified glycolipid as major

compounds. Moderate to minor amounts of two unidentified aminoglycolipids, one unidentified phospholipid, one unidentified glycopospholipid and three unidentified lipids are present. The quinone system is composed of the menaquinone MK-7.

The type strain is P5252^T (=CCM 8765^T=LMG 31495^T). All characteristics of the type strain P5252^T are in agreement with the species description, except for the strain-dependent test results of P5252^T that are presented in Tables S3 and S4. The DNA G+C content of strain P5252^T is 59.9 mol%, and the genome size is approximately 4.2 Mb. The GenBank/EMBL/DDBJ accession numbers for the 16S rRNA gene sequences of *Hymenobacter terrestris* P5252^T and P5353 are MH760415 and MH760416, respectively. The Whole-Genome Shotgun project of strain P5252^T has been deposited at DDBJ/ENA/GenBank under accession number JABKAV000000000. The strains of *H. terrestris* were isolated from different soil samples from James Ross Island, Antarctica.

DESCRIPTION OF HYMENOBACTER LAPIDIPHILUS SP. NOV.

Hymenobacter lapidiphilus sp. nov. (la.pi.di'phi.lus. L. masc. n. *lapis*, -*idis* rock, stone; Gr. masc. n. *philos* friend, loving; N.L. masc. adj. *lapidiphilus*, stone-loving). The description of the species is based on two strains.

Cells are Gram-stain-negative, non-spore-forming straight rods, 1070–1390 nm wide and 1730–6330 nm long, occurring singly and in clusters. Colonies on R2A agar are circular with irregular margins, flat, smooth, glistening, moderately slimy, reddish pigmented and 1–2 mm in diameter after 3 days of cultivation at 15 °C. Non-flexirubin-type pigment is present. Good growth occurs on R2A agar only. Variable growth is detected on PCA and nutrient agar. No growth occurs on TSA, BHI or MacConkey agar at 15 °C. Aerobic; no growth on R2A agar under anaerobic conditions. Good growth is observed between 1 and 25 °C, but not at 30 °C. Cells only grow in the pH range 7.0–8.0. Good growth on R2A medium in the presence of 0.5% (w/v) NaCl and weak growth in the presence of 1% NaCl; the presence of 2% NaCl inhibits growth. Glucose is not fermented to acid in OF test medium. Positive for acid production from maltose. Positive for catalase, alkaline phosphatase, acid phosphatase, esterase lipase (C8) (weak), *N*-acetyl- β -glucosaminidase, α -glucosidase (weak), naphthol-AS-BI-phosphohydrolase (weak), leucine arylamidase, valine arylamidase and cystine arylamidase (weak) by API ZYM. Positive for gelatin, casein, aesculin, DNA and starch hydrolysis. Negative for lipase (C14), trypsin, α -galactosidase, β -galactosidase, β -glucuronidase, β -glucosidase, α -mannosidase and α -fucosidase by API ZYM. Negative for nitrate and nitrite reduction, fluorescein (King B medium), acid from fructose, xylose and mannitol, urease, oxidase, lysine and ornithine decarboxylase, arginine dihydrolase, Simmons citrate, acetamide and malonate utilization. Negative for hydrolysis of Tween 80, ONPG, tyrosine and lecithin. Variable phenotypic

reactions of *H. lapidiphilus* strains are listed in Table S3. Resistant to aztreonam, cefixime, ceftazidime, gentamicin and kanamycin, but sensitive to ampicillin, carbenicillin, cephalothin, ciprofloxacin, chloramphenicol, imipenem, cotrimoxazole, piperacillin, polymyxin B, streptomycin and tetracycline. On GEN III MicroPlates (Biolog), positive for utilization of dextrin, α -D-glucose, D-aspartic acid, gelatine, glycyl-L-proline, L-serine, L-aspartic acid, L-glutamic acid, mucic acid, Tween 40, acetoacetic acid, propionic acid, acetic acid and formic acid as a carbon source. Negative for utilization of trehalose, cellobiose, gentiobiose, sucrose, turanose, stachyose, lactose, melibiose, methyl β -D-glucoside, D-salicin, *N*-acetyl-D-glucosamine, *N*-acetyl- β -D-mannosamine, *N*-acetyl neuraminic acid, D-mannose, 3-methyl glucose, L-rhamnose, inosine, D-arabitol, glycerol, D-serine, L-alanine, L-arginine, L-histidine, pectin, D-galacturonic acid, D-galactonic acid lactone, D-gluconic acid, quinic acid, *p*-hydroxy phenylacetic acid, methyl pyruvate, L-lactic acid, L-malic acid, bromosuccinic acid, γ -aminobutyric acid, α -hydroxy-butyric acid and α -ketobutyric acid. Borderline utilization of D-fructose 6-phosphate and L-malic acid. Variable results of *H. lapidiphilus* strains obtained on Biolog GEN III MicroPlates are shown in Table S4. Summed feature 3 ($C_{16:1}\omega7c/C_{16:1}\omega6c$), $C_{16:1}\omega5c$, summed feature 4 (anteiso- $C_{17:1}$ B/iso- $C_{17:1}$ I), anteiso- $C_{15:0}$ and iso- $C_{15:0}$ are the major cellular fatty acids. The polar lipid profile of strain P5342^T contains phosphatidylethanolamine and an unidentified glycolipid as the major compounds. Moderate to minor amounts of four aminoglycolipids, one unidentified glycopospholipid, one additional unidentified glycolipid and five unidentified lipids are also present. The quinone system is composed of menaquinone MK-7.

On GEN III MicroPlates (Biolog), positive for utilization of dextrin, α -D-glucose, D-aspartic acid, gelatine, glycyl-L-proline, L-serine, L-aspartic acid, L-glutamic acid, mucic acid, Tween 40, acetoacetic acid, propionic acid, acetic acid and formic acid as a carbon source. Negative for utilization of trehalose, cellobiose, gentiobiose, sucrose, turanose, stachyose, lactose, melibiose, methyl β -D-glucoside, D-salicin, *N*-acetyl-D-glucosamine, *N*-acetyl- β -D-mannosamine, *N*-acetyl neuraminic acid, D-mannose, 3-methyl glucose, L-rhamnose, inosine, D-arabitol, glycerol, D-serine, L-alanine, L-arginine, L-histidine, pectin, D-galacturonic acid, D-galactonic acid lactone, D-gluconic acid, quinic acid, *p*-hydroxy phenylacetic acid, methyl pyruvate, L-lactic acid, L-malic acid, bromosuccinic acid, γ -aminobutyric acid, α -hydroxy-butyric acid and α -ketobutyric acid. Borderline utilization of D-fructose 6-phosphate and L-malic acid. Variable results of *H. lapidiphilus* strains obtained on Biolog GEN III MicroPlates are shown in Table S4. Summed feature 3 ($C_{16:1}\omega7c/C_{16:1}\omega6c$), $C_{16:1}\omega5c$, summed feature 4 (anteiso- $C_{17:1}$ B/iso- $C_{17:1}$ I), anteiso- $C_{15:0}$ and iso- $C_{15:0}$ are the major cellular fatty acids. The polar lipid profile of strain P5342^T contains phosphatidylethanolamine and an unidentified glycolipid as the major compounds. Moderate to minor amounts of four aminoglycolipids, one unidentified glycopospholipid,

one additional unidentified glycolipid and five unidentified lipids are also present. The quinone system is composed of menaquinone MK-7.

The type strain is P5342^T (=CCM 8764^T=LMG 30613^T). All characteristics of the type strain P5342^T are in agreement with the species description except for the strain-dependent test results of P5342^T that are given in Tables S3 and S4. The DNA G+C content of strain P5342^T is 60.5 mol%, and the genome size is approximately 4.6 Mb. The GenBank/EMBL/DBJ accession numbers for the 16S rRNA gene sequences of *Hymenobacter lapidiphilus* P5342^T and P5314 are MN414324 and MN414325, respectively. The Whole-Genome Shotgun project of strain P5342^T has been deposited at DDBJ/ENA/GenBank under accession number JABKAU000000000. The strains of *H. lapidiphilus* species were isolated from different inorganic materials (regoliths) on James Ross Island, Antarctica.

Funding information

This work was supported by the Ministry of Education, Youth and Sports of the Czech Republic (LM2015078, LM2018121 and 02.1.01/0.0/0.0/18_046/0015975). R.P. and M.Z. were supported by the Grant Agency of Masaryk University (MUNI/A/0824/2019). CIISB research infrastructure project LM2018127 funded by MEYS CR is gratefully acknowledged for financial support of the measurements at the CEITEC Proteomics Core Facility. This study was also partially funded by MEYS CR (LM2015051 and CZ.02.1.01/0.0/0.0/16_013/0001761).

Acknowledgements

The authors wish to thank the scientific infrastructure of the J. G. Mendel Czech Antarctic Station, part of the Czech Polar Research Infrastructure (CzechPolar2), and its crew for their assistance. S.K. is a beneficiary of Brno PhD Talent financial aid. Dr Daniel Krsek (National Reference Laboratory for Diagnostic Electron Microscopy of Infectious Agents, National Institute of Public Health, Prague, Czech Republic) is gratefully acknowledged for transmission electron microscopy. We wish to thank Jana Bajerová for excellent technical assistance and Prof. Bernhard Schink (University of Konstanz, Germany) for nomenclature correction.

Conflicts of interest

The authors declare that there are no conflicts of interest.

References

- Hirsch P, Ludwig W, Hethke C, Sittig M, Hoffmann B et al. *Hymenobacter roseosalivarius* gen. nov., sp. nov. from continental Antarctica soils and sandstone: bacteria of the *Cytophaga/Flavobacterium/Bacteroides* line of phylogenetic descent. *Syst Appl Microbiol* 1998;21:374–383.
- Peeters K, Ertz D, Willems A. Culturable bacterial diversity at the Princess Elisabeth station (Utsteinen, Sør Rondane mountains, East Antarctica) harbours many new taxa. *Syst Appl Microbiol* 2011;34:360–367.
- Chang X, Zheng J, Jiang F, Liu P, Kan W et al. *Hymenobacter arcticus* sp. nov., isolated from glacial till. *Int J Syst Evol Microbiol* 2014;64:2113–2118.
- Gu Z, Liu Y, Xu B, Wang N, Jiao N et al. *Hymenobacter frigidus* sp. nov., isolated from a glacier ice core. *Int J Syst Evol Microbiol* 2017;67:4121–4125.
- Liu K, Liu Y, Wang N, Gu Z, Shen L et al. *Hymenobacter glaciicola* sp. nov., isolated from glacier ice. *Int J Syst Evol Microbiol* 2016;66:3793–3798.
- Liu L, Zhou EM, Jiao JY, Manikprabhu D, Ming H et al. *Hymenobacter mucosus* sp. nov., isolated from a karst cave soil sample. *Int J Syst Evol Microbiol* 2015;65:4121–4127.
- Zhu HZ, Yang L, Muhadesi JB, Wang BJ, Liu S. *Hymenobacter cavernae* sp. nov., isolated from a karst cave. *Int J Syst Evol Microbiol* 2017;67:4825–4829.
- Zhang G, Niu F, Busse H-J, Ma X, Liu W et al. *Hymenobacter psychrotolerans* sp. nov., isolated from the Qinghai-Tibet Plateau permafrost region. *Int J Syst Evol Microbiol* 2008;58:1215–1220.
- Han L, Wu S-J, Qin C-Y, Zhu YH, Lu Z-Q et al. *Hymenobacter qilianensis* sp. nov., isolated from a subsurface sandstone sediment in the permafrost region of Qilian mountains, China and emended description of the genus *Hymenobacter*. *Antonie van Leeuwenhoek* 2014;105:971–978.
- Kim MC, Kim CM, Kang OC, Zhang Y, Liu Z et al. *Hymenobacter rutilus* sp. nov., isolated from marine sediment in the Arctic. *Int J Syst Evol Microbiol* 2017;67:856–861.
- Sun J, Xing M, Wang W, Dai F, Liu J et al. *Hymenobacter profundus* sp. nov., isolated from deep-sea water. *Int J Syst Evol Microbiol* 2018;68:947–950.
- Kojima H, Watanabe M, Tokizawa R, Shinohara A, Fukui M. *Hymenobacter nivis* sp. nov., isolated from red snow in Antarctica. *Int J Syst Evol Microbiol* 2016;66:4821–4825.
- Sedláček I, Králová S, Kýrová K, Mašláňová I, Busse H-J et al. Red-pink pigmented *Hymenobacter coccineus* sp. nov., *Hymenobacter lapidarius* sp. nov. and *Hymenobacter glacialis* sp. nov., isolated from rocks in Antarctica. *Int J Syst Evol Microbiol* 2017;67:1975–1983.
- Jiang F, Danzeng W, Zhang Y, Zhang Y, Jiang L et al. *Hymenobacter rubripertinctus* sp. nov., isolated from Antarctic tundra soil. *Int J Syst Evol Microbiol* 2018;68:663–668.
- Sedláček I, Pantůček R, Králová S, Mašláňová I, Holochová P et al. *Hymenobacter amundsenii* sp. nov. resistant to ultraviolet radiation, isolated from regoliths in Antarctica. *Syst Appl Microbiol* 2019;42:284–290.
- Sedláček I, Pantůček R, Holochová P, Králová S, Staňková E et al. *Hymenobacter humicola* sp. nov., isolated from soils in Antarctica. *Int J Syst Evol Microbiol* 2019;69:2755–2761.
- Parte AC. LPSN - List of Prokaryotic names with Standing in Nomenclature (bacterio.net), 20 years on. *Int J Syst Evol Microbiol* 2018;68:1825–1829.
- Buczolits S, Busse H-J. *Hymenobacter*. In: Whitman WB (editor). *Bergey's Manual of Systematics of Archaea and Bacteria*, 2015. Indianapolis, IN: John Wiley & Sons; 2015. pp. 1–11.
- Klassen JL, Foght JM. Characterization of *Hymenobacter* isolates from Victoria upper glacier, Antarctica reveals five new species and substantial non-vertical evolution within this genus. *Extremophiles* 2011;15:45–57.
- Britton G. Structure and properties of carotenoids in relation to function. *Faseb J* 1995;9:1551–1558.
- Mumtaz R, Bashir S, Numan M, Shinwari ZK, Ali M. Pigments from soil bacteria and their therapeutic properties: a mini review. *Curr Microbiol* 2019;76:783–790.
- Kýrová K, Sedláček I, Pantůček R, Králová S, Holochová P et al. *Rufibacter ruber* sp. nov., isolated from fragmentary rock. *Int J Syst Evol Microbiol* 2016;66:4401–4405.
- Edwards U, Rogall T, Blöcker H, Emde M, Böttger EC. Isolation and direct complete nucleotide determination of entire genes. Characterization of a gene coding for 16S ribosomal RNA. *Nucleic Acids Res* 1989;17:7843–7853.
- Chun J, Oren A, Ventosa A, Christensen H, Arahall DR et al. Proposed minimal standards for the use of genome data for the taxonomy of prokaryotes. *Int J Syst Evol Microbiol* 2018;68:461–466.
- Nováková D, Švec P, Zeman M, Busse H-J, Mašláňová I et al. *Pseudomonas leptonychotis* sp. nov., isolated from Weddell seals in Antarctica. *Int J Syst Evol Microbiol* 2020;70:302–308.
- Tatusova T, DiCuccio M, Badretdin A, Chetvernin V, Nawrocki EP et al. NCBI prokaryotic genome annotation pipeline. *Nucleic Acids Res* 2016;44:6614–6624.

27. Na SI, Kim YO, Yoon S-H, Ha SM, Baek I et al. UBCG: up-to-date bacterial core gene set and pipeline for phylogenomic tree reconstruction. *J Microbiol* 2018;56:280–285.
28. Lee I, Ouk Kim Y, Park SC, Chun J. OrthoANI: an improved algorithm and software for calculating average nucleotide identity. *Int J Syst Evol Microbiol* 2016;66:1100–1103.
29. Buczolits S, Denner EB, Vybiral D, Wieser M, Kämpfer P et al. Classification of three airborne bacteria and proposal of *Hymenobacter aerophilus* sp. nov. *Int J Syst Evol Microbiol* 2002;52:445–456.
30. Zhang DC, Busse H-J, Liu HC, Zhou YG, Schinner F et al. *Hymenobacter psychrophilus* sp. nov., a psychrophilic bacterium isolated from soil. *Int J Syst Evol Microbiol* 2011;61:859–863.
31. Collins MD, Hutson RA, Grant IR, Patterson MF. Phylogenetic characterization of a novel radiation-resistant bacterium from irradiated pork: description of *Hymenobacter actinosclerus* sp. nov. *Int J Syst Evol Microbiol* 2000;50:731–734.
32. Freiwald A, Sauer S. Phylogenetic classification and identification of bacteria by mass spectrometry. *Nat Protoc* 2009;4:732–742.
33. Maier T, Klepel S, Renner U, Kostrzewa M. Fast and reliable MALDI-TOF MS-based microorganism identification. *Nature Methods* 2006;25:68–71.
34. Sedláček I, Kwon SW, Švec P, Mašláňová I, Kýrová K et al. *Aquitalea pelogenes* sp. nov., isolated from mineral peloid. *Int J Syst Evol Microbiol* 2016;66:962–967.
35. Švec P, Králová S, Busse H-J, Kleinhagauer T, Kýrová K et al. *Pedobacter psychrophilus* sp. nov., isolated from fragmentary rock. *Int J Syst Evol Microbiol* 2017;67:2538–2543.
36. Tamaoka J. Analysis of bacterial menaquinone mixtures by reverse-phase high-performance liquid chromatography. *Methods Enzymol* 1986;123:31–36.
37. Minnikin DE, O'Donnell AG, Goodfellow M, Alderson G, Athalye M et al. An integrated procedure for the extraction of bacterial isoprenoid quinones and polar lipids. *J Microbiol Methods* 1984;2:233–241.
38. Carlone GM, Valadez MJ, Pickett MJ. Methods for distinguishing Gram-positive from Gram-negative bacteria. *J Clin Microbiol* 1982;16:1157–1159.
39. Bernardet JF, Nakagawa Y, Holmes B, Subcommittee on the taxonomy of Flavobacterium and Cytophaga-like bacteria of the International Committee on Systematics of Prokaryotes. Proposed minimal standards for describing new taxa of the family *Flavobacteriaceae* and emended description of the family. *Int J Syst Evol Microbiol* 2002;52:1049–1070.
40. Da X, Jiang F, Chang X, Ren L, Qiu X et al. *Pedobacter ardeleyensis* sp. nov., isolated from soil in Antarctica. *Int J Syst Evol Microbiol* 2015;65:3841–3846.
41. Margesin R, Gander S, Zacke G, Gounot AM, Schinner F. Hydrocarbon degradation and enzyme activities of cold-adapted bacteria and yeasts. *Extremophiles* 2003;7:451–458.
42. CLSI. *Performance Standards for Antimicrobial Susceptibility Testing; Twenty-Fifth Informational Supplement (M100-S25)*, 35. Wayne, PA: No. 3, Clinical and Laboratory Standards Institute; 2015.
43. EUCAST. Breakpoint tables for interpretation of MICs and zone diameters, version 7.1, the European Committee on antimicrobial susceptibility testing. www.eucast.org 2017.
44. Nei M, Kumar S. *Molecular Evolution and Phylogenetics*. New York: Oxford University Press; 2000.
45. Felsenstein J. Confidence limits on phylogenies: an approach using the bootstrap. *Evolution* 1985;39:783–791.
46. Saitou N, Nei M. The neighbor-joining method: a new method for reconstructing phylogenetic trees. *Mol Biol Evol* 1987;4:406–425.
47. Tamura K, Nei M, Kumar S. Prospects for inferring very large phylogenies by using the neighbor-joining method. *Proc Natl Acad Sci USA* 2004;101:11030–11035.
48. Kumar S, Stecher G, Li M, Knyaz C, Tamura K. MEGA X: molecular evolutionary genetics analysis across computing platforms. *Mol Biol Evol* 2018;35:1547–1549.

Five reasons to publish your next article with a Microbiology Society journal

1. The Microbiology Society is a not-for-profit organization.
2. We offer fast and rigorous peer review – average time to first decision is 4–6 weeks.
3. Our journals have a global readership with subscriptions held in research institutions around the world.
4. 80% of our authors rate our submission process as 'excellent' or 'very good'.
5. Your article will be published on an interactive journal platform with advanced metrics.

Find out more and submit your article at microbiologyresearch.org.

1 ***Hymenobacter terrestris* sp. nov. and *Hymenobacter lapidiphilus* sp. nov., isolated from**
2 **regoliths in Antarctica**

3 Ivo Sedláček*¹, Roman Pantůček², Michal Zeman², Pavla Holochová¹, Ondrej Šedo³, Eva
4 Staňková¹, Pavel Švec¹, Stanislava Králová¹, Petra Vídeňská⁴, Lenka Micenková⁴, Vipin
5 Gupta⁵, Utkarsh Sood⁵, Urvashi⁶, Suresh Korpole⁶ and Rup Lal⁵

6

7 ¹Department of Experimental Biology, Czech Collection of Microorganisms, Faculty of
8 Science, Masaryk University, Kamenice 5, 625 00 Brno, Czech Republic

9 ²Department of Experimental Biology, Section of Genetics and Molecular Biology, Faculty of
10 Science, Masaryk University, Kamenice 5, 625 00 Brno, Czech Republic

11 ³Central European Institute of Technology, Masaryk University, Kamenice 5, 625 00 Brno,
12 Czech Republic

13 ⁴Research Centre for Toxic Compounds in the Environment, Faculty of Science, Masaryk
14 University, Kamenice 5, 625 00 Brno, Czech Republic

15 ⁵ Department of Zoology, North Campus, University of Delhi, Delhi-110007, India

16 ⁶ CSIR-Institute of Microbial Technology, Chandigarh, 160036 India

17

18 *Corresponding author:

19 Ivo Sedláček; E-mail: ivo@sci.muni.cz; Tel.: +420-549496922

20

21 **Supplementary materials**

22

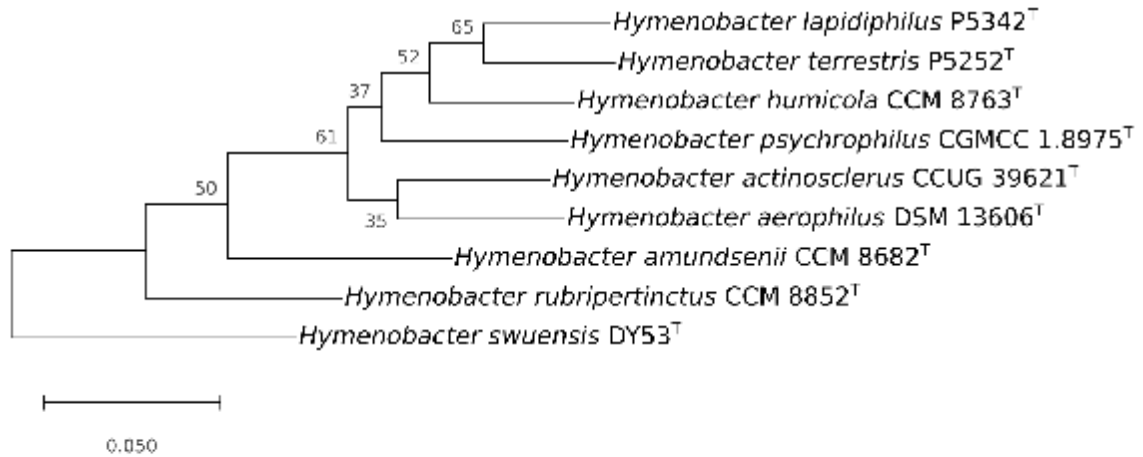
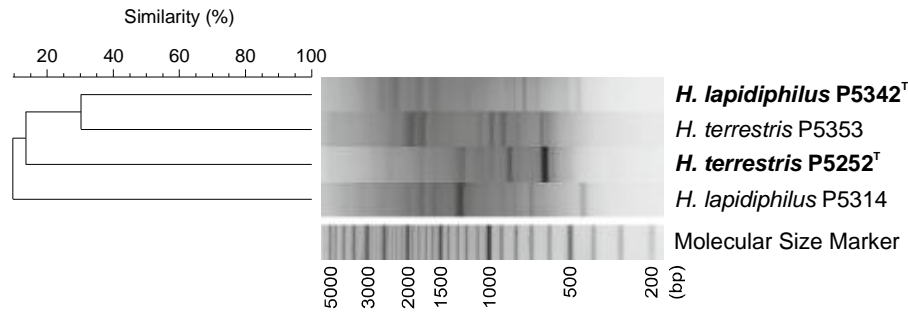


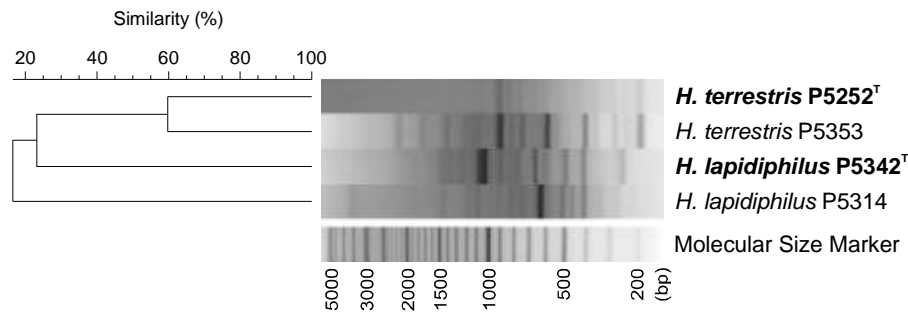
Fig. S1. Core gene set phylogenetic tree of *Hymenobacter lapidiphilus* sp. nov. P5342^T (CCM 8764^T), *Hymenobacter terrestris* sp. nov. P5252^T (CCM 8765^T) and closely related species.

Phylogenetic tree was constructed using Up-to-date bacterial core gene set (UBCG; concatenated alignment of 92 core genes). A total of 92,355 nucleotide positions were used. Maximum likelihood phylogenetic tree was inferred using Fasttree ver. 2.1.10 [Price, MN, Dehal PS, Arkin AP. FastTree 2 approximately maximum-likelihood trees for large alignments. *Plos One* 2010; 5(3):e9490] using GTR + CAT model. Alignments of UBCGs and concatenated gene sequences were done by default algorithm of UBCG v3.0. Gene support indices are given at branching points (maximal possible value is 92). Bar, 0.05 substitution per position.

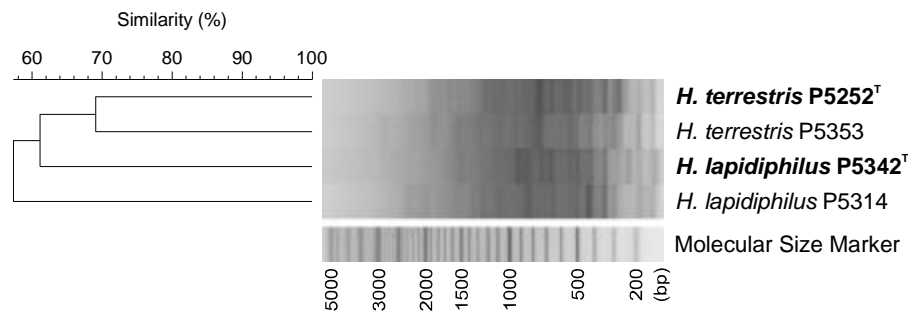
a) BOX-PCR



b) ERIC-PCR



c) (GTG)₅-PCR



d) REP-PCR

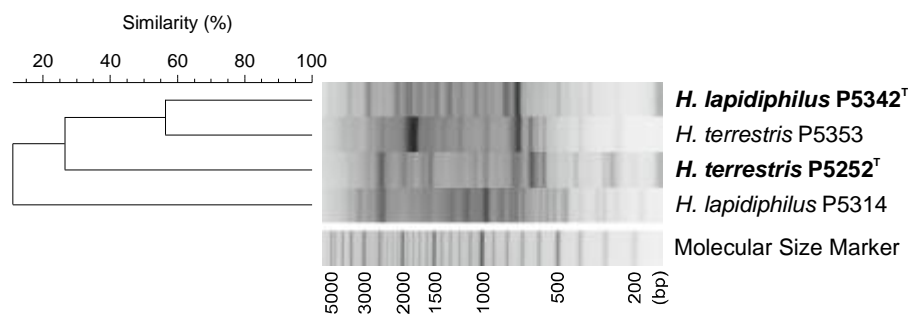
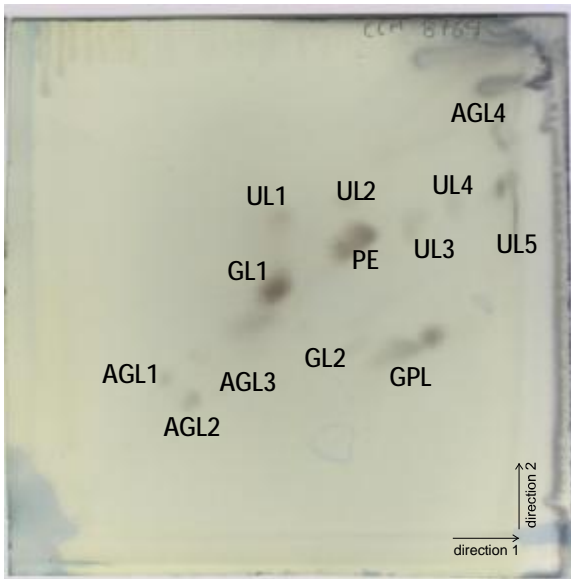


Fig. S2. Dendrograms based on cluster analysis of rep-PCR fingerprints obtained with **a)** BOX, **b)** ERIC, **c)** (GTG)₅, and **d)** REP primers from *Hymenobacter lapidiphilus* sp. nov. and *Hymenobacter terrestris* sp. nov. strains. The dendrograms were calculated with Pearson's correlation coefficients with UPGMA clustering method (r , expressed as percentage similarity values).

Hymenobacter lapidiphilus P5342^T



Hymenobacter terrestris P5252^T

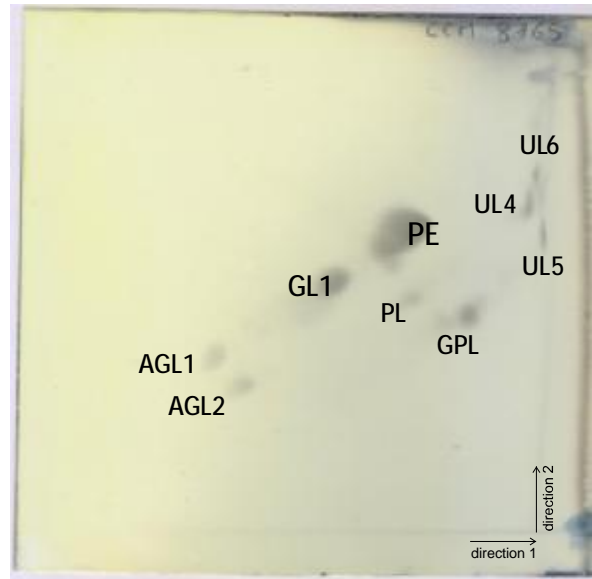
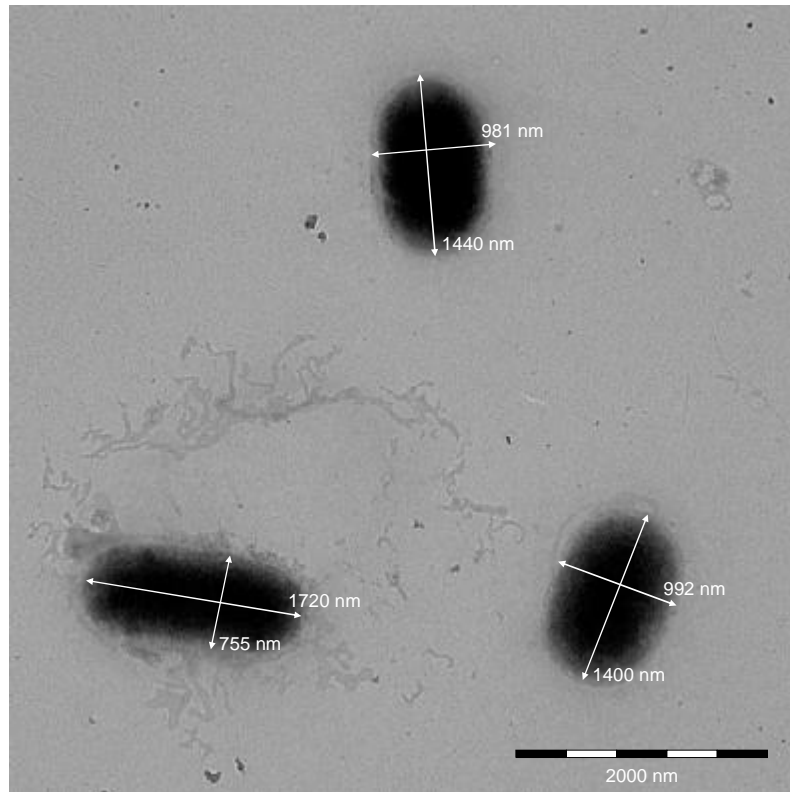


Fig S3. Two dimensional TLC showing the total polar lipids of the *Hymenobacter lapidiphilus* P5342^T (CCM 8764^T) and *Hymenobacter terrestris* P5252^T (CCM 8765^T). AGL1-AGL4: unidentified aminoglycolipids, GL1-GL2: unidentified glycolipids, GPL: glycophospholipid, PE: phosphatidylethanolamine, PL: unidentified phospholipid, UL1-UL6: unidentified polar lipids.

Hymenobacter terrestris P5252^T



Hymenobacter lapidiphilus P5342^T

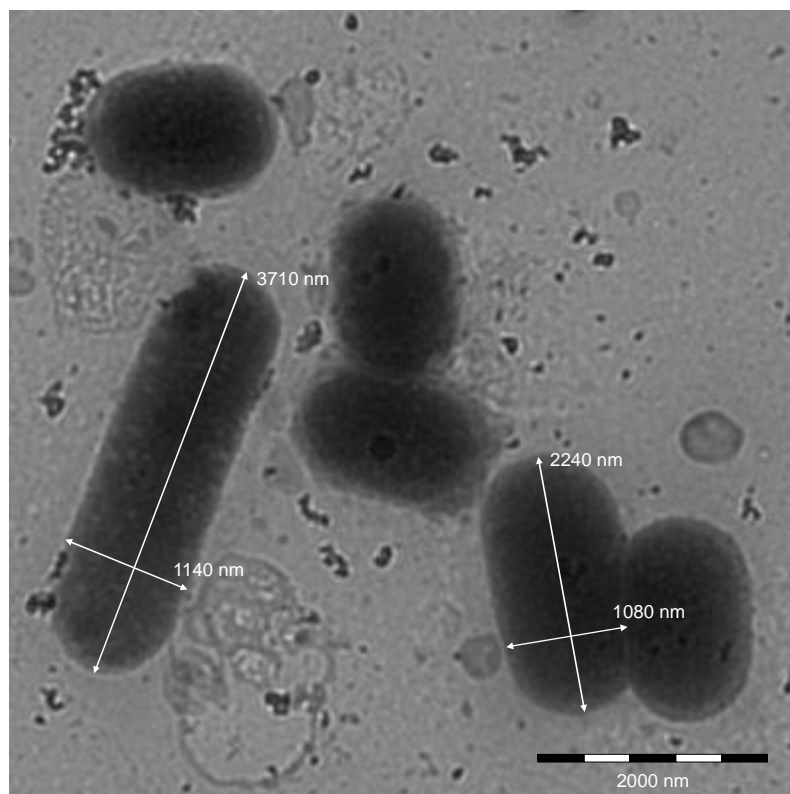


Fig. S4. Cell morphology of strains P5252^T (CCM 8765^T) and P5342^T (CCM 8764^T) observed using transmission electron microscopy performed with a Hitachi HT7800 (Hitachi, Japan). Negative staining with 0.25% ammonium molybdate. Bar represents 2000 nm (original magnification $\times 5000$).

Table S1. Pairwise 16S rRNA gene sequence similarities (above 96%), average nucleotide identities and dDDH values of strains P5342^T and P5252^T to close relatives.

Species	Strain	16S rRNA accession no.	16S rRNA pairwise similarity (%)				Genome accession no.	ANI value (%)		dDDH value (%)	
			P5342 ^T	P5314	P5252 ^T	P5353		P5342 ^T	P5252 ^T	P5342 ^T	P5252 ^T
<i>H. lapidiphilus</i> sp. nov.	P5342 ^T (CCM 8764 ^T)	MN414324	100.0	99.2	98.6	98.7	JABKAU000000000	100.0	89.6	-	39.2
<i>H. terrestris</i> sp. nov.	P5252 ^T (CCM 8765 ^T)	MH760415	98.6	99.3	100.0	99.7	JABKAV000000000	89.6	100.0	39.2	-
<i>H. humicola</i>	CCM 8763 ^T	MH760414	98.3	98.5	98.8	98.9	QVLT000000000	88.4	88.1	36.1	35.1
<i>H. aerophilus</i>	DSM 13606 ^T	EU155008	98.4	99.3	98.7	98.8	ARNJ000000000	85.2	84.9	30.0	29.4
<i>H. psychrophilus</i>	CGMCC 1.8975 ^T	GQ131579	97.9	98.8	98.8	98.7	FNOV000000000	85.5	85.2	30.8	29.6
<i>H. actinosclerus</i>	CCUG 39621 ^T	Y17356	97.1	97.6	97.9	98.1	FOHS01000001	85.5	85.1	30.2	29.5
<i>H. amundsenii</i>	CCM 8682 ^T	MF782439	96.1	96.6	97.4	97.3	NIRR000000000	81.7	81.5	26.1	25.5
<i>H. rubripertinctus</i>	NY03-3-30 ^T	MF770258	96.3	96.1	96.3	96.2	QYCN000000000	81.5	81.4	26.1	25.6

Table S2. Cellular fatty acid contents (%) of *Hymenobacter terrestris* sp. nov., *Hymenobacter lapidiphilus* sp. nov. and closely related *Hymenobacter* spp. type strains (pairwise 16S rRNA gene sequence similarities above 97%).

All data were taken from this study using cells grown to the late exponential phase (72 h) on R2A agar medium at 20 °C. TR, traces (< 1.0%); ND, not detected.

Fatty acid	<i>Hymenobacter terrestris</i>		<i>Hymenobacter lapidiphilus</i>		<i>Hymenobacter</i>	<i>Hymenobacter</i>	<i>Hymenobacter</i>	<i>Hymenobacter</i>	<i>Hymenobacter</i>
	P5252 ^T (CCM 8765 ^T)	P5353 (CCM 8963)	P5342 ^T (CCM 8764 ^T)	P5314 (CCM 8962)	<i>humicola</i> CCM 8763 ^T	<i>amundsenii</i> CCM 8682 ^T	<i>psychrophilus</i> CCM 8561 ^T	<i>actinosclerus</i> CCM 8740 ^T	<i>aerophilus</i> CCM 8584 ^T
C _{15:0} iso	7.1	8.6	4.4	11.9	9.9	7.5	14.0	16.4	7.6
C _{15:0} anteiso	6.8	8.3	8.1	10.9	13.2	6.0	11.0	21.4	16.8
C _{16:1} iso H	2.2	1.8	2.6	2.5	1.5	1.2	1.9	1.4	1.1
C _{16:0} iso	1.8	ND	1.4	1.4	ND	1.0	2.4	ND	ND
C _{16:1} ω5c	16.7	16.3	18.1	19.2	14.2	21.3	13.0	8.8	11.1
C _{16:0}	2.7	3.2	3.4	1.6	2.6	2.8	1.8	1.1	1.6
C _{15:0} iso 3OH	2.0	1.8	1.4	1.8	1.5	1.7	1.8	1.6	1.4
C _{15:0} 2OH	TR	TR	1.0	TR	TR	1.1	TR	1.0	1.1
C _{17:0} iso	2.0	2.3	TR	1.1	1.7	2.2	1.8	1.7	4.8
C _{17:0} anteiso	TR	TR	TR	TR	TR	TR	TR	TR	2.5
C _{17:0} iso 3OH	3.9	3.3	2.1	2.8	2.9	2.8	3.6	2.7	4.1
C _{17:0} 2OH	1.1	1.0	1.2	TR	1.1	1.7	TR	1.0	1.6
*Summed Feature 3	34.0	33.0	41.8	28.0	32.5	37.8	34.1	23.8	30.2
*Summed Feature 4	14.1	13.4	7.8	11.2	13.4	3.3	7.7	12.0	12.9

*Summed features are groups of two fatty acids that cannot be separated by gas chromatography using the MIDI system.

Summed Feature 3 contains C_{16:1} ω7c / C_{16:1} ω6c and Summed Feature 4 contains C_{17:1} anteiso B / iso I.

Table S3. Variable reactions of *Hymenobacter terrestris* sp. nov. and *Hymenobacter lapidiphilus* sp. nov. strains.

<i>Hymenobacter terrestris</i> sp. nov.									<i>Hymenobacter lapidiphilus</i> sp. nov.				
Strain	Growth at 25 °C	Esculine hydrolysis	Lipase (C 14)	Cystine arylamidase	N-acetyl-b-glucosaminidase	Cefixim	Gentamicin	Kanamycin	Strain	Growth on PCA	Growth on Nutrient agar CM03	Esterase (C 4)	a-chymotrypsin
P5252 ^T (CCM 8765 ^T)	-	-	-	-	-	R	S	S	P5314 (CCM 8962)	+	-	w	w
P5353 (CCM 8963)	+	+	w	w	+	S	R	I	P5342 ^T (CCM 8764 ^T)	-	+	-	-

+, positive; w, weakly positive; -, negative; S, sensitive; R, resistant; I, intermediate

Table S4. Variable reactions of *Hymenobacter terrestris* sp. nov. and *Hymenobacter lapidiphilus* sp. nov. strains on Biolog GEN III MicroPlate.

Test	<i>H. terrestris</i> sp. nov.		<i>H. lapidiphilus</i> sp. nov.	
	P5252 ^T (CCM 8765 ¹)	P5353 (CCM 8963)	P5314 (CCM 8962)	P5342 ^T (CCM 8764 ¹)
D-Maltose	-	+	+	-
D-Raffinose	-	-	b	-
N-Acetyl-D-galactosamine	+	-	+	-
D-Mannose	+	-	-	-
D-Fructose	-	-	+	-
D-Galactose	-	+	+	-
D-Fucose	-	-	b	-
L-Fucose	-	-	b	-
D-Sorbitol	+	-	b	-
D-Mannitol	-	-	b	-
myo-Inositol	-	-	b	-
D-Glucose-6-PO ₄	+	+	+	-
L-Pyroglutamic acid	-	-	b	-
Pectin	+	-	-	-
D-Glucuronic acid	-	+	-	b
Glucuronamide	+	-	b	-
D-Saccharic acid	b	-	b	-
D-Lactic acid methyl ester	-	-	b	-
Citric acid	-	-	+	-
α-keto Glutaric acid	-	-	-	b
Tween 40	-	+	+	+
γ-amino-Butyric acid	+	-	-	-
β-Hydroxy-D,L-butyric acid	+	+	+	-
Acetoacetic acid	-	+	+	+
Propionic acid	+	-	+	+
Acetic acid	-	b	+	+

All data were taken from this study using two replications.

+, positive; b, borderline; -, negative